©2019

Phillip Lavelle Vines

ALL RIGHTS RESERVED

MOLECULAR BREEDING TOOLS FOR IMPROVING MORPHOLOGICAL TRAITS AND BIOTIC AND ABIOTIC STRESS RESPONSES IN PERENNIAL RYEGRASS

By

PHILLIP LAVELLE VINES

A dissertation submitted to the

School of Graduate Studies

Rutgers, The State University of New Jersey

In partial fulfillment of the requirements

For the degree of

Doctor of Philosophy

Graduate Program in Plant Biology

Written under the direction of

Stacy A. Bonos

And approved by

_____

_____

_____

_____

_____

New Brunswick, New Jersey

May, 2019

ABSTRACT OF THE DISSERTATION

Molecular Breeding Tools for Improving Morphological Traits and Biotic and Abiotic Stress Responses in Perennial Ryegrass

by PHILLIP LAVELLE VINES

Dissertation Director:

Stacy A. Bonos

Perennial ryegrass (*Lolium perenne* L.) is a widely used cool-season turfgrass species. The primary breeding objectives for turf-type perennial ryegrass include improving tolerance to abiotic and biotic factors such as salinity stress and dollar spot disease, which is caused by *Clarireedia jacksonii* C. Salgado, L.A. Beirn, B.B. Clarke, and J.A. Crouch. These types of traits are often quantitatively inherited and present difficulties for the phenotypic selection breeding technique. Quantitative trait locus (QTL) mapping has been implemented in modern plant breeding programs as a basis for marker-assisted selection for complex, quantitatively inherited traits. The preliminary components for QTL mapping include developing an appropriate mapping population and constructing a genetic linkage map that is densely populated with markers. After these prerequisite tasks have been completed, and phenotypic data for the traits of interest have been collected, QTL analyses may be conducted.

The purpose of this dissertation was to exploit the QTL mapping technique for developing molecular breeding tools to help improve these complex traits in perennial ryegrass. The specific research objectives of this work were (i) to develop a diverse

perennial ryegrass mapping population that would accommodate QTL mapping studies for salinity tolerance and dollar spot resistance in perennial ryegrass, (ii) to construct a high-density, single nucleotide polymorphism (SNP)-based genetic linkage map for perennial ryegrass, (iii) to conduct QTL analyses for salinity tolerance, dollar spot resistance, and growth habit morphology traits in perennial ryegrass.

For the first objective, candidate parental genotypes were selected from a large population of perennial ryegrass clones in the Rutgers turfgrass breeding program. These genotypes were studied for response to salinity stress and dollar spot disease. Additionally, phenotypic variation in growth habit and leaf color was also observed among the candidate parental genotypes. Although these two traits were not of primary interest in developing the mapping population, they were also considered when pairing parents for cross-fertilization events. Nine biparental crosses were made in the summer of 2016. The selected population consisted of 118 pseudo-F_2 progeny derived from a cross between 15-8325 (maternal parent, referenced as I06) and 15-8343 (paternal parent, referenced as A89). Thus, the population is commonly referenced as the I06 × A89 perennial ryegrass mapping population and is comprised of the 2 parent genotypes and 118 progeny genotypes.

For the second objective, greater than 1.8 Gb of raw sequencing reads were generated for the 2 parent genotypes and the 118 progeny genotypes from the I06 × A89 population. In addition to the SNP markers that were generated in this study, a set of framework simple sequence repeat (SSR) markers from previous studies were also used for linkage map construction. Two linkage maps, one for each parent, were developed. After screening markers for polymorphisms, segregation distortion, redundancy, and

insufficient grouping support, 848 SNP markers and 52 SSR markers were included in the marker dataset for parent I06 while 769 SNP markers and 35 SSR markers were included in the marker dataset for parent A89. The 900 markers included in the I06 dataset mapped to a total distance of 677.5 cM with an average marker density of 0.75 cM. The 804 markers included in the A89 dataset mapped to a total distance of 687.9 cM with an average marker density of 0.86 cM.

For the third objective, the I06 × A89 population was evaluated for the traits of salinity tolerance, dollar spot resistance, and growth habit morphology using multiple field trials during 2017 and 2018 at the Rutgers Plant Science Research and Extension Farm in Adelphia, NJ. Subsequently, QTL analyses were conducted with the individual I06 and A89 parent maps and phenotypic data for the traits of interest.

The QTL analyses for salinity tolerance resulted in the identification of fifteen major-effect QTL and forty-three minor-effect QTL. Eleven salinity tolerance QTL were identified using two distinct assessment methods for salinity tolerance, seven salinity tolerance QTL were identified at multiple environmental locations, and one salinity tolerance QTL was identified on both parent maps. The QTL analyses for dollar spot resistance resulted in the identification of twelve major-effect QTL and nine minor-effect QTL. Coincident dollar spot resistance QTL were mapped to four distinct genomic regions and were consistently identified using multiple evaluation methods for dollar spot severity and/or multiple environments. The growth habit morphology QTL analyses resulted in the identification of twenty-one major effect QTL and seven minor-effect QTL. Four growth habit morphology QTL were identified across multiple environments,

and two growth habit morphology QTL were significantly associated with multiple morphological traits.

These are the first reported efforts for QTL mapping of salinity tolerance and dollar spot resistance in perennial ryegrass. Further, this is the first report of QTL mapping for growth habit traits in turf-type perennial ryegrass. These findings will be useful for future studies involving development of marker-assisted selection techniques for breeding applications, gene and mechanism discovery, and comparative genomics investigations using closely related plant species. These efforts will be used to develop improved perennial ryegrass cultivars, which will ultimately contribute to the sustainability of the turfgrass industry. Moreover, the I06 × A89 perennial ryegrass population will be useful to further study these and additional traits in perennial ryegrass, and the high-density genetic linkage map constructed herein will be a valuable resource for future QTL studies in turf-type perennial ryegrass breeding.

ACKNOWLEDGEMENTS

I would like to express my gratitude to each of the individuals who have made this research possible. I am certain that I will fail to mention someone who has helped me, and if that is so, I would like them to know that I am, indeed, very much appreciative for their assistance.

Firstly, to the director of my dissertation, Dr. Stacy A. Bonos. I thank her for the opportunity to study at Rutgers University and participate in the most successful cool-season breeding program in the world. In addition, I owe her a great deal of gratitude for the patience, belief, motivation, and guidance she presented to me throughout this research process. Her knowledge and supervision enabled me to complete this work, and for that, I am eternally grateful.

I extend my sincerest thanks to each of my committee members, Dr. Shaun B. Bushman, Dr. Bruce B. Clarke, Dr. Josh A. Honig, and Dr. William A. Meyer. The expertise and guidance they provided to me throughout my graduate studies at Rutgers University was extremely critical for my success. I have enjoyed getting to know each of them, and I am forever thankful for their contributions to this work.

I would also like to recognize other faculty, technical assistants, student workers, and fellow graduate students for their support in conducting this research. I am grateful to Ron Bara, Dirk Smith, and Eric Weibel for the help they provided in various aspects of my field research. To Christine Kubik and Jennifer Vaiciunas, I must express my appreciation for the countless hours they spent helping me in the laboratory. I am thankful for the support from Joseph Clark, Bryan Dzugan, Alan Habiak, T.J. Lawson, and George Ziemienski at the Rutgers Plant Science Research and Extension Farm in

Adelphia, NJ and the Rutgers Horticultural Research Farm II in North Brunswick, NJ. Thanks to Danielle Bara, Michael Bara, Tessa Catuogno, Lars Rasmussen, and Olivia Wright for their assistance, as undergraduate student workers. I am grateful to fellow graduate students, Ryan Daddio, Kyle Genova, Austin Grimshaw, Henry Qu, and Trent Tate, for their assistance with my research project, but more importantly, for their moral support and the comradery we shared. I extend thanks to Dr. Tom Gianfagna and Jeanne Peters for assistance in laboratory projects as part of my research, and I am grateful to Jeffrey Akers, Joseph Florentine, and Mark Peacos for their help with various greenhouse studies I conducted.

I would like to recognize the Center for Turfgrass Science, the Department of Plant Biology, the New Jersey Landscape Contractors Association, the New Jersey Turfgrass Association, the New Jersey Turfgrass Foundation, the Rutgers Turfgrass Alumni Association, and the United States Golf Association for the various scholarships and financial support provided to me during my graduate studies.

Lastly, but most importantly, I am thankful to God for placing such loving and supportive people in my life. I am grateful for the opportunities He has afforded me, and for the strength, knowledge, and guidance He has bestowed upon me. With God, all things are possible.

DEDICATION

This dissertation is dedicated to my wife, Elizabeth, and our parents, James and Tammie Vines and Bill and Janet Gullett. Words could never fully express my feelings for these individuals. The unending love and support our parents have provided has enabled me to be successful in the completion of this dissertation. I love them dearly, forever and always. Without Elizabeth, this accomplishment absolutely would not have been possible. I am truly thankful for the unconditional support, understanding, patience, and love she has shown me throughout the duration of this research. Simply put, I have the greatest wife in the entire world. She has my heart, and I will forever love her.

TABLE OF CONTENTS

ABSTRACT OF THE DISSERTATION ii

ACKNOWLEDGEMENTS vi

DEDICATION viii

TABLE OF CONTENTS ix

LIST OF TABLES xvi

LIST OF FIGURES xx

NOMENCLATURE xxx

I. LITERATURE REVIEW 1

Perennial ryegrass 2

Adaptation and use 2

Phytomorphology 3

Reproduction 4

Conventional breeding methods, achievements, and objectives 6

Salt-induced stress 9

Perspective and causation 9

Classification of salt-affected soils 10

Saline soils 14

Sodic soils 15

Saline-sodic soils 17

Salt-associated issues in turfgrass systems 18

Perennial ryegrass breeding efforts for salinity tolerance 20

Dollar spot disease 24

Symptoms and signs 24
Causal organism.....25
Disease development and epidemiology.....27
Control 28
Breeding efforts for dollar spot resistance in turfgrass systems 29
Molecular biology methods for plant breeding.....30
DNA sequencing.....30
Sanger sequencing technology.....33
Next-generation sequencing technology.....35
454 pyrosequencing 35
Illumina sequencing.....37
SOLiD sequencing.....39
Genetic markers 40
DNA markers.....41
Restriction fragment length polymorphisms.....42
Diversity array technologies 44
Random amplified polymorphic DNAs.....45
Arbitrary primed-PCRs.....48
Amplified fragment length polymorphisms.....49
Sequence-characterized amplified regions 51
Microsatellite markers 52
Inter-simple sequence repeats.....54
Cleaved amplified polymorphic sequences 56

Single-strand conformation polymorphisms.....56

Sequence-related amplified polymorphisms.....58

Target region amplification polymorphisms.....59

Single nucleotide polymorphisms.....61

Genotyping-by-sequencing.....63

Quantitative trait loci mapping.....66

Developing a mapping population.....67

Genotyping a mapping population.....68

Linkage mapping.....69

Phenotyping a mapping population.....70

Detection and mapping of quantitative trait loci.....71

Single-marker analysis.....72

Single interval mapping.....72

Composite interval mapping.....73

Multiple interval mapping.....74

Bayesian multiple quantitative trait locus mapping.....75

Quantitative trait loci confidence interval.....76

Quantitative trait loci mapping studies in ryegrass.....77

II. DEVELOPMENT OF THE I06 × A89 PERENNIAL RYEGRASS MAPPING POPULATION.....101

Abstract.....101

Introduction.....102

Materials and methods.....104

Phenotyping for traits of interest.....104

Biparental crosses and establishment of mapping population 106

Results 106

Discussion 108

Literature cited 111

III. A SNP-BASED GENETIC LINKAGE MAP OF PERENNIAL RYEGRASS USING NEXT-GENERATION DOUBLE-DIGEST RESTRICTION-SITE-ASSOCIATED DNA SEQUENCING 119

Abstract 119

Introduction 120

Materials and methods 123

Plant Material and DNA extraction 123

Construction and sequencing of ddRADseq libraries 124

SNP marker identification and genotyping 125

SSR framework marker genotyping 126

Genetic linkage map construction 127

Results 128

SNP marker identification and genotyping 128

SSR framework marker genotyping 130

Genetic linkage map construction 131

Parent I06 map 131

Parent A89 map 132

Discussion 134

Literature cited 136

IV. QUANTITATIVE TRAIT LOCUS MAPPING FOR SALINITY TOLERANCE IN PERENNIAL RYEGRASS 153

Abstract 153

Introduction 154

Materials and methods 156

Plant material 157

Genetic linkage mapping 157

Field assessment for salinity tolerance 158

Quantitative trait locus analysis 160

Results 161

Field assessment for salinity tolerance 161

Quantitative trait locus analysis 163

I06 parent map 163

A89 parent map 166

Discussion 169

Literature cited 174

V. QUANTITATIVE TRAIT LOCUS MAPPING FOR DOLLAR SPOT RESISTANCE IN PERENNIAL RYEGRASS 201

Abstract 201

Introduction 202

Materials and methods 205

Mapping population 205

Genetic linkage mapping 205

Field assessment for dollar spot resistance 206

Quantitative trait locus analysis 208

Results 209

Field assessment for dollar spot resistance 209

Quantitative trait locus analysis 210

I06 parent map 211

A89 parent map 213

Discussion 215

Literature cited 219

VI. QUANTITATIVE TRAIT LOCUS MAPPING FOR GROWTH HABIT MORPHOLOGY TRAITS IN PERENNIAL RYEGRASS 240

Abstract 240

Introduction 241

Materials and methods 243

Mapping population 243

Genetic linkage mapping 243

Field assessment for morphological traits 244

Quantitative trait locus analysis 245

Results 246

Field assessment for morphological traits 246

Analyses of Variance 247

Growth habit 248

Seedhead angle 248

Plant height 249

Vegetative plant width 249

Total plant width 250

Quantitative trait locus analysis 250

I06 parent map 251

A89 parent map 252

Discussion 253

Literature cited 257

VII. THESIS CONCLUSION 285

A. SUPPLEMENTARY MATERIAL FOR GENETIC LINKAGE MAPPING STUDIES 289

LIST OF TABLES

Table 2.1 Summary of clones selected as candidate parental genotypes for the I06 × A89 perennial ryegrass mapping population. 114

Table 3.1 Summary of sequence data for the I06 × A89 perennial ryegrass mapping population generated using next-generation double-digest restriction-site-associated DNA sequencing genotyping methods. 140

Table 3.2 Number and proportion of transitions and transversions in the identified SNP markers generated by next-generation sequencing-based genotyping of the I06 and A89 parent genotypes.....141

Table 3.3 Distribution and summary statistics of single nucleotide polymorphism and simple sequence repeat markers on the linkage groups of the I06 perennial ryegrass genetic linkage map. 142

Table 3.4 Distribution and summary statistics of single nucleotide polymorphism and simple sequence repeat markers on the linkage groups of the A89 perennial ryegrass genetic linkage map. 143

Table 4.1 Mean green cover as determined via visual ratings for the I06 × A89 perennial ryegrass population and each parent genotype on 28 Sep 2017 and 4 Sep 2018 at the Rutgers Plant Science Research and Extension Farm in Adelphia, NJ.....179

Table 4.2 Mean percent green cover as determined via pixel analysis for the I06 × A89 perennial ryegrass population and each parent genotype on 28 Sep 2017 and 4 Sep 2018 at the Rutgers Plant Science Research and Extension Farm in Adelphia, NJ. 179

Table 4.3 Analysis of variance for mean green cover as determined via visual ratings for the I06 × A89 perennial ryegrass mapping population on 28 Sep 2017 and 4 Sep 2018 at the Rutgers Plant Science Research and Extension Farm in Adelphia, NJ. 180

Table 4.4 Analysis of variance for mean percent green cover as determined via pixel analysis for the I06 × A89 perennial ryegrass mapping population on 28 Sep 2017 and 4 Sep 2018 at the Rutgers Plant Science Research and Extension Farm in Adelphia, NJ. 180

Table 4.5 Summary of the twenty-seven quantitative trait loci (QTL) identified for salinity tolerance at sixteen distinct genomic regions across six linkage groups of the I06 parent map. A multiple QTL model mapping analysis was conducted with phenotypic data for salinity tolerance generated from visual ratings and pixel analysis of field trials during 2017 on a loamy sand soil (2017LS) and a sandy loam soil (2017SL) and during 2018 on a sandy loam soil (2018SL) at the Rutgers Plant Science Research and Extension Farm in Adelphia, NJ. 181

Table 4.6 Summary of the thirty-one quantitative trait loci (QTL) identified for salinity tolerance at sixteen distinct genomic regions across six linkage groups of the A89 parent map. A multiple QTL model mapping analysis was conducted with phenotypic data for salinity tolerance generated from visual ratings and pixel analysis of field trials during 2017 on a loamy sand soil (2017LS) and a sandy loam soil (2017SL) and during 2018 on a sandy loam soil (2018SL) at the Rutgers Plant Science Research and Extension Farm in Adelphia, NJ. 184

Table 5.1 Mean dollar spot severity as determined via visual ratings for the I06 × A89 perennial ryegrass population on 23 Aug 2017 and 28 Aug 2018 at the Rutgers Horticultural Research Farm II in North Brunswick, NJ. 224

Table 5.2 Mean dollar spot severity (percent non-green area) as determined via pixel analysis for the I06 × A89 perennial ryegrass population on 23 Aug 2017 and 28 Aug 2018 at the Rutgers Horticultural Research Farm II in North Brunswick, NJ. 224

Table 5.3 Analysis of variance for mean dollar spot severity as determined via visual ratings for the I06 × A89 perennial ryegrass population on 23 Aug 2017 and 28 Aug 2018 at the Rutgers Horticultural Research Farm II in North Brunswick, NJ. 225

Table 5.4 Analysis of variance for mean dollar spot severity (percent non-green area) as determined via pixel analysis for the I06 × A89 perennial ryegrass population on 23 Aug 2017 and 28 Aug 2018 at the Rutgers Horticultural Research Farm II in North Brunswick, NJ. 225

Table 5.5 Summary of the twelve quantitative trait loci (QTL) identified for dollar spot resistance across six linkage groups of the I06 parent map. A multiple QTL model mapping analysis was conducted with phenotypic data for dollar spot severity generated from visual ratings and pixel analysis of field trials during 2017 and 2018 at the Rutgers Horticultural Research Farm II in North Brunswick, NJ....226

Table 5.6 Summary of the nine quantitative trait loci (QTL) identified for dollar spot resistance across five linkage groups of the A89 parent map. A multiple QTL model mapping analysis was conducted with phenotypic data for dollar spot severity generated from visual ratings and pixel analysis of field trials during 2017 and 2018 at the Rutgers Horticultural Research Farm II in North Brunswick, NJ....227

Table 6.1 Mean growth habit for the I06 × A89 perennial ryegrass population and each parent genotype on 27 Jun 2017 and 11 Jun 2018 at the Rutgers Plant Science Research and Extension Farm in Adelphia, NJ....259

Table 6.2 Mean seedhead angle (degree) for the I06 × A89 perennial ryegrass population and each parent genotype on 29 Jun 2017 and 12 Jun 2018 at the Rutgers Plant Science Research and Extension Farm in Adelphia, NJ. 259

Table 6.3 Mean plant height (mm) for the I06 × A89 perennial ryegrass population and each parent genotype on 27 Jun 2017 and 13 Jun 2018 at the Rutgers Plant Science Research and Extension Farm in Adelphia, NJ....259

Table 6.4 Mean vegetative plant width (mm) for the I06 × A89 perennial ryegrass population and each parent genotype on 29 Jun 2017 and 11 Jun 2018 at the Rutgers Plant Science Research and Extension Farm in Adelphia, NJ. 260

Table 6.5 Mean total plant width (mm) for the I06 × A89 perennial ryegrass population and each parent genotype on 28 Jun 2017 and 13 Jun 2018 at the Rutgers Plant Science Research and Extension Farm in Adelphia, NJ. 260

Table 6.6 Analysis of variance for mean growth habit of the I06 × A89 perennial ryegrass mapping population on 27 Jun 2017 and 11 Jun 2018 at the Rutgers Plant Science Research and Extension Farm in Adelphia, NJ. 261

Table 6.7 Analysis of variance for mean seedhead angle (degree) of the I06 × A89 perennial ryegrass mapping population on 29 Jun 2017 and 12 Jun 2018 at the Rutgers Plant Science Research and Extension Farm in Adelphia, NJ. 261

Table 6.8 Analysis of variance for mean plant height (mm) of the I06 × A89 perennial ryegrass mapping population on 27 Jun 2017 and 13 Jun 2018 at the Rutgers Plant Science Research and Extension Farm in Adelphia, NJ. 262

Table 6.9 Analysis of variance for mean vegetative plant width (mm) of the I06 × A89 perennial ryegrass mapping population on 29 Jun 2017 and 11 Jun 2018 at the Rutgers Plant Science Research and Extension Farm in Adelphia, NJ. 262

Table 6.10 Analysis of variance for mean total plant width (mm) of the I06 × A89 perennial ryegrass mapping population on 28 Jun 2017 and 13 Jun 2018 at the Rutgers Plant Science Research and Extension Farm in Adelphia, NJ. 263

Table 6.11 Summary of the twenty-one quantitative trait loci (QTL) identified for morphological traits across six linkage groups of the I06 parent map. A multiple QTL model mapping analysis was conducted with phenotypic data for growth habit, seedhead angle, plant height, vegetative plant width, and total plant width during 2017 and 2018 at the Rutgers Plant Science Research and Extension Farm in Adelphia, NJ. 264

Table 6.12 Summary of the seven quantitative trait loci (QTL) identified for morphological traits across four linkage groups of the A89 parent map. A multiple QTL model mapping analysis was conducted with phenotypic data for growth habit, seedhead angle, plant height, vegetative plant width, and total plant width during 2017 and 2018 at the Rutgers Plant Science Research and Extension Farm in Adelphia, NJ. 266

Table A.1 Library set, sample name, barcode identifier, total read number, and retained read number for parent and progeny genotypes of the I06 × A89 perennial ryegrass mapping population. 290

Table A.2 Characteristics for the set of framework SSR markers used for genetic linkage mapping of the I06 × A89 perennial ryegrass mapping population. 297

LIST OF FIGURES

Figure 2.1 Application of saline irrigation water to perennial ryegrass clones using an overhead irrigation technique. 117

Figure 2.2 Phenotypes of perennial ryegrass genotypes 15-8325 (left) and 15-8343 (right) maintained in a field nursery. Genotype 15-8325 represents a prostrate growth habit and light green leaf color morphology. Genotype 15-8343 represents an upright growth habit and dark green color morphology. 117

Figure 2.3 Isolated biparental cross between perennial ryegrass genotypes 15-8325 (left) and 15-8343 (right). 118

Figure 3.1 High-quality sequencing read numbers for the parents and progeny of the I06 × A89 perennial ryegrass mapping population. The first and second bars of the x-axis represent parent I06 and parent A89, respectively. The remaining bars represent the 118 progeny. The y-axis indicates the number of retained reads after quality filtering. 144

Figure 3.2 Number of single nucleotide polymorphisms generated by next-generation sequencing-based genotyping at missing data thresholds ranging from 0 percent to 20 percent. 145

Figure 3.3 Linkage group 1 of a SNP-based genetic linkage map for perennial ryegrass, constructed using the I06 × A89 pseudo-F_2 mapping population. Homeologous linkage groups are presented for parent I06 (left bar) and A89 (right bar). The I06 map includes 184 SNPs and 5 SSRs. The A89 map includes 148 SNPs and 6 SSRs. Marker names are provided to the right of each group; SNPs are in black font and SSRs are in red font. The centiMorgan map distance is provided to the left of each group. 146

Figure 3.4 Linkage group 2 of a SNP-based genetic linkage map for perennial ryegrass, constructed using the I06 × A89 pseudo-F_2 mapping population. Homeologous linkage groups are presented for parent I06 (left bar) and A89 (right bar). The I06 map includes 161 SNPs and 7 SSRs. The A89 map includes 55 SNPs and 6 SSRs. Marker names are provided to the right of each group; SNPs are in black font and SSRs are in red font. The centiMorgan map distance is provided to the left of each group. 147

Figure 3.5 Linkage group 3 of a SNP-based genetic linkage map for perennial ryegrass, constructed using the I06 × A89 pseudo-F_2 mapping population. Homeologous linkage groups are presented for parent I06 (left bar) and A89 (right bar). The I06 map includes 114 SNPs and 7 SSRs. The A89 map includes 85 SNPs and 3 SSRs. Marker names are provided to the right of each group; SNPs are in black font and SSRs are in red font. The centiMorgan map distance is provided to the left of each group.....148

Figure 3.6 Linkage group 4 of a SNP-based genetic linkage map for perennial ryegrass, constructed using the I06 × A89 pseudo-F_2 mapping population. Homeologous linkage groups are presented for parent I06 (left bar) and A89 (right bar). The I06 map includes 102 SNPs and 7 SSRs. The A89 map includes 140 SNPs and 3 SSRs. Marker names are provided to the right of each group; SNPs are in black font and SSRs are in red font. The centiMorgan map distance is provided to the left of each group.....149

Figure 3.7 Linkage group 5 of a SNP-based genetic linkage map for perennial ryegrass, constructed using the I06 × A89 pseudo-F_2 mapping population. Homeologous linkage groups are presented for parent I06 (left bar) and A89 (right bar). The I06 map includes 79 SNPs and 6 SSRs. The A89 map includes 100 SNPs and 5 SSRs. Marker names are provided to the right of each group; SNPs are in black font and SSRs are in red font. The centiMorgan map distance is provided to the left of each group.....150

Figure 3.8 Linkage group 6 of a SNP-based genetic linkage map for perennial ryegrass, constructed using the I06 × A89 pseudo-F_2 mapping population. Homeologous linkage groups are presented for parent I06 (left bar) and A89 (right bar). The I06 map includes 106 SNPs and 6 SSRs. The A89 map includes 106 SNPs and 5 SSRs. Marker names are provided to the right of each group; SNPs are in black font and SSRs are in red font. The centiMorgan map distance is provided to the left of each group.....151

Figure 3.9 Linkage group 7 of a SNP-based genetic linkage map for perennial ryegrass, constructed using the I06 × A89 pseudo-F_2 mapping population. Homeologous linkage groups are presented for parent I06 (left bar) and A89 (right bar). The I06 map includes 107 SNPs and 9 SSRs. The A89 map includes 135 SNPs and 7 SSRs. Marker names are provided to the right of each group; SNPs are in black font and SSRs are in red font. The centiMorgan map distance is provided to the left of each group. 152

Figure 4.1 Linear regression analysis between visual ratings and pixel analysis for salinity stress response of turfgrass plants on a loamy sand soil after salinity stress periods of 2017 at the Rutgers Plant Science Research and Extension Farm in Adelphia, NJ. 187

Figure 4.2 Linear regression analysis between visual ratings and pixel analysis for salinity stress response of turfgrass plants on a sandy loam soil after salinity stress periods of 2017 at the Rutgers Plant Science Research and Extension Farm in Adelphia, NJ. 188

Figure 4.3 Linear regression analysis between visual ratings and pixel analysis for salinity stress response of turfgrass plants on a sandy loam soil after salinity stress periods of 2018 at the Rutgers Plant Science Research and Extension Farm in Adelphia, NJ. 189

Figure 4.4 Linear regression analysis between visual ratings and pixel analysis for salinity stress response of turfgrass plants on a loamy sand soil and a sandy loam soil after salinity stress periods of 2017 and on a sandy loam soil after salinity stress periods of 2018 at the Rutgers Plant Science Research and Extension Farm in Adelphia, NJ. 190

Figure 4.5 Frequency distribution for mean green visual rating for the I06 × A89 perennial ryegrass mapping population on a loamy sand soil after salinity stress periods of 2017 at the Rutgers Plant Science Research and Extension Farm in Adelphia, NJ. The Visual rating scale ranged from 0 to 10, where 0 represented approximately 0% green cover and 10 represented approximately 100% green cover. 191

Figure 4.6 Frequency distribution for mean green visual rating for the I06 × A89 perennial ryegrass mapping population on a sandy loam soil after salinity stress periods of 2017 at the Rutgers Plant Science Research and Extension Farm in Adelphia, NJ. The Visual rating scale ranged from 0 to 10, where 0 represented approximately 0% green cover and 10 represented approximately 100% green cover. 192

Figure 4.7 Frequency distribution for mean green visual rating for the I06 × A89 perennial ryegrass mapping population on a sandy loam soil after salinity stress periods of 2018 at the Rutgers Plant Science Research and Extension Farm in Adelphia, NJ. The Visual rating scale ranged from 0 to 10, where 0 represented approximately 0% green cover and 10 represented approximately 100% green cover. 193

Figure 4.8 Frequency distribution for mean green visual rating for the I06 × A89 perennial ryegrass mapping population on a loamy sand soil and a sandy loam soil after salinity stress periods of 2017 and on a sandy loam soil after salinity stress periods of 2018 at the Rutgers Plant Science Research and Extension Farm in Adelphia, NJ. The Visual rating scale ranged from 0 to 10, where 0 represented approximately 0% green cover and 10 represented approximately 100% green cover. 194

Figure 4.9 Frequency distribution for mean percent green as determined via pixel analysis for the I06 × A89 perennial ryegrass mapping population on a loamy sand soil after salinity stress periods of 2017 at the Rutgers Plant Science Research and Extension Farm in Adelphia, NJ. 195

Figure 4.10 Frequency distribution for mean percent green as determined via pixel analysis for the I06 × A89 perennial ryegrass mapping population on a sandy loam soil after salinity stress periods of 2017 at the Rutgers Plant Science Research and Extension Farm in Adelphia, NJ. 196

Figure 4.11 Frequency distribution for mean percent green as determined via pixel analysis for the I06 × A89 perennial ryegrass mapping population on a sandy loam soil after salinity stress periods of 2018 at the Rutgers Plant Science Research and Extension Farm in Adelphia, NJ. 197

Figure 4.12 Frequency distribution for mean percent green as determined via pixel analysis for the I06 × A89 perennial ryegrass mapping population on a loamy sand soil and a sandy loam soil after salinity stress periods of 2017 and on a sandy loam soil after salinity stress periods of 2018 at the Rutgers Plant Science Research and Extension Farm in Adelphia, NJ. 198

Figure 4.13 Summary of the quantitative trait loci (QTL) identified for salinity tolerance on the I06 parent map. A multiple QTL model mapping analysis was conducted with phenotypic data for salinity tolerance generated from visual ratings and pixel analysis of field trials during 2017 on a loamy sand soil (2017LS) and a sandy loam soil (2017SL) and during 2018 on a sandy loam soil (2018SL) at the Rutgers Plant Science Research and Extension Farm in Adelphia, NJ. The genetic map distance (cM) is provided to the left, and linkage group (LG) numbers are indicated at the top of each linkage group. 199

Figure 4.14 Summary of the quantitative trait loci (QTL) identified for salinity tolerance on the A89 parent map. A multiple QTL model mapping analysis was conducted with phenotypic data for salinity tolerance generated from visual ratings and pixel analysis of field trials during 2017 on a loamy sand soil (2017LS) and a sandy loam soil (2017SL) and during 2018 on a sandy loam soil (2018SL) at the Rutgers Plant Science Research and Extension Farm in Adelphia, NJ. The genetic map distance (cM) is provided to the left, and linkage group (LG) numbers are indicated at the top of each linkage group. 200

Figure 5.1 Dollar spot susceptible parent I06 (left) and dollar spot resistant parent A89 (right) under high dollar spot disease pressure during 2017 at the Rutgers Horticultural Research Farm II in North Brunswick, NJ. 228

Figure 5.2 Linear regression analysis between visual ratings and pixel analysis for dollar spot severity on 23 Aug 2017 at the Rutgers Plan Biology Research and Extension Farm in North Brunswick, NJ. 229

Figure 5.3 Linear regression analysis between visual ratings and pixel analysis for dollar spot severity on 28 Aug 2018 at the Rutgers Plan Biology Research and Extension Farm in North Brunswick, NJ. 230

Figure 5.4 Linear regression analysis between visual ratings and pixel analysis for dollar spot severity on 23 Aug 2017 and 28 Aug 2018 at the Rutgers Plan Biology Research and Extension Farm in North Brunswick, NJ. 231

Figure 5.5 Frequency distribution for mean dollar spot severity (percent diseased area) as determined via visual ratings for the I06 × A89 perennial ryegrass mapping population on 23 Aug 2017 at the Rutgers Plan Biology Research and Extension Farm in North Brunswick, NJ. Dollar spot severity was estimated using a visual rating scale where 0 represented approximately 0% diseased leaf tissue and 10 represented approximately 100% diseased leaf tissue. 232

Figure 5.6 Frequency distribution for mean dollar spot severity (percent diseased area) as determined via visual ratings for the I06 × A89 perennial ryegrass mapping population on 28 Aug 2018 at the Rutgers Plan Biology Research and Extension Farm in North Brunswick, NJ. Dollar spot severity was estimated using a visual rating scale where 0 represented approximately 0% diseased leaf tissue and 10 represented approximately 100% diseased leaf tissue. 233

Figure 5.7 Frequency distribution for mean dollar spot severity (percent diseased area) as determined via visual ratings for the I06 × A89 perennial ryegrass mapping population on 23 Aug 2017 and 28 Aug 2018 at the Rutgers Plan Biology Research and Extension Farm in North Brunswick, NJ. Dollar spot severity was estimated using a visual rating scale where 0 represented approximately 0% diseased leaf tissue and 10 represented approximately 100% diseased leaf tissue. 234

Figure 5.8 Frequency distribution for mean dollar spot severity (percent non-green area) as determined via pixel analysis for the I06 × A89 perennial ryegrass mapping population on 23 Aug 2017 at the Rutgers Plan Biology Research and Extension Farm in North Brunswick, NJ. 235

Figure 5.9 Frequency distribution for mean dollar spot severity (percent non-green area) as determined via pixel analysis for the I06 × A89 perennial ryegrass mapping population on 28 Aug 2018 at the Rutgers Plan Biology Research and Extension Farm in North Brunswick, NJ. 236

Figure 5.10 Frequency distribution for mean dollar spot severity (percent non-green area) as determined via pixel analysis for the I06 × A89 perennial ryegrass mapping population on 23 Aug 2017 and 28 Aug 2018 at the Rutgers Plan Biology Research and Extension Farm in North Brunswick, NJ. 237

Figure 5.11 Summary of the quantitative trait loci (QTL) identified for dollar spot resistance on the I06 parent map. A multiple QTL model mapping analysis was conducted with phenotypic data for dollar spot severity generated from visual ratings and pixel analysis of a field trial on 23 Aug 2017 and 28 Aug 2018 at the Rutgers Plant Science Research and Extension Farm in Adelphia, NJ. The genetic map distance (cM) is provided to the left, and linkage group (LG) numbers are indicated at the top of each individual linkage group.....238

Figure 5.12 Summary of the quantitative trait loci (QTL) identified for dollar spot resistance on the A89 parent map. A multiple QTL model mapping analysis was conducted with phenotypic data for dollar spot severity generated from visual ratings and pixel analysis of a field trial on 23 Aug 2017 and 28 Aug 2018 at the Rutgers Plant Science Research and Extension Farm in Adelphia, NJ. The genetic map distance (cM) is provided to the left, and linkage group (LG) numbers are indicated at the top of each individual linkage group.....239

Figure 6.1 Measurement of seedhead angle for individuals of the I06 × A89 perennial ryegrass mapping population.....267

Figure 6.2 Frequency distribution for mean growth habit of the I06 × A89 perennial ryegrass mapping population on 27 Jun 2017 at the Rutgers Plant Science Research and Extension Farm in Adelphia, NJ. Growth habit was assessed for each plant using a visual rating scale that ranged from 1 to 9, where 1 represented an extremely prostrate growth habit and 9 represented an extremely upright growth habit. 268

Figure 6.3 Frequency distribution for mean growth habit of the I06 × A89 perennial ryegrass mapping population on 11 Jun 2018 at the Rutgers Plant Science Research and Extension Farm in Adelphia, NJ. Growth habit was assessed for each plant using a visual rating scale that ranged from 1 to 9, where 1 represented an extremely prostrate growth habit and 9 represented an extremely upright growth habit. 269

Figure 6.4 Frequency distribution for mean growth habit of the I06 × A89 perennial ryegrass mapping population on 27 Jun 2017 and 11 Jun 2018 at the Rutgers Plant Science Research and Extension Farm in Adelphia, NJ. Growth habit was assessed for each plant using a visual rating scale that ranged from 1 to 9, where 1 represented an extremely prostrate growth habit and 9 represented an extremely upright growth habit. 270

Figure 6.5 Frequency distribution for mean seedhead angle (degree) of the I06 × A89 perennial ryegrass mapping population on 29 Jun 2017 at the Rutgers Plant Science Research and Extension Farm in Adelphia, NJ. Seedhead angle was assessed for each plant using a protractor to measure the average seedhead angle from the ground level. 271

Figure 6.6 Frequency distribution for mean seedhead angle (degree) of the I06 × A89 perennial ryegrass mapping population on 12 Jun 2018 at the Rutgers Plant Science Research and Extension Farm in Adelphia, NJ. Seedhead angle was assessed for each plant using a protractor to measure the average seedhead angle from the ground level. 272

Figure 6.7 Frequency distribution for mean seedhead angle (degree) of the I06 × A89 perennial ryegrass mapping population on 29 Jun 2017 and 12 Jun 2018 at the Rutgers Plant Science Research and Extension Farm in Adelphia, NJ. Seedhead angle was assessed for each plant using a protractor to measure the average seedhead angle from the ground level. 273

Figure 6.8 Frequency distribution for mean plant height (mm) of the I06 × A89 perennial ryegrass mapping population on 27 Jun 2017 at the Rutgers Plant Science Research and Extension Farm in Adelphia, NJ. Plant height was assessed for each plant by measuring the maximum distance (mm) from the base of the plant to the top of the foliar leaf tissue. 274

Figure 6.9 Frequency distribution for mean plant height (mm) of the I06 × A89 perennial ryegrass mapping population on 13 Jun 2018 at the Rutgers Plant Science Research and Extension Farm in Adelphia, NJ. Plant height was assessed for each plant by measuring the maximum distance (mm) from the base of the plant to the top of the foliar leaf tissue. 275

Figure 6.10 Frequency distribution for mean plant height (mm) of the I06 × A89 perennial ryegrass mapping population on 27 Jun 2017 and 13 Jun 2018 at the Rutgers Plant Science Research and Extension Farm in Adelphia, NJ. Plant height was assessed for each plant by measuring the maximum distance (mm) from the base of the plant to the top of the foliar leaf tissue. 276

Figure 6.11 Frequency distribution for mean vegetative plant width (mm) of the I06 × A89 perennial ryegrass mapping population on 29 Jun 2017 at the Rutgers Plant Science Research and Extension Farm in Adelphia, NJ. Vegetative plant width was assessed for each plant by measuring the maximum distance (mm) from one side of the plant foliar leaf tissue to the other.....277

Figure 6.12 Frequency distribution for mean vegetative plant width (mm) of the I06 × A89 perennial ryegrass mapping population on 11 Jun 2018 at the Rutgers Plant Science Research and Extension Farm in Adelphia, NJ. Vegetative plant width was assessed for each plant by measuring the maximum distance (mm) from one side of the plant foliar leaf tissue to the other.....278

Figure 6.13 Frequency distribution for mean vegetative plant width (mm) of the I06 × A89 perennial ryegrass mapping population on 29 Jun 2017 and 11 Jun 2018 at the Rutgers Plant Science Research and Extension Farm in Adelphia, NJ. Vegetative plant width was assessed for each plant by measuring the maximum distance (mm) from one side of the plant foliar leaf tissue to the other.....279

Figure 6.14 Frequency distribution for mean total plant width (mm) of the I06 × A89 perennial ryegrass mapping population on 28 Jun 2017 at the Rutgers Plant Science Research and Extension Farm in Adelphia, NJ. Total plant width was assessed for each plant by measuring the maximum distance (mm) from one side of the plant seedheads to the other. 280

Figure 6.15 Frequency distribution for mean total plant width (mm) of the I06 × A89 perennial ryegrass mapping population on 13 Jun 2018 at the Rutgers Plant Science Research and Extension Farm in Adelphia, NJ. Total plant width was assessed for each plant by measuring the maximum distance (mm) from one side of the plant seedheads to the other. 281

Figure 6.16 Frequency distribution for mean total plant width (mm) of the I06 × A89 perennial ryegrass mapping population on 28 Jun 2017 and 13 Jun 2018 at the Rutgers Plant Science Research and Extension Farm in Adelphia, NJ. Total plant width was assessed for each plant by measuring the maximum distance (mm) from one side of the plant seedheads to the other. 282

Figure 6.17 Summary of the quantitative trait loci (QTL) identified for morphological traits on the I06 parent map. A multiple QTL model mapping analysis was conducted with phenotypic data for growth habit, seedhead angle, plant height, vegetative plant width, and total plant width during 2017 and 2018 at the Rutgers Plant Science Research and Extension Farm in Adelphia, NJ. The genetic map distance (cM) is provided to the left, and linkage group (LG) numbers are indicated at the top of each individual linkage group.....283

Figure 6.18 Summary of the quantitative trait loci (QTL) identified for morphological traits on the A89 parent map. A multiple QTL model mapping analysis was conducted with phenotypic data for growth habit, seedhead angle, plant height, vegetative plant width, and total plant width during 2017 and 2018 at the Rutgers Plant Science Research and Extension Farm in Adelphia, NJ. The genetic map distance (cM) is provided to the left, and linkage group (LG) numbers are indicated at the top of each individual linkage group.....284

NOMENCLATURE

ACS	Automatic Cofactor Selection
AFLP	Amplified Fragment Length Polymorphism
AMP-PCR	Anchored Microsatellite Polymerase Chain Reaction
AP-PCR	Arbitrary Primed-Polymerase Chain Reaction
ASSR	Anchored Simple Sequence Repeat
CAPS	Cleaved Amplified Polymorphic Sequence
CCD	Charge Coupled Device
cDNA	Complementary Deoxyribonucleic Acid
CEC	Cation Exchange Capacity
CIM	Composite Interval Mapping
cM	centiMorgan
CNV	Copy Number Variation
cSNP	Copy Single Nucleotide Polymorphism
DArT	Diversity Array Technology
DH	Doubled-Haploid
dS	Decisiemens
EC	Electrical Conductivity
ECe	Electrical Conductivity of a Saturated Soil Extract
eSNP	Electronic Single Nucleotide Polymorphism
ESP	Exchangeable Sodium Percentage
eSSR	Expressed Simple Sequence Repeat
EST	Expressed Sequence Tag

GBS	Genotyping-by-Sequencing
gSSR	Genomic Simple Sequence Repeat
GWAS	Genome-Wide Association Study
IM	Interval Mapping
InDels	Insertions and Deletions
ISA	Inter-Simple Sequence Repeat Amplification
isSNP	In Silico Single Nucleotide Polymorphism
ISSR	Inter-Simple Sequence Repeat
LOD	Logarithm of Odds
MCMC	Markov chain Monte Carlo
MIM	Multiple Interval Mapping
ML	Maximum Likelihood
MP-PCR	Microsatellite-Primed Polymerase Chain Reaction
MQM	Multiple QTL Model
ncSNP	Noncoding Single Nucleotide Polymorphism
NGS	Next-Generation Sequencing
NJAES	New Jersey Agriculture Experiment Station
nsSNP	Nonsynonymous Single Nucleotide Polymorphism
NTEP	National Turfgrass Evaluation Program
ORF	Open Reading Frame
PCR	Polymerase Chain Reaction
pSNP	Promoter Single Nucleotide Polymorphism
QTL	Quantitative Trait Loci

RAD	Restriction-Site Associated DNA
RAD-seq	Restriction-Site Associated DNA Sequencing
RAPD	Random Amplified Polymorphic DNA
refSNP	Reference Single Nucleotide Polymorphism
RFLP	Restriction Fragment Length Polymorphism
RIL	Recombinant Inbred Line
rsID	Reference Single Nucleotide Polymorphism Identifier
SAR	Sodium Adsorption Ratio
SCAR	Sequence-Characterized Amplified Region
SIM	Simple Interval Mapping
SMA	Single-Marker Analysis
SNP	Single Nucleotide Polymorphism
SOLiD	Sequencing by Oligonucleotide Ligation Detection
SPAR	Single Primer Amplification Reaction
SRAP	Sequence-Related Amplified Polymorphism
SSCP	Single-Strand Conformation Polymorphism
SSR	Simple Sequence Repeat
STS	Sequence-Tagged Sites
TDS	Total Dissolved Salts
TRAP	Target Region Amplified Polymorphism

CHAPTER I

LITERATURE REVIEW

This dissertation addresses molecular breeding tools for improving morphological traits, salt tolerance, and dollar spot resistance in perennial ryegrass. Accordingly, the literature review is divided into four sections. The first section introduces the adaptation and use, phytomorphology, reproduction, and conventional breeding methods, achievements, and objectives for perennial ryegrass. The second and third sections provide an overview of salt-induced stress and dollar spot disease, respectively, and summarize research efforts of each, with respect to perennial ryegrass and other turfgrass species. The fourth section provides a broad background of molecular biology methods for plant breeding including DNA sequencing technologies, descriptions of genetic markers, an overview of genotyping-by-sequencing, and QTL identification and mapping.

Perennial ryegrass

Adaptation and use

Perennial ryegrass (*Lolium perenne* L.) is a cool-season grass native to temperate regions of Asia, North Africa, and Europe (Beard, 1973; Terrell, 1968). The species is taxonomically classified in the plant Family Poaceae, Subfamily Pooideae, and Tribe Poeae (Beard and Beard, 2005; Thorogood, 2003). In early years, man heavily disseminated perennial ryegrass for crop use (Jenkin, 1936). This complicated the determination of perennial ryegrass distribution patterns from its origin to current locales (Jenkin, 1936). Records indicate that perennial ryegrass was used for pasture grass in Britain as early as the seventeenth century (Funk and Clarke, 1989; Plot, 1677). Currently, the species has been introduced to all parts of the world and, with the exception of Antarctica, is grown on every continent (Thorogood, 2003).

Perennial ryegrass grows in alkaline and acidic soils with a pH range of 5.1 to 8.4, but it thrives in moist, well-drained soils at a pH near 6.5 (Beard, 1973; Funk and Clarke, 1989; Thorogood, 2003). The grass exhibits optimal growth between air temperatures of 20 and 25°C and requires a minimum of 46 to 63 cm of rainfall, or equivalent irrigation, annually (Beard, 1973; Funk and Clarke, 1989; Thorogood, 2003). The species is tolerant of various mowing heights, has good wear tolerance, and produces little thatch (Beard, 1973; Beard and Beard, 2005). However, the grass is only moderately resistant to heat, cold, drought, salt, and sulfur dioxide stresses (Beard and Beard, 2005).

Furthermore, perennial ryegrass is poorly adapted to shaded conditions and has a high evapotranspiration rate (Beard and Beard, 2005).

This species is an important forage and turfgrass crop, grown throughout much of the temperate world (Funk and Clarke, 1989; Thorogood, 2003). In mild climates, perennial ryegrass is managed as a turfgrass in parks, golf fairways and roughs, athletic fields, racetracks, and general landscaping areas (Beard, 1973; Beard and Beard, 2005; Thorogood, 2003). In lower latitudes, the species is used to overseed warm-season turf during periods of winter dormancy (Beard and Beard, 2005; Thorogood, 2003; Turgeon, 2008). Additionally, perennial ryegrass may be grown as low maintenance or utility turf in areas such as roadsides (Beard and Beard, 2005).

Phytomorphology

Perennial ryegrass is a medium to high density, bunch-type perennial, which has a low to high tillering rate and grows to a height of 10 to 90 cm (Beard, 1973; Beard and Beard, 2005; Thorogood, 2003; Turgeon, 2008). Stems are prostrate or erect, smooth, and contain 2 to 4 nodes (Beard, 1973; Beard and Beard, 2005; Thorogood, 2003). Leaves are medium- to fine-textured and mid- to dark-green (Beard and Beard, 2005; Thorogood, 2003; Turgeon, 2008). Leaf blades are 2 to 4 mm wide, pointed or blunted at the tip, smooth and waxy on the abaxial side, and rough and rigid on the adaxial side (Beard, 1973; Beard and Beard, 2005; Thorogood, 2003; Turgeon, 2008). Leaf sheaths are smooth, folded in the shoot, mid-green, and commonly have pinkish-red bases (Beard, 1973; Beard and Beard, 2005; Thorogood, 2003; Turgeon, 2008). Ligules are 1

to 2 mm long, membranous, and serrated at the tip and the collar is narrow (Beard, 1973; Beard and Beard, 2005; Thorogood, 2003; Turgeon, 2008).

The inflorescence of perennial ryegrass is a green to reddish colored spike that is 3 to 30 cm in length (Beard, 1973; Beard and Beard, 2005; Thorogood, 2003). Spikes contain 10 to 30 sessile spikelets that are flat, narrow, and alternately arranged on opposite sides of the central rachis (Beard, 1973; Beard and Beard, 2005; Thorogood, 2003). Spikelets consist of 4 to 14 alternating florets and are delimited by upper and lower glumes that measure 4 to 15 mm in length (Beard, 1973; Beard and Beard, 2005; Thorogood, 2003). Individual flowers are enclosed by lemma and palea, which are 3 to 9 mm long (Beard, 1973; Beard and Beard, 2005; Thorogood, 2003). The lemma are awnless, rounded, and contain 5 to 7 veins. As seed develops, the lemma and palea fuse with it to produce a caryopsis (Beard, 1973; Beard and Beard, 2005; Thorogood, 2003).

Reproduction

Perennial ryegrass is predominantly diploid ($2n = 2x = 14$) in nature; however tetraploid ($2n = 4x = 28$) specimens have been observed (Barker et al., 2001; Evans, 1926; Richardson et al., 2007; Wang, 2009). The ploidy levels of 194 perennial ryegrass accessions from the United States Department of Agriculture National Plant Germplasm System and six commercial perennial ryegrass cultivars were assessed via flow cytometry (Wang et al., 2009). Only six of the 200 total accessions and cultivars tested were tetraploid, while the remaining 194 were diploid (Wang et al., 2009). Another exception is colchicine-treated autotetraploid lines that have been developed for forage use (Thorogood, 2003).

The species can persist vegetatively for numerous years; however, seed is the primary mode of propagation (Beard, 1973; Thorogood, 2003). Perennial ryegrass is self-incompatible and dependent upon wind-pollination for outcrossing with neighboring plants (Beard, 1973; Bonos and Huff, 2013; Thorogood, 2003). Environmental conditions required for flower development include short, cool days with air temperatures less than 7°C, followed by increased photoperiods of 12 hours or more of light (Thorogood, 2003).

Single ovules are contained inside each floret (Thorogood, 2003). At the tips of the ovules, emerge two feathery stigmas, and three stamens protrude from the base (Thorogood, 2003). Upon maturation of florets, lodicules, located near the floret base, swell with cell sap and force the lemma and palea to open (Thorogood, 2003). Anthers, extended on long versatile filaments, emerge simultaneously with the stigmas, which protrude from either side of the floret, receptive to pollen (Thorogood, 2003). Lengthwise splitting of the anthers, from tip to base, releases clouds of pollen, which is wind-blown onto stigmas, initiating pollination (Thorogood, 2003). Anthesis occurs around midday and proliferates during bright, warm weather conditions (Thorogood, 2003). Flowering begins with older basal florets of the mid-spike spikelets, and progresses toward the basal and apical spikelets and the outermost floret (Thorogood, 2003).

The self-incompatible characteristic of perennial ryegrass is a result of a multiallelic, two-locus (SZ), gametophytic incompatibility system that is present in numerous grasses (Cornish et al., 1979; Cornish et al., 1980; Hayman, 1956; Lundqvist, 1956). At least 17 different S and Z alleles are documented in this system, inhibiting

inbreeding depression from self-seed setting (Bean and Yok-Hwa, 1972; Jenkin, 1931; Fearon et al., 1994). The relationship between the S and Z loci is complementary, meaning a pollen grain is compatible if it does not share both S and Z alleles with the stigmatic surface of the female plant; if both S and Z alleles are shared, the pollen grain is incompatible (Thorogood, 2003). Deposition of an incompatible pollen grain leads to inhibition of germination tube growth and formation of callus tissue in both germination tube cell wall and pollen grain (Thorogood, 2003).

Conventional breeding methods, achievements, and objectives

The allogomous, self-incompatible, and wind-pollinated characteristics of perennial ryegrass have made it an ideal species for recurrent phenotypic selection (Bonos and Huff, 2013; Bonos et al., 2006; Thorogood, 2003). This breeding method involves the selection of desirable phenotypes and subsequent interpollination, typically in isolation, of selected individuals (Poehlman and Sleper, 1995). Recurrent selection has been widely applied to perennial ryegrass breeding programs to produce composite cultivars with improved traits including increased disease resistance, more desirable growth habits, and enhanced aesthetic properties (Bonos and Huff, 2013; Bonos et al., 2006; Brilman, 2005; Thorogood, 2003).

The Rutgers University turfgrass breeding program at the New Jersey Agriculture Experiment Station (NJAES) is the largest breeding program for cool-season turfgrasses in the world (Honig, 2011). Thorogood (2003) referenced the NJAES-based program as the most effective perennial ryegrass breeding program in the U.S. The program was started in 1961 by Dr. C. Reed Funk, and ‘Manhattan’, a landmark perennial ryegrass

cultivar, was released a short time later, in 1967 (Funk et al., 1969; Funk and Meyer, 2001). By 2010, the turfgrass breeding program had flourished to release more than 400 turf cultivars (Honig, 2011).

For many years, the NJAES turfgrass breeding program was based on a relatively small sampling of the total perennial ryegrass germplasm worldwide (Thorogood, 2003). However, in 1996, turf breeders from the program began collecting diverse germplasm from various countries across Europe and Asia to diversify and improve the germplasm base of the species at the NJAES; an excess of 15,000 new germplasm sources had been collected as of 2010 (Bonos et al., 2004; Honig, 2011). Collected perennial ryegrass germplasm potentially harbors desirable traits, which, once identified, can be introduced into elite NJAES perennial ryegrass germplasm via population improvement techniques (Bonos et al., 2004).

Objectives for perennial ryegrass breeding programs are dependent upon intended applications and locations of usage (Thorogood, 2003). In general, breeders select for improvements in turf appearance and growth habit, increased disease resistance, higher grain yields, and enhanced tolerance to abiotic and environmental stresses (Bonos and Huff, 2013; Thorogood, 2003). Since 1982, perennial ryegrasses have been evaluated by the National Turfgrass Evaluation Program (NTEP), a non-profit, self-supporting program, sponsored by the National Turfgrass Federation, Inc. and the Beltsville Agricultural Research Center (Morris, 1996; Thorogood, 2003). The usefulness of the NTEP is the ability to test a given cultivar across a large geographical location; this offers information for range of adaptability for turfgrass breeders (Morris, 1996). Additionally, both standard and elite cultivars are included in NTEP evaluation studies, providing

instant feedback of how a given cultivar performs compared to those individuals (Morris, 1996).

Perennial ryegrass is affected by numerous fungal and Oomycete diseases (Bonos and Huff, 2013; Bonos et al., 2006; Thorogood, 2003). To date, disease-related breeding efforts of perennial ryegrass have primarily been directed toward improving gray leaf spot (*Pyricularia oryzae* Cavara), stem rust (*Puccinia graminis* subsp. *graminicola* Z. Urb.), and crown rust (*Puccinia coronata* Corda) resistance (Bonos and Huff, 2013; Bonos et al., 2006). The dollar spot (*Sclerotinia homoeocarpa* F.T. Bennet) disease, discussed in detail in a later section, is a commonly occurring foliar disease of perennial ryegrass, and is a primary focus of this dissertation. Additional diseases affecting perennial ryegrass include anthracnose (*Colletotrichum cereale* Manns), brown patch (*Rhizoctonia solani* Kuhn), *Pythium* blight (*Pythium* spp.), and red thread (*Laetisaria fuciformis* McAlpine) (Bonos et al., 2006; Smiley et al., 2005).

Improvement of environmental and abiotic stress tolerances is another targeted objective for many turfgrass breeders (Bonos and Huff, 2013; Thorogood, 2003). Examples of such stress tolerances include drought tolerance, winter hardiness, wear tolerance, and salinity tolerance (Bonos and Huff, 2013; Thorogood, 2003). Much attention has been devoted to breeding for these traits, and improvements have been made, but such characters remain viable and necessary breeding improvement objectives for future directions of turfgrass breeding programs (Bonos and Huff, 2013; Thorogood, 2003). Salinity tolerance is another primary focus of this dissertation, and is discussed in the following section.

Salt-induced stress

Perspective and causation

Salt-affected soils span an excess of 320 million hectares of land, worldwide, with the largest affected land areas located in Africa, Asia, Australia, and South America (Brady and Weil, 2004; Carrow and Duncan, 1998, 2012). Such soils are characterized by excessive levels of exchangeable sodium ions and soluble salts, which are detrimental to the growth of many plant species (Carrow and Duncan, 1998, 2012). Salt-affected soils are naturally confined to arid and semiarid regions and low-lying landscapes; however, human involvement has expanded the development of salt-affected soils to additional regions and landscapes (Carrow and Duncan, 1998, 2012; Havlin et al., 2005).

Salts exist as soluble and insoluble mineral forms in soils. Soluble minerals include chloride chemicals such as calcium chloride and potassium chloride, sulfate compounds such as calcium sulfate and potassium sulfate, and bicarbonate compounds such as sodium carbonate and sodium hydrocarbonate (Carrow and Duncan, 1998, 2012). Soluble minerals dissolve into various salt ions in the soil solution and are problematic for plant growth (Carrow and Duncan, 1998, 2012). Insoluble minerals include compounds such as calcium carbonate and magnesium carbonate as well as soil minerals like apatites (Carrow and Duncan, 1998, 2012). Insoluble minerals, unlike soluble minerals, do not dissolve into the soil solution and are not problematic for plant growth (Carrow and Duncan, 1998, 2012).

The most common salt ions recovered from salt-affected soils include bicarbonate (HCO_3^-), calcium (Ca^{+2}), carbonate (CO_3^{-2}), chloride (Cl^-), magnesium (Mg^{+2}), nitrate (NO_3^-), potassium (K^+), sodium (Na^+), and sulfate (SO_4^{-2}) (Carrow and Duncan, 1998, 2012). In addition to dissolution of minerals, salt ions in soil solutions originate from fertilizers, soil amendments, rainwater, floodwater, salt water sprays, and irrigation water (Carrow and Duncan, 1998, 2012).

Soils of arid and semiarid regions that receive less than 380 mm of rainfall, annually, are most prone to being naturally salt-affected (Brady and Weil, 2004; Carrow and Duncan, 1998, 2012). These soils accrue salts from groundwater, rainwater, and weathering of minerals, and become salt-affected via insufficient leaching of accumulated salts (Brady and Weil, 2004; Carrow and Duncan, 1998, 2012; Havlin et al., 2005). Sodium and sulfate salts, including $NaSO_4$, $CaSO_4$, and $MgSO_4$, are the most common salt forms observed in soils of arid and semiarid climates (Carrow and Duncan, 1998, 2012).

Classification of salt-affected soils

Salt-affected soils are most widely classified as saline, sodic, and saline-sodic soils according to their total soluble salt concentrations and quantities of exchangeable sodium ions (Brady and Weil, 2004; Carrow and Duncan, 1998, 2012). Soil salinity, the total soluble salt concentration of a soil, is a relation of the salt-induced drought stress potential (Brady and Weil, 2004; Carrow and Duncan, 1998, 2012). Soil sodicity, the concentration of exchangeable sodium ions of a soil, is related to ion toxicity and soil

physical deterioration that results from the presence of sodium ions (Brady and Weil, 2004; Carrow and Duncan, 1998, 2012).

Soil salinity can be indirectly measured based on the electrical conductivity (EC) of a soil solution (Brady and Weil, 2004). Purified water acts as a poor electrical conductor, but as the concentration of salts dissolved in pure water increases, the EC increases as well (Brady and Weil, 2004; Carrow and Duncan, 1998). The EC of a saturated soil-water paste extract (ECe) is commonly used to measure the total soluble salt concentration in a soil (Bandyopadhyay et al., 2001; Brady and Weil, 2004; Carrow and Duncan, 1998, 2012). The ECe is a measurement of total salts present in a soil; it does not discern which salts are present (Carrow and Duncan, 1998, 2012). Soil ECe increases as total salt concentration increases (Brady and Weil, 2004; Carrow and Duncan, 1998). A soil ECe greater than 4 decisiemens (dS) m^{-1} is considered to be of high salinity or total soluble salts (Bandyopadhyay et al., 2001; Brady and Weil, 2004; Carrow and Duncan, 1998, 2012).

The simplest method, conceptually, to determine soil salinity is to measure the total dissolved solids (TDS) in a solution extracted from a soil sample (Brady and Weil, 2004). This method requires heat-mediated evaporation of water from a solution so that only dry residue remains (Brady and Weil, 2004). The dry residue is weighed and the TDS is presented as milligrams of solid residue per liter of water (mg L^{-1}) (Brady and Weil, 2004). The TDS of irrigation water ranges from 5 to 1,000 mg L^{-1}; whereas the TDS of a solution extracted from a soil sample may range from 500 to 12,000 mg L^{-1} (Brady and Weil, 2004).

Soil sodicity was initially measured as the exchangeable sodium percentage (ESP), which assesses saturation of soil exchange complexes with sodium ions (Bandyopadhyay et al., 2001; Brady and Weil, 2004; Carrow and Duncan, 1998, 2012). The ESP method remains favored by many labs and is calculated as:

$$\mathbf{ESP} = \frac{exchangeable\ sodium}{cation\ exchange\ capacity} \times \mathbf{100}$$

where the exchangeable sodium, expressed as cmol kg^{-1} or meq $100g^{-1}$, is the quantity of sodium ions on the cation exchange capacity (CEC) sites (Brady and Weil, 2004; Carrow and Duncan, 1998, 2012; Havlin et al., 2005). The CEC, also expressed as cmol kg^{-1}, is comprised of all exchangeable cations, such as Al^{+3}, Ca^{+2}, H^{+}, K^{+}, Mg^{+2}, and Na^{+}, on the CEC sites (Brady and Weil, 2004; Carrow and Duncan, 1998, 2012). The potential for soil structure deterioration increases as the percentage of sodium ions on the CEC increases (Carrow and Duncan, 1998, 2012). Severely deteriorated physical properties of soils and pH values greater than 8.5 are associated with ESP values above 15 (Brady and Weil, 2004).

An easier and more widely used method for determining soil sodicity is the sodium adsorption ratio (SAR) (Bandyopadhyay et al., 2001; Brady and Weil, 2004; Carrow and Duncan, 1998, 2012). The SAR is calculated as:

$$\mathbf{SAR} = \frac{[Na]}{\sqrt{(0.5[Ca] + 0.5[Mg]}}$$

where the sodium, calcium, and magnesium ion concentrations, determined in a saturation paste extract in $mmol_c\ L^{-1}$, in the soil solution are represented by [Na], [Ca], and [Mg], respectively (Bandyopadhyay et al., 2001; Brady and Weil, 2004; Carrow and Duncan, 1998, 2012; Havlin et al., 2005). The SAR increases as sodium ion concentration increases (Carrow and Duncan, 1998).

Many scientists prefer the SAR method to the ESP method because of the increased error potential associated with the ESP method (Carrow and Duncan, 1998, 2012). The SAR method considers the quantities of calcium and magnesium ions relative to sodium ions in the soil solution, while the ESP method only considers the sodium concentration as determined as the sodium present on the CEC sites (Carrow and Duncan, 1998, 2012). The previous statement implies that the calculation of ESP is dependent upon determination of CEC, which presents an issue because it is a pH dependent process (Carrow and Duncan, 1998, 2012). To exemplify, a CEC calculated at a different pH in the laboratory than the pH in the field would be misleading as some of the CEC sites are pH dependent (Carrow and Duncan, 1998). Another source of error is the reporting of non-CEC associated cations in salt affected soils, which may be dissolved into solution, as CEC (Carrow and Duncan, 1998, 2012). In lieu of the shortcomings of the ESP method, both SAR and ESP methods resolve closely related soil sodicity values over a broad range of sodium levels (Carrow and Duncan, 1998, 2012).

Saline soils

Soils that contain soluble salts at levels sufficient to adversely affect the growth of most plants, and also contain low levels of exchangeable sodium, are classified as saline soils (Brady and Weil, 2004; Carrow and Duncan, 1998; Havlin et al., 2005). These soils have ECe threshold values greater than 4 dS m^{-1} and ESP threshold values less than 15% in the saturation extract (Brady and Weil, 2004; Carrow and Duncan, 1998; Havlin et al., 2005; Leinauer and Devitt, 2013). However, plants that are salt-sensitive may be affected at levels lower than the ECe threshold values; likewise, plants that are salt-tolerant may not be affected at levels even slightly higher than the ECe threshold values (Carrow and Duncan, 1998). Because sodium levels are relatively low in saline soils, calcium and magnesium cations typically dominate the exchange sites (Brady and Weil, 2004). The pH of saline soils is normally between 7.0 and 8.5, but acidic pH can be observed on sandy sites (Brady and Weil, 2004; Carrow and Duncan, 1998; Havlin et al., 2005). As water evaporates from these soils, salts are deposited on the surface, resulting in a white crust appearance; this led to the original term 'white alkali' that was formerly used as the designation for saline soils (Brady and Weil, 2004; Carrow and Duncan, 1998; Havlin et al., 2005).

Physical properties, such as structure and permeability, of saline soils are not affected by the soluble salts; however, these soils are prone to water deficits, ion toxicities, and ion imbalances (Carrow and Duncan, 1998). Water deficits in saline soils occur because the salts attract soil water, thereby decreasing the amount of water in the soil available for uptake by the plants (Carrow and Duncan, 1998). The high soil osmotic potential exhibited by the salts causes physiological drought stress on the plants (Carrow

and Duncan, 1998). Ion toxicities can affect shoot and root tissues and are dependent upon the specific chemistry of irrigation water and soil salts (Carrow and Duncan, 1998). Toxicities can arise from B, HCO_3^-, and SO_4^-, but are most common from high levels of Cl^- (Carrow and Duncan, 1998). Ion imbalances are present in some saline soils and lead to deficiencies of Ca^{+2}, K^+, Mg^{+2}, Mn, NO_3^-, and P (Carrow and Duncan, 1998).

Field symptoms of soils and plants are associated with saline soils (Carrow and Duncan, 1998). As stated earlier, the most indicative symptoms of saline soils is the presence a white crust on the soil surface, which results from salt deposition during evaporation (Carrow and Duncan, 1998). Plants grown in saline soils most commonly exhibit symptoms of drought stress, independent of soil moisture levels (Carrow and Duncan, 1998). Drought symptoms include a bluish-green leaf color, leaf wilting, and, in severe instances, leaf firing (Carrow and Duncan, 1998). Wilt symptoms may become exacerbated by ion toxicities of roots, and roots may become blackened and deteriorated (Carrow and Duncan, 1998).

Sodic soils

Soils that contain high levels of exchangeable sodium ions (ESP greater than 15%), low levels of soluble salts (ECe less than 4 dS m^{-1}), and adversely affect soil structure and plant growth are referred to as sodic soils (Brady and Weil, 2004; Carrow and Duncan, 1998; Havlin et al., 2005). High levels of Na^+ and Na_2CO_3 on CEC sites are prone to hydrolysis, which increases OH^- ions and, subsequently, pH to levels greater than 8.5 and often in excess of 10.0 (Brady and Weil, 2004; Carrow and Duncan, 1998).

Organic matter becomes solubilized under high pH conditions and is deposited at the soil surface as water evaporates from the soil (Carrow and Duncan, 1998). This deposition of organic matter results in a dark surface appearance; for this reason, sodic soils were formerly referred to as 'black alkali' soils (Carrow and Duncan, 1998; Havlin et al., 2005).

Sodic soils most commonly result in issues of deteriorated soil structure, ion toxicities, and ion imbalances (Carrow and Duncan, 1998; Havlin et al., 2005). Soil structure issues arise as clay and organic matter colloids swell and disperse, soil structural units breakdown, and soil colloids plug pores via migration (Carrow and Duncan, 1998). A compromised soil structure is an extreme detriment to the movement of water in the soil (Carrow and Duncan, 1998). Ion toxicities in sodic soils are primarily derived from Na^{+} and Cl^{-}, but Al^{+3}, B, HCO_3^{-}, and OH^{-} can also accumulate to toxic levels (Carrow and Duncan, 1998). Sodic soils are most prone to imbalances of Ca^{+2}, K^{+}, and Mg^{+2} ions (Carrow and Duncan, 1998).

Sodic soils present visible field symptoms of both soil and plants materials (Carrow and Duncan, 1998). As mentioned previously, sodic soils affect soil permeability (Carrow and Duncan, 1998). This can be perceived as low oxygen levels in moist soils and decreased drainage, infiltration, or percolation rates of a given soil (Carrow and Duncan, 1998). Another indicator of sodic soils that was previously mentioned is the presence of a dark surface color, which results from solubilizing and deposition of organic matter at the surface of the soil (Carrow and Duncan, 1998). Further symptoms of sodic soils include a lack of colloid aggregation in moist soils and presence of cracking or clod formation in dry soils due to shrinkage (Carrow and Duncan,

1998). Plant symptoms include foliar toxicities and reduced root viability and growth (Carrow and Duncan, 1998). Roots grown in sodic soils are often discolored and thin due to Na^{+}, OH^{-}, or Al^{+3} toxicities and low oxygen levels (Carrow and Duncan, 1998). The lack of proper root function typically manifests as symptoms of drought stress in the plant (Carrow and Duncan, 1998). Toxicities of the leaves in sodic soils generally arise from heightened levels of Na^{+}, Cl^{-}, or B (Carrow and Duncan, 1998).

Saline-sodic soils

Soils that contain high levels of soluble salts (ECe greater than 4 dS m^{-1}) and high levels of exchangeable sodium ions (ESP greater than 15%) are referenced as saline-sodic soils (Brady and Weil, 2004; Carrow and Duncan, 1998; Havlin et al., 2005). The heightened levels of soluble salts adversely affect normal plant growth, but also interact with the excess exchangeable sodium ions in such a manner that the soil physical properties are not compromised (Brady and Weil, 2004; Carrow and Duncan, 1998). However, a saline-sodic soil can transform to a sodic soil in the instance that the soluble salts are leached through the soil profile by rainfall or irrigation water that is low in soluble salts (Brady and Weil, 2004; Carrow and Duncan, 1998; Havlin et al., 2005). This situation is prevented through Ca^{+2} supplementation when Na^{+} ions are displaced by leaching processes (Carrow and Duncan, 1998).

Saline-sodic soils present similar issues as saline soils, especially water deficits that result from high soil osmotic potential (Carrow and Duncan, 1998). As described previously, additional problems associated with sodic soil structural properties arise when

Na^+ ions are leached through the soil profile and not replaced with Ca^{+2} ions (Carrow and Duncan, 1998). Soils and plants will display various symptoms in the field depending upon whether saline or sodic conditions are most prevalent in the soil; nonetheless, the most commonly observed symptoms are those of saline soils (Carrow and Duncan, 1998).

Salt-associated issues in turfgrass systems

Historically, salt-affected turfgrass issues were confined to arid and semiarid regions that are characterized by low levels of precipitation and high levels of evaporation (Brady and Weil, 2004; Carrow and Duncan, 1998). However, human involvement has expanded salt-affected areas through events including the establishment of golf courses in environmentally conducive areas for salt issues, applications of deicing salts to sidewalks and roadways, and use of recycled water for irrigation (Carrow and Duncan, 1998; Leinauer and Devitt, 2013; Marcum, 2006; Steinke and Ervin, 2013). Many of these activities are not at all careless; in fact, most are responses to advance environmental stewardship of the turfgrass community.

Golf courses are often constructed in coastal regions, which are typically accompanied by swamps and marshes (Carrow and Duncan, 1998). Swamps and marshes contain high levels of Na^+ and Cl^- and, when drained, lead to salt-affected soils (Carrow and Duncan, 1998). Additional sources for salt issues in coastal regions include intrusion of salt water into irrigation aquifers, flooding, and saltwater sprays (Carrow and Duncan, 1998; Marcum, 2006). Moreover, these areas can have heightened water tables that contain water of poor quality (Carrow and Duncan, 1998). These factors increase the likelihood that a given soil will become affected by salt.

Deicing salts (NaCl) are often applied to paved surfaces from late autumn through early spring in areas that are subject to regular snow cover and freezing temperatures (Steinke and Ervin, 2013). As snow melts, deicing salts are distributed through runoff and are suggested to contaminate lakes, streams, and groundwater (Mason et al., 1999; Steinke and Ervin, 2013). The effects of deicing salts on turfgrass sites has increased in parallel with urban development and population size (Steinke and Ervin, 2013). Turfgrasses located adjacent to paved surfaces are prone to severe injury or death from deicing salts; this ultimately results in regrowth of other plant species or soil erosion issues (Steinke and Ervin, 2013). As mentioned, deicing salts contain Cl^- ions, which can accumulate in soil solutions and trigger nutrient imbalances via displacement of adsorbed cations such as Ca^{+2}, K^+, and Mg^{+2} (Howard and Beck, 1993; Shanley, 1994).

Municipal water, including surface water and ground water, which meets recommended standards, is primarily used for irrigation of turfgrass (Ayers and Westcot, 1985; Committee on Water Quality Criteria, 1972; Farnham et al., 1985; Lazoarova and Bahri, 2004; Pescod, 1992; Pettygrove and Asano, 1985; USEPA, 1992). However, numerous states in the U.S. have transitioned to the use of recycled water for turfgrass irrigation (Devitt et al., 2004; Leinauer and Devitt, 2013; Marcum, 2006). This transition has occurred voluntarily and involuntarily; in some instances the use of recycled water has been mandated or catalyzed by heightened water prices and drinking water shortages (Devit et al., 2004; Leinauer and Devitt, 2013; Marcum, 2006; Steinke and Ervin, 2013). Recycled water includes effluent, reused, and reclaimed water, and the nomenclature indicates that the water has been cycled through an industrial or residential usage and treated in accordance to state or federal standards for water quality (Harivandi, 2004).

Recycled water has approximately twice as much salt content as municipal water and contains heightened levels of ions such as Na^+, Cl^-, or B (Devitt et al., 2005; Leinauer and Devitt, 2013).

Recycled water is used for irrigation on an approximated 13% of all golf courses in the U.S.; an overwhelming 34% of the golf courses in the state of Florida rely upon recycled irrigation water (Cisar et al., 2006; National Golf Foundation, 1999). Steinke and Ervin (2013) suggest that the use of recycled water for golf course irrigation purposes will continue to increase as demands for human needs of fresh water continue to increase. It is important to indicate that no illnesses have been associated with the use of recycled water for turfgrass irrigation purposes (USEPA, 2004). The same is not true for plants, however. It is well understood that turfgrass health and productivity, as well as physical components of soil structure, are influenced by the quality of irrigation water (Bresler et al., 1982; USGA, 1994). Furthermore, concerns of plant stress and water quality may slow the acceptance of recycled water for irrigation purposes (Devitt et al., 2004). The aforementioned salt-associated issues, and consideration that potable water use will become increasingly more restricted, intensifies the importance of development and usage for salt-tolerant turfgrass species (Bonos and Huff, 2013; Koch and Bonos, 2010; Marcum, 2006).

Perennial ryegrass breeding efforts for salinity tolerance

Salinity tolerance is emphasized in current perennial ryegrass breeding programs and, in consideration of increasing salinity issues, will remain a primary focus (Bonos et al., 2009a; Bonos and Huff, 2013; Marcum, 2006). Regardless of the importance of

developing perennial ryegrass cultivars with improved salinity tolerance, the complex inheritance of this trait has slowed the progress (Bonos and Huff, 2013; Rose-Fricker and Wipff, 2001; Winicov, 1998). Salinity tolerance in turfgrass systems is influenced by a number of components including edaphic factors, environmental conditions, inheritance mechanisms, and morphological and physiological plant traits (Harivandi, 1988; Hoffman and Rawlins, 1977; Hughes et al., 1975; Koch et al., 2015; Flowers, 2004; Maas, 1986; Marcum, 2006; Neumann, 1997; Qian and Suplick, 2001; Shannon, 1984).

Koch et al. (2015) studied the inheritance of salinity tolerance in perennial ryegrass. Broad-sense heritability, estimated at 0.78, provided evidence that phenotypic variation of salinity tolerance in perennial ryegrass is based on genetics (Koch et al., 2015). Further analyses of narrow-sense heritability indicated additive gene action is responsible for salinity tolerance in perennial ryegrass (Koch et al., 2015). In addition to inheritance, plant growth stages, such as seedlings, juveniles, and mature plants, have been associated with differing salinity tolerances (Hughes et al., 1975; Neumann, 1997; Qian and Suplick, 2001). The variability of salinity tolerance among factors such as humidity, temperature, edaphic conditions, and the previously mentioned plant morphological and physiological characters have prompted researchers and breeders to explore a number of methods for salinity tolerance screening (Bauer et al., 2009; Bonos and Huff, 2013; Dudeck et al., 1993; Koch and Bonos, 2010; Koch and Bonos, 2011a; Lee et al., 2002; Marcum, 2001; Marcum, 2006; Marcum and Murdoch, 1990; Peabody, 2004; Peacock et al., 1993; Peel et al., 2004; Qian et al., 2000; Rose-Fricker and Wipff, 2001).

The earliest method for screening perennial ryegrass germplasm for salinity tolerance includes growing plants in a hydroponic salt water solution (Rose-Fricker and Wipff, 2001). This method is effective in identifying salt tolerant germplasm as it led to the development of 'Brightstar SLT', a perennial ryegrass cultivar with improved salinity tolerance (Rose-Fricker and Wipff, 2001). However, the hydroponic method does not provide salt stress to leaves, which readily occurs in routine irrigation practices by turf managers (Koch and Bonos, 2010; Qian et al., 2001; Rose-Fricker and Wipff, 2001). A greenhouse-based overhead irrigation protocol was developed by Koch and Bonos (2010) to screen for salinity tolerance in a fashion that better represented typical irrigation practices of routine management conditions. The overhead irrigation screening technique was further adapted to a field setting to screen a larger number of perennial ryegrass germplasm (Koch and Bonos, 2011a). Each of the three screening methods, the hydroponic salt water solution, the greenhouse-based overhead irrigation, and the field-based overhead irrigation, are sufficiently capable of screening germplasm for salinity tolerance (Koch and Bonos, 2011a).

Another issue faced by turfgrass breeders is the inconsistent use of measurement criteria and units in salinity tolerance research among breeding programs (Marcum, 2006). Examples of measurement criteria for salinity tolerance in turfgrass systems include plant survival (Ahti et al., 1980), root length and weight (Kik, 1989), shoot and leaf length (Horst and Beadle, 1984), shoot weight (Dudeck and Peacock, 1985; Hughes et al., 1975), shoot visual injury (Greub et al., 1985), and seed germination (Marcar, 1987). Koch and Bonos (2010) found that ratings for percent green leaf material were highly correlated with the more intensive ratings of shoot and root weights and clipping

yields. Therefore, percent green ratings could be used to predict the more intensive measurements for salinity tolerance (Koch and Bonos, 2010). Salinity measurement units used among turfgrass evaluation studies include conductivity, presented as mmho cm^{-1} or dS m^{-1}; total dissolved solids in milliequivalents per liter, presented as meq L^{-1}; and total dissolved solids on a weight basis, presented as ppm or mg L^{-1} (Marcum, 2006). Nonetheless, if a single entry is common between two studies, the relative salinity tolerance can be ascertained (Marcum, 2006).

Improving salinity tolerance in turfgrass cultivars would provide a means of maintaining high turf quality traits in turfgrasses grown at salt-affected sites and potentially increase the usage potential for recycled water (Koch and Bonos, 2011a). As mentioned previously, 'Brightstar SLT' was a salinity tolerant perennial ryegrass cultivar selected by hydroponic salt water screening methods (Rose-Fricker and Wipff, 2001). A study by Koch and Bonos (2011b) demonstrated the effectiveness of the overhead irrigation technique for identifying salt tolerant genotypes in a total of 23 perennial ryegrass experimental selections and cultivars. The cultivar, Gator 3, RKS (now named Rukus), and MSH Comp perennial ryegrasses had the greatest salinity tolerance, and the cultivar, Fiesta III, had the least salinity tolerance (Koch and Bonos, 2011b). The implementation of salinity tolerance screening methods in a recurrent selection breeding program will be a leading contributor to the development of turfgrass cultivars with increased concentrations of the additive salinity tolerance alleles (Koch and Bonos, 2011a; Koch et al., 2015).

Dollar spot disease

Dollar spot is a prevalent and tenacious foliar disease of many warm- and cool-season turfgrass species (Smiley et al., 2005; Watschke et al., 2013). The disease occurs throughout the world and is of great economic importance; more money is spent by U.S. golf courses to manage dollar spot than any other turfgrass disease (Smiley et al., 2005; Vargas, 1994). The name, dollar spot, references the characteristic quarter to silver dollar sized spots the disease causes in the turf canopy (Vargas, 1994).

Symptoms and signs

Symptoms of dollar spot disease vary depending on the height at which a given turf is managed (Couch, 2000). Taller turfs, such as those found in residential lawns, typically exhibit 1.9-15.2 cm diameter irregularly shaped, bleached patches (Smiley et al., 2005; Vargas, 1994). As disease development progresses, patches may expand and coalesce, resulting in large areas of blighted turf (Smiley et al., 2005; Vargas, 1994). Symptoms on golf greens and other shorter turfs include sunken patches of blighted grass (Couch, 2000; Smiley et al., 2005; Tani and Beard, 1997). Patches are generally circular and between 1.2 and 5.0 cm in diameter; however, greater zones of infection can occur as individual patches coalesce (Couch, 2000; Smiley et al., 2005; Tani and Beard, 1997). A grayish to white, cobwebby or cottony growth of mycelium may be visible on affected turf when the pathogen is active and dew is present on the blades of grass (Couch, 2000;

Smiley et al., 2005; Tani and Beard, 1997). As leaves dry, the mycelium becomes less apparent (Smiley et al., 2005).

Dollar spot infection causes lesion development on leaves of affected turfgrass plants (Couch, 2000; Smiley et al., 2005; Tani and Beard, 1997). Leaf lesions initiate as chlorosis, progress to a water-soaked appearance, and ultimately transition to a straw or bleached white color (Couch, 2000; Smiley et al., 2005; Tani and Beard, 1997). A single leaf blade may have one lesion, have many lesions, or may be entirely blighted (Couch, 2000; Smiley et al., 2005; Tani and Beard, 1997). Individual lesions may span across an entire leaf blade, are delimited by characteristic reddish brown to tan margins, and frequently appear in the shape of an hourglass (Couch, 2000; Smiley et al., 2005; Tani and Beard, 1997). On some grass species, leaf lesions are oval or oblong with brown borders (Smiley et al., 2005). Foliar symptoms of dollar spot may not be readily distinguishable from other turfgrass diseases such as brown patch, red thread, *Pythium* blight, and *Nigrospora* blight caused by *Nigrospora sphaerica* (Sacc.) E. Mason (Smiley et al., 2005)

Causal organism

Taxonomic classification of the causal fungus of dollar spot has been unclear since the disease was first described (Couch, 1995; Smiley et al., 2005). In the 1920s, the fungus was thought to be a species of *Rhizoctonia*, and the disease was called small brown patch to distinguish it from large brown patch, which is incited by *Rhizoctonia solani* (Monteith and Dahl, 1932). During the 1930s, an extensive study of isolates from the U.S., Britain, and Australia concluded that the fungus belonged to the genus

Sclerotinia (Bennett, 1937). The specific epithet, *homoeocarpa*, was assigned to the fungus because of its unusual conidial state (Bennett, 1937). Later, culture-based studies of *Sclerotinia homoeocarpa* isolates from North America designed to induce the teleomorph (ascocarp) were unsuccessful. Apothecial initials and aborted apothecia were observed, but ascospores and conidia were not identified (Fenstermacher, 1970, 1980).

Morphological examinations, immunological and biochemical studies of stromatal proteins, and sequenced DNA have disputed the taxonomical designation of this organism and suggested this fungus was incorrectly placed in the genus *Sclerotinia* (Jackson, 1973; Kohn, 1979; Kohn and Greenville, 1989; Novak and Kohn, 1991). Members of *Sclerotinia* are characterized by tuber-like sclerotia production; however, the fungus that causes dollar spot produces a flat stroma, thereby eliminating it from the genus *Sclerotinia* (Smiley et al., 2005). Jackson (1973) suggested that the name of the fungus should remain stable until additional examinations of the teleomorph were conducted. Unfortunately, teleomorph observation is rare and the original specimen, observed by Bennett (1937) no longer exists (Smiley et al., 2005).

Recently, taxonomic revisions using multiple gene loci have resulted in the establishment of a new genus, *Clarireedia*, to accommodate four species associated with dollar spot of turfgrass (Salgado-Salazar et al., 2018). *Clarireedia homoeocarpa* was designated as the type specimen of the genus as a tribute to the former specific epithet, *Sclerotinia homoeocarpa*. The remaining three species in the genus include *C. bennettii*, *C. jacksonii*, and *C. monteithiana*. *Clarireedia monteithiana* and *C. jacksonii* appear to be the most common pathogenic species worldwide on warm- and cool-season turfgrasses, respectively (Salgado-Salazar et al., 2018). *Clarireedia homoeocarpa* and *C.*

bennettii are believed to primarily affect red fescue (*Festuca rubra* L.) and appear to be confined to the United Kingdom (Salgado-Salazar et al., 2018).

Clarireedia spp. grow well on PDA at pH 5 to pH 7, with optimum temperatures for mycelium growth between 20 and 30°C (Endo, 1963; Fenstermacher, 1970). Cultured strains are readily identified by characteristic floccose, white mycelium that matures into a felt-like texture and turns shades of brown, yellow, olive, or gray (Couch, 1995; Smiley et al., 2005). Darkly pigmented stroma appears on the agar surface two to four weeks after plating (Smiley et al., 2005).

Disease development and epidemiology

The dollar spot fungus survives unfavorable weather conditions as dormant mycelium in crowns and shoots of infected plants and as stromata on the surface of leaves (Couch, 1995; Smiley et al., 2005; Tani and Beard, 1997). As microclimatic temperatures reach 16°C, *Clarireedia jacksonii* (reported as *Sclerotinia homoeocarpa*) resumes growth, and grows maximally when microclimate temperatures are between 21 and 27°C with atmospheric humidity greater than 85% at night (Couch, 1995; Tani and Beard, 1997). Dissemination of the fungus is primarily through dispersal of diseased or infected plant material (Couch, 1995; Smiley et al., 2005; Tani and Beard, 1997). Mycelium protrudes from zones of active colonization and extends, from leaf to leaf, to infect healthy foliage via direct penetration or entrance through natural or mechanically induced openings of leaf surfaces (Couch, 1995; Smiley et al., 2005). In nature, immature asci and conidia are of miniscule importance for dissemination and infection of dollar spot (Couch, 1995).

Numerous soil properties have been documented to affect dollar spot disease. Wagner and Halisky (1981) found that thatch accumulations greater than 13 mm led to severe outbreaks of dollar spot. Low soil moisture and low nitrogen fertility are shown to increase dollar spot severity (Couch, 1995; Smiley et al., 2005; Tani and Beard, 1997). Soil pH and phosphorous levels do not affect dollar spot severity (Couch and Bloom, 1960; Smiley et al., 2005).

Control

Historically, dollar spot disease of turfgrass has been best controlled by applications of fungicides (Walsh et al., 1999). Concerns of fungicide efficacy for dollar spot control arose in the 1960s, as isolates of *Clarireedia jacksonii* (reported as *Sclerotinia homoeocarpa*) with tolerance to cadmium were identified (Cole et al., 1968). Furthermore, *Clarireedia jacksonii* resistance to heavy metal-based fungicides (Cole et al., 1968; Massie, 1968), triazines (Nicholson, 1971), benzimidazoles (Cole et al, 1974; Goldberg and Cole, 1973), dicarboximides (Detweiler, 1983), demethylation inhibitors (Golembiewski et al., 1995), and succinate dehydrogenase inhibitors (Popko et al., 2018) has been documented. Currently, control guidelines for dollar spot include various cultural management practices in concert with strategic fungicide applications (Smiley et al., 2005; Watschke et al., 2013).

Cultural management recommendations are targeted at promoting plant health and growth and reducing environmental conditions conducive for disease progression (Couch, 1995; Smiley et al., 2005; Tani and Beard, 1997; Williams et al., 1993). Mowing practices should be conducted at the appropriate height of cut and frequency for a given

turfgrass species (Smiley et al., 2005). Accumulations of guttation fluids and dew should be removed from leaf surfaces early in the morning by lightweight rolling, poling, or mowing (Couch, 1995; Smiley et al., 2005; Williams et al., 1993). Heavy irrigation should be supplied at low frequencies to decrease leaf wetness periods and avoid moisture stress (Couch, 1995; Smiley et al., 2005; Tani and Beard, 1997). Air circulation across the turf surface should be improved by installing fans, pruning or removing shrubs and trees or addressing various other physical barriers that may restrict airflow (Smiley et al., 2005). Aerification should be employed throughout the year to reduce thatch accumulations and compaction (Smiley et al., 2005). When dollar spot is active, nitrogen fertility should be maintained at adequate to high levels to promote foliar growth and enhance recovery (Couch, 1995; Smiley et al., 2005; Tani and Beard, 1997; Watschke et al., 2013).

Breeding efforts for dollar spot resistance in turfgrass systems

Dollar spot is a troublesome disease of perennial ryegrass, and a number of cultivars such as 'Silver Dollar' have been developed that provide improved dollar spot resistance (Bonos and Huff, 2013; Bonos et al., 2006). Unfortunately, research on the genetic basis for dollar spot resistance in perennial ryegrass is limited (Bonos and Huff, 2013). Dollar spot resistance mechanisms are much better understood in creeping bentgrass (*Agrostis stolonifera* L.) (Bonos and Huff, 2013). Oxalate oxidase, an enzyme that degrades the pathogenicity factor oxalic acid to CO_2 and H_2O_2, has higher activity in dollar spot resistant creeping bentgrass plants, compared with dollar spot susceptible creeping bentgrass plants (DaRoche and Hammerschmidt, 2004). Thus, it is suggested

that an increase in oxalate oxidase production is a possible mechanism for dollar spot resistance in creeping bentgrass (Orshinsky et al., 2012; Rioux, 2014).

Bonos and Huff (2013) indicate that future research in the area of perennial ryegrass breeding should address the inheritance of resistance to dollar spot. Inheritance studies in creeping bentgrass support a quantitative inheritance of dollar spot resistance (Bonos, 2006, 2011; Bonos et al., 2003). The cross of dollar spot susceptible and dollar spot resistant parental lines resulted in transgressive segregation and continual phenotype distributions in progeny (Bonos et al., 2003). Furthermore, dollar spot resistance is most likely due to additive gene action and influenced by environmental effects (Bonos, 2006, 2011; Bonos et al., 2003). These findings provide a basis for studying dollar spot resistance in perennial ryegrass and suggest that quantitative inheritance may exist.

Molecular biology methods for plant breeding

DNA sequencing

Numerous individuals have contributed to the current understanding, conceptualization, and sequencing methodologies of DNA, which was first isolated in 1869 by Swiss scientist Johann Friedrich Miescher while studying the chemical composition of leukocytes (Dahm, 2005). Miescher noticed that the precipitate of an unknown substance contained rich amounts of phosphorous and resisted digestion by protease enzymes (Dahm, 2008; Glass, 1965). These findings suggested the substance was not a protein or lipid; rather, it was a novel molecule (Dahm, 2008). Miescher

termed the substance nuclein because it was isolated from the nuclei of cells; the name is preserved in the modern nomenclature, deoxyribonucleic acid (Dahm, 2008; Glass, 1965).

The chemical properties of DNA were further elucidated by Russian biochemist Phoebus Levene during the early twentieth century (Masoudi-Nejad et al., 2013). Levene discovered that ribose and deoxyribose were the carbohydrate components of RNA and DNA, respectively (Masoudi-Nejad et al., 2013). Levene was the first to observe the order of the phosphate, sugar, and base components of a single nucleotide, and he is credited with the resolution of DNA and RNA assembly (Masoudi-Nejad et al., 2013).

Erwin Chargaff, an Austrian biochemist, continued studies to resolve the structural characteristics of DNA (Masoudi-Nejad et al., 2013). Chargaff found that the nucleotide base composition of DNA between species varied much more than that of DNA within species (Chargaff, 1951; Chargaff et al., 1949). A second discovery, recognized as Chargaff's rule, concluded that the concentration of adenine was usually similar to that of thymine and the concentration of guanine was usually similar to cytosine (Chargaff, 1951; Chargaff et al., 1949; Masoudi-Nejad et al., 2013).

Shortly after the findings of Chargaff, two English scientists, Rosalind Franklin and Maurice Wilkins, disclosed a regularly repeating helical structure of DNA via use of X-ray technology (Masoudi-Nejad et al., 2013). These findings provided a basis for the three-dimensional, double helical structure proposal by American researchers James Watson and Francis Crick (Watson and Crick, 1953).

Prior to the discovery of the structure of DNA, Avery and colleagues (1944) proposed that DNA carried the genetic information of an organism, a concept dissimilar

to the widely accepted theory that proteins were responsible for harboring such genetic material. This notion was later confirmed by Hersley and Chase (1952) through their studies of viral DNA transmission to bacteria.

After much effort by numerous persons, the structure and functionality of the DNA molecule is well understood. In 1957, Francis Crick proposed the central dogma, which suggested that information in the DNA is transferred to proteins through RNA (Dahm, 2005). Further speculations by Crick were that three nucleotide bases in the DNA specify a single amino acid in the protein sequence (Dahm, 2005). This concept was proven by Robert W. Holley and colleagues as they successfully cracked the genetic code (Dahm, 2005; Singer, 1968).

An overview of DNA synthesis is provided by Masoudi-Nejad et al. (2013) and summarized below. A phosphodiester linkage between two nucleotides generates the chains of a double helix DNA molecule. Each of the two strands of a DNA molecule has a 3' and 5' end, and the strands exist in opposite directional orientation. A hydroxyl group from an enlarging strand of DNA targets the phosphate group on the subsequent base to be added; this occurs in a 5' to 3' direction. The added base forms a phosphodiester linkage with the enlarging strand of DNA, releasing a pyrophosphate. The remaining free hydroxyl group targets the next base to be added. These reactions are catalyzed by DNA polymerase enzymes.

After the genetic code was cracked and the central dogma was established, researchers increasingly valued the genetic information contained in DNA (Dahm, 2005). Therefore, scientists focused on methods for determining the sequences of nucleotides bases in DNA for various organisms. Sanger sequencing, developed by Fredrick Sanger,

and Maxam-Gilbert chemical degradation DNA sequencing, developed by Allan Maxam and Walter Gilbert, are regarded as first-generation DNA sequencing technologies (Masoudi-Nejad et al., 2013). The Sanger sequencing method, compared to the Maxam-Gilbert sequencing method, was more user friendly and did not require heavy use of toxic chemicals; this led to a preferred usage of the Sanger sequencing technology (Masoudi-Nejad et al., 2013). For many years, the Sanger method was the sole technology utilized for DNA sequencing applications (Masoudi-Nejad et al., 2013). In recent years, various other DNA sequencing methods have emerged, which are referenced as the second- or next-generation DNA sequencing technologies (Masoudi-Nejad et al., 2013).

Sanger sequencing technology

Sanger sequencing was first introduced in 1977 as a method for DNA sequencing using chain-terminating inhibitors (Sanger et al., 1977). Alternatively known as dideoxy or chain termination sequencing, Sanger sequencing makes use of dideoxynucleotides, which lack a 3' hydroxyl group that is necessary for extension of the DNA strand (Masoudi-Nejad et al., 2013). Classical Sanger sequencing required four separate reactions, each of which were conducted with a single-stranded template DNA, DNA polymerase, DNA primers, the four normal DNA nucleotide bases, and a small amount of one of the four dideoxynucleotide bases (Masoudi-Nejad et al., 2013). As the dideoxynucleotides were incorporated into the growing DNA strands, elongation was terminated (Masoudi-Nejad et al., 2013). Such events resulted in various length DNA fragments, which were separated by size via polyacrylamide gel electrophoresis

(Masoudi-Nejad et al., 2013). The relative position of DNA fragment bands were visualized to determine the nucleotide sequences (Masoudi-Nejad et al., 2013). In later years, the process became increasingly automated by the addition of fluorescent labels on the dideoxynucleotides in such a manner that each emitted light at distinct wavelengths (Masoudi-Nejad et al., 2013).

Sanger sequencing was the standard procedure for DNA sequencing applications for nearly 30 years (Metzker, 2010). Numerous DNA sequencing studies were conducted with Sanger technology including complete genome sequencing of the bacterium *Haemophilus influenzae* (Fleischmann et al., 1995), the yeast *Saccharomyces cerevisiae* (Goffeau et al., 1996), the nematode *Caenorhabditis elegans* (Worm Sequencing Consortium, 1998), the plant *Arabidopsis thaliana* (The Arabidopsis Genome Initiative, 2000), and the human (Venter et al., 2001). Although such landmark studies were conducted with this DNA sequencing technology, notable weaknesses of this method existed (Masoudi-Nejad et al., 2013).

The primary limitation of Sanger sequencing for high throughput systems was that it could only accommodate up to about 1,000 base pairs (Masoudi-Nejad et al., 2013). This method required large DNA molecules to be fragmented and amplified prior to sequencing and reassembly (Masoudi-Nejad et al., 2013). These procedures were carried out through map-based or shotgun sequencing (Masoudi-Nejad et al., 2013). Additional drawbacks to Sanger sequencing included the lack of complete automation, limited parallel analyses, and high costs (Masoudi-Nejad et al., 2013).

Next-generation sequencing technology

DNA sequencing via next-generation sequencing (NGS) technologies has been steadily practiced since 2010 (Dolezel et al., 2014). NGS sequencing methods have reduced labor requirements and costs associated with resolving genome sequences (Dolezel et al., 2014). Various genomes have been sequenced with NGS technologies, and expectations include genomic sequencing of many additional scientifically and economically important species (Dolezel et al., 2014). Numerous NGS tools have been developed and are available for DNA sequencing; however, this review will only cover three of the most commonly used technologies.

454 pyrosequencing

The 454 pyrosequencing technology was commercialized in 2005 and was the first NGS platform released to the market (Ansorge, 2009X; Margulies et al., 2005). The method is based on pyrophosphate detection, which was first described by Nyren and Lundin (1985). The principle of pyrophosphate detection was first used in a DNA sequencing method introduced by Hyman (1988) and further developed into a routinely functioning method by Ronaghi and colleagues (1996). The 454 pyrosequencing technology was the first NGS platform to successfully sequence an entire human genome; befittingly, the genome was that of Dr. James D. Watson (Wheeler et al., 2008).

A sequencing-by-synthesis concept underlies the pyrosequencing technology (Masoudi-Nejad et al., 2013). Individual nucleotide bases are added to extending chains of DNA, releasing pyrophosphate molecules. In the presence of 5’ phosphosulfate, ATP

sulfurylase can enzymatically convert pyrophosphate to ATP. The ATP molecule, subsequently, acts as a substrate for luciferase, a chemical luminescence enzyme, which transforms luciferine into oxyluciferine and generates visible light. The light is detectable by a charged coupled device (CCD) camera and, importantly, the level of intensity is indicative of the number of nucleotides added to the growing DNA chain.

The sequencing process has been widely reviewed (Ansorge, 2009; Margulies et al., 2005; Masoudi-Nejad et al., 2013; Metzker, 2010; Shendure and Ji, 2008; Singh and Singh, 2013) and is summarized as follows. Genomic DNA is fragmented, ligated with short adapters, and hybridized to streptavidin-coated beads in such a manner that a single fragment is associated with a given bead. DNA fragments are amplified via emulsion PCR, a process where all necessary reagents, present in a single droplet of water, are introduced to an oil mixture containing a single bead. This amplification procedure ensures that numerous copies of DNA fragments of only one type are present on the surface of each bead. Each bead is pre-treated with DNA polymerase enzymes and transferred to a single well of a Pico TiterPlate. Smaller-sized beads, coated with the pyrosequencing enzymes, sulfurylase and luciferase, are added to the wells, and the loaded plates are transferred to a sequencing instrument.

Each of the four nucleotides is sequentially delivered to the wells of the plate, initiating the pyrosequencing technique. The generation of light from the incorporation of a nucleotide base into a growing DNA chain is recorded as a signal on a CCD camera. The DNA sequence is determined by knowing the nucleotide base identity and detecting its incorporation into the extending DNA chain as emitted light. As noted previously, the number of nucleotides incorporated is proportional to the signal intensity; however,

accuracy of homopolymer detection appears to be limited to about 10 nucleotide long stretches (Mardis, 2008). Subsequently, observed errors associated with the pyrosequencing-based sequencing approach are most commonly in the form of insertions and deletions (Shendure and Ji, 2008).

The 454 pyrosequencing technology is capable of producing 400 to 500 base pair read lengths using paired-end reads, and it is highly useful for numerous applications including transcriptome analysis, de novo sequencing and assembly, genome sequencing and mapping, and analysis of epigenetic changes (Ansorge, 2009). Primary drawbacks to the approach include the aforementioned reduced read accuracy associated with homopolymer stretches of identical bases and a relatively high cost of operation (Ansorge, 2009; Shendure and Ji, 2008).

Illumina sequencing

The Illumina Genome Analyzer, formerly owned by the Solexa company, was first introduced for commercial application in 2006 and is the most widely used NGS technology (Ansorge, 2009; Masoudi-Nejad et al., 2013; Singh and Singh, 2015). The technology makes use of the sequencing-by-synthesis chemistry along with a novel reversible terminator nucleotide component (Ansorge, 2009). Each of the four nucleotide bases are labelled with different fluorophores, which serve as chain terminators (Singh and Singh, 2015). The original Genome Analyzer platform generated very short reads of about 36 base pairs (Masoudi-Nejad et al., 2013). In 2009, Illumina introduced the Genome Analyzer IIX, which increased output from 1 Gb per run to 3 Gb per run (Masoudi-Nejad et al., 2013; Singh and Singh, 2015). Another improvement was

observed with the 2010 release of the HiSeq 2000 platform, which initially generated output up to 200 Gb per run (Masoudi-Nejad et al., 2013). The HiSeq 2000 output was improved to 600 Gb per run, an analysis that could be completed in eight days (Masoudi-Nejad et al., 2013). Another platform release came in 2011 with the introduction of the MiSeq, a benchtop version of the favored HiSeq 2000 platform (Masoudi-Nejad et al., 2013).

The Illumina sequencing methodology has been widely reviewed (Ansorge, 2009; Margulies et al., 2005; Masoudi-Nejad et al., 2013; Metzker, 2010; Shendure and Ji, 2008; Singh and Singh, 2013) and is summarized as follows. Sample genomic DNA is fragmented and ligated to adapters, which flank the 5' and 3' ends of the fragment. A solid surface flow cell is populated with primers that contain complementary sequences to those of the adapters. The adapter-flanked DNA fragments are hybridized to the flow cell-bound primers, and bridge amplification is conducted to generate up to 1,000 identical copies of each DNA fragment. The many copies of a single DNA fragment form a cluster on the flow cell, and they are referenced as the in vitro fragment clone. All of the fragments on a given flow cell comprise the in vitro DNA library.

Sequencing primers are ligated to the unbound ends of the DNA fragments and the fluorophore-labelled nucleotides are introduced. As the nucleotides incorporate onto the 3' end of the extending DNA chain, the fluorophores emit a fluorescence, which is captured by a CCD camera. The fluorophore terminator is removed, and the added nucleotide is rendered functional for continued DNA synthesis. The previous steps are repeated; a fluorophore-labeled nucleotide is added to the reaction mixture and incorporated into the extending DNA chain, fluorescence is recorded, the fluorophore is

removed, and the nucleotide is again functional. This process is repeated until the entire sequence of each DNA fragment is elucidated.

As mentioned, the Illumina sequencing platforms are the most widely used NGS technologies (Singh and Singh, 2015). Applications of Illumina sequencers include transcript profiling, de novo genome sequencing, and genome resequencing for discovery of insertions and deletions (InDels), copy number variations (CNV), SNPs, and structural variation (Singh and Singh, 2015). Potential issues associated with the Illumina sequencing technology include a heightened error rate via PCR amplification, potential for terminator malfunction, and tendency of the fluorescent properties of the dyes to create substitutions of G for T, A for C, and vice versa (Shendure and Ji, 2008; Singh and Singh, 2015). It should be noted that insertion and deletion errors are considerably lower than with 454 pyrosequencing (Shendure and Ji, 2008).

SOLiD sequencing

The sequencing by oligonucleotide ligation and detection (SOLiD) procedure was first described by Shendure et al. (2005) and McKernan et al. (2006), and it was commercialized in 2007 by the Applied Biosciences company (Ansorge, 2009; Masoudi-Nejad et al., 2013). The original platform was capable of generating an output of nearly 2 to 4 Gb of DNA sequence data in just over 8 days (Ansorge, 2009; Mardis, 2008). In 2008, the SOLiD 2.0 platform was introduced and increased sequence data output to nearly 10 Gb in a little over 4 days (Ansorge, 2009). The SOLiD platforms are desired for generating quality reads with low error rates; however, they do have drawbacks including short sequence read lengths of about 25 to 35 base pairs as well as the technical

challenges that accompany emulsion PCR (Ansorge, 2009; Mardis, 2008; Shendure and Ji, 2008)

A description of the sequencing methodology for SOLiD is provided as reviewed by Ansorge (2009), Mardis (2008), Masoudi-Nejad and colleagues (2013), and Shendure and Ji (2008). Genomic DNA is fragmented, ligated to adapters that flank 5' and 3' termini, and amplified via emulsion PCR in such a manner that each bead contains numerous copies of a single type of DNA fragment. Bead clones are selectively deposited onto a glass flow cell via 3' DNA strand modifications. As mentioned, SOLiD makes use of a sequencing by ligation approach, whereby a primer is annealed to adapters of each DNA fragment, subsequently initiating DNA sequencing reactions. Oligonucleotide octamers, labelled with fluorescent probes encoded by dinucleotides of the octamer sequence, are added to the sequencing mixture and ligated to the DNA fragments. The ligation reaction activates a fluorescent signal, which, when detected, triggers cleavage of the octamer after the fifth nucleotide. Multiple cycles of ligation are conducted, with a single nucleotide offset annealing of the primer each time. This allows each base to be analyzed on multiple occasions, increasing the resulting read accuracy.

Genetic markers

The biological features of individual organisms or species, determined by allelic forms, are recognized as genetic markers (Collard, 2005; Xu, 2010). Such features can be generationally transmitted, and serve as tags or experimental probes for tracing an individual, a chromosome, gene, tissue, nucleus, or cell (Jiang, 2013; Xu, 2010). Genetic markers are classified as classical markers or DNA markers (Singh and Singh, 2015; Xu,

2010). Classical markers are further categorized as morphological markers, cytological markers, and protein markers (Xu, 2010). DNA markers, commonly referenced as molecular markers, are further categorized as hybridization-based markers, PCR-based markers, and DNA sequencing-based markers (Collard, 2005).

The components of an ideal genetic marker have been outlined previously (Singh and Singh, 2015; Xu, 2010). The desirable marker should be codominant so that heterozygous and homozygous individuals may be distinguished, polymorphic and multiallelic to allow classification of more than two groups, and abundantly and evenly distributed across the genome. The marker should not be affected by environmental variation, nor should it exhibit epistasis or pleiotropic properties. Furthermore, the ideal genetic marker should generate high reproducibility and require minimal monetary input for both development and genotyping procedures. Given the scope of this dissertation, only DNA markers will be discussed in further detail.

DNA markers

Genetic variation among individuals in a group is predominately attributed to chromosomal rearrangement during recombination or abnormal pairing of sister chromosomes (Yang et al., 2015). Chromosomal rearrangements vary in size from only a few base pairs to millions of base pairs and include insertions, deletions, substitutions, reduplications, translocations, and inversions (Yang et al., 2015). DNA markers identify such sequence variations in the genomic DNA of different individuals via DNA

hybridization, PCR, and DNA sequencing techniques (Singh and Singh, 2015; Xu, 2010; Yang et al., 2015).

DNA marker development began in 1974, with the analysis of DNA fragments generated by restriction enzyme digestion (Grodzicker et al., 1974; Singh and Singh, 2015). Later improvements to DNA marker technologies led to increased marker abundance, higher throughput, improved reproducibility, reduced costs, and enhanced user friendliness (Singh and Singh, 2015). Currently, DNA markers are the most readily used marker types for such applications as linkage map construction, genetic diversity assessments, and cultivar identification (Collard, 2005; Jahufer et al., 2003; Langridge and Chalmers, 2004; Winter and Kahl, 1995).

Restriction fragment length polymorphisms

Regarded as the first generation molecular marker, the hybridization-based restriction fragment length polymorphism (RFLP) markers provided a basis for many of the more popular DNA markers used today (Langridge and Chalmers, 2004; Singh and Singh, 2015; Xu, 2010; Yang et al., 2015). RFLP markers were extensively used throughout the 1980s and 1990s, but are not as heavily used in current times (Singh and Singh, 2015; Yang et al., 2015). However, RFLP markers remain useful as anchor marker in synteny and comparative mapping studies (Singh and Singh, 2015; Xu, 2010).

Grodzicker and colleagues (1974) first used RFLP technology to determine locations of temperature-sensitive mutations on a physical map of restriction fragments of adenoviruses. A short time thereafter, a detailed description of the procedure and principle for the use of RFLPs was provided through the construction of the first human

linkage map (Botstein et al., 1980). These studies pioneered the use of polymorphic DNA as genetic markers and led to the extensive use of RFLPs for genomic linkage mapping in plants and animals (Bernatzky and Tanksley, 1986; Helentjaris et al., 1986; Xu, 2010; Singh and Singh, 2015).

The general methodology for RFLP detection has been summarized by Xu (2010) and Singh and Singh (2015). Large quantities of genomic DNA are isolated from several individuals of the target genotypes. The DNA is purified and restriction enzymes are added to cleave the DNA at recognition sites throughout the genome. The resulting fragments are separated by gel electrophoresis, denatured, and transferred to a nitrocellulose membrane via Southern blotting (Southern, 1975). Membrane-bound DNA fragments are hybridized to labeled probes. Non-specifically hybridized DNA molecules are washed from the membrane and sizes of remaining fragments are determined by radioactive methods. Two or more differentially sized fragments may be identified by the probe-restriction enzyme combination. Polymorphism is presented as non-identical lengths of the fragmented DNA.

Advantages of the RFLP marker system include high reproducibility, even distribution of markers across the genome, and primarily codominant inheritance patterns (Singh and Singh, 2015; Xu, 2010; Yang et al., 2015). Disadvantages include intense labor and time requirements, need for large quantities of high purity DNA, and inability for automation or high-throughput analyses (Singh and Singh, 2015; Xu, 2010; Yang et al., 2015). Notably, useful hybridization-based RFLP markers have been converted into more user-friendly and convenient PCR-based systems including cleaved amplified

polymorphic sequence (CAPS) markers, single-strand conformation polymorphism (SSCP) markers, and sequence-tagged site markers (Singh and Singh, 2015).

Diversity array technologies

The diversity array technology (DArT) marker is a low-cost, microarray hybridization-based genotyping system introduced by Jaccoud and colleagues (2001). DArT was originally proposed for interspecific genetic diversity studies, but has since been applied to various other principles (Xu, 2010). The DArT method is amendable to high-throughput automation and enables simultaneous genotyping of numerous genome-wide polymorphic loci (Wenzl et al., 2004).

DArT analyses consist of microarray construction and genotyping of samples; these procedures have been summarized by Singh and Singh (2015) and Xu (2010). The microarray, alternatively termed diversity array or genotyping array, is constructed so that it contains polymorphic segments of genomic DNA across a range of germplasm for a given species. Such an array is developed by digesting representative genomic DNA with restriction enzymes and ligating restricted fragments to adaptors. Genome complexity is reduced via PCR with primers complementary to sequences of the selective overhangs and adaptors. The resulting restriction fragments, which represent the gene pool, are cloned to produce a representation library. Array inserts from a random set of clones are used to identify polymorphic clones in the library. Cloned inserts are amplified via vector-specific primers, purified, and arrayed across a solid support, producing the microarray.

Genotyping involves fluorescent labelling of representative DNA for a sample and hybridization against the discovery array. The array is scanned to measure the hybridization signal for each location. If multiple labels are added, hybridization signals of a representative from one sample can be compared to a control probe or another sample. Polymorphic clones, or DArT markers, are those that differentially express hybridization signals for different samples. Such clones are gathered onto a genotyping array for routine genotype analyses.

DArT markers are commonly used to assemble genetic linkage maps of medium-density for species of various genome sizes. DArT markers are biallelic and behave in both codominant and dominant fashion, and are capable of detecting insertions, deletions, and single base changes (Singh and Singh, 2015). The DArT system has been successfully applied to many plant species including barley (*Hordeum vulgare* L.) (Wenzl et al., 2006), wheat (*Triticum aestivum* L.) (Semagn et al., 2006), and cassava (*Manihot esculenta* Crantz) (Xia et al., 2005).

Primary weaknesses of DArT marker systems are the technically demanding nature and the dominant inheritance (Xu, 2010). Additionally, concerns exist regarding marker distribution across plant genomes (Singh and Singh, 2015; Xu, 2010). In barley, DArT markers appeared to be localized in distal chromosome regions that were hypomethylated and gene rich (Wenzl et al., 2006).

Random amplified polymorphic DNAs

The PCR-based random amplified polymorphic DNA (RAPD) markers were first introduced by Willliams et al. (1990). This marker system is dominant, scored as

presence or absence, and capable of detecting high levels of polymorphisms in plants in a relatively short time period without prior sequence knowledge of the template DNA (Singh and Singh, 2015 Staub et al. 1996). RAPD markers do not require radioactive components, large amounts of DNA, or prerequisite procedures such as preparation of hybridization filters or development of cloned DNA probes (Singh and Singh, 2015). The technology accommodates automation and has been utilized to construct high-density maps in many crop and model plant species including alfalfa (*Medicago sativa* L.), apple (*Malus domestica* Borkh.), lettuce (*Lactuca sativa* L.), and Arabidopsis (*Arabidopsis thaliana* Heynh.) (Echt et al., 1994; Hemmat et al., 1994; Kesseli et al., 1994; Reiter et al., 1992; Singh and Singh, 2015). Moreover, RAPDs have been employed to identify molecular markers associated with desired genes such as disease resistance in crops like tomato (*Lycopersicon esculentum* L.) and faba bean (*Vicia faba* L.) (Avila et al., 2003; Stevens et al., 1995).

An overview of RAPD marker development is provided by Singh and Singh (2015). High molecular weight genomic DNAs are acquired from test individuals. Sequences are targeted and amplified by a single, arbitrary base oligonucleotide primer, usually 10 nucleotides in length. The single primer, which acts as both the forward and reverse primer, anneals at multiple sites of the genomic DNA, and sequence amplification progresses when the primer anneals at locations within approximately 2 kb of each other. Conditions are adjusted so that each reaction yields less than 20 amplified fragments, which can be separated via polyacrylamide or agarose gel electrophoresis and visualized by silver or ethidium bromide staining (Staub et al., 1996). Multiple loci are rapidly evaluated because fragments are typically amplified from various genomic regions

(Edwards, 1998). Of important notation, only RAPD markers that generate intense, reproducible bands should be used to ensure the marker genotypes are reliably scored (Singh and Singh, 2015).

The dominant characteristic of RAPD markers does not readily permit distinction between heterozygous and homozygous individuals (Williams et al., 1990). To differentiate the two types, RAPD markers should be chosen that are tightly linked to the locus of interest. Additionally, one marker should be in repulsion phase with the target locus, while the other marker should be in coupling phase with the target locus; identifying such markers is not likely to be an easily accomplished task (Singh and Singh, 2015). As a result, this strategy requires twice as many marker assays as a codominant marker.

RAPD markers are relatively easy to develop and simple to analyze; however, poor experimental reproducibility, along with dominant inheritance patterns, have limited the widespread application of this system (Singh and Singh, 2015; Xu, 2010). RAPD polymorphism reproducibility is affected by numerous factors including primer-to-template ratio, annealing temperature, and magnesium concentration (Williams et al., 1990). To illustrate these effects, Singh and Singh (2015) indicated that a slight 1°C change in annealing temperature might produce an entirely different RAPD banding profile. Additionally, experimental error could lead to failure of amplification, which could be scored as an absent allele (Singh and Singh, 2015).

Despite the aforementioned shortcomings, the RAPD system remains relevant for some genetic studies (Babu et al., 2014). More importantly, various modifications to this system have led to more applicable and useful marker systems including arbitrary

primed-PCR (AP-PCR), allele-specific associated primers, and sequence-characterized amplified region (SCAR) markers (Singh and Singh, 2015).

Arbitrary primed-PCRs

Welsh and McClelland (1990) first introduced the AP-PCR markers as a method of PCR-based amplification using 18-32 nucleotide long arbitrary sequence primers. AP-PCRs are similar to, and often considered synonymous with, RAPDs; however, there are distinct differences among the two marker types (Singh and Singh, 2015). In consideration of an arbitrary sequence greater than 20 nucleotides in length, it is highly unlikely that even complex genomes would contain sequence complementarity (Singh and Singh, 2015). Consequently, successful amplification occurs only when annealing temperatures are adjusted to permit primer-to-template base pairing mismatches at some base pairs (Singh and Singh, 2015).

The methodology for AP-PCR marker amplification is summarized by Singh and Singh (2015). The first two PCR cycles are conducted with reduced annealing temperatures. This lowers the stringency and enables primer-to-template mismatch annealing. In subsequent PCR cycles, the annealing temperatures are raised, and stringency is increased to promote primer-to-template base pairing integrity. This methodology generates up to 100 distinct bands for each individual, which are separated via polyacrylamide gel electrophoresis and scored as present or absent.

This approach has since been modified to permit agarose gel electrophoresis-based fragment separation, and is an adequate tool for DNA fingerprinting (Singh and Singh, 2015). The AP-PCR marker system differs from the RAPD system in annealing

conditions, length of primers, and the number of generated fragments (de Vienne et al., 2003). Currently, AP-PCR is not widely implemented, primarily due to autoradiography usage requirements (Singh and Singh, 2015).

Amplified fragment length polymorphisms

The PCR-based amplified fragment length polymorphism (AFLP) marker system, introduced by Zabeau and Vos (1993) and Vos (1995), combines PCR flexibility with the powerful restriction digestion component of the RFLP method (Singh and Singh, 2015; Xu, 2010). This generates a highly polymorphic, robust DNA marker system that is applicable to all sources of genome complexity (Singh and Singh, 2015; Xu, 2010).

An overview of the AFLP procedure is provided by Singh and Singh (2015) and Xu (2010). Genomic DNAs are acquired from samples and digested with both rare- and frequent-cutting enzymes. This digestion procedure yields fragments with both ends generated by rare-cutting enzymes, fragments with both ends generated by frequent-cutting enzymes, and fragments with one end generated by rare-cutting enzymes and one end generated by frequent-cutting enzymes. Those fragments that are generated solely by rare-cutting enzymes are expected to represent the smallest fraction of the fragment population, and those fragments that are generated solely by frequent-cutting enzymes are expected to represent the largest fraction of the fragment population. All fragments are ligated with appropriate adapters and subjected to a two-phase PCR procedure.

The first phase of PCR, termed the preamplification step, makes use of AFLP primers with arbitrary nucleotides, called selection nucleotides, to reduce the total number of fragments amplified. Preamplification products are diluted and used as a

template for the second phase of PCR. AFLP primers in the second phase have an increased number of selection nucleotides, and the primers corresponding to the rare-cutting enzymes are radioactive- or fluorescent-labelled. Noteworthy, amplification conditions and AFLP primers are designed to promote amplification of fragments with one end generated by the rare-cutting enzymes and one end generated by the frequent-cutting enzymes.

PCR amplified fragments are denatured and separated via polyacrylamide gel electrophoresis, and the bands are visualized with autoradiography or, preferentially, fluorescence (Vos et al., 1995). Genotyping data is automatically collected and analyzed when fragments are evaluated by an automated DNA sequencer, a process that is permitted with the use of fluorescent labelling (Singh and Singh, 2015). A typical number of amplified restriction fragments ranges from 50 to 100, and about 80 percent of those are polymorphic and useful as markers (Singh and Singh, 2015; Xu, 2010).

AFLP markers, compared to RFLP markers, are less labor intensive, quicker, and detect larger numbers of loci that supply greater information (Singh and Singh, 2015; Yang et al., 2015). General advantages of AFLP markers include no requirement for marker development or prior sequence knowledge and applicability to all species, including model organisms (Singh and Singh, 2015; Xu, 2010; Yang et al., 2015). AFLP markers exhibit higher reproducibility compared to RAPD markers; however, the reproducibility of AFLP markers is less than RFLP markers and SSR markers (Singh and Singh, 2015; Xu, 2010).

Disadvantages of AFLP markers include technically demanding, laborious, and time-consuming procedures (Singh and Singh, 2015; Xu, 2010). Additionally, AFLP is

expensive to set up, requires highly pure DNA preparation, uses restriction enzymes, and yields a relatively low polymorphic content (Singh and Singh, 2015; Xu, 2010). Studies in barley (Qi et al., 1998) and sunflower (*Helianthus annuus* L.) (Gedil et al., 2001) have demonstrated the tendency of AFLP markers to concentrate near centromeric regions of the chromosome (Xu, 2010). Lastly, AFLP markers are dominantly inherited; however, distinctions between heterozygosity and homozygosity can be made based on fragment band intensity (Staub et al., 2006).

Sequence-characterized amplified regions

The PCR-based SCAR markers were originally developed from desirable RAPD markers (Paran and Michelmore, 1993). The term SCAR is often applied to PCR markers derived from other markers like AFLPs, as well (Singh and Singh, 2015). SCARs are highly similar to STS markers in both application and construction, and they are used for phylogenetic relationship studies, physical and genetic mapping, and comparative analysis (Singh and Singh, 2015; Staub et al., 1996). SCAR markers are typically dominant and scored as either the presence or absence of a single, unique band (Singh and Singh, 2015; Staub et al., 1996). The requirement of electrophoresis can be eliminated by developing the SCAR markers into presence-absence arrays (Singh and Singh, 2015).

A general outline for development and application of SCAR markers is provided by Singh and Singh (2015). SCAR marker development includes eluting an amplified fragment of a desirable RAPD marker from a gel, cloning the fragment, and determining the nucleotide sequence of both termini of the fragment. Forward and reverse primers,

20-24 nucleotides in length and specific to terminal sequences of the fragment, are designed. Primer pairs are evaluated, and those that amplify the polymorphism represented by the RAPD marker give rise to SCAR markers. In the instance that SCAR markers fail to detect polymorphisms, both alleles of the RAPD fragment must be sequenced, and primers designed based on sequence differences; this ensures polymorphism detection (Vosman, 1998).

Microsatellite markers

Microsatellite markers, alternatively referred to as simple sequence repeat (SSR) markers, short tandem repeat (STR) markers, sequence-tagged microsatellite site (STMS) markers, and simple sequence length polymorphism (SSLP) markers, is a repeated unit of nucleotide motifs (Singh and Singh, 2015; Xu, 2010). The term 'microsatellite' was first presented to describe the PCR-generated simple sequence fragments (Litt and Luty, 1989). Microsatellites are tandem di-, tri-, and tetranucleotide repeats such as $(GA)_n$, $(AAG)_n$, and $(GATA)_n$, respectively, where 'n' represents the number of repeats, which can vary from 5 to 50, or more (Singh and Singh, 2015; Xu, 2010). Microsatellites are distinguished from minisatellites by genome-wide distribution pattern and size of repeating unit (Singh and Singh, 2015). Microsatellites are evenly distributed across the plant genome, whereas minisatellites are most commonly localized at the telomeric regions of eukaryotic chromosomes (Tautz, 1989; Tautz and Renz, 1984; Weber and May, 1989). The repeating motif of microsatellites is typically 1 to 6 base pairs in length, while that of minisatellites is 11 to 60 base pairs in length (Singh and Singh, 2015; Xu, 2010).

Microsatellites exhibit high levels of allelic variation, which is solely based on the number of repeat units; this is the most important property of microsatellites as it validates their usefulness as genetic markers (Singh and Singh, 2015; Xu, 2010). Microsatellite polymorphisms have been studied to establish SSR markers and inter-simple sequence repeat (ISSR) markers (Singh and Singh, 2015). The SSR markers are further described in this section whereas the ISSR markers are outlined in the section immediately following.

An SSR marker locus may be identified via a number of methods including exploring sequences deposited in databases and evaluating clone libraries or fragments from genomic DNA restriction digestion (Singh and Singh, 2015). Markers that are derived from genomic sequence data are referred to as genomic SSR (gSSR) markers, while those derived from EST data are referred to as expressed SSR (eSSR) markers (Singh and Singh, 2015). For *de novo* marker development, microsatellite sequences are identified by sequencing DNA inserts or restriction fragments (Singh and Singh, 2015; Xu, 2010). Regardless of the method used to identify SSR marker loci, the associated primers should be developed in such a manner that they are 'AT' rich at the 3' ends, have about 50 percent 'GC' content, and yield low frequencies of primer dimers (Singh and Singh, 2015).

SSR markers are routinely used for practices such as characterizing germplasm, developing linkage maps, identifying plant cultivars, and analyzing genetic variation (Powell et al., 1996). During the 1990s and early 2000s, SSR makers were predominantly chosen for molecular-based plant research (Singh and Singh, 2015). However, SNP markers, which are discussed in a later section, have gained popularity

over SSR marker for many applications due to their high-throughput nature and general abundance (Singh and Singh, 2015; Xu, 2010).

The SSR marker system is primarily limited by the costly, labor intensive, and complex development procedures (Singh and Singh, 2010). Generally speaking, SSR marker development includes genomic library construction, constructing specific primers, and characterizing chromosomal position and size of an SSR marker locus (Singh and Singh, 2015; Xu, 2010). Multiplexing with SSR markers is limited and automation is costly and provides insufficient coverage of desired genomic regions (Singh and Singh, 2010). Moreover, various genotyping platforms yield different allele sizes; which can complicate the sharing of SSR marker data (Singh and Singh, 2015).

Inter-simple sequence repeats

The ISSR markers are PCR-based markers that utilize microsatellite sequences as primers to amplify genomic regions adjacent to those microsatellite sequences (Singh and Singh, 2015). Simply put, ISSR polymorphisms are assessed as the length of the genomic region that is located between two adjacent microsatellite sequences (Singh and Singh, 2015). ISSR markers may consist of anchored or non-anchored primers (Singh and Singh, 2015). Anchored primers, which are more common of the two types, include a microsatellite sequence plus a short, arbitrary nucleotide sequence located at the 3' or the 5’ end (Singh and Singh, 2015). Non-anchored primers, as the name implies, do not have the short nucleotide 'anchor' sequence, and consists only of the microsatellite sequence (Singh and Singh, 2015).

The markers that result from non-anchored primers, generally referenced as microsatellite-primed PCR (MP-PCR) markers or single primer amplification reactions (SPARs) markers, are only of use when trinucleotide, tetranucleotide, or pentanucleotide repeats constitute the primers (Singh and Singh, 2015). Non-anchored primers are also prone to annealing at various locations within the microsatellite repeats, which is undesirable as it produces different fragment lengths from a single ISSR region (Caldeira et al., 2002). Fortunately, anchored primers are able to eliminate this type of issue and greatly reduce ISSR fragment amplification variability (Singh and Singh, 2015).

The markers that result from anchored primers are alternatively referenced as anchored microsatellite-primed PCR (AMP-PCR) markers, anchored simple sequence repeat (ASSR) markers, inter-SSR amplification (ISA) markers, or inter-SSR PCR markers (Singh and Singh, 2015). The position of the anchor in the primer dictates the region amplified by anchored primers (Singh and Singh, 2015). When the anchor is attached to the 3' end of the primer, the amplified product consists only of the primer and the region between the two microsatellites (Singh and Singh, 2015). Alternatively, when the anchor is attached to the 5' end of the primer, the region between the two microsatellites and the entire microsatellite sequence will be included in the amplified fragment (Singh and Singh, 2015).

Largely, ISSR markers are inexpensive, identify multiple polymorphic loci, and are easy to use (Singh and Singh, 2015). Furthermore, ISSR makers have a high throughput and do require prior knowledge of sequence information for development (Singh and Singh, 2015). A primary limitation of ISSR markers is that some primer sets are prone to amplification of non-reproducible banding patterns (Singh and Singh, 2015).

Additionally, ISSR markers are mostly dominant; however, some codominant markers can be established via the use of a 5' anchor sequence (Singh and Singh, 2015).

Cleaved amplified polymorphic sequences

The PCR-based CAPS markers were developed by Konieczny and Ausubel (1993) as a method for genotyping RFLP markers. Also referenced as PCR-RFLP, the CAPS marker system involves restriction enzyme digestion of PCR-amplified fragments and detection of polymorphisms as the lengths of the digested fragments (Jarvis et al., 1994; Konieczny and Ausubel, 1993; Singh and Singh, 2015). CAPS markers exhibit codominant inheritance and arise from genetic variations at recognition loci within the amplified fragments for a given set of restriction enzymes (Singh and Singh, 2015; Staub et al., 1996). The use of restriction enzymes increases the cost and renders this system undesirable for automation and high-throughput analyses; however, CAPS is favored over the hybridization-based RFLP approach (Singh and Singh, 2015).

Single-strand conformation polymorphisms

The SSCP markers were proposed by Orita et al. (1989), and are classified as PCR-based markers because PCR amplification is the primary origin of the DNA fragments used in such analyses (Singh and Singh, 2015). The premise of SSCP marker systems is that nucleotide sequences dictate internal complementary base pairing, which results in short double-stranded regions along the single-stranded DNA (Singh and Singh, 2015). Such double-stranded interactions provide stability for the folding patterns and

establish secondary structures, which affect mobility of the resulting single-stranded DNA molecule (Singh and Singh, 2015).

A general description of the SSCP marker detection procedure is outlined by Singh and Singh (2015). SSCP detection begins with denaturing double-stranded DNA molecules by heat exposure at 95°C. Separated single-stranded DNA molecules are quickly cooled in such a way that complementary DNA strands are unable to pair with each other. Rather, the single-stranded DNA molecules are encouraged to internally base pair so that characteristic secondary structures are formed. SSCP markers are detected by differential migration patterns of single-stranded DNA molecules on agarose gel electrophoresis in the presence of non-denaturing conditions.

Estimates suggest that the SSCP marker system is capable of exposing 100 percent of sequence variants for DNA molecules up to 200 base pair in length (Singh and Singh, 2015). However, percentage of sequence variants detected decreases as length of DNA tested increases (Singh and Singh, 2015). Nonetheless, when highly detailed information is not desired, SSCP provides a quick assay for differences among DNA samples (Singh and Singh, 2015). The SSCP marker system has also been utilized for genetic and mapping studies in plants (de Vienne, 2003). SSCP is more convenient and straightforward than other systems such as CAPS, which requires restriction digestion of PCR products (Singh and Singh, 2015). The primary limitations to use of SSCP include costly marker development, intense labor requirements, and lack of automation for high-throughput analyses (Singh and Singh, 2015)

Sequence-related amplified polymorphisms

Sequence-related amplified polymorphism (SRAP) is a simple, PCR-based marker developed by Li and Quiros (2001) for the amplification of open reading frames (ORFs). SRAP markers have been used for many studies including linkage mapping, genetic diversity analyses, and identification of markers linked to useful genes (Singh and Singh, 2015). Additionally, SRAPs have been applied to numerous crops including celery (*Apium gravedens* Pers.), Chinese cabbage (*Brassica rapa* L.), wild cabbage (*Brassica oleraceae* L.), garlic (*Allium sativum* L.), potato (*Solanum tuberosum* L.), rapeseed (*Brassica napus* L.), and rice (*Oryza sativa* L.) (Li and Quiros, 2001).

An overview of the experimental conditions for the SRAP marker system is provided by Li and Quiros (2001). The SRAP marker system is based on two primers, forward and reverse, for amplification. Each primer is 17 or 18 nucleotides long and is composed of core nucleotides and selective nucleotides. Core nucleotides include a filler sequence of 10 or 11 arbitrary bases at the 5' end, followed by the sequences 'CCGG' and 'AATT' for the forward and reverse primers, respectively. Notably, the filler sequences of the forward and reverse primers should be different from each other. The sequence 'CCGG' is targeted at exons, which are typically GC-rich regions; the sequence 'AATT' is targeted at promoter and introns, which are typically AT-rich regions. The core sequence is followed by three selective nucleotides, which are assembled at the 3' end of the forward and reverse primers. The initial five cycles of PCR are conducted with an annealing temperature of 35°C, and the following 35 cycles are conducted with an annealing temperature of 50°C. DNA fragment amplifications are denatured in an

acrylamide gel electrophoresis for separation, and bands are visualized via autoradiography.

In a study of recombinant inbred line (RIL) and doubled-haploid (DH) populations of *B. oleracea*, Li and Quiros (2001) found a large number of SRAPs included exons in ORFs, suggesting the markers were evenly distributed across the genome. SRAP markers can manifest as dominant and codominant markers depending on the type of genetic variation (Li and Quiros, 2001). For example, insertions and deletions (InDels) create polymorphisms in amplified fragment size and generate codominant markers, whereas SNPs that affect primer binding generate dominant markers (Singh and Singh, 2015).

The SRAP method is simple and reliable, and has become widely used in plant genetics (Li and Quiros, 2001; Poczai et al., 2013). Attractive attributes include high reproducibility, no requirement for prior sequence knowledge of target specimen, moderate throughput, readily applicable to any species, generates a fair proportion of codominant markers, is easy to perform, and is cost effective (Li and Quiros, 2001; Poczai et al., 2013; Sing and Singh, 2015).

Target region amplification polymorphisms

The PCR-based target region amplification polymorphism (TRAP) marker system, introduced by Hu and Vick (2003), is similar to SRAP markers, but makes use of bioinformatics resources and expressed sequence tag (EST) databases to develop polymorphic DNA markers located near the targeted candidate gene. The TRAP method

uses a fixed primer and an arbitrary primer, each of 18 nucleotides, for marker generation (Hu and Vick, 2003).

An overview of the experimental conditions for the TRAP marker system is provided by Hu and Vick (2003). The fixed primer is complementary to the known sequences of a targeted EST, as determined from an EST database. The arbitrary primer for the TRAP method is designed in the same manner as with the SRAP method; the primer is composed of core nucleotides and selective nucleotides. Core nucleotides include a filler sequence of 10 or 11 arbitrary bases at the 5' end, followed by the sequences 'CCGG' or 'AATT' to promote exon annealing or intron annealing, respectively. The core sequence is followed by three selective nucleotides, which are assembled at the 3' end. The initial five cycles of PCR are conducted with an annealing temperature of 35°C, and the following 35 cycles are conducted with an annealing temperature of 50°C. DNA fragment amplifications are analyzed via electrophoresis on a 6.5% polyacrylamide gel.

Single PCR reactions with TRAP markers have generated up to 50 scorable polymorphisms of 50-900 base pairs from various plant species. TRAP markers are proven reproducible, and are more desirable than SRAP markers in terms of yielding markers near targeted candidate genes. TRAPs have been applied to various studies including genotype fingerprinting analyses, mapping of genes and quantitative trait loci (QTL), and characterizing germplasm (Singh and Singh, 2015).

Single nucleotide polymorphisms

Single nucleotide polymorphisms (SNPs, pronounced 'snips') describe individual nucleotide base variations between DNA sequences among individuals of a given species (Bernardo, 2001; Singh and Singh, 2015; Xu, 2010). A SNP locus is the genomic position where variants of nucleotides occur; SNP loci are characterized by the flanking sequences of the polymorphic nucleotide (Singh and Singh, 2015). A given SNP is categorized as transitions or transversions based on the type of nucleotide substitution, and, in general, transitions are considered more common than transversions (Singh and Singh, 2015; Xu, 2010). Transitions include C ↔ T or G ↔ A, whereas transversions include C ↔ G, A ↔ T, C ↔A, or T ↔ G (Singh and Singh, 2015; Xu, 2010). Furthermore, InDels are also analyzed as SNPs (Singh and Singh, 2015). As an example, fragment DNA sequences from two individuals of a given species are 'TTCGCAT' and 'TTCGTAT'. In this example, there is a SNP (C ↔ T transition), which yields 'C' and 'T' alleles.

The minor allele of a given nucleotide polymorphism must be present in at least 1% of the individuals in order for that polymorphism to be considered as a SNP (Singh and Singh, 2015; Xu, 2010). In plants, it is estimated that a SNP occurs once every 100 to 300 base pairs (Edwards et al., 2007a). SNP markers are easy to detect, extremely abundant, and have low rates of mutation (Singh and Singh, 2015). Moreover, given that a single nucleotide is the smallest inherited unit, they are regarded as the ultimate form of molecular markers (Xu, 2010). Noncoding regions of genes are the most common location for SNP; however, they are also present in coding sequences and in intergenic regions (Singh and Singh, 2015; Xu, 2010). Phenotypic variants from SNPs arise from

mechanisms such as altered promoter activity, disrupted splicing patterns of RNA transcripts, and changed protein sequence (Singh and Singh, 2015; Xu, 2010). Distinctions of various SNP factors such as genomic location and effect on phenotype have led to a plethora of SNP classification nomenclatures, which have been summarized by Singh and Singh (2015).

The majority of SNPs do not produce a phenotype and have no effect on gene function and are termed anonymous SNPs. Some SNPs, however, do affect gene function and lead to variant phenotypes; these are classified as functional SNPs or candidate SNPs. Functional SNPs and candidate SNPs, which are located in genes, are further characterized as genic SNPs. Genic SNPs can be localized in introns (intronic SNPs), exons (exonic SNPs or coding SNPs), and promoter regions (promoter SNPs, pSNPs). Intronic SNPs are noncoding SNPs (ncSNPs) that are located in noncoding gene regions. Exonic SNPs are similar to copy SNPs (cSNPs) or cDNA SNPs, which are identified from cDNAs. Exonic SNPs that result in altered amino acid sequences are called non-synonymous SNPs (nsSNPs) whereas exonic SNPs that do not result in altered amino acid sequences are called synonymous SNPs (synSNPs). A reference SNP (refSNP) is one that serves as a location determinant for neighboring SNPs. Upon submission to a databank, a given refSNP is assigned to a particular refSNP identifier (rsID) number. Subsequently, databanks and ESTs can be mined for SNP discovery; the resulting SNPs from these approaches are generally termed in silico SNPs (isSNPs) or electronic SNPs (eSNPs). Such ‘virtual’ polymorphisms must be resequenced for validation.

Numerous methods have been developed for SNP discovery; these methods have been categorized as indirect discovery, in vitro discovery, and in silico discovery (Edwards et al., 2007b). The in vitro discovery methods are the only one of the three that pertains to generating novel polymorphic sequence data (Edwards et al., 2007b; Xu, 2010). The in silico method makes use of previously sequenced polymorphism data and in the indirect discovery method, the underlying polymorphic sequence remains unknown (Edwards et al., 2007b; Xu, 2010). However, regardless of the method used for SNP discovery, all SNPs were originally discovered by sequencing of entire genomes, transcriptomes, or targeted regions of genomes (Singh and Singh, 2015). The following section details a novel reduced-representation sequencing method for SNP discovery and genotyping.

Genotyping-by-sequencing

A focal objective of molecular plant breeding is accurately predicting phenotypes based on genotype associations (Xu, 2010). The procedure for genotyping germplasm includes identifying polymorphic DNA sequences and assaying resulting markers across the complete set of plant material (Poland and Rife, 2012). Historically, this process has existed in two distinct steps involving marker discovery prior to assay design and genotyping (Poland and Rife, 2012).

Limited density and high costs of molecular markers such as RFLPs, AFLPs, and SSRs have increased the usage of SNPs for genotyping applications (Beissinger et al., 2013). Accordingly, sequencing-based and array-based technologies are available to discover large numbers of SNPs for constructing haplotype maps, exploring within-

species diversity, conducting genome-wide association studies (GWAS), and linkage mapping (Beissinger et al., 2013; Fan et al., 2006, Hegarty et al., 2013; Metzker, 2010; Pfender et al., 2011). Examples of sequencing-based SNP allele calling methods include whole-genome sequencing (Hillier et al., 2008), methylated DNA sequencing (Brunner et al., 2009), exome capture (Ng et al., 2009), restriction enzyme digestion (Davey et al., 2011), and RNA sequencing (Hansey et al., 2012).

Restriction enzyme digestion is a readily used approach, which generates a reduced representation of the genome (Davey et al., 2011). Reduced-representation sequencing, or sequencing of small, targeted genomic regions, was first exploited by Altshuler and colleagues (2000). The method was later combined with NGS by Baird et al. (2008) in a process described as restriction-site associated DNA sequencing (RAD-seq). Elshire et al. (2011) introduced genotyping-by-sequencing (GBS) as a simplified and streamlined alternative to RAD-seq that could be applied to any species in a cost efficient manner. GBS combines genome-wide molecular marker discovery and genotyping in a single step, enabling application to new species and new germplasm without prior efforts to discover and characterize genetic variants (Poland and Rife, 2012).

The introductory demonstration of GBS library construction was performed on the highly diverse maize (*Zea mays* L.) and barley species (Elshire et al., 2011). The original GBS protocol, provided by Elshire and colleagues (2011) and Poland and Rife (2012), is summarized as follows. High molecular weight genomic DNAs are extracted from individuals of interest, normalized to ensure equal representation among samples, and digested with restriction enzymes. Bar code and common adapters are ligated to

fragmented DNA and samples are pooled and cleaned, constituting libraries. Libraries are amplified via PCR, cleaned, evaluated for size via capillary electrophoresis, and sequenced on an Illumina platform.

Adaptability and low cost have resulted in the application of the GBS method to various studies including genetic linkage mapping and QTL analysis (Fiedler et al., 2015; Mahoney et al., 2016; Poland et al., 2012a; Ward et al., 2013), characterization of genetic diversity (Byrne et al., 2013; Lu et al., 2013; Pembleton et al., 2016), genomic selection (GS), prediction, and heritability (Ashraf et al., 2016; Crossa et al., 2013; Poland et al., 2012b), and GWAS (Arruda et al., 2016).

The original GBS approach was extended to a two-enzyme method by Poland et al. (2012a) for the establishment of high-density genetic maps of the complex diploid barley and hexaploid wheat genomes. Greater than 34,000 SNPs and 240,000 tags were assigned to a reference map of barley and greater than 20,000 SNPs and 367,000 tags were assigned to a reference map of wheat. The two-enzyme method included rare- and common-cutting restriction enzymes, which allowed for generation of uniform libraries. This method is preferential for large, complex genomes and provides a viable approach for analyzing species lacking reference genomes (Poland et al., 2012a).

Linkage maps have been constructed with GBS for additional plant species including perennial ryegrass, red raspberry (*Rubus idaeus* L.), switchgrass (*Panicum virgatum* L.), and the ancestral diploid strawberry (*Fragaria iinumae* Makino). An ultra-high density linkage map was constructed in perennial ryegrass by Vemururgan et al. (2016) using GBS-derived SNP and presence-absence variation markers. Ward and colleagues (2013) used GBS to establish two parental red raspberry linkage maps, to

which they mapped 6,912 SNP markers across seven linkage groups. Timeliness and cost-effectiveness of generating linkage maps with GBS-derived SNP markers was presented in the outcrossing switchgrass species (Fiedler et al., 2015). Linkage maps generated with 4,611 SNP markers from genotype analyses of 231 F_1 progeny shared collinearity with prior SSR marker-based maps. In addition, SNP markers were localized to regions of the genome that were previously unpopulated (Fiedler et al., 2015). Mahoney et al (2016) established a linkage map of the ancestral diploid strawberry via 893 GBS-based SNP markers.

Quantitative trait loci mapping

Plant traits can be broadly classified as qualitative or quantitative in nature (Bernardo, 2002; Poehlman and Sleper, 1995). Qualitative traits are those that have distinct phenotypes and are genetically controlled by only one or a few genes (Bernardo, 2002; Poehlman and Sleper, 1995). Such traits are minimally influenced by environmental effects and are studied by analyses of inheritance patterns or phenotypic ratios (Bernardo, 2002; Poehlman and Sleper, 1995). Quantitative traits, conversely, are those that have a continuum of phenotypes and are genetically controlled by the combined action of many genes (Bernardo, 2002; Poehlman and Sleper, 1995). Quantitative traits are under greater influence by environmental effects and are studied by analyses of central tendency and dispersion (Bernardo, 2002; Poehlman and Sleper, 1995).

The term quantitative trait loci (QTL) references genomic regions where genes associated with quantitative traits are located (Collard et al., 2005; Geldermann, 1975;

Sing and Singh, 2015; Xu, 2010). Such regions are not identifiable based on evaluations of phenotypes alone (Collard et al., 2005). However, the development of molecular markers in the 1980s revolutionized the characterization of quantitative traits (Collard et al., 2005; Xu, 2010). The construction of high-density molecular maps, genome-wide mapping, and manipulation of genes affecting quantitative traits has been enabled through the increased interchange between molecular biology and quantitative genetics since the 1990s (Xu, 2010). Marker-based genetic analyses are employed to identify QTL and estimate QTL effects, a process often termed as QTL mapping (Xu, 2010).

The mapping of QTL requires an appropriate mapping population, a linkage map of the species containing a dense population of markers, accurate and dependable phenotyping of the trait of interest, and suitable software packages for analysis of the data (Bernardo, 2002; Singh and Singh, 2015; Xu, 2010). The generalized procedure for QTL mapping includes developing, genotyping, and phenotyping a mapping population, generating linkage maps with the resulting data, and establishing associations between markers and traits (Langridge and Chalmers, 2004; Singh and Singh, 2015).

Developing a mapping population

A mapping population is a group of segregating individuals, which are derived by cross-fertilization of parents that differ for one or more traits. The structure of mapping populations can vary greatly depending on numerous factors including the mode of reproduction of a given plant species and the aims of a particular mapping project. The size of mapping populations vary as well; for example, high-resolution mapping requires

a larger number of individuals than other projects such as preliminary mapping. In general, mapping populations for cross-pollinated species are more complex than self-pollinated species because the cross-pollinated species are typically intolerant of inbreeding. A proven mapping population structure for cross-pollinated species was exemplified in white clover (*Trifolium repens* L.) and perennial ryegrass (Barrett et al., 2004; Forster et al., 2000). For these species, biparental pseudo-F_2 generation mapping populations were established from two heterozygous parents that were phenotypically different for traits of interest (Barrett et al., 2004; Forster et al., 2000).

Genotyping a mapping population

Genotyping a mapping population involves identifying polymorphic markers between the parental lines and assaying those markers across all individuals in the population. This is typically conducted in two distinct steps; however, in the GBS procedure, identifying polymorphic markers and assaying the markers across individuals is completed in a single step. It is imperative that polymorphic markers are both high in number and sufficiently distributed across the entire genome for quality linkage analyses (Collard et al., 2005; Singh and Singh, 2015; Xu, 2010; Young, 1994). Cross-pollinated species tend to exhibit greater DNA polymorphism compared to self-pollinated species (Collard et al., 2005).

Linkage mapping

Linkage maps provide visual representations of the relative locations of genetic markers across the chromosomes of an organism. The locations of the markers are determined via estimation of recombination frequencies between pairs of markers, defined in units of genetic distances known as centiMorgan (cM) or map units (Bernardo, 2002). The underlying principle for linkage map construction is that more recombination events occur between loci that are further apart on the same chromosome compared to loci that are closer together on the same chromosome (Bernardo, 2002). A map unit of 1 cM represents one recombination event out of 100 possible recombination events (Bernardo, 2002).

Linkage analyses are conducted with various computer software programs such as JoinMap (Stam, 1993), Mapmaker/EXP (Lander et al., 1987; Lincoln et al., 1993a), and MapManager QTX (Manly et al., 2001). The ratio of linkage versus no linkage, also known as the odds ratio, is commonly used to calculate linkage between markers (Collard et al., 2005). The odds ratio is most often referenced as the logarithm of odds (LOD) value or LOD score as it is most suitably written as the logarithm of the odds ratio (Bernardo, 2002; Collard et al., 2005; Risch, 1992). A LOD value of 3.0 between two markers means that linkage is 1,000 time more likely than no linkage; values greater than 3.0 are commonly used to construct linkage maps (Bernardo, 2002; Collard et al., 2005). Within a marker interval, the highest LOD score indicates the most plausible location of a QTL (Bernardo, 2002). However, LOD value thresholds can be adjusted according to demands of the study (Collard et al., 2005).

Linked markers are placed into linkage groups, which represent entire chromosomes or chromosomal segments (Collard et al., 2005). In instances, the number of linkage groups and the number of chromosomes for a species do not agree (Collard et al., 2005). These findings can result from uneven distribution of molecular markers or non-uniform recombination frequencies across a given genome (Collard et al., 2005; Hartl and Jones, 2001; Paterson, 1996; Xu, 2010; Young, 1994). It is possible that polymorphic markers are dense in certain chromosomal regions and completely absent in others (Paterson, 1996). With respect to non-uniform recombination frequencies, heterochromatic and centromeric regions are well characterized to exhibit suppressed recombination (cold spots), whereas other regions are known to exhibit frequent recombination (hot spots) (Hartl and Jones, 2001; Singh and Singh, 2015; Xu, 2010; Young, 1994).

Phenotyping a mapping population

Phenotyping a mapping population involves determining the type and level of expression of a target trait among all individuals in the population (Singh and Singh, 2015). Accurately phenotyping an individual is generally considered more difficult than accurately genotyping an individual due to environmentally sensitive quantitative traits (Singh and Singh, 2015). Ideally, phenotypic data should be collected from replicated trials, across multiple locations and years to limit environmental effects (Singh and Singh, 2015).

Detection and mapping of quantitative trait loci

There are a number of approaches for analyzing QTL; each of which can be assigned to one of two primary groups: (i) single QTL mapping or (ii) multiple QTL mapping (Singh and Singh, 2015). The single QTL mapping group consists of approaches such as single-marker analysis (SMA) and simple interval mapping (SIM) (Bernardo, 2002; Singh and Singh, 2015; Xu, 2010). The multiple QTL mapping group includes approaches such as composite interval mapping (CIM), multiple interval mapping (MIM), and Bayesian multiple QTL mapping (Bernardo, 2002; Singh and Singh, 2015; Xu, 2010). The majority of these approaches detect QTL via the use of Bayesian models, regression analysis, or estimation of maximum likelihood (ML) parameters (Singh and Singh, 2015).

Single QTL mapping, as implied by the name, identify a single QTL at a given time (Bernardo, 2002; Singh and Singh, 2015). These were the earliest developed and most simplistic methods and they remain relevant for some applications today (Sing and Singh, 2015; Xu, 2010). As indicated previously, quantitative traits are generally considered to be under control of many genes, which are likely distributed across multiple QTL. Single QTL mapping methods, however, do not account for additional QTL that may be present in other regions of the genome (Singh and Singh, 2015). This implies that single QTL mapping methods may be less reliable than multiple QTL mapping methods, which consider all QTL that affect a target trait. Multiple QTL mapping methods increase the power to detect QTL, allow for separation and identification of two linked QTL, and enable detection of QTL × QTL interaction.

Single-marker analysis

The SMA, also known as single-point analysis, is a single QTL mapping method in which each marker is independently monitored for association with the target trait (Collard et al., 2005; Singh and Singh, 2015). This is the least computationally intensive method; it does not require construction of marker linkage maps and it can be conducted with commonly used statistical software (Collard et al., 2005; Singh and Singh, 2015). The SMA uses tests such as analysis of variance, linear regression, or maximum likelihood estimation to evaluate phenotypic means of individuals with different marker genotypes (Bernardo, 2002; Collard et al., 2005; Singh and Singh, 2015).

The SMA approach for single QTL mapping has a low QTL detection power and is limited by a number of factors. This method is unable to determine if one or multiple QTL are associated with a marker and it is highly influenced by the rate of recombination (Collard et al., 2005; Singh and Singh, 2015). For instance, if the recombination rate increased, the likelihood of identifying a given QTL would decrease (Singh and Singh, 2015). Further, the SMA approach does not assess the recombination rate between a marker and a QTL, which leads to an inability to locate a given QTL in the genome (Singh and Singh, 2015).

Single interval mapping

Interval mapping, generally referenced as SIM, was established by Lander and Botstein (1989), and is currently noted as a standard single QTL mapping approach (Bernardo, 2002; Singh and Singh, 2015). This method requires that a linkage map be constructed, and localizes QTL onto the map by providing a LOD score curve (Collard et

al., 2005; Singh and Singh, 2015). With respect to QTL detection, the SIM procedure is regarded as being more statistically influential than SMA (Collard et al., 2005; Lander and Botstein, 1989; Liu, 1998; Singh and Singh, 2015). The SIM approach searches for QTL within marker intervals, which are defined by neighboring marker pairs, in a systematic fashion whereby each marker interval is assessed independently of other marker intervals (Collard et al., 2005; Singh and Singh, 2015). Software packages such as MapMaker/QTL (Lincoln et al., 1993b) and QGene (Nelson, 1997) have been used to conduct SIM (Collard et al., 2005).

Limitations of the SIM procedure pertain to computational intensity and assessments of single marker intervals independent from other marker intervals. As mentioned previously, the SIM procedure provides more statistical power than the SMA procedure; however, this requires more computational input (Singh and Singh, 2015). When there is linkage between two or more QTL affecting a target trait, the estimates of QTL localization in the genome and QTL effect tend to be biased (Singh and Singh, 2015). Moreover, when two QTL are located close to one another, SIM tends to identify 'ghost' QTL (Singh and Singh, 2015).

Composite interval mapping

The CIM procedure is a relatively simplistic multiple QTL mapping approach that combines multiple regression analysis with interval mapping (Jansen, 1993; Jansen and Stam, 1994; Zeng, 1993,1994; Singh and Singh, 2015). The CIM begins as a SMA then develops into a multiple QTL model via forward or stepwise regression (Singh and Singh, 2015). Precision of QTL detection is increased in CIM because effects of QTL

located in other marker intervals are controlled (Collard et al., 2005; Singh and Singh, 2015). Due to widespread implementation in software programs such as QTL Cartographer (Basten et al. 1994, 2001), MapManager QTX (Manly et al., 2001), and PLABQTL (Utz and Melchinger, 1996), CIM is now the preferred approach for QTL mapping in biparental populations (Collard et al., 2005; Singh and Singh, 2015). The CIM procedure is only limited by the arbitrary selection of cofactors and the inability to detect QTL × QTL interaction, a drawback that restricts use when epistatic interactions are present (Singh and Singh, 2015).

The generalized procedure for CIM has been summarized by Zhang and Zhang (2015). To begin, the single marker with the highest LOD score is selected and added to the model. Immediately following, the marker with the second highest LOD score is selected and added to the model. The two markers are then reevaluated for significance. In the case that both remain significant, the marker with the third highest LOD score is selected and incorporated into the model. Again, the significance of all three markers is reevaluated. This process is continued, and all the markers that are significant when jointly evaluated are added to the models as cofactors. The entire genome is evaluated for QTL detection and mapping.

Multiple interval mapping

The MIM procedure is a multiple QTL mapping approach developed to simultaneously map QTL in multiple marker intervals (Kao et al., 1999; Singh and Singh, 2015). As with CIM, the MIM procedure is implemented in software programs such as QTL Cartographer (Basten et al., 1994, 2001), but unlike the CIM procedure, MIM does

not require complicated selections of background markers (Singh and Singh, 2015). Instead, MIM utilizes forward and backward selection methods and forward search methods to identify the most appropriate genetic models; model selection processes are guided by the QTL Cartographer software program (Singh and Singh, 2015). An advantage to MIM, compared with CIM, is that it can accommodate epistatic interactions that may be present among QTL in the model (Singh and Singh, 2015).

A primary limitation to MIM implementation is the computational intensity that arises due to an exponential increase in the number of parameters resulting from an increase in the number of QTL included in the model (Singh and Singh, 2015). The MIM procedure is also characterized by saturation that prevails when the number of covariates exceeds the number of samples, and when a large number of QTL are present in the model (Singh and Singh, 2015). The final challenge of MIM is the selection of an appropriate model as there is no reliable model selection criterion to aid in selection among the large number of possible models (Singh and Singh, 2015).

Bayesian multiple quantitative trait locus mapping

The Bayesian multiple QTL mapping procedure, like CIM, utilizes ML functions to detect QTL (Singh and Singh, 2015; Xu, 2010). In the Bayesian multiple QTL mapping method, the number of QTL is treated as a random variable and reversible-jump Markov chain Monte Carlo (MCMC) procedures are used for specific modeling (Banerjee et al., 2008; Satgopan et al., 1996). Bayesian modeling involves selecting a prior distribution and inferring results from a posterior distribution, which is derived from the prior (Singh and Singh, 2015). The Bayesian multiple QTL mapping procedures are

capable of handling uncertainties associated with location, number, and missing genotypes of QTL (Singh and Singh, 2015). The primary advantage of Bayesian procedures is that they estimate the probability of QTL existence in a given marker interval (Singh and Singh, 2015).

Bayesian multiple QTL mapping may not offer much advantage compared to conventional QTL mapping procedures (CIM and MIM, for example) in cases where genotype data are near completion and detailed genetic maps are available (Singh and Singh, 2015). The widespread use of Bayesian methods for multiple QTL mapping has been limited due to computation complexities, difficulty in prior distribution selection, and lack of user-friendly software programs (Singh and Singh, 2015).

Quantitative trait loci confidence interval

The location of a given QTL is presented as a bar alongside a linkage maps whereby the bar length depicts the interval in which the QTL is most likely positioned (Singh and Singh, 2015). The interval is referenced as the confidence interval or the support interval and can be calculated by various methods including two of the most common, the LOD score drop-off method and the bootstrapping method (Collard et al., 2005; Hackett, 2002; Lander and Botstein, 1989; Sing and Singh, 2015; Xu, 2010). The LOD score drop-off method, also called the one-LOD support interval, is defined as the interval to either side of the peak LOD score where the LOD score drops to one value less than the peak LOD score value (Collard et al., 2005; Hackett, 2002; Lander and Botstein, 1989; Sing and Singh, 2015). The bootstrapping method is a statistical

approach that utilizes resampling procedures, which are implemented in computer software programs such as MapManager QTX (Collard et al., 2005; Manly et al., 2001; Singh and Singh, 2015; Talbot et al., 1999; Visscher et al., 1996).

Quantitative trait loci mapping studies in ryegrass

Hayward et al. (1994, 1998) established the primary low-density genetic map of ryegrass using isozymes, RFLPs, and RAPDs. In recent years, high-density genetic maps for intraspecific perennial ryegrass populations and interspecific perennial × Italian ryegrass (*Lolium multiflorum* Lam.) populations have been generated (Bushman and Warnke, 2013). High-density intraspecific linkage maps have been based on various combinations of genetic markers including AFLPs, ESTs, and isozymes (Bert et al., 1999), AFLPs, RFLPs, and SSRs (Jones et al., 2002a), AFLPs, ESTs, RFLPs, and isozymes (Jones et al., 2002b); AFLPs, CAPS, RFLPs, SSRs, and STSs (Armstead et al., 2004), AFLPs, RFLPs, SSRs, and STSs (Muylle et al., 2005), and ESTs, RFLPs, and SSRs (Gill et al., 2006). High-density interspecific linkage maps have been based on RAPDs, RFLPs, and isozymes (Hayward et al., 1998) and AFLPs, RAPDs, RFLPs, SSRs, isozymes, and morphological characters (Warnke et al., 2004). Most recently, as discussed in a prior section, a perennial ryegrass linkage map was constructed with SNP markers derived from a GBS study (Velmurugan et al., 2016).

Numerous QTL mapping studies have been conducted for traits such as disease resistance, morphology and development, and abiotic stress tolerance (Bushman and Warnke, 2013). Pfender et al. (2011) constructed linkage maps with combinations of

SSR, STS, and SNP markers to identify three QTL for stem rust resistance in perennial ryegrass. QTL have also been discovered for resistance to crown rust in ryegrass (Dumsday et al., 2003; Muylle et al., 2005; Sim et al., 2007; Studer et al., 2007). A single QTL for crown rust resistance was found by using SSR markers alone (Dumsday et al., 2003). Two crown rust resistance QTL were identified when SSR and AFLP markers were utilized for the construction of linkage maps (Studer et al., 2007). The use of either AFLP, RAPD, RFLP, SSR, isozyme, and morphological markers (Sim et al., 2007) or AFLP, RFLP, SSR, and STS markers (Muylle et al., 2005) led to the identification of four QTL for crown rust resistance.

Gray leaf spot resistance in ryegrass has also been analyzed via QTL mapping methods (Curley et al., 2005; Curley et al., 2008). In an initial study, a combination of AFLP, RAPD, RFLP, SSR, isozyme, and morphological markers were used for linkage map construction (Curley et al., 2005). This led to the discovery of four QTL for gray leaf spot resistance in ryegrass, two of which were considered major QTL (Curley et al., 2005). As a follow up, Curley et al (2008) studied the durability of the four gray leaf spot resistance QTL in a subsequent generation population. A single gray leaf spot resistant individual from the original population was selected and crossed to an unrelated gray leaf spot susceptible individual (Curley et al., 2008). Linkage maps were constructed with RAPD, RFLP, and SSR markers, and, indeed, one of the two major QTL previously described by Curley and colleges (2005) were recovered by Curley et al. (2008).

A study for forage quality traits included an AFLP, RFLP, and SSR marker based linkage map whereby 42 QTL were identified for herbage quality traits, which is an important characteristic for perennial ryegrass in forage usage (Cogan et al., 2005).

Jensen et al. (2005) identified five QTL for vernalization response in perennial ryegrass by constructing linkage maps with AFLP, CAPS, and SSR markers. A single QTL for winter hardiness and multiple QTL for morphological and developmental traits were identified via the use of AFLP, RFLP, and SSR markers (Yamada et al., 2004).

Literature cited

Ahti, K., A. Moustafa, and H. Kaerwer. 1980. Tolerance of turfgrass cultivars to salt. In: Proceedings of the 3rd International Turfgrass Research Conference, p. 165–171

Altshuler, D., V.J. Pollara, C.R. Cowles, W.J. Van Etten, J. Baldwin, L. Linton, and E.S. Lander. 2000. An SNP map of the human genome generated by reduced representation shotgun sequencing. Nature. 407:513–516

Ansorge, W.J. 2009. Next-generation DNA sequencing techniques. New Biotechnology. 25:195–203

Armstead, I.P., L.B. Turner, M. Farrell, L. Skot, P. Gomez, T. Montoya, I.S. Donnison, I.P. King, and M.O. Humphreys. 2004. Synteny between a major heading-date QTL in perennial ryegrass (*Lolium perenne* L.) and the *Hd3* heading-date locus in rice. Theor. Appl. Genet. 108:822–828

Arruda, M.P., P. Brown, G. Brown-Guedira, A.M. Krill, C. Thurber, K.R. Merrill, B.J. Foresman, F.L. Kolb. 2016. Genome-wide association mapping of Fusarium head blight resistance using genotyping by sequencing. The Plant Genome. 9. doi: 10.3835/plantgenome2015.04.0028

Ashraf, B.H., S. Byrne, D. Fe, A. Czaban, T. Asp, M.G. Pederson, I. Lenk, N. Roulund, T. Didion, C.S. Jensen, J. Jensen, L.L. Janss. 2016. Estimating genomic heritabilities at the level of family-pool samples of perennial ryegrass using genotyping-by-sequencing. Theor. Appl. Genetics. 129:45–52

Avila, C.M., J.C. Sillero, D. Rubiales, M.T. Moreno, and A.M. Torres. 2003. Identification of RAPD markers linked to the Uvf-1 gene conferring hypersensitive resistance against rust (*Uromyces vicia-fabae*) in *Vicia faba* L. Theor. Appl. Genet. 107:353–358

Ayers, R.S., and D.W. Westcot. 1985. Water quality for agriculture. FAO Irrig. Drainage Paper 29 CSS–200059097

Babu, K.N., M.K. Rajesh, K. Samsudeen, D. Minoo, E.J. Suraby, K. Anupama, and P. Ritto. 2014. Randomly amplified polymorphic DNA (RAPD) and derived techniques. Methods Mol. Biol. 1115:191–209

Baird, N.A., P.D. Etter, T.S. Atwood, M.C. Currey, A.L. Shiver, Z.A. Lewis, E.U. Selker, W.A. Cresko, and E.A. Johnson. 2008. Rapid SNP discovery and genetic mapping using RAD markers. Plos One. 3:e3376

Bandyopadhyay, B.K., H.S. Sen, B. Maji, and J.S.P. Yadav. 2001. Saline and alkali soils and their management. Monogram Series 1, Indian Society of Coastal Agricultural Research, Coastal Soil Salinity Research Institute, Canning Town, West Bengal, India. 72 pp.

Banerjee, S., B.S. Yandell, and N. Yi. 2008. Bayesian quantitative trait loci mapping for multiple traits. Genetics179:2275–2289

Barker, R.E., J.A. Kilgore, R.L. Cook, A.E. Garay, and S.E. Warnke. 2001. Use of flow cytometry to determine ploidy level of ryegrass. Seed Sci. Tech. 29: 493–502

Barrett, B., A. Griffiths, M. Schreiber, N. Ellison, C. Mercer, J. Bouton, B. Ong, J. Forster, T. Sawbridge, G. Spangenburg, G. Bryan, and D. Woodfield. 2004. A microsatellite map of white clover. Theor. Appl. Genet. 109: 596–608

Basten, C.J., B.S. Weir, and Z.B. Zeng. 1994. Zmap - a QTL cartographer. *In*: J.S.G.C. Smith, B.J. Benke, W.F. Chesnais, J.P. Gibson, B.W. Kennedy, and E.B. Burnside (Eds.), Proceedings of the 5th World Congress on Genetics Applied to Livestock Production: Computing Strategies and Software, Guelph, Ontario, Canada. Published by the Organizing Committee, 5th World Congress on Genetics Applied to Livestock Production

Basten, C., B. Weir, Z.B. Zeng. 2001. QTL Cartographer. Department of Statistics, North Carolina State University, Raleigh, NC

Bauer, B.K., R.E. Poulter, A.D. Troughton, and D.S. Loch. 2009. Salinity tolerance of twelve hybrid bermudagrass [*Cynodon dactylon* (L.) pers. × *C. transvaalensis* burtt davy] genotypes. Int. Turfgrass Soc. Res. J. 11:313–326

Bean, E.W., and C. Yok-Hwa. 1972. An analysis of the growth of inbred progeny of *Lolium*. J. Agric. Sci. 79: 147–153

Beard, J.B. 1973. Turfgrass: Science and Culture. Prentice Hall, Englewood Cliffs, NJ.

Beard, J.B., and H.J. Beard. 2005. Beard's Turfgrass Encyclopedia for Golf Courses, Grounds, Lawns, Sports Fields. Michigan State University Press

Beissinger, T.M., C.N. Hirsch, R.S. Sekhon, J.M. Foerster, J.M. Johnson, G. Muttoni, B. Vaillancourt, C.R. Buell, S.M. Kaeppler, and N. de Leon. 2013. Marker density and read depth for genotyping populations using genotyping-by-sequencing. Genetics. 193:1073–1081

Bennett, F.T. 1937. Dollarspot disease of turf and its causal organism, *Sclerotinia homoeocarpa* n. sp. Annals Appl. Biol. 24:236–257

Bernardo, R. 2002. Breeding for quantitative traits in plants. Stemma Press, Woodbury, MN, USA.

Bernatzky, R., and S.D. Tansley. 1986. Toward a genetic map in tomato based on isozymes and random cDNA sequences. Genetics. 112:887–898

Bert, P.F., G. Charmet, P. Sourdille, M.D. Hayward, and F. Balfourier. 2999. A high-density map for ryegrass (*Lolium perenne* L.) using AFLP markers. Theor. Appl. Genet. 99:445–452

Bonos, S.A. 2011. Gene action of dollar spot resistance in creeping bentgrass. Phytopathology 159: 12–18

Bonos, S.A., and D.R. Huff. 2013. Cool-season grasses: biology and breeding. In: J.C. Stier, B.P. Horgan, and S.A. Bonos, editors, Turfgrass: biology, use, and management. ASA, CSSA, and SSSA, Madison, WI. p.591–660

Bonos, S.A., B.B. Clarke, and W.A. Meyer. 2006. Breeding for disease resistance in the major cool-season turfgrasses. Annu. Rev. Phytopathol. 44:213–234

Bonos, S.A., C. Kubik, B.B. Clarke, and W.A. Meyer. 2004. Breeding perennial ryegrass for resistance to gray leaf spot. Crop Sci. 44: 575–580

Bonos, S.A., M.D. Casler, and W.A. Meyer. 2003. Inheritance of dollar spot resistance in creeping bentgrass. Crop Sci. 43: 2189–2196

Bonos, S.A., M. Koch, J.A. Honig, T. Gianfagna, and B. Huang. 2009. Evaluating cool-season turfgrasses for salinity tolerance. USGA Green Section Record 47: 6–9

Brady, N.C., and R.R. Weil. 2004. Elements of the nature and properties of soils. Prentice Hall, Upper Saddle River, NJ.

Bresler, E., B.L. McNeal, and D.L. Carter. 1982. Saline and sodic soils. Springer Verlag, NY.

Brilman, L.A. 2005. Turfgrass breeding in the United States: public private cool- and warm-season. Int. Turf. Soc. Res. 10:508–515

Brunner, A.L., D.S. Johnson, S.W. Kim, A. Valouev, T.E. Reddy et al. 2009. Distinct DNA methylation patterns characterize differentiated human embryonic stem cells and developing human fetal liver. Genome Res. 19:1044–1056

Bushman, B.S., and S.E. Warnke. 2013. Genetic and genomic approaches for improving turfgrass. In: J.C. Stier, B.P. Horgan, and S.A. Bonos, editors, Turfgrass: biology, use, and management. ASA, CSSA, and SSSA, Madison, WI. p.683–712

Byrne, S.A. Czaban, B. Studer, F. Panitz, C. Bendixen, and T. Asp. 2013. Genome wide allele frequency fingerprints (GWAFFs) of populations via genotyping by sequencing. Plos One. 8:e57438

Caldeira R.L., O.S. Carvalho, R.C.G. Lage, P.C.M. Cardosa, and G.C. Oliveira. 2002. Sequencing of simple sequence repeat anchored polymerase chain reaction

amplification products of *Biomphalaria glabrata*. Mem. Inst. Oswaldo Cruz, Rio de Janeiro 97:23–26

Carrow, R.N., and R.R. Duncan. 1998. Salt-affected turfgrass sites: Assessment and management. Ann Arbor Press. Chelsea, MI.

Carrow, R.N., and R.R. Duncan. 2012. Best management practices for saline and sodic turfgrass soils. CRC Press, Boca Raton, FL.

Casler, M.D., and R.R. Duncan. 2003. Turfgrass biology, genetics, and breeding. John Wiley & Sons

Chargaff, E. 1951. Structure and function of nucleic acid as cell constituent. Fed. Proc. 10:654–659

Chargaff, E., E. Vischer, R. Doniger, C. Green, and F. Misani. 1949. The composition of the desoxypentose nucleic acid of thymus and spleen. J. Biol. Chem. 177:405–416

Cisar, J.L., M. Reuter, G.H. Snyder, M.A. Fidanza. 2006. The use of non-saline reclaimed water for golf course irrigation in Florida. Appl. Turfgrass Sci. doi:10.1094/ATS–2006–0210–02–TT.

Cogan, N.O.I., K.F. Smith, T. Yamada, M.G. Francki, A.C. Vecchies, E.S. Jones, G.C. Spangenberg, and J.W. Forster. 2005. QTL analysis and comparative genomics of herbage quality traits in perennial ryegrass (*Lolium perenne* L.). Theor. Appl. Genet. 110:364–380

Cole, H., B. Taylor, J. and Duich. 1968. Evidence of differing tolerances to fungicides among isolates of *Sclerotinia homoeocarpa*. Phytopathology. 58:683–686

Cole, H., C.G. Warren, and P.L. Sanders. 1974. Fungicide tolerance - A rapidly emerging problem in turfgrass disease control. Int. Turfgrass Res. J. 2:344–349

Collard, B.C.Y, M.Z.Z. Jahufer, J.B. Brouwer, and E.C.K. Pang. 2005. An introduction to markers, quantitative trait loci (QTL) mapping and marker-assisted selection for crop improvement: the basic concepts. Euphytica. 142:169–196

Committee on Water Quality Criteria (National Academy of Sciences and national Academy of Engineering). 1972. Water quality criteria, 1972. Natl. Serv. Cent. Environ. Publ. (NSCEP) Rep. No. EPA–R3–73–033. USEPA, Washington, D.C.

Cornish, M.A., M.D. Hayward, and M.J. Lawrence. 1979. Self-incompatibility in ryegrass. I. Genetic control in diploid *Lolium perenne* L. Heredity. 43: 95–106

Cornish, M.A., M.D. Hayward, and M.J. Lawrence. 1980. Self-incompatibility in ryegrass. V. Genetic control, linkage and seed set in diploid *Lolium perenne* L. Heredity. 44:333–340

Crossa, J., Y. Beyene, S. Kassa, P. Perez, J.M. Hickey, C. Chen, G. de los Campos, J. Burgueno, V.S. Windhausen, E. Buckler, J.L. Jannink, M.A.L. Cruz, and R. Babu. 2013. Genomic prediction in maize breeding populations with genotyping-by-sequencing. G3 Genes | Genomes | Genetics. 3:1903–1926

Couch, H. B. 1995. Diseases of Turfgrasses. Krieger Publishing Company, Malabar, FL.

Couch, H. B. 2000. The Turfgrass Disease Handbook. Krieger Publishing Company, Malabar, FL.

Couch, H.B., and J.R. Bloom. 1960. Influence of environment on diseases of turfgrasses. II. Influence of nutrition, pH and soil moisture on Sclerotinia dollar spot. Phytopathol. 50:761–763

Curley, J., N. Chakrabory, S. Chang, and G. Jung. 2008. QTL mapping of resistance to gray leaf spot in ryegrass: consistency of QTL between two mapping populations. Kor. Turfgrass Sci. 22:85–100

Curley, J., S.C. Sim, S. Warnke, S. Leong, and R. Barker. 2005. QTL mapping of resistance to gray leaf spot in ryegrass. Theor. Appl. Genet. 111:1107–1117

Dahm, R. 2005. Friedrich Miescher and the discovery of DNA. Developmental Bio. 278:274–288

Dahm, R. 2008. Discovering DNA: Friedrich Miescher and the early years of nucleic acid research. Human Genetics. 122:565–581

DaRocha, A.B., R. Hammerschmidt. 2004. Increase in oxalate oxidase activity in bentgrass response to *Sclerotinia homoeocarpa* and chemical treatment. Phytopahthology 94:S157.

Davey, J.W., P.A. Hohenlohe, P.D. Etter, J.Q. Boone, J.M. Catchen, and M.L. Baxter. 2011. Genome-wide genetic marker discovery and genotyping using next-generation sequencing. Nat. Rev. Genet. 12:499–510

de Viennne, D. (ed.) 2003. Molecular markers in plant genetics and biotechnology. Science Publisher, Inc. Enfield, NH, USA.

Detweiler, A.R., J.M. Vargas, and T.K. Danneberger. 1983. Resistance of *Sclerotinia homoeocarpa* to iprodione and benomyl. Plant Dis. 67:627–632

Devitt, D.A., R.L. Morris, M. Baghzouz, and M. Lockett. 2005. Water quality changes in golf course irrigation ponds transitioning to reuse water. HortScience 40:2151–2156

Devitt, D.A., R.L. Morris, D. Kopec, and M. henry. 2004. Golf course superintendents' attitudes and perceptions toward using reuse water for irrigation in the southwestern United States. hortTechnology 14:1–7

Dolezel, J., J. Vrana, P. Capal, M. Kubalakava, V. Buresova, and H. Simkova. 2014. Advances in plant chromosome genomics. Biotechnology Advances. 32:122–136

Dressman, D., H. Yan, G. Traverso, K.W. Kinzler, and B. Vogelstein. 2003. Transforming single DNA molecules into fluorescent magnetic particles for detection and enumeration of genetic variations. Proc. Natl. Acad. Sci. USA 100:8817–8822

Dudeck, A.E., and C.H. Peacock. 1985. Salinity effects on warm-season turfgrasses. In: Proceedings of the 33rd Annual Florida Turfgrass Conference 33. p. 22–24

Dudeck, A.E., C.H. Peacock, and J.C. Wildmon. 1993. Physiological and growth responses of St. Augustinegrass cultivars to salinity. HortScience 28:46–48

Dumsday, J.L., K.F. Smith, J.W. Forster, and E. Jones, 2003. SSR-based genetic linkage analysis of resistance to crown rust (*Puccinia coronate* f. sp. *lolii*) in perennial ryegrass (*Lolium perenne* L.). Plant Pathol. 52:628–637

Echt, C.S., K.K. Kidwell, J.S. Knapp, T.C. Osborn, and T.J. McCoy. 1994. Linkage mapping in diploid alfalfa (*Medicago saiva*). Genome. 37:61–71

Edwards, D., J.W. Forster, D. Chagne, and J. Batley. 2007a. What is SNPs? In: N.C. Oraguzie, E.H.A. Rikkerink, S.E. Gardiner, and H.N. Silva, editors, Association Mapping in Plants. Springer, Berlin, p.41–52

Edwards, D., J.W. Forster, D. Chagne, and J. Batley. 2007b. Single nucleotide polymorphism discovery. In: N.C. Oraguzie, E.H.A. Rikkerink, S.E. Gardiner, and H.N. Silva, editors, Association Mapping in Plants. Springer, Berlin, p. 53–76

Elshire, R.J., J.C. Glaubitz, Q. Sun, J.A. Poland, K. awamoto, E.S. Buckler, and S.E. Mitchell. 2011. A robust, simple genotyping-by-sequencing (GBS) approach for high diversity species. Plos One. 6:e19379

Endo, R.M. 1963. Influence of temperature on rate of growth of five fungus pathogens of turfgrass and on rate of disease spread. Phytopathology. 55:857–861

Evans, G. 1926. Chromosome complements in grasses. Nature. 118:841

Fan, J., M.S. Chee, and K.L. Gunderson. 2006. Highly parallel genomic assays. Nat. Rev. Genet. 7:632–644

Farnham, D.S., R.F. Hasek, and J.L. Paul. 1985. Water quality: Its effects on ornamental plants. Univ. of Calif. Coop. Ext. Leaflet 2995. Div. of Agric. Nat. Resources, Oakland, CA.

Fearon, C.H., M.A. Cornish, M.D. Hayward, and M.J. Lawrence. 1994. Self-incompatibility in ryegrass. X. Number and frequency of alleles in a natural population of *Lolium perenne* L. Heredity. 73: 254–261

Fenstermacher, J.M. 1970. Variation within *Sclerotinia homoeocarpa* F.T. Bennett. M.S. Thesis, Univ. Rhode Island, Kingston. 68p.

Fenstermacher, J.M. 1980. Certain features of dollar spot disease and its causal organism. In: Advances in Turfgrass Pathology, B.G. Joyner and P.O. Larson, Ed. Harcourt Brace Jovanovich: Duluth. p.49–53

Fiedler, J.D., C. Lanzatella, M. Okada, J. Jenkins, J. Schmutz, and C.M. Tobias. 2015. High–density single nucleotide polymorphism linkage maps of lowland switchgrass using genotyping-by-sequencing. The Plant Genome. 8. doi:10.3835/plantgenome2014.10.0065

Fleischmann, R.D., M.D. Adams, O. White, et al. 1995. Whole-genome random sequencing and assembly of *Haemophilus influenza* Rd. Science. 269:496–512

Flowers, T.J. 2004. Improving crop salt tolerance. J. Exp. Bot. 55:307–319.

Forster, J.W., E.S. Jones, R. Kolliker, M.C. Drayton, J.L. Dumsday, M.P. Dupal, K.M. Guthridge, N.L. Mahoney, E. van Zijll de Jong, and K.F. Smith. 2000. Development and implementation of molecular markers for crop improvement. *In*: Molecular Breeding of Forage Crops. In: G. Spangenberg, editor, Proceedings of the 2nd International Symposium, Lorne and Hamilton, Victoria Australia, November 19–24, pp. 101–133, Kluwer Academic Publishers, London

Funk, C.R., and B.B. Clarke. 1989. Turfgrass breeding - with special reference to turf-type perennial ryegrass, tall fescue, and endophytes. In: H. Takotoh, editor, Proceedings of the 6th International Turfgrass Research Conference, Tokyo, Japan. 31 July – 5 Aug. 1989. p.3–10

Funk, C.R., and W.A. Meyer. 2001. 70 years of turfgrass improvement at the New Jersey Agricultural Experiment Station: The Garden State's Rutgers University has long been in the forefront of turfgrass development. USGA Green Section Record. 39:19–23

Funk, C.R., R.E. Engel, and P.M. Halisky. 1969. Registration of ‘Manhattan’ perennial ryegrass. Crop Sci. 9:679–680

Gedil, M.A., C. Wye, S. Berry, B. Segers, J. Peleman, R. Jones, A. Leon, M.B. Slabaugh, and S.J. Knapp. 2001. An integrated restriction fragment length polymorphism-

amplified fragment length polymorphism linkage map for cultivated sunflower. Genome. 44:213–221

Geldermann, H. 1975. Investigations on inheritance of quantitative characters in animals by gene markers. I. Methods. Theor. Appl. Genetics 46:319–330

Gill, G.P., P.L. Wilcox, D.J. Whittaker, R.A. Winz, P. Bickerstaff, C.E. Echt, J. Kent, M.O. Humphreys. K.M. Elborough, and R.C. Gardner. 2006. A framework linkage map of perennial ryegrass based on SSR markers. Genome 49:354–364

Glass, B. 1965. A century of biochemical genetics. Proc. Am. Philos. Soc. 109:227–236

Goffeau, A., B.G. Barrell, H. Bussey, R.W. Davis, B. Dujon, H. Feldmann, F. Galibert, J.D. Hoheisel, C. Jacq, M. Johnston, E.J. Louis, H.W. Mewes, Y. Murakami, P. Philippsen, H. Tettelin, S.G. Oliver. 1996. Life with 6000 genes. Science. 274:546, 563–567

Goldberg, C.W., and H. Cole. 1973. In vitro study of benomyl tolerance exhibited by *Sclerotinia homoeocarpa*. Phytopathology. 63:201–202

Golembiewski, R.C., J.M. Vargas, A.L. Jones, and A.R. Detweiler. 1995. Detection of demethylation inhibitor (DMI) resistance in *Sclerotinia homoeocarpa* populations. Plant Dis. 79:491–493

Greub, L.J., P.N. Drolsom, and D.A. Rohweder. 1985. Salt tolerance of grasses and legumes for roadside use. Agron. J. 77: 76–80

Grodzicker, T., J. Williams, P. Sharp, and J. Sambrook. 1974. Physical mapping of temperature-sensitive mutations of adenoviruses. Cold Spring Harb. Symp. Quant Biol. 39:439–446

Hackett, C. 2002. Statistical methods for QTL mapping in cereals. Plant Mol. Biol. 48: 585–599

Hansey, C.N., B. Vaillancourt, R.S. Sekhon, N. de Leon, S.M. Kaeppler et al. 2012. Maize (*Zea mays* L.) genome diversity as revealed by RNA-sequencing. Plos One. 7:e33071

Harivandi, A. 1988. Irrigation water quality and turfgrass management. California Turfgrass Culture 38: 3–4

Harivandi, M.A. 2004. A review of sports turf irrigation with municipal recycled water. Acta Hortic. 661:131–136

Hartl, D., and E. Jones. 2001. Genetics: analysis of genes and genomes. Jones and Bartlett Publishers, Dudbury, MA.

Havlin, J.L., J.D. Beaton, S.L. Tisdale, and W.L. Nelson. 2005. Soil fertility and fertilizers: an introduction to nutrient management. Prentice Hall, Upper Saddle River, NJ.

Hayman, D.L. 1956. The genetical control of incompatibility in *Phalaris coerulescens* Desf. Austral. J. of Biol. Sci. 9: 321–331

Hayward, M.D., J.W. Forster, J.G. Jones, O. Dolstra, C. Evans, N.J. McAdam, K.G. Hossain, M. Stammers, J.K. Will, M.O. Humphreys, and G.M. Evans. 1998. Genetic analysis of *Lolium* I. Identification of linkage groups and the establishment of a genetic map. Plant Breed. 117:451–455

Hayward, M.D., N.J. McAdam, J.G. Jones, C. Evans, G.M. Evens, J.W. Forster, A. Ustin, K.G. Hossain, B. Quader, M. Stammers, and J.K. Will. 1994. Genetic markers and the selection of quantitative traits in forage grasses. Euphytica 77:269–275

Hegarty, M. R. Yadav, M. Lee, I. Armstead, R. Sanderson, N. Scollan, et al. 2013. Genotyping by RAD sequencing enables mapping of fatty acid composition traits in perennial ryegrass (*Lolium perenne* (L.)). Plant Biotechnology J. 11:572–581

Helentjaris, T., M. Slocum, S. Wright, A. Schaefer, and J. Nienhuis. 1986. Construction of genetic linkage maps in maize and tomato using restriction fragment length polymorphisms. Theoretical and Applied Genetics. 72:761–769

Hemmat, M., N.F. Weeden, A.G. Manganaris, and D.M. Lawson. 1994. Molecular marker linkage map for apple. J. of Heredity. 85:4–11

Hillier, L.W., G.T. Marth, A.R. Quinlan, D. Dooling, G. Gewell, et al. 2008. Whole-genome sequencing and variant discovery in *C. elegans*. Nat. Methods. 5:183–188

Hoffman, G.J., and S.L. Rawlins. 1971. Growth and water potential of root crops as influenced by salinity and relative humidity. Agron. J. 63: 877–880

Honig, J.A., 2011. The use of molecular genetics tools to complement a traditional field based turfgrass breeding program. Doctoral dissertation, Rutgers, The State Univ. of New Jersey-New Brunswick, New Brunswick, NJ.

Horst, G.L., and N.B. Beadle. 1984. Salinity affects germination and growth of tall fescue cu1tivars. J. Am. Soc. Hortic. Sci. 109: 419–422

Howard, K.W.F., and P.J. Beck. 1993. Hydrogeochemical implications of groundwater contamination by road de-icing chemicals. J. Contam. Hydrol. 12:245–268

Hu, J., B.A. Vick. 2003. Target region amplification polymorphism: a novel marker technique for plant genotyping. Plant Mol. Biol. Rep. 21:289–294

Hughes, T.D., J.D. Butler, and G.D. Sanks. 1975. Salt tolerance and suitability of various grasses for saline roadsides. J. Environ. Quality 4: 65–68

Hyman, E.D. 1988. A new method of sequencing DNA. Anal. Biochem. 174:423–436

Jaccoud, D., K. Peng, D, Feinstein, and A. Killian. 2001. Diversity arrays: a solid state technology for sequence information independent genotyping. Nucleic Acids Research. 29:e25

Jackson, N.E. 1973. Apothecial production in *Sclerotinia homoeocarpa* F.T. Bennett. Jour. Sports Turf Res. Inst. 49:58–63

Jahufer, M. B. Barret, A. Griffiths, and D. Woodfield. 2003. DNA fingerprinting and genetic relationships among white clover cultivars. *In*: J. Morton (ed.) Proceeding of the New Zealand Grassland Association. Taieri Print Limited, Dunedin. 65:163–169

Jansen, R. 1993. Interval mapping of multiple quantitative trait loci. Genetics 135:205–211

Jansen, R., and P. Stam. 1994. High resolution of quantitative traits into multiple loci via interval mapping. Genetics 136:1447–1455

Jarvis, P., C. Lister, V. Szabo, and C. Dean. 1994. Integration of CAPS markers into the RFLP map generated using recombinant inbred lines of *Arabidopsis thaliana*. Plant Mol. Biol. 24:685–687

Jenkin, T.J. 1931. The method and technique of selection, breeding and strain building in grasses. Imp. Bureau Plant Genet. Herbage Plants Bull. No. 3:5–34

Jenkin, T.J. 1936. Natural selection in relation to the grasses. In A Discussion on the Present State of the Theory of Natural Selection. Proc. Roy Soc, Ser. B. 121: 52–56

Jensen, L.B., J.R. Andersen, U. Frei, Y. Xing, C. Taylor, P.B. Holm, and T. Lubberstedt. 2005. QTL mapping of vernalization response in perennial ryegrass (*Lolium perenne* L.) reveals co-location with an orthologue of wheat *VRN1*. Theor. Appl. Genet. 110:527–536

Jiang, G.L. 2013. Molecular markers and marker-assisted breeding in plants. *In*: Anderson, S.B. (ed.) Agricultural and biological science. Plant Breeding from Laboratories to Fields. pp.45–83

Jones, E.S., M.P. Dupal, J.LO. Dumsday, L.J. Hughes, and J.W. Forster. 2002a. An SSR-based genetic linkage map for perennial ryegrass (*Lolium perenne* L.). Theor. Appl. Genet. 105:577–584

Jones, E.S., N.L. Mahoney, M.D. Hayward, I.P. Armstead, J.G. Jones, M.O. Humpreys, I.P. King, T. Kishida, T. Yamada, F. Balfourier, C. Charmet, and J.W. Forster. 2002b. An enhanced molecular marker-based map of perennial ryegrass (*Lolium perenne* L.) reveals comparative relationships with other Poaceae species. Genomes 45:282–295

Kao, C.H., Z.B. Zeng, and R.D. Teasdale.1999. Multiple interval mapping. Genetics 152:1203–1216

Kesseli, R.V., I. Paran, and R.W. Michelmore. 1994. Analysis of a detailed genetic linkage map of *Lactuca sativa* (Lettuce) constructed from RFLP and RAPD markers. Genetics. 136:1435–1446

Kik, C. 1989. Ecological genetics of salt resistance in the clonal perennial *Agrostis stolonifera* L. New Phytol. 113: 453–458

Koch, M.J., and S.A. Bonos. 2010. An overhead irrigation screening technique for salinity tolerance in cool-season turfgrasses. Crop Sci. 50:2613–2619

Koch, M.J., and S.A. Bonos. 2011a. Correlation of three salinity tolerance screening methods for cool-season turfgrasses. HortScience 46: 1198–1201

Koch, M.J., and S.A. Bonos. 2011b. Salinity tolerance of cool-season turfgrass cultivars under field conditions. Appl. Turfgrass Sci. doi:10.2135/cropsci2011.03.0174

Koch, M.J., W.A. Meyer, and S.A. Bonos. 2015. Inheritance of salinity tolerance in perennial ryegrass. Crop Sci. 55:1834–1842

Kohn, L.M. 1979. Delimitation of the economically important plant pathogenic *Sclerotinia* species. Phytopathology. 69:881–886

Kohn, L.M., and Greenville, D.J. 1989. Anatomy and biochemistry of stromatal anamorphs in the Sclerotiniaceae. Canadian Jour. Bot. 67:371–393

Konieczny, A., and F.M. Ausubel. 1993. A procedure for mapping *Arabidopsis* mutations using co-dominant ecotype-specific PCR-based markers. Plant J. 4:403–410

Lander, E., and D. Botstein. 1989. Mapping Mendelian factors underlying quantitative traits using RFLP linkage maps. Genetics 121:185–199

Lander, E.S., P. Green, J. Abrahamson, A. Barlow, M.J. Daly, S.E. Lincoln, and L. Newburg. 1987. Mapmaker an interactive computer package for constructing primary genetic linkage maps of experimental and natural populations. Genomics 1: 174–181

Langridge, P., and K. Chalmers. 2004. The principle: identification and application of molecular markers. In: H. Lorz and G. Wenzel, editors, Biotechnology in

agriculture and forestry: molecular marker systems in plant breeding and crop improvement. Springer-Verlag Berlin Heidelberg, Germany. p. 3–22

Lazarova, V., and A. Bahri. 2004. Water reuse for irrigation: Agriculture, landscapes, and turf grass. CRC Press, Boca Raton, FL.

Lee, G., R.R. Duncan, and R.N. Carrow. 2002. Initial Selection of salt tolerant seashore paspalum ecotypes. USGA Turfgrass Environ. Res. Online 1(11):1–7

Leinauer, B., and D.A. Devitt. 2013. Irrigation science and technology. In: J.C. Stier, B.P. Horgan, and S.A. Bonos, editors, Turfgrass: biology, use, and management. ASA, CSSA, and SSSA, Madison, WI. p.1075–1132

Li, G., and C.F. Quiros. 2001. Sequence-related amplified polymorphism (SRAP), a new marker system based on a simple PCR reaction: its application to mapping and gene tagging in *Brassica*. Theor. Appl. Genet. 103:455–461

Lincoln, S., M. Daly, and E. Lander. 1993a. Constructing genetic linkage maps with MAPMAKER/EXP. Version 3.0. Whitehead Institute for Biomedical Research Technical Report, 3rd Edn.

Lincoln, S., M. Daly, and E. Lander. 1993b. Mapping genes controlling quantitative traits using MAPMAKER/QTL. Version 1.1. Whitehead Institute for Biomedical Research Technical Report, 2nd Edn.

Litt, M., and J.A. Luty. 1989. A hypervariable microsatellite revealed by in vitro amplification of a dinucleotide repeat within the cardiac muscle actin gene. Am. J. Hum. Genet. 44:397–401

Liu, B. 1998. Statistical genomics: linkage, mapping and QTL analysis. CRC Press, Boca Raton

Lu, F., A.E. Lipka, J. Glaubitz, R. Elshire, J.H. Cherney, M.D. Casler, E.S. Buckler, D.E. Costich. 2013. Switchgrass genomic diversity, ploidy and evolution: novel insights from a network-based SNP discovery protocol. Plos Genetics. 9:e1003215

Lundqvist, A. 1956. Self-incompatibility in the rye. I. Genetic control in the diploid. Hereditas. 42: 293–348

Maas, E.V. 1986. Salt tolerance of plants. Appl. Agricult. Res. 1:12–26

Mahoney, L.L., D.J. Sargent, F. Abebe-Akele, D.J. Wood, J.A. Ward, N.V. Bassil, J.F Hancock, K.M. Falta, and T.M. Davis. 2016. A high-density linkage map of the ancestral diploid strawberry, *Fragaria iinumae*, constructed with single nucleotide polymorphism markers from the IStraw90 array and genotyping by sequencing. The Plant Genome. 9 doi:10.3835/plantgenome2015.08.0071

Manly, K.F., H. Cudmore Robert, Jr., and J.M. Meer. 2001. Map Manager QTX, cross-platform software for genetic mapping. Mamm. Genome 12: 930–932

Marcar, N.E. 1987. Salt tolerance in the genus *Lolium* (ryegrass) during germination and growth. Aust. J. Agricult. Res. 38: 297–307

Marcum, K.B. 2001. Salinity tolerance of 35 bentgrass cultivars. HortScience 36:374–376

Marcum, K.B., and C.L. Murdoch. 1990. Growth responses, ion relations, and osmotic adaptations of eleven C_4 turfgrasses to salinity. Agron. J. 82:892–896

Marcum, K.B. 2006. Use of saline and non-potable water in the turfgrass industry: Constraints and developments. Agric. Water Manage. 80:132–146

Mardis, E.R. 2008. Next-generation DNA sequencing methods. Annu. Rev. Genomics Hum. Genet. 9:387–402

Margulies, M. et al. 2005. Genome sequencing in micro fabricated high-density picolitre reactors. Nature. 437:376–380

Mason, C.F., S.A. Norton, I.J. Fernandez, and L.E. Katz. 1999. Deconstruction of the chemical effects of road salt on stream water chemistry. J. Environ. Qual. 28:82–91

Masoudi-Nejad, A., Narimani, Z. and Hosseinkhan, N. 2013. Next generation sequencing and sequence assembly: methodologies and algorithms. Springer New York, Heidelberg, Dordrecht, London

Massie, L.B., Cole, H., and Duich, J. 1968. Pathogen variation in relation to disease severity and control of Sclerotinia dollar spot of turfgrass by fungicides. Phytopathology. 58:1616–1619

McKernan, K., A. Blanchard, L. Kotler, and G. Costa. 2006. Reagents, methods, and libraries for bead-based sequencing. U.S. Patent Application No. 20080003571

Metzker, M.L. 2010. Sequencing technologies - the next generation. Nat. Rev. Genet. 11:31–46

Monteith, J. and Dahl. A.S. 1932. Turf diseases and their control. The Bulletin, U.S. Golf Assoc. 12:8–126

Morris, K. 1996. National turfgrass evaluation program. NTEP. 96:84–95

Muylle, H., J. Baert, E. Van Bockstaele, J. Pertijs, and I. Roldan-Ruiz. 2005. Four QTL determine crown rust (*Puccinia coronate* f. sp. *lolii*) resistance in a perennial ryegrass (*Lolium perenne*) population. Heredity 95:348–357

National Golf Foundation. 1999. Operating and financial performance data of 18–hole golf facilities. Nat. Golf Found., Jupiter, FL.

Nelson, J.C. 1997. Qgene - software for marker-based genomic analysis and breeding. Mol. Breed. 3:239–245

Neumann, P. 1997. Salinity resistance and plant growth revisited. Plant Cell Environ. 20:1193–1198

Ng, S.B., E.H. Turner, P.D. Robertson, S.D. Flygare, A.W. Bigham et al. 2009. Targeted capture and massively parallel sequencing of 12 human exomes. Nature. 461:272–276

Nicholson, J.G., Meyer, W.A., Sinclair, J.B., and Butler, J.D. 1971. Turf isolates of *Sclerotinia homoeocarpa* tolerant to dyrene. Phytopathol. 72:169–172

Novak, L.A. and Kohn, L.M. 1991. Electrophoretic and immunological comparisons of developmentally regulated proteins in members of the Sclerotiniaceae and other sclerotial fungi. App. Environ. Microbiol. 57:525–534

Nyren, P. and A. Lundin. Enzymatic method for continuous monitoring of inorganic phosphate synthesis. Anal. Biochem. 151:504–509

Orita, M., H. Iwahana, H. Kanazawa, H. Kenshi, and S. Takao. 1989. Detection of polymorphisms of human DNA by gel electrophoresis as single-strand conformation polymorphisms. Proc. Natl. Acad. Sci. U.S.A. 86:2766–2770

Orshinsky, A.M., J. Hu, S.O. Opiyo, V. Reddyvari-Channarayappa, T.K. Mitchell, M.J. Boehm. 2012. RNA-Seq analysis of the *Sclerotinia homoeocarpa* – creeping bentgrass pathosystem. Plos One 7:e41140.

Paran, I., and R.W. Michelmore. 1993. Development of reliable PCR-based markers linked to downy mildew resistance genes in lettuce. Theor. Appl. Genet. 85:985–993

Paterson, A.H. 1996. Making genetic maps. In: A.H. Paterson, editor, Genome mapping in plants. R.G. Landes Company, San Diego, California; Academic Press, Austin, TX. p.23–39

Peabody, A. 2004. Salt-worthy flowers are stunning and sensible. Agric. Res. 52:5–7

Peacock, C.H., A.E. Dudeck, and J.C. Wildmon. 1993. Growth and mineral content of St. Augustinegrass cultivars in response to salinity. J. Am. Soc. Hortic. Sci. 118:464–469

Peel, M.D., B.L. Waldron, K.B. Jensen, N.J. Chatterton, H. Horton, and L.M. Dudley. 2004. Screening for salinity tolerance in alfalfa: A repeatable method. Crop Sci. 44:2049–2053

Pembleton, L.W., M.C. Drayton, M. Bain, R.C. Baillie, C. Inch, G.C. Spangenberg, J. Wang, J.W. Forester, N.O.I. Cogan. 2016. Targeted genotyping-by-sequencing permits cost-effective identification and discrimination of pasture grass species and cultivars. Theor. Appl. Genet. doi 10.1007/s00122–016–2678–2

Pescod, M. 1992. Wastewater treatment and use in agriculture. FAO, Rome, Italy.

Pettygrove, G.S., and T. Asano, editors. 1985. Irrigation with reclaimed municipal wastewater: A guidance manual. Lewis Publishers, Chelsea, MI.

Pfender, W., M. Saha, E. Johnson, M. Slabaugh. Mapping with RAD (restriction-site associated DNA) markers to rapidly identify QTL for stem rust resistance in *Lolium perenne*. Theor. Appl. Genet. 122:1467–1480

Plot, R. 1677. The Natural History of Oxfordshire. Oxford University Press.

Poczai, P., I. Varga, M, Laos, A. Cseh, N. Bell, J.P.T. Valkonen, and J. Hyvonen. 2013. Advances in plant gene-targeted and functional markers: a review. Plant Methods. 9:6. doi:10.1186/1746–4811–9–6

Poehlman, J.M., and D.A. Sleper. 1995. Breeding field crops. Third ed. Iowa State Univ. Press, Ames

Poland, J.A., and T.W. Rife. 2012. Genotyping-by-sequencing for plant breeding and genetics. The Plant Genome. 5:92–102

Poland, J., J. Endelman, J. Dawson, J. Rutkoski, S. Wu, Y. Manes, S. Dreisigacker, J. Crossa, H. Sanchez-Villeda, M. Sorrells, and J.L. Jannink. 2012a. Genomic selection in wheat breeding using genotyping-by-sequencing. The Plant Genome. 5:103–113

Poland, J.A., P.J. Brown, M.E. Sorrells, and J.L. Jannink. 2012b. Development of high-density genetic maps for barley and wheat using a novel two-enzyme genotyping-by-sequencing approach. Plos One. 7:e32253

Popko, J.T., H. Sang, J. Lee, T. Yamada, Y. Hoshino, and G. Jung. 2018. Resistance of *Sclerotinia homoeocarpa* field isolates to succinate dehydrogenase inhibitor fungicides. Plant Dis. doi:10.1111/mpp.12174

Qi, X., P. Stam, and P. Lindhout. 1998. Use of locus-specific AFLP markers to construct a high-density molecular map in barley. Theor. Appl. Gen. 109:1485–1493

Qian, Y.L., and M.R. Suplick. 2001. Interactive effects of salinity and temperature on Kentucky bluegrass ad tall fescue seed germination. Int. Turfgrass Soc. Res. J. 9: 334–339

Qian, Y.L., M.C. Engelke, and M.J.V. Foster. 2000. Salinity effects on Zoysiagrass cultivars and experimental lines. Crop Sci. 40:488–492

Qian, Y.L., S.J. Wilhelm, and K.B. Marcum. 2001. Comparative response of two Kentucky bluegrass cultivars to salinity stress. Crop Sci. 41:1895–1900

Reiter, R.S., J.G.K. Williams, K.A. Feldman, A. Rafalski, S.V. Tingey, and P.A. Scolnik. 1992. Global and local genome mapping in *Arabidopsis thaliana* by using recombinant inbred lines and random amplified polymorphic DNAs. Proc. Natl. Acad. Sci. USA. 89:1477–1481

Richardson, M.D., Hignight, K.W., Walker, R.H., Rodgers, C.A., Rush, D., McCalla, J.H., and Karcher, D.E. 2007. Meadow fescue and tetraploid perennial ryegrass-two new species for overseeding dormant bermudagrass turf. Crop Sci. 47:83–90

Rioux, R.A. 2014. New insights on the biology and host-pathogen interactions of the dollar spot pathogen *Sclerotinia homoeocarpa*. Doctoral dissertation, University of Wisconsin-Madison, Madison, WI.

Risch, N. 1992. Genetic linkage: interpreting LOD scores. Science 255: 803–804

Ronaghi, M. S. Karamohamed, B. Pettersson, M. Uhlen, and P. Nyren. 1996. Real-time DNA sequencing using detection of pyrophosphate release. Anal. Biochem. 242:84–89

Rose-Fricker, C., and J. Wipff . 2001. Breeding for salt tolerance in cool-season turfgrasses. Int. Turf. Soc. Res. J. 9:206–212

Salgado-Salazar, C., L.A. Beirn, A. Ismaiel, M. J. Boehm, I. Carbone, A.I. Putman, L.P. Tredway, B.B. Clarke, and J.A. Crouch. 2018. *Clarireedia*: A new fungal genus comprising four pathogenic species responsible for dollar spot disease of turfgrass. Fungal Biol. 122:761–773

Sanger, F., S. Nicklen, and A.R. Coulson. 1977. DNA sequencing with chain-terminating inhibitors. Proc. Natl. Acad. Sci. USA. 74:5463–5467

Satgopan, J.M., B.S. Yandell, M.A. Newton, and T.C. Osborn.1996. A Bayesian approach to detect quantitative trait loci using Markov chain Monte Carlo. Genetics 144:805–816

Semagn, K. A. Bjornstad, H, Skinnes, A.G. Maroy, Y. Tarkegne, and M. William. 2006. Distribution of DArT, AFLP, and SSR markers in a genetic linkage map of a doubled-haploid hexaploid wheat population. Genome. 49:545–555

Shanley, J.B. 1994. Effects of ion exchange on a stream solute fluxes in a basin receiving highway deicing salts. J. Environ. Qual. 23:977–986

Shannon, M.C. 1984. Breeding, selection, and the genetics of salt tolerance. In: R.C. Staples and G.H. Toenniessen, editors, Salinity tolerance in plants: Strategies for crop improvement. John Wiley & Sons, New York. p.231–254

Shendure J, J.P. Gregory, N.B. Reppas, X. Lin, J.P. McCutcheon, A.M Rosenbaum, M.D. Wang, K. Zhang, R.D. Mitra, and G.M. Church. 2005. Accurate multiplex colony sequencing of an evolved bacterial genome. Science 309:1728–1732

Shendure, J., and H. Ji. 2013. Next-generation DNA sequencing. Nature Biotech. 26:1135–1145

Sim, S., K. Diesburg, M. Casler, and G. Jung. 2007. Mapping and comparative analysis of QTL for crown rust resistance in an Italian × perennial ryegrass population. Phytopathology 97:767–776

Singer, M.F. 1968. 1968 Nobel Laureate in Medicine or Physiology. Science. 162:433–436

Singh, B.D. and Singh, A.K. 2015. Marker-assisted plant breeding: principles and practices. Springer, New Delhi.

Smiley, R.W., Dernoeden, P.H., Clarke, B.B. 2005. Compendium of Turfgrass Diseases. St. Paul, MN: Am. Phytopathol. Soc. 3rd ed. 167pp.

Southern, E.M. 1975. Detection of specific sequences among DNA fragments separated by gel electrophoresis. Journal of Molecular Biology. 98:503–517

Stam, P. 1993. Construction of integrated genetic linkage maps by means of a new computer package: JoinMap. Plant J. 3: 739–744

Staub, J.E., F.C. Serquen, and M. Gupta. 1996. Genetic marker, map construction, and their application in plant breeding. HortSci. 31:729–741

Steinke, K., and E.H. Ervin. 2013. Turfgrass ecology. In: J.C. Stier, B.P. Horgan, and S.A. Bonos, editors, Turfgrass: biology, use, and management. ASA, CSSA, and SSSA, Madison, WI. p.347–382

Stevens, M.R., E.M. Lamb, and D.D. Rhoads. 1995. Mapping the Sw-5 locus for tomato spotted wilt virus resistance in tomatoes using RAPD and RFLP analyses. Theor. Appl. Genet. 90:451–456

Studer, B., B. Boller, E. Bauer, U.K. Posselt, F. Widmer, and R. Kolliker. 2007. Consistent detection of QTL for crown rust resistance in an Italian ryegrass

(*Lolium multiflorum* Lam.) across environments and phenotyping methods. Theor. Appl. Genet. 115:9–17

Talbot, C.J., A. Nicod, S.S. Cherny, D.W. Fulker, A.C. Collins, and J. Flint. 1999. High-resolution mapping of quantitative trait loci in outbred mice. Nature Genetics 21: 305–308

Tani, T., and Beard, J.B. 1997. Color Atlas of Turfgrass Diseases. Ann Arbor Press, Chelsea, MI.

Tautz, D. 1989. Hypervariability of simple sequence as a general source of polymorphic DNA markers. Nucleic Acids Res. 17:6462–6471

Tautz, D., and M. Renz. 1984. Simple sequences are ubiquitous repetitive components of eukaryotic genomes. Nucleic Acids Res. 12:4127–4138

Terrell, E.E. 1968. A taxonomic revision of the genus *Lolium*. Technical Bulletin No. 1392. United States Department of Agriculture, Washington, D.C.

The Arabidopsis Genome Initiative. 2000. Analysis of the genome sequence of the flowering plant *Arabidopsis thaliana*. 408:796–815

Thorogood, D. 2003. Perennial ryegrass (*Lolium perenne* L.), p. 75–105. In: M.D. Casler and R.R. Duncan, editors, Turfgrass biology, genetics, and breeding. John Wiley and Sons, Hoboken, NJ. p.75–106

Turgeon, A.J. 2008. Turfgrass management, Eighth Edition. Pearson Prentice Hall, Upper Saddle River, NJ.

USEPA. 1992. Manual: Guidelines for water use. EPA/625/R–92/004, Office of Water, Office of Wastewater Enforcement and Compliance, U.S. Agency for Int. Dev., Washington, D.C.

USEPA. 2004. Guidelines for water reuse. EPA/645/R–04/108

USGA. 1994. Wastewater reuse for golf course irrigation. Lewis Publishers, NY.

Utz, H., and A. Melchinger. 1996. PLABQTL: A program for composite interval mapping of QTL. J. Quant. Trait Loci 2:1–5

Vargas, J.M., Jr. 1994. Management of Turfgrass Diseases. 2nd ed. Lewis Publ., Boca Raton, FL

Velmurugan, J., E. Molison, S. Barth, D. Marshall, L. Milne, C.J. Creevey, B. Lynch, H. Meally, M. McCabe, and D. Milbourne. 2016. An ultra-high density genetic linkage map of perennial ryegrass (*Lolium perenne*) using genotyping by sequencing (GBS) based on a reference shotgun genome assembly. Annals of

Botany doi:10.1093/aob/mcw081

Venter, J.C., M.D. Adams, E.W. Myers, et al. 2001. The Sequence of the Human Genome. Science. 291:1304–1351

Visscher, P.M., R. Thompson, and C.S. Haley. 1996. Confidence intervals in QTL mapping by bootstrapping. Genetics 143: 1013–1020

Vos, P., R. Hogers, M. Bleeker, M. Reijans, T. van de Lee, M. Hornes, A. Frijters, J. Pot, H. Peleman, M. Kuiper, and M. Zabeau. 1995. AFLP: a new technique for DNA fingerprinting. Nucleic Acids Res. 23:4407–4414

Vosman, B. 1998. Variations on a theme. *In*: Karp, A., P.G. Isaac, and D.S. Ingram (eds.) Molecular tools for screening biodiversity. Chapman and Hall, London. pp 262–264

Walsh, B., S.S. Ikeda, and G.J. Boland. 1999. Biology and management of dollar spot (*Sclerotinia homoeocarpa*); an important disease of turfgrass. HortScience. 34:13–21

Wagner, R.E., and P.M. Halisky. 1981. Influence of thatch accumulation on disease incidence and fungicidal effectiveness in Kentucky bluegrass turf. Phytopathol. 71:565

Wang, Y., C.A. Bigelow, and Y. Jiang. 2009. Ploidy level and DNA content of perennial ryegrass germplasm as determined by flow cytometry. HortScience. 44:2049–2052

Ward, J.A., J. Bhangoo, F. Fernandez-Fernandez, P. Moore, J.D. Swanson, R. Viola, R. Velasco, N. Bassil, C.A. Weber, D.J. Sargent. 2013. Saturated linkage map construction in *Rubus idaeus* using genotyping by sequencing and genome-independent imputation. BMC Genomics. 14:2

Warnke, S.E., R.E. Barker, G. Jung, S.C. Sim, M.A.R. Mian, M.C. Saha, L.A. Brilman, M.P. Dupal, and J.W. Forster. 2004. Genetic linkage mapping of an annual × perennial ryegrass population. Theor. Appl. Genet. 109:294–304

Watschke, T.L., P.H. Dernoeden, and D.J. Shetlar. 2013. Managing Turfgrass Pests. 2nd ed. CRC Press, Boca Raton, FL.

Watson, J.D, and F.H.C. Crick. 1953. A structure for deoxyribose nucleic acid. Nature. 171:737–738

Weber, J.L., and P.E. May. 1989. Abundant class of human DNA polymorphism, which can be typed using the polymerase chain reaction. Am. J. Hum. Genet. 44:388–396

Wenzl, P., J. Carling, D. Kudrna, D. Jaccoud, E. Huttner, A. Kleinhofs, and A. Kilian. 2004. Diversity array technology (DArT) for whole-genome profiling of barley. Proc. Natl. Acad. Sci. U.S.A. 101:9915–9920

Wenzl, P., H. Li, J. Carling, M. Zhou, H. Raman, E. Paul, P. Hearnden, C. Maier, L. Xia, V. Caig, J. Ovesna, M. Cakir, D. Poulsen, J. Wang, R. Raman, K.P. Smith, G.J. Muehlbauer, K.J. Chalmers, A. Kleinhofs, E. Huttner, and A. Kilian. 2006. A high-density consensus map of barley linking DArT markers to SSR, RFLP, and STS loci and agricultural traits. BMC Genomics. 7:206

Wheeler, D.A., et al. 2008. The complete genome of an individual by massively parallel DNA sequencing. Nature. 452:872–877

Williams, J.G.K., A.R. Kubelik, K.J. Livak, J.A. Rafalski, and S.V. Tingey. 1990. DNA polymorphisms amplified by arbitrary primers are useful as genetic markers. Nucleic Acidds Res. 18:6531–6535

Williams, D.W., A.J. Powell, and P.C. Vincelli. 1993. Response of dollar spot to dew removal from creeping bentgrass. Agronomy Abstracts: 1993 Annual Meetings. American Soc. Agron., Madison, Wisc. p. 165

Winicov, I. 1998. New molecular approaches to improving salt tolerance in crop plants. Ann. Bot. (London) 82:703–710

Winter, P., and G. Kahl. 1995. Molecular marker technologies for plant improvement. World Journal of Microbiology and Biotechnology. 11:438–448

Worm Sequencing Consortium. 1998. Genome sequence of the nematode *C. elegans*: a platform for investigating biology. The *C. elegans* Sequencing Consortium. Science. 282:2012–2018

Xia, L., K. Peng, S. Yang, P. Wenzl, M.C. de Vincente, M. Fregene, and A. Kilian. 2005. DArT for high-throughput genotyping of cassava (*Manihot esculenta*) and its wild relatives. Theor. Appl. Gen. 110:1092–1098

Xu, Y. 2010. Molecular plant breeding. CAB International, Wallingford. p. 734.

Yamada, T., E.S. Jones, N.O.I. Cogan, A.C. Vecchies, T. Nomura, H. Hisano, Y. Shimamoto, K.F. Smith, M.D. Hayward, and J.W. Forster. 2004. QTL analysis of morphological, developmental, and winter hardiness-associated traits in perennial ryegrass. Crop Sci. 44:925–935

Yang, H.B., Kang, W.H., Nahm, S.H., and Kang, B.C. 2015. Methods for developing molecular markers, p.15–50. In: Koh, H.J., Kwon, S.Y., and Thomson, M. (eds.). Current technologies in plant molecular breeding. Springer, Netherlands.

Young, N.D. 1994. Constructing a plant genetic linkage map with DNA markers, pp. 39–57 *In*: I.K.V. Ronald and L. Phillips (Eds.) DNA-based markers in plants. Kluwer, Dordrecht/Boston/London.

Zabeau, M. and P. Voss. 1993. Selective restriction fragment amplification: a general method for DNA fingerprinting. European Patent Application. 92402629.7. Publ. 0534858A1

Zeng, Z.B. 1993. Theoretical basis for separation of multiple linked gene effects in mapping quantitative trait loci. Proc. Natl. Acad. Sci. USA 90:10972–10976

Zeng, Z.B. 1994. Precision mapping of quantitative trait loci. Genetics 136:1457–1468

CHAPTER II

DEVELOPMENT OF THE I06 × A89 PERENNIAL RYEGRASS MAPPING POPULATION

Abstract

Primary breeding objectives for turf-type perennial ryegrass (*Lolium perenne* L.) include improving tolerance to stress factors such as salinity and dollar spot disease. These types of traits are often quantitatively inherited and present complexities for the phenotypic selection breeding technique. Quantitative trait locus (QTL) mapping is a viable means for overcoming limitations of traditional, field-based breeding efforts. In this study, we aimed to fulfill the primary prerequisite for QTL mapping, which is the development of a mapping population. Candidate parental genotypes were selected from a large population of perennial ryegrass clones in the Rutgers turfgrass breeding program. These genotypes were studied for response to salinity stress and dollar spot disease. Additionally, phenotypic variation in growth habit and leaf color was also observed among the candidate parental genotypes. Although these two traits were not of primary interest in developing the mapping population, we also considered them when selecting and pairing parents for cross-fertilization events. Nine biparental crosses were made in the summer of 2016. The selected population consisted of 118 pseudo-F_2 progeny derived from a cross between 15-8325 (maternal parent, referenced as I06) and 15-8343 (paternal parent, referenced as A89). Thus, the population is referenced as the I06 × A89

perennial ryegrass mapping population and is comprised of the 2 parent genotypes and 118 progeny genotypes. This population will be a valuable resource for future QTL mapping studies for traits such as salinity tolerance, dollar spot resistance, growth habit, and leaf color morphology.

Introduction

Perennial ryegrass (*Lolium perenne* L.) is a predominantly diploid (2n = 2x = 14), cool-season forage and turfgrass species native to temperate regions of Asia, North Africa, and Europe (Beard, 1973; Funk and Clarke, 1989; Terrell, 1968; Thorogood, 2003). With the exception of Antarctica, this medium to high density, bunch-type perennial is grown on every continent and managed as a turfgrass in general landscaping areas, parks, racetracks, golf fairways and roughs, and athletic fields (Beard, 1973; Beard and Beard, 2005; Thorogood, 2003). Furthermore, perennial ryegrass is used in lower latitudes to overseed warm-season turf during winter dormancy periods (Beard and Beard, 2005; Thorogood, 2003; Turgeon, 2008). Current breeding efforts for turf-type perennial ryegrass are primarily aimed at improving tolerance to abiotic and biotic stress factors such as salinity stress and dollar spot disease (Bonos and Huff, 2013; Bonos et al., 2006; Brilman, 2005; Thorogood, 2003).

Salinity stress can occur naturally in arid and semi-arid climates that do not receive adequate rainfall to leach salts through soil profiles and along coastal regions that are prone to saltwater sprays (Brady and Weil, 2004; Carrow and Duncan, 1998, 2012; Havlin et al., 2005). In addition, salinity stress can occur due to human practices such as

the use of ice melting salts to clear roadways, applications of fertilizer and other soil amendments, and, most notably, irrigation with reclaimed water sources (Carrow and Duncan, 1998; Leinauer and Devitt, 2013; Marcum, 2006; Steinke and Ervin, 2013). Koch et al. (2015) found that salinity tolerance is quantitatively inherited in perennial ryegrass and controlled by additive gene effects.

Dollar spot is a prevalent and persistent foliar disease that occurs throughout the world on many warm- and cool-season turfgrass species (Smiley et al., 2005; Watschke et al., 2013). In the U.S., dollar spot of cool-season turfgrass species, such as perennial ryegrass, is caused by the fungal pathogen *Clarireedia jacksonii* C. Salgado, L.A. Beirn, B.B. Clarke, and J.A. Crouch (formerly *Sclerotinia homoeocarpa* F.T. Bennet) (Salgado-Salazar et al., 2018; Smiley et al., 2005). Dollar spot is of great economic importance; more money is spent by U.S. golf courses to manage dollar spot than any other turfgrass disease (Smiley et al., 2005; Vargas, 1994). Unfortunately, research on the genetic basis for dollar spot resistance in perennial ryegrass is limited (Bonos and Huff, 2013). However, studies on another cool-season turfgrass species, creeping bentgrass (*Agrostis stolonifera* L.), suggest that dollar spot resistance is quantitatively inherited and largely influenced by additive gene effects (Bonos, 2006, 2011; Bonos et al., 2003; Chakraborty et al., 2006).

A recurrent phenotypic selection breeding scheme has been widely and successfully applied to perennial ryegrass breeding programs to produce composite cultivars with improved traits (Bonos and Huff, 2013; Bonos et al., 2006; Brilman, 2005; Thorogood, 2003). However, phenotypic selection for quantitative traits, particularly for perennial crop breeding, can be laborious and time-consuming (Grinberg et al., 2016).

Marker assisted selection based on quantitative trait locus (QTL) mapping has been successfully implemented to overcome limitations of phenotypic selection for quantitative traits (Curley et al., 2005; Lespinasse et al., 2000; Portyanko et al., 2005; Tanksley et al., 1993; Wang et al., 2000).

The initial step for the QTL mapping procedure is developing an appropriate mapping population (Bernardo, 2002; Langridge and Chalmers, 2004; Singh and Singh, 2015; Xu, 2010). A mapping population is a collection of phenotypically segregating individuals that are derived by cross-fertilization of parents that differ for the specific trait(s) of interest (Bernardo, 2002). Barrett et al. (2004) and Forster et al. (2000) studied white clover (*Trifolium repens* L.) and perennial ryegrass, respectively, and demonstrated that a biparental pseudo-F_2 generation was a suitable mapping population structure for cross-pollinated species. Thus, the goals for this research were to (i) identify candidate parental genotypes with varying responses to salinity stress and dollar spot disease, (ii) conduct biparental cross-fertilizations between parent genotypes, and (iii) establish a pseudo-F_2 perennial ryegrass mapping population.

Materials and methods

Phenotyping for traits of interest

A field trial of 400 perennial ryegrass genotypes was established at the Rutgers Plant Science Research and Extension Farm in Adelphia, NJ in Oct 2013. Plants were

spaced 30.5 cm apart and mowed weekly at a cutting height of 5 cm. During the summer of 2015, the clones were screened for salinity stress response by irrigating with a saline water solution that was made using equal parts of $CaCl_2$ and NaCl salts, as described by Koch and Bonos (2010). The electrical conductivity of the solution was adjusted to 10 dS m^{-1} in a 1,893 L tank, which was equipped with a gasoline-powered pump and an internal agitator. A flow meter (McMaster-Carr, Elmhurst, IL, USA) was attached to the spray system and used to apply 0.5 L of the saline water solution to each plant (Fig. 2.1). Irrigation with saline water was applied three times per week until phenotypic segregation for salinity tolerance was observed. Salinity stress tolerant and susceptible clones were identified as candidate parental genotypes and transplanted to a field nursery on 22 Sep 2015. Candidate parental genotypes were maintained in the field nursery and segregation of growth habits and leaf color morphologies were also observed (Fig. 2.2). During May 2016, all candidate parental genotypes were evaluated for growth habit and leaf color morphology.

The candidate parental genotypes were also maintained in a mowed spaced-plant nursery at the Rutgers Plant Science Research and Extension Farm in Adelphia, NJ and screened for dollar spot response during September 2015. Plants were spaced 30.5 cm apart and mowed weekly at a height of 5 cm. Two virulent isolates (PRG and JP236941) of *Clarireedia jacksonii* were used to inoculate the candidate parental genotypes. The isolates were grown for 3 weeks on 90 mm diameter Petri plates, cut into 1 cm^2 pieces, and added to double sterilized Kentucky bluegrass (*Poa pratensis* L.) seed. The isolates were grown on the Kentucky bluegrass seed for 4 weeks and the resulting inoculum was

applied to the candidate parental genotypes at a rate of 0.8 g m^{-2}. Dollar spot tolerant and susceptible clones were identified.

Biparental crosses and establishment of mapping population

Individual clones were selected from the field nursery of candidate parental genotypes and paired for cross-fertilization events based on similarity of flowering time and differences of salinity stress response, dollar spot stress response, growth habit, and leaf color (Fig. 2.3). Biparental crosses were conducted from late May to early Jul 2016. Seed was harvested from both parents in all biparental crosses on 22 Aug 2016 and sown into round pots (15.2 cm diameter) containing Pro-mix growing media (Premier Tech, Riviere-du-Loup, QC) on 22 Aug 2016 and allowed to germinate.

Results

Thirty clones were identified as candidate parental genotypes based on field screening for salinity stress response. A summary of the traits for each candidate parental genotype is provided in Table 2.1. The selected genotypes originated from seven distinct sources including selections from the Rutgers University/NJAES turfgrass breeding material, collections from the U.S., and collections from other countries. With respect to salinity stress response, 21 tolerant genotypes and 9 susceptible genotypes were selected. Of these genotypes, 4 were tolerant and 26 were susceptible to dollar spot.

The population was further characterized by growth habit and leaf color morphologies (Table 2.1, Fig. 2.2). There were two leaf color classes, light green and dark green. Fourteen of the genotypes were characterized as light green and sixteen genotypes were characterized as dark green. With respect to growth habit, four morphological classes were observed; twelve of the genotypes were upright, eleven of the genotypes were prostrate, five of the genotypes were semi-upright, and two of the genotypes were semi-prostrate. These criteria were also used to determine the pairing of clones for cross-fertilization events.

Nine biparental crosses were made during the summer of 2016 (Fig. 2.3). The crosses included 15-8305 × 15-8337, 15-8309 × 15-8337, 15-8311 × 15-8339, 15-8320 × 15-8341, 15-8320 × 15-8343, 15-8321 × 15-8337, 15-8325 × 15-8341, 15-8325 × 15-8343, and 15-8336 × 15-8337. The point of origin was different between the two parents in all the crosses that were made (Table 2.1). The parents in crosses 15-8305 × 15-8337, 15-8309 × 15-8337, 15-8311 × 15-8339, 15-8321 × 15-8337, and 15-8336 × 15-8337 differed in only two of the four traits of interest. However, parents in crosses 15-8320 × 15-8341, 15-8320 × 15-8343, 15-8325 × 15-8341, and 15-8325 × 15-8343 differed in all four of the traits of interest.

Seed was harvested from both parents of all nine biparental crosses and sown into growing media on 22 Aug 2016. The population derived from the cross between 15-8325 and 15-8343, with genotype 15-8325 as the maternal parent, was selected based on phenotypic variation among the parents and sufficient germination and establishment of progeny genotypes (Fig. 2.3). This cross-fertilization event resulted in 118 pseudo-F_2 progeny, which were transferred to single cells (5.1 × 5.1 cm) of plastic flats containing

Pro-mix growing media and labeled with a unique mapping population designation on 14 Sep 2016.

Parent 15-8325 has higher salinity tolerance, greater susceptibility to dollar spot, lighter green leaf color, and a more prostrate growth habit than parent 15-8343. Furthermore, parent 15-8325 originates from a collection made in Italy in 2006; hence, this parent is referenced as I06. Parent 15-8343 originates from a selection in Adelphia, NJ in 1989; hence, this parent is referenced as A89.

Discussion

Improved tolerance to abiotic and biotic factors such as salinity stress and dollar spot disease are primary objectives for breeding efforts of turf-type perennial ryegrass (Bonos and Huff, 2013; Bonos et al., 2006; Brilman, 2005; Thorogood, 2003). These are quantitatively inherited traits, and the use of traditional phenotypic selection breeding techniques for quantitative traits often requires a great deal of time, labor, and resource inputs (Bonos, 2006, 2011; Bonos et al., 2003; Grinberg et al., 2016; Koch et al, 2015). Quantitative trait locus mapping is a proven solution for the limitations of phenotypic selection (Curley et al., 2005; Lespinasse et al., 2000; Poryanko et al., 2005; Tanksley et al., 1993; Wang et al., 2000). In this work, we have completed a prerequisite for QTL mapping, which is the development of a mapping population.

Candidate parental genotypes were initially selected by identifying salinity stress tolerant and susceptible clones from a large population of perennial ryegrasses in the Rutgers turfgrass breeding program. These candidate parental genotypes were from

various origins, both within the U.S. and abroad. In addition to developing a population to segregate for salinity tolerance, we also aimed to create the population in such a way that it would also segregate for tolerance to dollar spot disease. Thus, we inoculated the candidate parental genotypes with two isolates of *Clarireedia jacksonii*, the causal organism for dollar spot disease. We noted that many genotypes were indeed susceptible to dollar spot disease; however, some were tolerant, showing very little to no disease symptoms after inoculation.

Inadvertently, we observed differences in growth habit and leaf color among the candidate parental genotypes. Although, these traits were not of primary interest for development of the mapping population, we documented the phenotypes of all the candidate parental genotypes. In general, there were four growth habit classes and two leaf color classes. These observations, along with flowering time and tolerance to dollar spot disease and salinity stress, were primary criteria for cross-fertilization pairings and selection of the mapping population.

The population we selected was derived from a cross between 15-8325 and 15-8343, where 15-8343 was the paternal parent and 15-8325 was the maternal parent. This population had the greatest phenotypic variation for all the traits of interest. Parent 15-8325 is a light green, prostrate individual that is tolerant to salinity stress and susceptible to dollar spot disease. Conversely, parent 15-8343 is a dark green, upright individual that is susceptible to salinity stress and tolerant to dollar spot disease. Parent 15-8325 was collected from Italy in 2006 and is called parent I06. Parent 15-8343 was selected from Adelphia, NJ in 1989 and is called parent A89. Thus, the mapping population is commonly referenced as the I06 × A89 perennial ryegrass mapping population.

Other studies have demonstrated the usefulness of developing populations for QTL mapping of various traits in perennial ryegrass (Bushman and Warnke, 2013). Mapping populations were used by Pfender et al. (2011), for example, to identify QTL for stem rust (*Puccinia graminis* subsp. *graminicola* Z. Urb.) resistance in perennial ryegrass. Moreover, mapping populations have also proven useful for identifying QTL for resistance to crown rust (*Puccinia coronata* Corda) and gray leaf spot (*Pyricularia oryzae* Cavara) diseases (Curley et al., 2005; Curley et al., 2008; Dumsday et al., 2003; Muylle et al., 2005; Sim et al., 2007; Studer et al., 2007). In addition, QTL for vernalization response, winter hardiness, and morphological and developmental traits were also identified by developing and studying mapping populations (Jensen et al., 2005; Yamada et al., 2004). We consider the I06 × A89 population to be a valuable resource for future studies including linkage mapping construction and QTL analyses for salinity tolerance, dollar spot resistance, growth habit, and leaf color morphology.

Literature cited

Barrett, B., A. Griffiths, M. Schreiber, N. Ellison, C. Mercer, J. Bouton, B. Ong, J. Forster, T. Sawbridge, G. Spangenburg, G. Bryan, and D. Woodfield. 2004. A microsatellite map of white clover. Theor. Appl. Genet. 109: 596–608

Beard, J.B. 1973. Turfgrass: Science and Culture. Prentice Hall, Englewood Cliffs, NJ.

Beard, J.B., and H.J. Beard. 2005. Beard's Turfgrass Encyclopedia for Golf Courses, Grounds, Lawns, Sports Fields. Michigan State University Press.

Bernardo, R. 2002. Breeding for quantitative traits in plants. Stemma Press, Woodbury, MN, USA.

Bonos, S.A. 2011. Gene action of dollar spot resistance in creeping bentgrass. Phytopathology 159: 12–18

Bonos, S.A., and D.R. Huff. 2013. Cool-season grasses: biology and breeding. In: J.C. Stier, B.P. Horgan, and S.A. Bonos, editors, Turfgrass: biology, use, and management. ASA, CSSA, and SSSA, Madison, WI. p.591–660

Bonos, S.A., B.B. Clarke, and W.A. Meyer. 2006. Breeding for disease resistance in the major cool-season turfgrasses. Annu. Rev. Phytopathol. 44:213–234

Bonos, S.A., M.D. Casler, and W.A. Meyer. 2003. Inheritance of dollar spot resistance in creeping bentgrass. Crop Sci. 43: 2189–2196

Brady, N.C., and R.R. Weil. 2004. Elements of the nature and properties of soils. Prentice Hall, Upper Saddle River, NJ.

Brilman, L.A. 2005. Turfgrass breeding in the United States: public private cool- and warm-season. Int. Turf. Soc. Res. 10:508–515

Carrow, R.N., and R.R. Duncan. 1998. Salt-affected turfgrass sites: Assessment and management. Ann Arbor Press. Chelsea, MI.

Carrow, R.N., and R.R. Duncan. 2012. Best management practices for saline and sodic turfgrass soils. CRC Press, Boca Raton, FL.

Chakraborty, N., J. Curley, S. Warnke, M.D. Casler, G. Jung. 2006. Mapping QTL for dollar spot resistance in creeping bentgrass (*Agrostis stolonifera* L.). Theor. Appl. Genet. 113:1421–1435.

Curley, J., S.C. Sim, S. Warnke, S. Leong, and R. Barker. 2005. QTL mapping of resistance to gray leaf spot in ryegrass. Theor. Appl. Genet. 111:1107–1117.

Forster, J.W., E.S. Jones, R. Kolliker, M.C. Drayton, J.L. Dumsday, M.P. Dupal, K.M. Guthridge, N.L. Mahoney, E. van Zijll de Jong, and K.F. Smith. 2000. Development and implementation of molecular markers for crop improvement. *In*: Molecular Breeding of Forage Crops. In: G. Spangenberg, editor, Proceedings of the 2nd International Symposium, Lorne and Hamilton, Victoria Australia, November 19–24, pp. 101–133, Kluwer Academic Publishers, London

Funk, C.R., and B.B. Clarke. 1989. Turfgrass breeding – with special reference to turf-type perennial ryegrass, tall fescue, and endophytes. In: H. Takotoh, editor, Proceedings of the 6th International Turfgrass Research Conference, Tokyo, Japan. 31 July – 5 Aug. 1989. p.3–10

Grinberg, N.F., A. Lovatt, M. Hegarty, A. Lovatt, K.P. Skøt, R. Kelly, T. Blackmore, D. Thorogood, R.D. King, I. Armstead, W. Powell, L. Skøt. 2016. Implementation of genomic prediction in *Lolium perenne* (L.) breeding populations. Front. Plant Sci. 7:133

Havlin, J.L., J.D. Beaton, S.L. Tisdale, and W.L. Nelson. 2005. Soil fertility and fertilizers: an introduction to nutrient management. Prentice Hall, Upper Saddle River, NJ.

Koch, M.J., W.A. Meyer, and S.A. Bonos. 2015. Inheritance of salinity tolerance in perennial ryegrass. Crop Sci. 55:1834–1842

Langridge, P., and K. Chalmers. 2004. The principle: identification and application of molecular markers. In: H. Lorz and G. Wenzel, editors, Biotechnology in agriculture and forestry: molecular marker systems in plant breeding and crop improvement. Springer-Verlag Berlin Heidelberg, Germany. p. 3–22

Leinauer, B., and D.A. Devitt. 2013. Irrigation science and technology. In: J.C. Stier, B.P. Horgan, and S.A. Bonos, editors, Turfgrass: biology, use, and management. ASA, CSSA, and SSSA, Madison, WI. p.1075–1132

Lespinasse, D., L. Grivet, V. Troispoux, M. Rodier-Goud, F. Pinard, M. Sequin. 2000. Identification of QTL involved in the resistance to South American leaf blight (*Microcyclus ulei*) in the rubber tree. Theor. Appl. Genet. 100:975–984

Marcum, K.B. 2006. Use of saline and non-potable water in the turfgrass industry: Constraints and developments. Agric. Water Manage. 80:132–146

Portyanko, V.A., G. Chen, H.W. Rines, R.L. Phillips, K.J. Leonard, G.E. Ochocki, D.D. Stuthman. 2005. Quantitative trait loci for partial resistance to crown rust, *Puccinia coronoata*, in cultivated oat, *Aevena sativa* L. Theor. Appl. Genet. 111:313–324

Salgado-Salazar, C., L.A. Beirn, A. Ismaiel, M. J. Boehm, I. Carbone, A.I. Putman, L.P. Tredway, B.B. Clarke, and J.A. Crouch. 2018. *Clarireedia*: A new fungal genus

comprising four pathogenic species responsible for dollar spot disease of turfgrass. Fungal Biol. 122:761–773

Singh, B.D. and Singh, A.K. 2015. Marker-assisted plant breeding: principles and practices. Springer, New Delhi

Smiley, R.W., Dernoeden, P.H., Clarke, B.B. 2005. Compendium of Turfgrass Diseases. St. Paul, MN: Am. Phytopathol. Soc. 3rd ed. 167pp.

Steinke, K., and E.H. Ervin. 2013. Turfgrass ecology. In: J.C. Stier, B.P. Horgan, and S.A. Bonos, editors, Turfgrass: biology, use, and management. ASA, CSSA, and SSSA, Madison, WI. p.347–382

Tanksley, S.D., N.D. Young, A.H. Paterson, M.W. Bonierbale. 1993. RFLP mapping in plant breeding: new tools for an old science. Bio/Technol. 7:257–264

Terrell, E.E. 1968. A taxonomic revision of the genus *Lolium*. Technical Bulletin No. 1392. United States Department of Agriculture, Washington, D.C.

Thorogood, D. 2003. Perennial ryegrass (*Lolium perenne* L.), p. 75-105. In: M.D. Casler and R.R. Duncan, editors, Turfgrass biology, genetics, and breeding. John Wiley and Sons, Hoboken, NJ. p.75–106

Turgeon, A.J. 2008. Turfgrass management, Eighth Edition. Pearson Prentice Hall, Upper Saddle River, NJ.

Vargas, J.M., Jr. 1994. Management of Turfgrass Diseases. 2nd ed. Lewis Publ., Boca Raton, FL.

Wang, D., R. Karle, A.F. Iezzoni. 2000. QTL analysis of flower and fruit traits in sour cherry. Theor. Appl. Genet. 100:535–544

Watschke, T.L., P.H. Dernoeden, and D.J. Shetlar. 2013. Managing Turfgrass Pests. 2nd ed. CRC Press, Boca Raton, FL.

Xu, Y. 2010. Molecular plant breeding. CAB International, Wallingford. p. 734.

Table 2.1 Summary of clones selected as candidate parental genotypes for the I06 × A89 perennial ryegrass mapping population.

Plant ID	Origin[a]	Salinity[b]	Dollar Spot[c]	Leaf Color[d]	Growth Habit[e]	Maturity[f]
15-8304	collection from Poland	tolerant	susceptible	light green	upright	late
15-8305	selection from SPL III	tolerant	susceptible	light green	prostrate	early
15-8306	selection from SR 4200	tolerant	susceptible	light green	prostrate	early
15-8307	collection from Poland	tolerant	susceptible	light green	prostrate	late
15-8308	collection from Bulgaria	tolerant	susceptible	dark green	prostrate	medium
15-8309	collection from GCC	tolerant	susceptible	dark green	upright	early
15-8310	selection from A89 patch	tolerant	susceptible	dark green	upright	medium
15-8311	selection from A89 patch	tolerant	tolerant	dark green	upright	late
15-8312	collection from Poland	tolerant	susceptible	light green	prostrate	late
15-8313	collection from Poland	tolerant	susceptible	light green	semi-upright	medium
15-8314	collection from Poland	tolerant	susceptible	light green	semi-prostrate	late
15-8318	selection from SPL III	tolerant	susceptible	light green	prostrate	medium

Table 2.1 (continued)

Plant ID	Origin	Salinity	Dollar Spot	Leaf Color	Growth Habit	Maturity
15-8319	collection from Poland	tolerant	susceptible	dark green	upright	late
15-8320	collection from Poland	tolerant	susceptible	light green	prostrate	late
15-8321	collection from Poland	tolerant	susceptible	dark green	upright	early
15-8322	collection from Poland	tolerant	susceptible	light green	upright	medium
15-8323	collection from Bulgaria	tolerant	susceptible	light green	prostrate	early
15-8324	collection from Poland	tolerant	susceptible	light green	semi-upright	medium
15-8325	collection from Italy	tolerant	susceptible	light green	prostrate	late
15-8328	collection from Poland	tolerant	susceptible	dark green	upright	medium
15-8329	collection from Bulgaria	tolerant	susceptible	dark green	upright	early
15-8337	collection from Bulgaria	susceptible	susceptible	dark green	prostrate	early
15-8338	collection from Poland	susceptible	susceptible	light green	semi-upright	medium
15-8339	collection from Poland	susceptible	tolerant	dark green	prostrate	late

Table 2.1 (continued)

Plant ID	Origin	Salinity	Dollar Spot	Leaf Color	Growth Habit	Maturity
15-8340	selection from SPL III	susceptible	susceptible	dark green	semi-upright	late
15-8341	selection from SPL III	susceptible	tolerant	dark green	upright	medium
15-8342	collection from Poland	susceptible	susceptible	dark green	semi-upright	late
15-8343	selection from A89 patch	susceptible	tolerant	dark green	upright	late
15-8344	selection from A89 patch	susceptible	susceptible	dark green	semi-prostrate	late
15-8345	collection from GCC	susceptible	susceptible	dark green	upright	late

[a] Point of origin and introduction into the Rutgers germplasm collection.
[b] Salinity stress response, visually assessed after repeated irrigation with saline water solution.
[c] Dollar spot stress response, visually assessed after inoculation with two virulent isolates of *Clarireedia jacksonii*.
[d] Leaf color, visually assessed when grown in a field nursery.
[e] Growth habit, visually assessed when grown in a field nursery.
[f] Maturity, visually assessed when grown in a field nursery.

Figure 2.1 Application of saline irrigation water to perennial ryegrass clones using an overhead irrigation technique.

Figure 2.2 Phenotypes of perennial ryegrass genotypes 15-8325 (left) and 15-8343 (right) maintained in a field nursery. Genotype 15-8325 represents a prostrate growth habit and light green leaf color morphology. Genotype 15-8343 represents an upright growth habit and dark green color morphology.

Figure 2.3 Isolated biparental cross between perennial ryegrass genotypes 15-8325 (left) and 15-8343 (right).

CHAPTER III

A SNP-BASED GENETIC LINKAGE MAP OF PERENNIAL RYEGRASS USING NEXT-GENERATION DOUBLE-DIGEST RESTRICTION-SITE-ASSOCIATED DNA SEQUENCING

Abstract

Quantitative trait locus (QTL) mapping is implemented in modern plant breeding programs as a basis for marker-assisted selection of complex, quantitatively inherited traits. Prior to QTL mapping, DNA markers must be identified and used to generate genetic linkage maps. Recently, the I06 × A89 population was developed to study salinity tolerance, dollar spot resistance, and morphological traits in perennial ryegrass (*Lolium perenne* L.). In this study, we aimed to use the next-generation double digestion restriction-site-associated DNA sequencing strategy to efficiently identify DNA markers, genotype the I06 × A89 population, and construct high-density genetic linkage maps for perennial ryegrass. Sequencing of the 2 parents and 118 progeny in the I06 × A89 population yielded greater than 1.8 Gb of raw sequencing reads. In addition to the SNP markers that were generated in this study, a set of framework SSR markers from previous studies were also used for linkage map construction. Two linkage maps, one for each parent, were developed. After screening markers for polymorphisms, segregation

distortion, redundancy, and insufficient grouping support, 848 SNPs and 52 SSRs were included in the marker dataset for parent I06 while 769 SNPs and 35 SSRs were included in the marker dataset for parent A89. The 900 markers included in the I06 dataset mapped to a total distance of 677.5 cM with an average marker density of 0.75 cM. The 804 markers included in the A89 dataset mapped to a total distance of 687.9 cM with an average marker density of 0.86 cM. These high-density genetic linkage map will be valuable resources for future QTL mapping studies in turf-type perennial ryegrass breeding.

Introduction

Perennial ryegrass (*Lolium perenne* L.) is a major cool-season turf and forage grass (Beard, 1973; Funk and Clarke, 1989; Terrell, 1968; Thorogood, 2003). This diploid (2n = 2x = 14) species has seven chromosomes and a genome size of approximately 2.5 Gb (Beard, 1973; Kopecky et al., 2010). Enhanced tolerance to abiotic and biotic stresses is a primary breeding objective for turf-type perennial ryegrass (Bonos and Huff, 2013; Bonos et al., 2006; Brilman, 2005; Thorogood, 2003). Many of these traits, however, are quantitatively inherited and are difficult to improve using the traditional, field-based breeding approach of phenotypic recurrent selection (Grinberg et al., 2016). Thus, many researchers have implemented molecular or laboratory-oriented strategies such as quantitative trait locus (QTL) mapping to overcome these difficulties (Curley et al., 2005; Lespinasse et al., 2000; Portyanko et al., 2005; Tanksley et al., 1993; Wang et al, 2000).

Preliminary components for QTL mapping include developing an appropriate mapping population and constructing a genetic linkage map that is densely populated with markers (Bernardo, 2002; Singh and Singh, 2015; Xu, 2010). Recently, the I06 × A89 population was developed to study the genetic basis of salinity tolerance, dollar spot resistance, growth habit, and leaf color in perennial ryegrass (Chapter II). This pseudo-F_2 generation population is composed of 2 parent genotypes and 118 progeny genotypes.

Genetic linkage maps for perennial ryegrass have been constructed from combinations of various marker types including amplified fragment length polymorphisms (AFLPs), expressed sequence tags (ESTs), isozymes, restriction fragment length polymorphisms (RFLPs), and simple sequence repeats (SSRs) (Bert et al., 1999; Bushman and Warnke, 2013; Faville et al., 2004; Gill et al., 2006; Jensen et al., 2005; Jones et al., 2002a, 2002b; Studer et al., 2010). Bert et al. (1999) mapped 463 AFLPs, 3 isozymes, and 5 ESTs to 930 cM of total map distance, resulting in an average marker density of approximately 2.0 cM. Faville (2004) constructed two separate parent maps, one for parent NA_6 and another for parent AU_6. For the NA_6 parent map, 88 EST-RFLPs and 71 EST-SSRs were mapped to 963 cM of total map distance, resulting in an average marker density of approximately 6.1 cM. For the AU_6 parent map, 67 EST-RFLPs and 58 EST-SSRs were mapped to 757 cM of total map distance, resulting in an average marker density of approximately 6.1 cM. Gill et al. (2006) mapped 376 SSRs and 9 RFLPs to 675.6 cM of total map distance, resulting in an average marker density of approximately 1.8 cM. Jensen (2005) mapped 317 SSRs to 772 cM of total map distance, resulting in an average marker density of approximately 2.4 cM. Jones (2002a) mapped 391 SSRs to 814 cM of total map distance, resulting in an average marker density of

approximately 2.1 cM. Jones (2002b) mapped 241 markers (AFLPs, ESTs, isozymes, and RFLPs) to 811 cM of total map distance, resulting in an average marker density of approximately 3.4 cM. Studer (2010) mapped 284 SSRs to 742 cM of total map distance, resulting in an average marker density of approximately 2.6 cM.

More recently, the decreased cost of next-generation sequencing (NGS) technologies has prompted the development of new marker discovery strategies (Baird et al., 2008; Davey et al., 2011; Elshire et al., 2011; Poland and Rife, 2012; Poland et al., 2012a). Restriction-site associated DNA (RAD) tagging was the first demonstration of combining NGS with complexity reduction (Baird et al., 2008). Elshire et al. (2011) introduced the genotyping-by-sequencing approach as a robust and simple method for complexity reduction in large genomes. A double digestion RAD sequencing (ddRADseq) approach was later introduced by Poland et al. (2012b). These reduced representation NGS strategies generate a subset of complex genomes and have been extended to non-model species (Deschamps et al, 2010; Gore et al, 2009; Hyten et al, 2010 Nelson et al., 2011).

The genotyping-by-sequencing approach has been utilized to construct an ultra-high density genetic linkage map for perennial ryegrass (Velmurugan et al., 2016). By using the NGS-based genotyping strategy, Velmurugan et al. (2016) mapped 3,092 single nucleotide polymorphisms (SNPs) and 7,260 presence and absence variants (PAVs) to 952.6 cM of total map distance, resulting in an average marker density of approximately 0.1 cM. These results, compared with earlier linkage maps for perennial ryegrass, demonstrate the advantages of implementing NGS-based genotyping approaches to construct much denser genetic linkage maps.

The objectives of this study were to implement the next-generation ddRADseq strategy to efficiently (i) identify single nucleotide polymorphism markers, (ii) genotype the I06 × A89 population, and (iii) construct high-density genetic linkage of perennial ryegrass.

Materials and methods

Plant Material and DNA extraction

In 2015, two heterozygous perennial ryegrass clones, I06 and A89, were selected from an evaluation of 400 clones at the Rutgers Plant Science Research and Extension Farm in Adelphia, NJ (Chapter II). These clones exhibit differences in salinity stress response, disease response to dollar spot, leaf color, and growth habit. Parent I06 has higher salinity tolerance, greater susceptibility to dollar spot, lighter leaf color, and a more prostrate growth habit than A89.

A pseudo-F_2 perennial ryegrass population was developed from a controlled cross between I06 and A89 during the summer of 2016. The cross-fertilization event was conducted in a greenhouse at the New Jersey Agricultural Experiment Station in New Brunswick, NJ with I06 as the maternal parent and A89 as the paternal parent. Maternally derived seeds were sown into round pots (15.2 cm diameter) containing Pro-mix growing media (Premier Tech, Riviere-du-Loup, QC) on 22 Aug 2016 and allowed to germinate. The resulting 118 pseudo-F_2 progeny were transferred to single cells (5.1 ×

5.1 cm) of plastic flats containing Pro-mix growing media and labeled with a unique mapping population designation on 14 Sep 2016.

Young leaf tissue of both parents and all 118 progeny was ground under liquid nitrogen using mortar and pestle and genomic DNA (gDNA) was extracted via manufacturer's recommendations for the DNeasy Plant Mini Kit (Qiagen, Hilden, Germany). Purity and concentration of gDNA was determined by quantifying the 260/280 and 260/230 absorbance ratios with a NanoDrop 2000/2000c spectrophotometer (Thermo Fischer Scientific, Waltham, MA, USA).

Construction and sequencing of ddRADseq libraries

As outlined by Poland et al. (2012), gDNA was double digested in 30 µl reaction volumes containing 200 ng gDNA, 8 units each of the common-cutting *Msp*I (New England Biolabs, Ipswich, MA, USA) and the rare-cutting *Pst*I-HF (New England Biolabs, Ipswich, MA, USA) enzymes, and 1× NEBuffer 4 (New England Biolabs, Ipswich, MA, USA). Double digest reaction mixtures were incubated at 37°C for 2 hours.

Restricted fragments were ligated with adapters in 40 µl reaction volumes containing 1 mM ATP, 1× NEBuffer, 1 µM *Msp*I adapter, 0.1 pmol double-stranded barcode adapter, 200 units of T4 DNA Ligase (New England Biolabs, Ipswich, MA, USA), and 20 µl of restricted fragments. The ligation reaction was incubated at 22°C for 2 hours, then temperatures were increased to 65°C for 20 minutes to denature the ligase. Adaptor-ligated DNA fragments were purified with the AMPure XP PCR purification kit

(Agencourt Bioscience, Beverly, MA, USA) as instructed by the manufacturer. Samples were amplified via PCR in 25 µl reaction volumes containing 1× NEB Taq MasterMix (New England Biolabs, Ipswich, MA, USA), 10 µM each of forward and reverse primer, and 3 µl of purified, adaptor-ligated DNA fragments. PCR included an initial denaturation at 95°C for 30 seconds followed by 16 cycles of denaturation at 95°C for 30 seconds, annealing at 62°C for 20 seconds, and extension at 68°C for 15 seconds. A final extension was performed at 68°C for 5 minutes.

The resulting libraries were quantified with a Qubit 3.0 fluorometer (Thermo Fischer Scientific, Waltham, MA, USA), an Agilent 2100 bioanalyzer (Agilent Technologies, Santa Clara, CA, USA), and real-time quantitative PCR. The library concentrations were normalized to 8 ng μl^{-1}, and the 48-plex pooled samples were submitted to GeneWiz (GeneWiz, South Plainfield, NJ, USA) for sequencing via the Illumina HiSeq 2500 sequencing platform (Illumina, San Diego, CA, USA). Nine individual libraries were sequenced for each of the two parent genotypes with the HiSeq 2500 sequencing platform. Additionally, 12 individual libraries were sequenced for each of the two parent genotypes with the Illumina MiSeq sequencing platform (Illumina, San Diego, CA, USA). Thus, 21 total libraries were sequenced for each of the two parent genotypes to generate a 21× sequencing depth relative to the progeny genotypes.

SNP marker identification and genotyping

Sequence reads from raw FASTQ files were converted into genotype data using the Stacks v.1.47 pipeline (Catchen et al., 2011). All reads were trimmed to 100 bases,

quality filtered with the '-q' flag, and demultiplexed according to their barcode (Table A.1) using the process_radtags program. Single and paired end reads were concatenated and matching reads within each sample were grouped using the ustacks program. Each group had a minimum of three matching reads and a maximum of three mismatching nucleotides; this was ensured using the '-m' and '-M' flags, respectively. SNPs were called within each group of reads to generate individual haplotype alleles. The cstacks program was used to create a catalog of loci from the groups that were polymorphic between the parent genotypes. The progeny genotypes were matched to the catalog using the sstacks program, and SNPs were called to identify putative loci. The genotypes program was used to summarize the population genotypes. To limit low-quality genotypes in the SNP dataset, loci missing in greater than 5 % of the genotyped progeny were excluded from subsequent analyses.

SSR framework marker genotyping

A set of 247 framework SSRs were selected from previous studies for linkage group assignments (Gill et al., 2006; Jensen et al., 2005; Kubik et al., 2001; Studer et al., 2008; Studer et al., 2010). The PCR primers for regions flanking the SSR motifs are provided in Table A.2. The M13(-21) 18 base pair sequence (5'–TGTAAAACGACGGCCAGT–3') was added to the 5' end of PCR primer sequences as a means for cost-efficient fluorescent labelling (Schuelke, 2000) and synthesized by Integrated DNA Technologies (Coralville, IA, USA). A PIG-tail (5'–GTTTCTT–3') was added to the 5' end of the reverse primer to promote adenylation (Brownstein et al.,

1996). The PCR reactions for SSR marker genotyping were carried out in a total reaction volume of 13 µL, which contained 5 ng gDNA, 1× ImmoBuffer PCR buffer (Bioline, Memphis, TN, USA), 2 mM $MgCl_2$, 0.25 mM of each dNTP (Bioline, Memphis, TN, USA), 0.5 units of IMMOLASE™ DNA polymerase (Bioline, Memphis, TN, USA), 0.5 pmol of the forward primer with M13(-21) label, 1 pmol of the reverse primer, and 1 pmol of the of the forward fluorescent dye-labeled M13(-21) primer (FAM, NED, PET, or VIC).

Parameters for thermal cycling included an initial denaturation of 5 minutes at 94°C, followed by 30 cycles at 94°C for 30 seconds, 55°C for 45 seconds, and 72°C for 45 seconds, followed by 20 cycles of 94°C for 30 seconds, 53°C for 45 seconds, and 72°C for 45 seconds, and a final extension of 10 minutes at 72°C. An ABI 3500xL Genetic Analyzer (Applied Biosystems, Foster City, CA, USA) was used to analyze PCR products. Genemapper 5.0 software (Thermo Fisher Scientific, Waltham, MA, USA) and LIZ 600 size standard (Thermo Fisher Scientific, Waltham, MA, USA) were used to determine sizes of PCR products.

Genetic linkage map construction

Linkage mapping analyses were conducted using JoinMap 4.1 (Van Ooijen, 2006). The SSR and SNP markers generated from the cross-pollinated population were initially coded as dominant marker types, using lm × ll coding when they were identified as heterozygous in the maternal parent and nn × np coding when they were identified as heterozygous in the paternal parent (Van Ooijen, 2006). Maternal (lm × ll) and paternal

(nn × np) marker datasets were used, independently, to construct two linkage maps. The marker datasets were recoded according to the doubled haploid (DH) coding scheme and analyzed using the two-way pseudo testcross approach (Van Ooijen, 2006). For both the maternal and paternal DH datasets, a chi-square goodness-of-fit test was used to filter out markers with severe segregation distortion ($P < 0.001$). Grouping trees were constructed from the logarithm of odds (LOD) estimation, and linkage groups were selected using a LOD score threshold of 10. The regression mapping algorithm was used to estimate marker recombination and order within each linkage group. Parameters for the regression mapping calculation included a pairwise recombination estimation using $r < 0.49$ and a LOD score > 0.5 with a ripple value = 1 and a jump threshold = 5. Map distances were estimated using the Kosambi mapping function (Kosambi, 1944). The genetic linkage maps were visualized using MapChart 2.3 (Voorrips, 2002). Linkage groups were numbered according to prior placement of the set of framework SSR markers (Gill et al., 2006; Jensen et al., 2005; Kubik et al., 2001; Studer et al., 2008, 2010). Characteristics for the framework SSR markers are provided in Table A.2.

Results

SNP marker identification and genotyping

A summary of the NGS results for the ddRADseq libraries of 118 progeny and 2 parent genotypes is provided in Table 3.1 and Fig. 3.1. The overall total number of raw

reads was 1,824,660,958 (Table 3.1). The number of raw reads for each of the two parent genotypes was 134,329,748 for parent I06 and 129,598,326 for parent A89 (Table 3.1). The total number of raw reads for both parent genotypes was 263,928,074 (Table 3.1). The number of raw reads for the 118 progeny genotypes ranged from 9,659,846 to 17,446,066 with a mean of 13,226,550 (Table 3.1). The total number of raw reads for the progeny genotypes was 1,560,732,884 (Table 3.1).

After trimming read lengths to 100 bases, demultiplexing, and filtering low quality reads, the overall total number of retained reads for all parent and progeny genotypes was 1,741,496,073 (95.4% of total raw reads) (Table 3.1). The number of retained reads for each of the two parents was 124,927,377 for parent I06 and 121,944,604 for parent A89 (Table 3.1, Fig. 3.1). The total number of retained reads for both parent genotypes was 246,871,981 (Table 3.1). The number of retained reads for the 118 progeny genotypes ranged from 9,367,557 to 16,973,767 with a mean of 12,666,077 (Table 3.1, Fig. 3.1). The total number of retained reads for the progeny genotypes was 1,494,597,092 (Table 3.1). The retained read number for the parent genotypes was approximately 10× greater than the retained read number for the 118 progeny genotypes (Table 3.1).

Sequence data from the parent genotypes was used to construct a catalog, which consisted of 548,785 loci for SNP discovery. There were three observed nucleotides for 1,922 loci, resulting in 550,707 total SNPs in the catalog. Transitions were more common than transversions (Table 3.2). The 177,534 C ↔ T and 173,696 A ↔ G transitions accounted for 32.2 and 21.5 % of the total observed SNP loci, respectively. Meanwhile, the 50,704 G ↔ T, 45,136 G ↔ C, 58,087 A ↔ C, and 45,550 A ↔ T

transversions combined for only 36.2 % of the total observed SNPs. The number of SNP loci that appeared in at least one progeny genotype was 104,681. After removing loci with > 5% missing data (SNP observed in ≥ 112 progeny), a total of 2,330 SNPs were considered informative and used to genotype the progeny (Fig. 3.2).

Maternal (lm × ll) and paternal (nn × np) marker datasets were constructed. The initial maternal dataset included 1,219 SNPs, which were heterozygous in the I06 background. The initial paternal dataset included 1,382 SNPs, which were heterozygous in the A89 background. Chi-square goodness-of-fit tests provided evidence for segregation distortion for 320 SNP markers from the maternal dataset and 590 SNP markers for the paternal dataset; those SNPs were removed. In addition, 21 SNP markers were removed from the maternal dataset due to genotype redundancy, and 23 SNP markers were removed from the paternal dataset due to genotype redundancy. Lastly, SNPs were removed from the maternal and paternal datasets based on insufficient grouping support (LOD < 10). Thus, the final maternal (parent I06) and paternal (parent A89) SNP marker datasets included 848 and 769 SNPs, respectively.

SSR framework marker genotyping

Of the 247 selected framework SSR markers, 112 were identified as polymorphic between the I06 and A89 parent genotypes; 72 were identified as monomorphic between the parent genotypes and removed from the set (Table A.2). An additional 63 SSRs were removed from the set due to an inability to produce consistent PCR products among the progeny genotypes. The set of 112 polymorphic markers were used to genotype the 118

progeny. After removing additional SSRs due to non-Mendelian inheritance patterns, 81 informative SSRs were used to genotype the progeny. Sixty-five SSRs were heterozygous in the I06 background and were included in the initial maternal (lm × ll) marker dataset. Forty-nine SSRs were heterozygous in the A89 background and were included in the initial paternal (nn × np) marker dataset. Chi-square goodness-of-fit tests provided evidence for segregation distortion for three SSR markers from both the maternal and paternal datasets; those SSRs were removed. In addition, one SSR marker was removed from the maternal dataset and two SSR markers were removed from the paternal dataset due to genotype redundancy. Lastly, SSRs were removed from the maternal and paternal datasets based on insufficient grouping support (LOD < 10). The final maternal (parent I06) and paternal (parent A89) SSR marker datasets included 52 and 35 SSRs, respectively; these are presented in boldface font in Table A.2.

Genetic linkage map construction

Parent I06 map

After screening markers for segregation distortion, redundancy, and insufficient grouping support, 848 SNP and 52 SSR markers were included in the final dataset for parent I06. As expected, based on the haploid chromosome number for perennial ryegrass (n=7), these 900 markers resolved into seven LGs. The parent I06 linkage map

was 677.5 cM in length (Table 3.3). The lengths of the LGs ranged from 79.2 cM to 135.1 cM, with an average of 96.8 cM (Table 3.3). The number of markers at each LG ranged from 85 markers to 189 markers, with an average of 129 markers (Table 3.3). The marker density ranged from 0.55 cM to 1.08 cM with an average of 0.75 cM (Table 3.3). The SSR markers mapped across each of the seven LGs, providing necessary PCR-based framework associations with previously published perennial ryegrass maps.

Linkage group 1 was 135.1 cM in length and included 184 SNP and 5 SSR markers at a marker density of 0.71 cM (Table 3.3, Fig. 3.3). Linkage group 2 was 93.1 cM in length and included 161 SNP and 7 SSR markers at a marker density of 0.55 cM (Table 3.3, Fig. 3.4). Linkage group 3 was 92.9 cM in length and included 114 SNP and 7 SSR markers at a marker density of 0.77 cM (Table 3.3, Fig. 3.5). Linkage group 4 was 90.3 cM in length and included 102 SNP and 7 SSR markers at a marker density of 0.83 cM (Table 3.3, Fig. 3.6). Linkage group 5 was 91.9 cM in length and included 79 SNP and 6 SSR markers at a marker density of 1.08 cM (Table 3.3, Fig. 3.7). Linkage group 6 was 79.2 cM in length and included 106 SNP and 6 SSR markers at a marker density of 0.71 cM (Table 3.3, Fig. 3.8). Linkage group 7 was 95.0 cM in length and included 107 SNP and 9 SSR markers at a marker density of 0.82 cM (Table 3.3, Fig. 3.9).

Parent A89 map

There were 769 SNP and 35 SSR markers included in the final dataset for parent A89 after screening markers for segregation distortion, redundancy, and insufficient

grouping support. As with the map for parent I06, these 804 markers were mapped to seven LGs for parent A89, which was expected for perennial ryegrass. The parent A89 linkage map was 687.9 cM in length (Table 3.4). The lengths of the LGs ranged from 69.0 cM to 121.7 cM, with an average of 98.3 cM (Table 3.4). The number of markers at each LG ranged from 61 markers to 154 markers, with an average of 115 markers (Table 3.4). The marker density ranged from 0.62 cM to 1.77 cM with an average of 0.86 cM (Table 3.4). Similar to the results with the parent I06 map, the SSR markers mapped across each of the seven LGs in the parent A89 map. This was critical in providing PCR-based framework associations with perennial ryegrass maps published previously.

Linkage group 1 was 113.6 cM in length and included 148 SNP and 6 SSR markers at a marker density of 0.74 cM (Table 3.4, Fig. 3.3). Linkage group 2 was 108.1 cM in length and included 55 SNP and 6 SSR markers at a marker density of 1.77 cM (Table 3.4, Fig. 3.4). Linkage group 3 was 74.0 cM in length and included 85 SNP and 3 SSR markers at a marker density of 0.84 cM (Table 3.4, Fig. 3.5). Linkage group 4 was 121.7 cM in length and included 140 SNP and 3 SSR markers at a marker density of 0.85 cM (Table 3.4, Fig. 3.6). Linkage group 5 was 102.2 cM in length and included 100 SNP and 5 SSR markers at a marker density of 0.97 cM (Table 3.4, Fig. 3.7). Linkage group 6 was 69.0 cM in length and included 106 SNP and 5 SSR markers at a marker density of 0.62 cM (Table 3.4, Fig. 3.8). Linkage group 7 was 99.3 cM in length and included 135 SNP and 7 SSR markers at a marker density of 0.70 cM (Table 3.4, Fig. 3.9).

Discussion

We recently developed the I06 × A89 mapping population, which is a useful resource for studying salinity tolerance, dollar spot resistance, growth habit, and leaf color in perennial ryegrass (Chapter II). Some of these traits, however, are complex, quantitatively inherited traits (Bonos, 2006, 2011; Bonos et al., 2003; Koch et al., 2015). Quantitative trait locus mapping is used in modern breeding programs to improve selection efficiency for quantitative traits through a process called marker-assisted selection (Curley et al, 2005; Lespinasse et al., 2000; Portyanko et al., 2005; Somers et al., 2004; Tanksley et al., 1993; Wang et al., 2000). Prior to QTL mapping, linkage maps must be constructed and densely populated with markers (Bernardo, 2002; Singh and Singh, 2015; Xu, 2010).

The earliest perennial ryegrass linkage maps were constructed with PCR-based markers such as AFLPs, ESTs, isozymes, RFLPs, and SSRs (Bert et al., 1999; Bushman and Warnke, 2013; Faville et al., 2004; Gill et al., 2006; Jensen et al., 2005; Jones et al., 2002a, 2002b; Studer et al., 2010). The number of markers included in the PCR-based maps ranged from 125 (Faville, 2004) to 471 (Bert et al., 1999). The total mapping distances ranged from 675.6 cM (Faville, 2004) to 930 cm (Bert et al., 1999). Marker densities in the PCR-based maps ranged from 1.8 cM (Gill et al., 2006) to 6.1 cM (Faville, 2004).

In the present study, we implemented NGS-based genotyping methods to simultaneously develop and genotype SNP markers for our mapping population. Additionally, a set of SSR framework markers were used in this study to anchor our linkage maps with previously published perennial ryegrass linkage maps. We

constructed two parent maps, one for parent I06 and one for parent A89. The I06 parent map consisted of 900 SNP and SSR markers mapped across a total distance of 677.5 cM with an average marker density of 0.75 cM. The A89 parent map consisted of 804 SNP and SSR markers mapped across a total distance of 687.9 cM with an average marker density of 0.86 cM. Clearly, the linkage maps we have constructed herein are much more densely populated than the early linkage maps for perennial ryegrass.

Although our maps are densely populated with markers, they are not the most densely populated perennial ryegrass maps constructed to date. Valmurugan et al. (2016) mapped 10,352 markers (3,092 SNPs and 7,260 PAVs) across a total map distance of 952.6 cM, yielding an average marker density of 0.1 cM. In that study, Valmurugan et al. used a shotgun assembly approach to generate a reference perennial ryegrass sequence on which GBS reads were aligned. This strategy enabled the researchers to map lower confidence SNPs and PAVs, effectively increasing the total number of markers on the linkage maps (Valmurugan et al., 2016).

Future analyses will include aligning our marker dataset to reference genomic resources (Byrne et al., 2016; Valmurugan et al., 2016) to increase the number of mapped markers for our population and improve the marker density of our genetic linkage maps. Nonetheless, the marker density of the genetic linkage maps we have produced from the I06 × A89 mapping population is a marked increase compared with the former, PCR-based maps (Bert et al., 1999; Bushman and Warnke, 2013; Faville et al., 2004; Gill et al., 2006; Jensen et al., 2005; Jones et al., 2002a, 2002b; Studer et al., 2010). This will provide a valuable resource for QTL mapping studies of traits including salinity tolerance, dollar spot resistance, growth habit, and leaf color in perennial ryegrass.

Literature cited

Baird, N.A., P.D. Etter, T.S. Atwood, M.C. Currey, A.L. Shiver, Z.A. Lewis, E.U. Selker, W.A. Cresko, and E.A. Johnson. 2008. Rapid SNP discovery and genetic mapping using RAD markers. Plos One. 3:e3376.

Beard, J.B. 1973. Turfgrass: Science and Culture. Prentice Hall, Englewood Cliffs, NJ.

Bernardo, R. 2002. Breeding for quantitative traits in plants. Stemma Press, Woodbury, MN, USA.

Bert, P.F., G. Charmet, P. Sourdille, M.D. Hayward, and F. Balfourier. 2999. A high-density map for ryegrass (*Lolium perenne* L.) using AFLP markers. Theor. Appl. Genet. 99:445–452.

Bonos, S.A., and D.R. Huff. 2013. Cool-season grasses: biology and breeding. In: J.C. Stier, B.P. Horgan, and S.A. Bonos, editors, Turfgrass: biology, use, and management. ASA, CSSA, and SSSA, Madison, WI. p.591–660.

Bonos, S.A., B.B. Clarke, and W.A. Meyer. 2006. Breeding for disease resistance in the major cool-season turfgrasses. Annu. Rev. Phytopathol. 44:213–234.

Brilman, L.A. 2005. Turfgrass breeding in the United States: public private cool- and warm-season. Int. Turf. Soc. Res. 10:508–515.

Brownstein, M.J., J.D. Carpten, and J.R. Smith. 1996. Modulation of non-templated nucleotide addition by Taq DNA polymerase: primer modifications that facilitate genotyping. BioTechniques. 20:1004–1010.

Bushman, B.S., and S.E. Warnke. 2013. Genetic and genomic approaches for improving turfgrass. In: J.C. Stier, B.P. Horgan, and S.A. Bonos, editors, Turfgrass: biology, use, and management. ASA, CSSA, and SSSA, Madison, WI. p.683–712.

Catchen, J., A. Amores, P. Hohenlohe, W. Cresko, J. Postlethwait. 2011. Stacks: Building and genotyping loci de nevo from short-read sequences. G3 1:171–182.

Curley, J., S.C. Sim, S. Warnke, S. Leong, and R. Barker. 2005. QTL mapping of resistance to gray leaf spot in ryegrass. Theor. Appl. Genet. 111:1107–1117.

Davey, J.W., P.A. Hohenlohe, P.D. Etter, J.Q. Boone, J.M. Catchen, and M.L. Baxter. 2011. Genome-wide genetic marker discovery and genotyping using next-generation sequencing. Nat. Rev. Genet. 12:499–510.

Deschamps S., M. Rota, J. Ratashak, P. Biddle, D. Thureen, A. Farmer, S. Luck, M. Beatty, N. Nagasawa, L. Michael, V. Llaca, H. Sakai, G. May, J. Lightner, M. Campbell. 2010. Rapid genome-wide single nucleotide polymorphism discovery in soybean and rice via deep resequencing of reduced representation libraries with the Illumina genome analyzer. The Plant Genome 3:53–68.

Elshire, R.J., J.C. Glaubitz, Q. Sun, J.A. Poland, K. awamoto, E.S. Buckler, and S.E. Mitchell. 2011. A robust, simple genotyping-by-sequencing (GBS) approach for high diversity species. Plos One. 6:e19379.

Faville, M.J., A.C. Vecchies, M. Schreiber, M.C. Drayton, L.J. Hughes, E.S. Jones, K.M. Guthridge, K.F. Smith, T. Sawbridge, G.C. Spangenberg, G.T. Bryan, J.W. Forster. 2004. Functionally associated molecular genetic marker map construction in perennial ryegrass (*Lolium perenne* L.). Theor. Appl. Genet. 110:12–32.

Funk, C.R., and B.B. Clarke. 1989. Turfgrass breeding – with special reference to turf-type perennial ryegrass, tall fescue, and endophytes. In: H. Takotoh, editor, Proceedings of the 6th International Turfgrass Research Conference, Tokyo, Japan. 31 July – 5 Aug. 1989. p.3–10.

Gill, G.P., P.L. Wilcox, D.J. Whittaker, R.A. Winz, P. Bickerstaff, C.E. Echt, J. Kent, M.O. Humphreys. K.M. Elborough, and R.C. Gardner. 2006. A framework linkage map of perennial ryegrass based on SSR markers. Genome 49:354–364.

Gore M.A., J. Chia, R.J. Elshire, Q. Sun, E.S. Ersoz, B.L. Hurwitz, J.A. Peiffer, M.D. McMullen, G.S. Grills, J. Ross-Ibarra, D.H. Ware, E.S. Buckler. 2009. A first-generation haplotype map of maize. Science 326:1115–1117.

Grinberg, N.F., A. Lovatt, M. Hegarty, A. Lovatt, K.P. Skøt, R. Kelly, T. Blackmore, D. Thorogood, R.D. King, I. Armstead, W. Powell, L. Skøt. 2016. Implementation of genomic prediction in *Lolium perenne* (L.) breeding populations. Front. Plant Sci. 7:133.

Hyten D., Q. Song, E. Fickus, C. Quigley, J. Lim I. Choi, E. Hwang, M. Pastor-Corrales, P.B. Cregan. 2010. High-throughput SNP discovery and assay development in common bean. BMC Genomics 11:475.

Jensen, L.B., H. Muylle, P. Arens, C.H. Andersen, P.B. Holm, M. Ghesquiere, B. Julier, T. Lubberstedt, K.K. Nielsen, J.D. Riek, I. Roldan-Ruiz, N. Roulund, C. Taylor, B. Vosman, P. Barre. 2005. Development and mapping of a public reference set of SSR markers in *Lolium perenne* L. Mol. Ecol. Notes doi:10.1111/j.1471–8286.2005.01043.x.

Jones, E.S., M.P. Dupal, J.LO. Dumsday, L.J. Hughes, and J.W. Forster. 2002a. An SSR-based genetic linkage map for perennial ryegrass (*Lolium perenne* L.). Theor. Appl. Genet. 105:577–584.

Jones, E.S., N.L. Mahoney, M.D. Hayward, I.P. Armstead, J.G. Jones, M.O. Humpreys, I.P. King, T. Kishida, T. Yamada, F. Balfourier, C. Charmet, and J.W. Forster. 2002b. An enhanced molecular marker-based map of perennial ryegrass (*Lolium perenne* L.) reveals comparative relationships with other Poaceae species. Genomes 45:282–295.

Koch, M.J., W.A. Meyer, and S.A. Bonos. 2015. Inheritance of salinity tolerance in perennial ryegrass. Crop Sci. 55:1834-1842.

Kopecky, D., M. Havrankova, J. Loureiro, S. Castro, A.J. Lukaszewski, J. Bartos, J. Kopecka, J. Dolezel. 2010. Physical distribution of homeologous recombination in individual chromosomes of *Festuca pratensis* in *Lolium multiflorum*. Cytogenetic and Genome Research 129:162–172.

Kosambi, D.D. 1944. The estimation of map distances from recombination values. Ann Eugen 12:172–175.

Kubik, C. M. Sawkins, W.A. Meyer, B.S. Gaut. 2001. Genetic diversity in seven perennial ryegrass (*Lolium perenne* L.) cultivars based on SSR markers. Crop Sci. 41:1565–1572.

Lespinasse, D., L. Grivet, V. Troispoux, M. Rodier-Goud, F. Pinard, M. Sequin. 2000. Identification of QTL involved in the resistance to South American leaf blight (*Microcyclus ulei*) in the rubber tree. Theor. Appl. Genet. 100:975–984.

Nelson J., S. Wang, Y. Wu, X. Li, G. Antony, F.F. White, J. Yu. 2011. Single-nucleotide polymorphism discovery by high-throughput sequencing in sorghum. BMC Genomics 12:352.

Poland, J.A., and T.W. Rife. 2012a. Genotyping-by-sequencing for plant breeding and genetics. The Plant Genome. 5:92–102.

Poland, J.A., P.J. Brown, M.E. Sorrells, and J.L. Jannink. 2012b. Development of high-density genetic maps for barley and wheat using a novel two-enzyme genotyping-by-sequencing approach. Plos One. 7:e32253.

Portyanko, V.A., G. Chen, H.W. Rines, R.L. Phillips, K.J. Leonard, G.E. Ochocki, D.D. Stuthman. 2005. Quantitative trait loci for partial resistance to crown rust, *Puccinia coronoata*, in cultivated oat, *Aevena sativa* L. Theor. Appl. Genet. 111:313–324.

Schuelke, M. 2000. An economic method for florescent labeling of PCR fragments. Nature Biotechnology 18:233–234.

Singh, B.D. and Singh, A.K. 2015. Marker-assisted plant breeding: principles and practices. Springer, New Delhi.

Somers, D.J., P. Isaac, K. Edwards. 2004. A high-density microsatellite consensus map for wheat (*Triticum aestivum* L.). Theor. Appl. Genet. 109:1105–1114.

Studer, B., T. Asp, U. Frei, S. Hentrup, H. Meally, A. Guillard, S. Barth, H. Muylle, Roldan-Ruiz, P. Barre, C. Koning, Boucoiran, G. Uenk-Stunnenberg, O. Dolstra, L. Skot, K.P. Skot, L.B. Turner, M. O. Humphreys, R. Kolliker, N. Roulund, K.K. Nielson, T. Lubberstedt. 2008. Expressed sequence tag-derived microsatellite markers of perennial ryegrass (*Lolium perenne* L.). Mol. Breed. 21:533–548.

Studer, B., R. Kolliker, H. Muylle, T. Asp, U. Frei, I. Roldan-Riuz, P. Barre, C. Tomaszewski, H. Meally, S. Barth, L. Skot, I.P. Armstead, O. Dolstra, T. Lubberstedt. 2010. EST-derived SSR markers used as anchor loci for the construction of a consensus linkage map in ryegrass (*Lolium* spp.). BMC Plant Biology 10: 533–548.

Tanksley, S.D., N.D. Young, A.H. Paterson, M.W. Bonierbale. 1993. RFLP mapping in plant breeding: new tools for an old science. Bio/Technol. 7:257–264.

Terrell, E.E. 1968. A taxonomic revision of the genus *Lolium*. Technical Bulletin No. 1392. United States Department of Agriculture, Washington, D.C.

Thorogood, D. 2003. Perennial ryegrass (*Lolium perenne* L.), p. 75-105. In: M.D. Casler and R.R. Duncan, editors, Turfgrass biology, genetics, and breeding. John Wiley and Sons, Hoboken, NJ. p.75–106.

Van Ooijen, J.W. 2006. JoinMap 4.0, software for the calculation of genetic linkage maps in experimental populations. Kyazma B.V., Wageningen, Netherlands.

Velmurugan, J., E. Molison, S. Barth, D. Marshall, L. Milne, C.J. Creevey, B. Lynch, H. Meally, M. McCabe, and D. Milbourne. 2016. An ultra-high density genetic linkage map of perennial ryegrass (*Lolium perenne*) using genotyping by sequencing (GBS) based on a reference shotgun genome assembly. Annals of Botany doi:10.1093/aob/mcw081.

Voorrips, R.E. 2002. MapChart: software for the graphical presentation of linkage maps and QTL. J. Hered. 93:77–78.

Wang, D., R. Karle, A.F. Iezzoni. 2000. QTL analysis of flower and fruit traits in sour cherry. Theor. Appl. Genet. 100:535–544.

Xu, Y. 2010. Molecular plant breeding. CAB International, Wallingford. p. 734.

Table 3.1 Summary of sequence data for the I06 × A89 perennial ryegrass mapping population generated using next-generation double-digest restriction-site-associated DNA sequencing genotyping methods.

Genotype	Total read number	Retained read number
Parent		
I06	134,329,748	124,927,377
A89	129,598,326	121,944,604
Total	263,928,074	246,871,981
Progeny		
Minimum	9,659,846	9,367,557
Maximum	17,446,066	16,973,767
Mean	13,226,550	12,666,077
Total	1,560,732,884	1,494,597,092
Overall	1,824,660,958	1,741,469,073

Table 3.2 Number and proportion of transitions and transversions in the identified SNP markers generated by next-generation sequencing-based genotyping of the I06 and A89 parent genotypes.

SNP type	Number	Proportion of total
Transitions (C ↔ T)		
C → T	97411	17.7
T → C	80123	14.5
Total	177534	32.2
Transitions (A ↔G)		
A → G	87178	15.8
G → A	86518	15.7
Total	173696	31.5
Transitions Total	351230	63.8
Transversions (G ↔ T)		
G → T	27862	5.1
T → G	22842	4.1
Total	50704	9.2
Transversions (G ↔ C)		
G → C	21299	3.9
C → G	23837	4.3
Total	45136	8.2
Transversions (A ↔ C)		
A → C	31144	5.7
C → A	26943	4.9
Total	58087	10.5
Transversions (A ↔ T)		
A → T	23885	4.3
T → A	21665	3.9
Total	45550	8.3
Transversions Total	199477	36.2
Overall	550707	

Table 3.3 Distribution and summary statistics of single nucleotide polymorphism and simple sequence repeat markers on the linkage groups of the I06 perennial ryegrass genetic linkage map.

Linkage group	Total Markers	Length (cM)	Marker density (cM/marker)
LG1	189	135.1	0.71
LG2	168	93.1	0.55
LG3	121	92.9	0.77
LG4	109	90.3	0.83
LG5	85	91.9	1.08
LG6	112	79.2	0.71
LG7	116	95.0	0.82
Average	129	96.8	0.75

Table 3.4 Distribution and summary statistics of single nucleotide polymorphism and simple sequence repeat markers on the linkage groups of the A89 perennial ryegrass genetic linkage map.

Linkage group	Number of markers	Length (cM)	Marker density (cM/marker)
LG1	154	113.6	0.74
LG2	61	108.1	1.77
LG3	88	74.0	0.84
LG4	143	121.7	0.85
LG5	105	102.2	0.97
LG6	111	69.0	0.62
LG7	142	99.3	0.70
Average	115	98.3	0.86

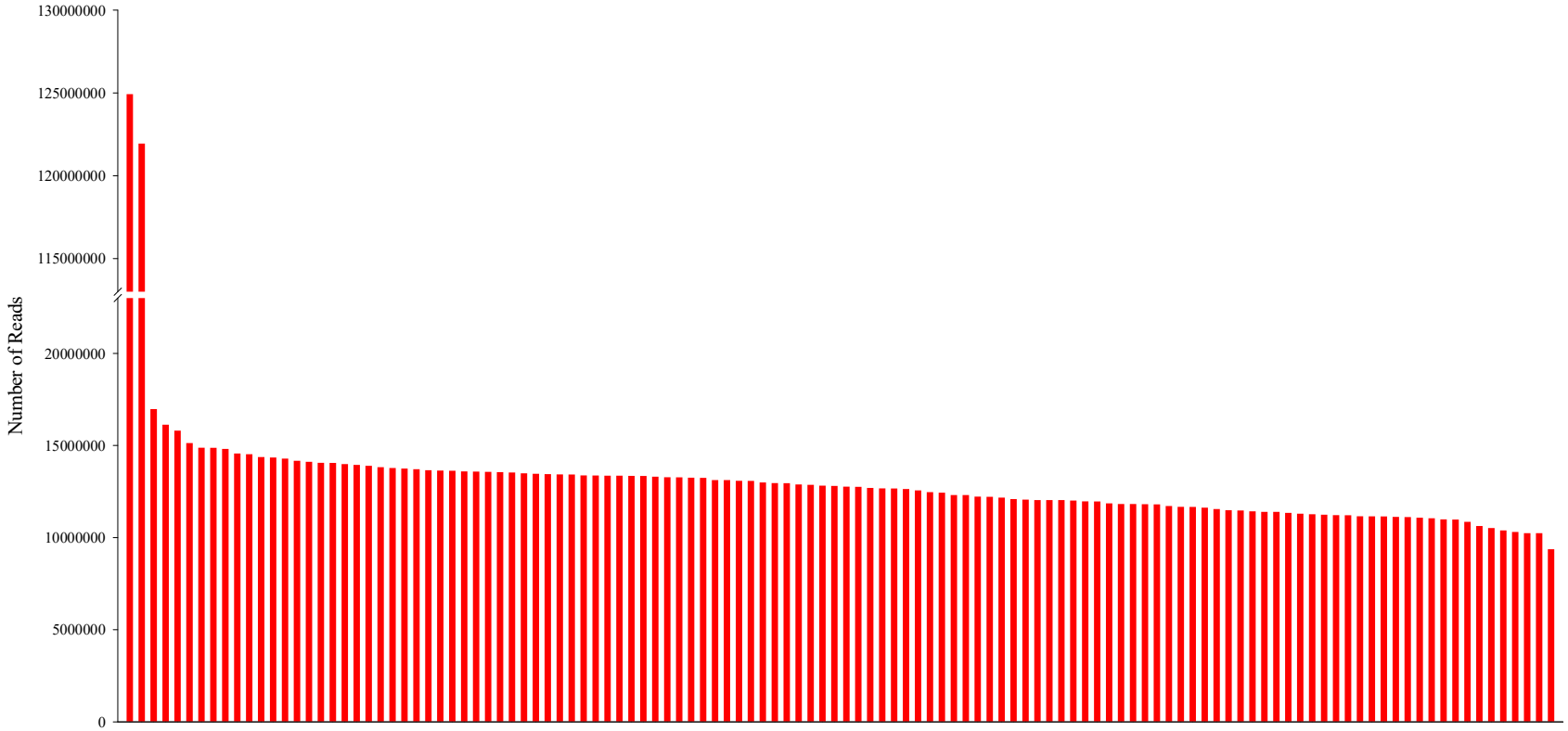

Figure 3.1 High-quality sequencing read numbers for the parents and progeny of the I06 × A89 perennial ryegrass mapping population. The first and second bars of the x-axis represent parent I06 and parent A89, respectively. The remaining bars represent the 118 progeny. The y-axis indicates the number of retained reads after quality filtering.

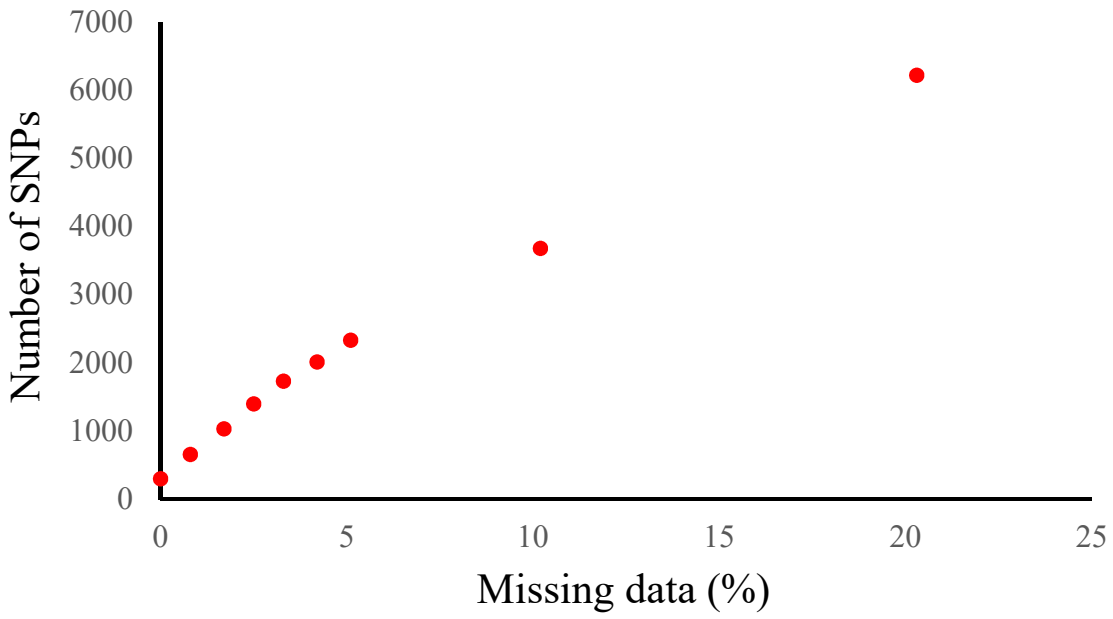

Figure 3.2 Number of single nucleotide polymorphisms generated by next-generation sequencing-based genotyping at missing data thresholds ranging from 0 percent to 20 percent.

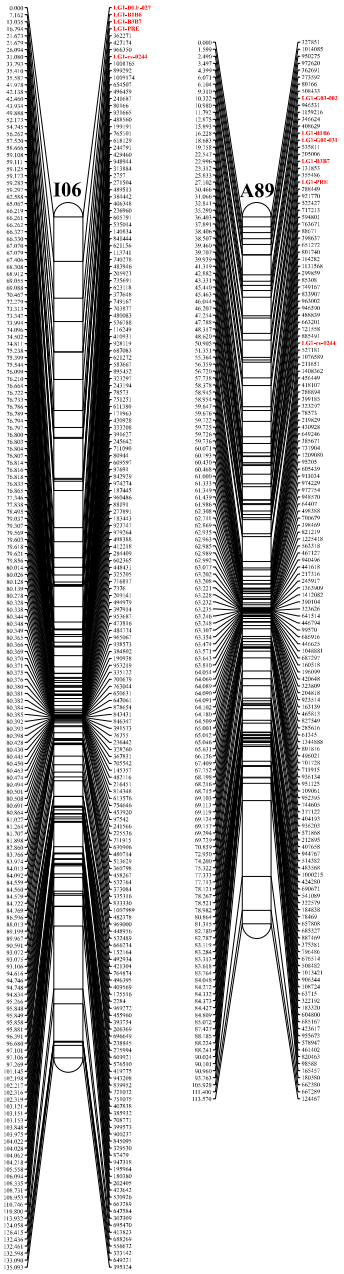

Figure 3.3 Linkage group 1 of a SNP-based genetic linkage map for perennial ryegrass, constructed using the I06 × A89 pseudo-F_2 mapping population. Homeologous linkage groups are presented for parent I06 (left bar) and A89 (right bar). The I06 map includes 184 SNPs and 5 SSRs. The A89 map includes 148 SNPs and 6 SSRs. Marker names are provided to the right of each group; SNPs are in black font and SSRs are in red font. The centiMorgan map distance is provided to the left of each group.

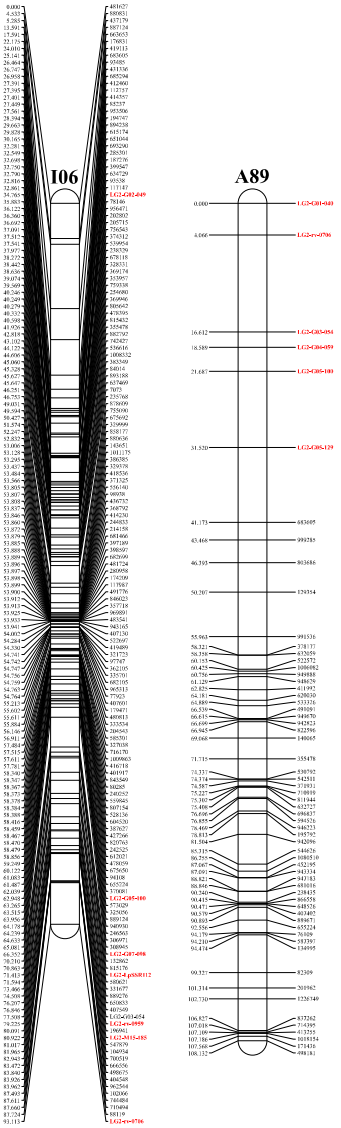

Figure 3.4 Linkage group 2 of a SNP-based genetic linkage map for perennial ryegrass, constructed using the I06 × A89 pseudo-F_2 mapping population. Homeologous linkage groups are presented for parent I06 (left bar) and A89 (right bar). The I06 map includes 161 SNPs and 7 SSRs. The A89 map includes 55 SNPs and 6 SSRs. Marker names are provided to the right of each group; SNPs are in black font and SSRs are in red font. The centiMorgan map distance is provided to the left of each group.

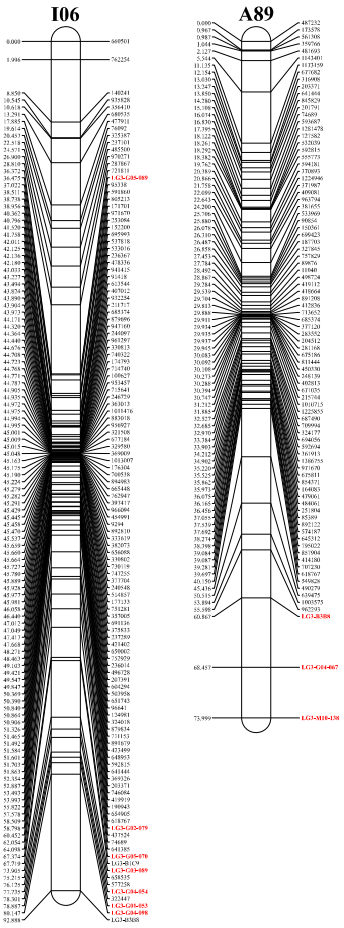

Figure 3.5 Linkage group 3 of a SNP-based genetic linkage map for perennial ryegrass, constructed using the I06 × A89 pseudo-F_2 mapping population. Homeologous linkage groups are presented for parent I06 (left bar) and A89 (right bar). The I06 map includes 114 SNPs and 7 SSRs. The A89 map includes 85 SNPs and 3 SSRs. Marker names are provided to the right of each group; SNPs are in black font and SSRs are in red font. The centiMorgan map distance is provided to the left of each group.

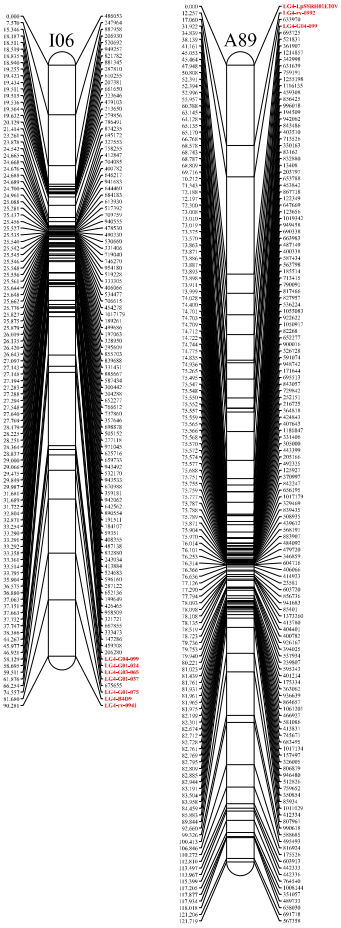

Figure 3.6 Linkage group 4 of a SNP-based genetic linkage map for perennial ryegrass, constructed using the I06 × A89 pseudo-F_2 mapping population. Homeologous linkage groups are presented for parent I06 (left bar) and A89 (right bar). The I06 map includes 102 SNPs and 7 SSRs. The A89 map includes 140 SNPs and 3 SSRs. Marker names are provided to the right of each group; SNPs are in black font and SSRs are in red font. The centiMorgan map distance is provided to the left of each group.

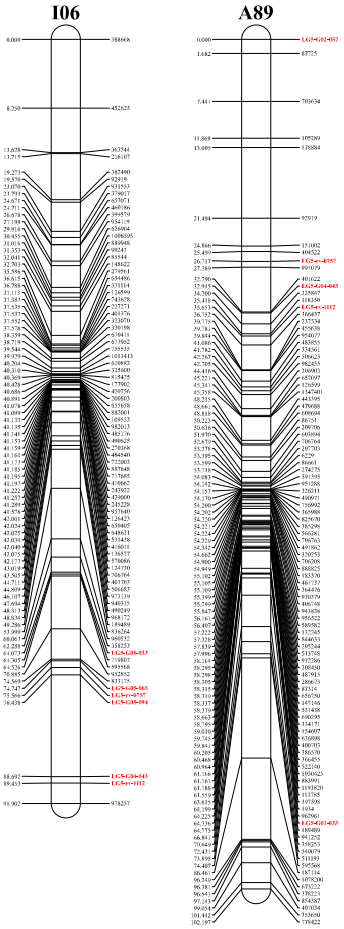

Figure 3.7 Linkage group 5 of a SNP-based genetic linkage map for perennial ryegrass, constructed using the I06 × A89 pseudo-F_2 mapping population. Homeologous linkage groups are presented for parent I06 (left bar) and A89 (right bar). The I06 map includes 79 SNPs and 6 SSRs. The A89 map includes 100 SNPs and 5 SSRs. Marker names are provided to the right of each group; SNPs are in black font and SSRs are in red font. The centiMorgan map distance is provided to the left of each group.

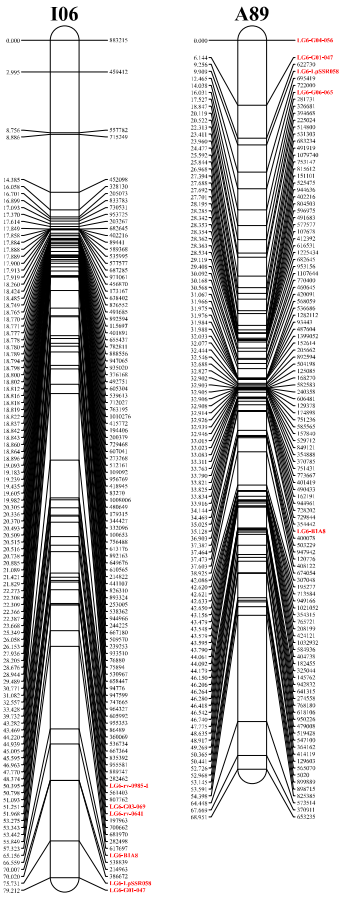

Figure 3.8 Linkage group 6 of a SNP-based genetic linkage map for perennial ryegrass, constructed using the I06 × A89 pseudo-F_2 mapping population. Homeologous linkage groups are presented for parent I06 (left bar) and A89 (right bar). The I06 map includes 106 SNPs and 6 SSRs. The A89 map includes 106 SNPs and 5 SSRs. Marker names are provided to the right of each group; SNPs are in black font and SSRs are in red font. The centiMorgan map distance is provided to the left of each group.

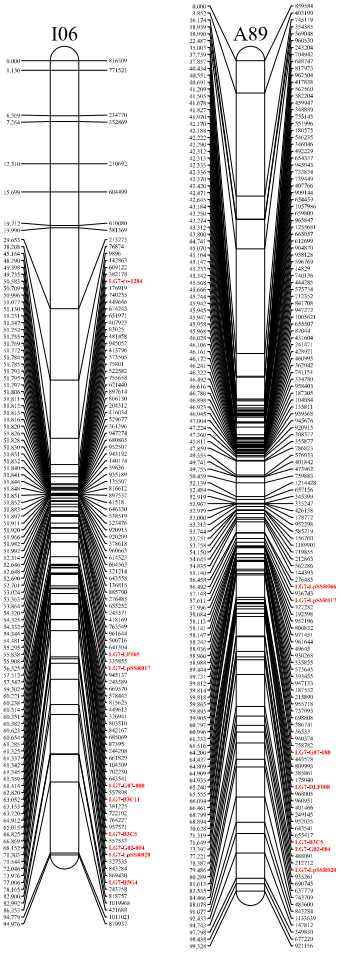

Figure 3.9 Linkage group 7 of a SNP-based genetic linkage map for perennial ryegrass, constructed using the I06 × A89 pseudo-F_2 mapping population. Homeologous linkage groups are presented for parent I06 (left bar) and A89 (right bar). The I06 map includes 107 SNPs and 9 SSRs. The A89 map includes 135 SNPs and 7 SSRs. Marker names are provided to the right of each group; SNPs are in black font and SSRs are in red font. The centiMorgan map distance is provided to the left of each group.

CHAPTER IV

QUANTITATIVE TRAIT LOCUS MAPPING FOR SALINITY TOLERANCE IN PERENNIAL RYEGRASS

Abstract

Fresh water conservation has led to an increased use of alternative water sources for turfgrass irrigation. Alternative water sources often contain high levels of total dissolved salts; therefore, salinity tolerant turfgrass cultivars will be required for successful implementation of this irrigation strategy. Breeders are working to develop turfgrass cultivars with improved salinity tolerance; however, this multigenic, quantitatively inherited trait is difficult to improve using traditional, field-based breeding strategies. To better understand the underlying genetics of salinity tolerance in perennial ryegrass (*Lolium perenne* L.), a quantitative trait locus (QTL) analysis was conducted using the I06 × A89 pseudo-F_2 perennial ryegrass mapping population. The QTL analyses were conducted utilizing the individual I06 and A89 parent maps and phenotypic data for salinity tolerance collected from three field trials during 2017 and 2018. Fifteen major-effect QTL and forty-three minor-effect QTL were identified from the I06 and A89 parent genetic linkage maps. Eleven QTL were identified using both visual ratings and pixel analysis for salinity tolerance, seven QTL were identified at

multiple environmental locations, and one QTL was identified on both parent maps. This is the first reported effort for QTL mapping of salinity tolerance in perennial ryegrass. These findings will be useful for future studies involving development of marker-assisted selection techniques for breeding applications, salinity tolerance gene and mechanism discovery, and comparative genomics investigations for salinity tolerance using closely related plant species. These efforts will lead to the development of improved salinity tolerance in cultivars of perennial ryegrass, which will ultimately contribute to fresh water conservation.

Introduction

Fresh water conservation is a primary concern of the 21st century; the United Nations estimates that water shortages will affect 2.7 billion people by the year 2025 (Montiagne, 2002). Turfgrass, a non-food crop, is considered a low priority for fresh water irrigation (Kjelgren et al., 2000). Thus, laws and regulations have mandated the use of alternative water sources for the irrigation of turfgrass (Dean et al., 1996; Hayes et al., 1990; Shannon and Grieve, 1999). Alternative water sources, such as effluent water, gray water, or seawater, contain high levels of total dissolved salts and can lead to increased salinity stress, which can result in decreased turf quality (Qian and Mecham, 2005).

Salinity stress also occurs naturally along coastal regions that are prone to saltwater sprays and in arid and semi-arid climates that do not receive adequate rainfall to leach salts through soil profiles (Brady and Weil, 2004; Carrow and Duncan, 1998, 2012;

Havlin et al., 2005). In addition, salinity stress can occur due to human involvement through practices such as the use of ice melting salts to clear roadways and applications of fertilizers and other soil amendments (Carrow and Duncan, 1998; Leinauer and Devitt, 2013; Marcum, 2006; Steinke and Ervin, 2013). The growing concerns of salinity stress issues in turfgrass systems have prompted turfgrass breeders to focus their efforts on breeding for improved salinity tolerance in important turfgrass species such as perennial ryegrass (*Lolium perenne* L.) (Duncan and Carrow, 1999; Koch et al., 2015; Lee et al., 2004; Marcum and Pessarakli, 2000; Pessarakli, 2007; Rose-Fricker and Wipff, 2001).

Perennial ryegrass is a major cool-season forage and turfgrass species native to temperate regions of Asia, North Africa, and Europe (Beard, 1973; Funk and Clarke, 1989; Terrell, 1968; Thorogood, 2003). This diploid ($2n = 2x = 14$) species has seven chromosomes and a genome size of approximately 2.5 Gb (Beard, 1973; Kopecky et al., 2010). Koch et al. (2015) found that salinity tolerance is quantitatively inherited in perennial ryegrass and controlled by additive gene effects. Although traditional breeding strategies have yielded perennial ryegrass cultivars with improved salinity tolerance (Friell et al., 2013; Koch and Bonos, 2011), quantitatively inherited traits like salinity tolerance are difficult to improve using the traditional, field-based breeding approach of phenotypic recurrent selection (Grinberg et al., 2016). Thus, many researchers have implemented molecular or laboratory-oriented strategies such as quantitative trait locus (QTL) mapping to help overcome these difficulties (Bushman and Warnke, 2013; Curley et al., 2005; Lespinasse et al., 2000; Portyanko et al., 2005; Tanksley et al., 1993; Wang et al, 2000).

The QTL mapping approach has been used to identify QTL in perennial ryegrass for traits such as disease resistance for stem rust (*Puccinia graminis* subsp. *graminicola* Z. Urb), crown rust (*Puccinia coronata* Corda), and gray leaf spot (*Pyricularia oryzae* Cavara) diseases, vernalization response, winter hardiness, herbage quality characteristics, and morphological and developmental traits (Bushman and Warnke, 2013; Cogan et al., 2005; Curley et al., 2005; Curley et al., 2008; Dumsday et al., 2003; Jensen et al., 2005; Muylle et al., 2005; Pfender et al., 2011; Sartie et al., 2011; Schejbel et al., 2007; Sim et al., 2007; Studer et al., 2008; Yamada et al., 2004). The initial steps for the QTL mapping procedure include the development of an appropriate mapping population and constructing a genetic linkage map that is densely populated with markers (Bernardo, 2002; Langridge and Chalmers, 2004; Singh and Singh, 2015; Xu, 2010). Recently, high-density genetic linkage maps were constructed using the I06 × A89 perennial ryegrass mapping population (Chapters II and III). This is a pseudo-F_2 population composed of 2 parent genotypes and 118 progeny genotypes that segregate for salinity tolerance.

The aims of this research were (i) to conduct QTL analyses using the I06 × A89 mapping population to detect genomic regions involved in salinity tolerance for perennial ryegrass and (ii) to identify molecular markers associated with salinity tolerance for potential future use in a marker-assisted selection breeding approach.

Materials and methods

Plant material

During the summer of 2016, a pseudo-F_2 perennial ryegrass population was constructed to analyze QTL for salinity tolerance (Chapter II). The population was derived from a controlled cross between two diploid heterozygous genotypes, I06 and A89, using I06 as the maternal parent and A89 as the paternal parent. The cross-fertilization event was conducted in a greenhouse at the New Jersey Agricultural Experiment Station in New Brunswick, NJ. On 22 Aug 2016, maternally derived seeds were sown into round pots (15.2 cm diameter) containing Pro-mix growing media (Premier Tech Ltd., Riviere-du-Loup, QC) and allowed to germinate. The resulting 118 pseudo-F_2 progeny were transferred to single cells (5.1 × 5.1 cm) of plastic flats containing Pro-mix growing media and labeled with a unique mapping population designation on 14 Sep 2016.

Genetic linkage mapping

Separate parent genetic linkage maps, I06 and A89, were constructed in JoinMap 4.1 using the doubled haploid two-way pseudo testcross approach (Van Ooijen, 2006, Chapter III). The I06 map included 848 SNPs and 52 SSRs mapped across a total distance of 677.5 cM. The average density of the 900 markers in the I06 map was 0.75 cM. The A89 map included 769 SNPs and 35 SSRs mapped across a total distance of 687.9 cM. The average density of the 804 markers in the A89 map was 0.86 cM. Both the I06 and A89 marker datasets and both genetic linkage maps were used for QTL mapping analyses.

Field assessment for salinity tolerance

The I06 × A89 mapping population was screened for salinity tolerance using three field trials at the Rutgers Plant Science Research and Extension Farm in Adelphia, NJ. Prior to planting in field trials, three replicates of each progeny genotype (n=118) and 24 replicates of each parent genotype (n=2) were established in single cells (6.4 × 6.4 cm) of plastic flats containing Pro-mix growing media. The plants were grown in greenhouse conditions for four weeks where they received daily irrigation and biweekly fertilizer (10N-4.4P-8.3K) applications.

The mapping population was established as two separate mowed spaced-plant trials on 2 Jun 2017 using a Freehold loamy sand soil for one trial (2017LS) and a Holmdel sandy loam soil for the other trial (2017SL). A third mowed spaced-plant trial was established on 25 May 2018 using a Holmdel sandy loam soil (2018SL). Each of the three trials were arranged in a randomized complete block design with 3 replications of each progeny genotype and 24 replications of each parent genotype. Plants were spaced 30.5 cm apart and fertilized with a balanced fertilizer (10N-4.4P-8.3K) at a rate of 98 Kg N Ha^{-1} at time of planting. Fresh water irrigation was supplied during establishment as needed to promote plant growth and limit drought stress. The trials were mowed weekly at a cutting height of 5 cm.

After the establishment period, plants were irrigated with a saline water solution that was made using equal parts of $CaCl_2$ and NaCl salts, as outlined by Koch and Bonos (2010). The saline water solution was mixed in a 1,893 L tank, and the electrical

conductivity (EC) was adjusted to 10 dS m^{-1}. The tank was equipped with a gasoline-powered pump and an internal agitator. The pump was connected to hoses and an attached flow meter (McMaster-Carr, Elmhurst, IL, USA) was used to deliver 0.5 L of the solution to each plant. Irrigation with the saline water solution was applied three times per week, weather permitting, until a desired variation in phenotypic segregation for salinity tolerance was observed.

Salinity tolerance was assessed via visual ratings and digital imagery on 28 Sep 2017 and 4 Sep 2018. Visual ratings were performed to estimate the portion of each plant that was alive at the time of rating. These data were recorded as green cover using a 0-10 rating scale where zero represented approximately 0% green leaf tissue, one represented approximately 10% green leaf tissue, two represented approximately 20% green leaf tissue, three represented approximately 30% green leaf tissue, four represented approximately 40% green leaf tissue, five represented approximately 50% green leaf tissue, six represented approximately 60% green leaf tissue, seven represented approximately 70% green leaf tissue, eight represented approximately 80% green leaf tissue, nine represented approximately 90% green leaf tissue, and ten represented approximately 100% green leaf tissue. Digital images of each plant were taken with a light box when phenotypic variation was at maximum, and the images were subjected to a pixel analysis for percent green cover using TurfAnalyzer software (Karcher et al., 2017). Data for salinity tolerance generated from visual ratings and pixel analysis were analyzed using an analysis of variance (ANOVA) in SAS (SAS Institute, NC, USA) and used to assign a phenotypic mean for each genotype, which was used for QTL analyses. In addition, the relationship between the visual rating and pixel analysis methods was

determined by a simple linear regression analysis using the REG procedure in SAS (SAS Institute, NC, USA).

Quantitative trait locus analysis

The I06 × A89 parent genetic linkage maps, marker datasets for all markers included in the linkage maps, and phenotypic data for salinity tolerance were used for QTL mapping analyses in MapQTL 6 (Van Ooijen, 2009). Permutation testing was conducted to establish genome-wide logarithm of odds (LOD) thresholds using 10,000 permutations and at $\alpha = 0.05$ significance level (Churchill and Doerge, 1994). Initially, QTL regions were identified by interval mapping (IM) procedures with default parameters including a regression algorithm with a mapping step size of 1.0 cM and a maximum number of neighboring markers equal to 5 (Jung et al., 1996; Lander and Botstein, 1989). The automatic cofactor selection (ACS) tool was used to detect significantly ($P < 0.02$) associated markers, which were subsequently used for multiple QTL model (MQM) mapping. The MQM mapping procedures were implemented with default parameters as described for the IM procedures. Positions for QTL were defined as the locations where the LOD scores reached maximum values, and 2-LOD support intervals were used to calculate 99% confidence intervals (Lander and Botstein, 1989; Li, 2011). The significance of identified QTL were further evaluated by testing with the nonparametric, single-marker-based Kruskal-Wallis analysis. The percentage of phenotypic trait variation explained by each marker (R^2) was calculated and used to identify major- and minor-effect QTL. Major-effect QTL were defined by R^2 values ≥ 10.0, while minor-effect QTL were defined by R^2 values < 10.0 (Collard et al., 2005).

Results

Field assessment for salinity tolerance

The visual rating and pixel analysis methods were well correlated with coefficient of determination values ranging from 0.87 to 0.95 across the three environments and the overall, pooled dataset (Figs. 4.1-4.4). Continuous phenotypic variation was observed for salinity stress among the individuals of the mapping population generated from the cross between salinity stress tolerant I06 and salinity stress susceptible A89 among all environments (Tables 4.1, 4.2; Figs. 4.5-4.12).

A summary of mean green cover data generated by visual ratings is presented in Table 4.1. Mean green cover for the progeny genotypes was 4.4, 5.5, and 5.5 at environments 2017LS, 2017SL, and 2018SL, respectively. The overall progeny mean green cover averaged across all three trials was 5.1. Mean green cover for the salinity stress tolerant I06 parent genotype was 5.7, 7.0, and 5.7 at environments 2017LS, 2017SL, and 2018SL, respectively. The overall parent I06 mean green cover averaged across all three trials was 6.1. Mean green cover for the salinity stress susceptible A89 parent genotype was 2.0, 3.8, and 2.6 at environments 2017LS, 2017SL, and 2018SL, respectively. The overall parent A89 mean green cover averaged across all three trials was 2.8.

A summary of mean percent green cover generated by pixel analysis is presented in Table 4.2. Mean percent green cover for the progeny genotypes was 32.4, 61.0, and 56.9 at environments 2017LS, 2017SL, and 2018SL, respectively. The overall progeny mean percent green cover averaged across all three trials was 50.1. Mean percent green cover for the salinity stress tolerant I06 parent genotype was 41.6, 72.7, and 58.8 at environments 2017LS, 2017SL, and 2018SL, respectively. The overall parent I06 mean percent green cover averaged across all three trials was 57.7. Mean percent green cover for the salinity stress susceptible A89 parent genotype was 15.2, 42.5, and 29.4 at environments 2017LS, 2017SL, and 2018SL, respectively. The overall parent A89 mean percent green cover averaged across all three trials was 29.0.

The analyses of variance for salinity tolerance data generated by visual ratings and pixel analysis were similar (Tables 4.3, 4.4). The interaction effect, genotype × environment, significantly affected mean green cover as determined by visual ratings ($P = 0.0003$) and pixel analysis ($P = 0.0002$). The main effect, genotype, significantly affected mean green cover as determined by visual ratings ($P < 0.0001$) and pixel analysis ($P < 0.0001$). The main effect, environment, did not significantly affect mean green cover as determined by visual ratings ($P = 0.4004$) but did significantly affect mean percent green cover as determined by pixel analysis ($P = 0.0347$). Accordingly, QTL analyses were conducted using the phenotypic means for each genotype at each trial location. Additionally, the QTL analyses were conducted on the overall datasets, which were generated by combining the data across all trial locations to increase the consistency in the observed genotype mean response.

Quantitative trait locus analysis

The QTL analyses resulted in the identification of seven major-effect QTL and twenty minor-effect QTL for salinity tolerance at sixteen distinct genomic regions across six linkage groups of the I06 parent map. Additionally, eight major-effect QTL and twenty-three minor-effect QTL were identified for salinity tolerance at twenty distinct genomic regions across seven linkage groups of the A89 parent map (Tables 4.5, 4.6; Figs. 4.13, 4.14). The LOD scores for the QTL identified from the I06 parent map ranged from 3.21 to 12.40, and the percent phenotypic variation for salinity tolerance explained by the QTL ranged from 5.0 to 24.2. The LOD scores for the QTL identified from the A89 parent map ranged from 3.28 to 9.41, and the percent phenotypic variation for salinity tolerance explained by the QTL ranged from 5.1 to 16.9. Eleven QTL were identified using both assessment methods (visual ratings and pixel analysis) for salinity tolerance, and five QTL were identified at more than one environmental location. One QTL was identified on linkage group three of both the I06 and A89 parent maps. The following sections describe the mapping results from each of the parent maps, separately.

<u>I06 parent map</u>

Four QTL with significant LOD scores above the genome-wide LOD thresholds were identified across four regions of linkage group one (Table 4.5; Fig. 4.13). The LOD scores for these QTL ranged from 6.16 to 12.40. All four of the QTL were identified from the visual rating assessment for green cover. Three of the QTL were identified from the environment 2017LS and the remaining QTL was identified from the combined data

from all three environmental locations. A region at 21.194 cM was defined by a single QTL explaining 6.4% phenotypic variation for salinity stress. A single QTL explaining 24.2% phenotypic variation for salinity tolerance was identified at 33.793 cM. Another QTL explaining 6.9% phenotypic variation for salinity tolerance was identified at 42.460 cM. A fourth region at 55.045 cM was defined by a single QTL explaining 6.8% phenotypic variation for salinity stress.

Nine QTL with significant LOD scores above the genome-wide LOD thresholds were identified for salinity tolerance across five regions of linkage group three (Table 4.5; Fig. 4.13). The LOD scores for the QTL ranged from 3.97 to 7.70. Five of the QTL were identified from the pixel analysis and the remaining four QTL were identified from the visual rating assessment. Of the nine total QTL, three were identified from the environment 2017LS, five were identified from the environment 2018SL, and one was identified from the combined data from all three environmental locations. One QTL explaining 8.9% phenotypic variation for salinity tolerance was identified at 42.125 cM. Three QTL explaining between 6.1 and 14.9% phenotypic variation for salinity tolerance were identified at a region between 44.935 and 45.637 cM. One QTL explaining 5.9% phenotypic variation for salinity tolerance was identified at 49.487 cM. Three QTL explaining between 5.0 and 15.3% phenotypic variation for salinity tolerance were identified at a region between 53.793 and 55.693 cM. A final region at 58.509 cM was defined by a single QTL explaining 11.3% phenotypic variation for salinity tolerance.

Four QTL with significant LOD scores above the genome-wide LOD thresholds were identified across two regions of linkage group four (Table 4.5; Fig. 4.13). The LOD scores for the QTL ranged from 4.46 to 10.79. Three of the QTL were identified from

the visual rating assessment and one QTL was identified from the pixel analysis. One QTL was identified from the environment 2017LS, two QTL were identified from the environment 2017SL, and the remaining two QTL were identified from the combined data from all three environmental locations. Three QTL explaining between 6.1 and 16.2% phenotypic variation for salinity tolerance were identified at a region between 58.695 and 62.676 cM. Another region was identified at 73.454 cM and defined by a single QTL explaining 5.8% phenotypic variation for salinity tolerance.

Four QTL with significant LOD scores above the genome-wide LOD thresholds were identified at a single region of linkage group five (Table 4.5; Fig. 4.13). The LOD scores for the QTL ranged from 5.01 to 8.16. Two of the QTL were identified from the visual rating assessment and two QTL were identified from the pixel analysis. Two QTL were identified from the environment 2017LS, one QTL was identified from the environment 2017SL, and the remaining QTL was identified from the combined data from all three environmental locations. Four QTL explaining between 7.6 and 10.6% phenotypic variation for salinity tolerance were identified at a region between 86.138 and 88.892 cM.

Three QTL with significant LOD scores above the genome-wide LOD thresholds were identified across two regions of linkage group six (Table 4.5; Fig. 4.13). The LOD scores for the QTL ranged from 3.21 to 5.65. Two of the QTL were identified from the visual rating assessment and one QTL was identified from the pixel analysis. One QTL was identified from the environment 2017LS, one QTL was identified from the environment 2017SL, and the remaining QTL was identified from the combined data from all three environmental locations. Two QTL explaining 5.7 and 7.6% phenotypic

variation for salinity tolerance were identified at a region between 18.424 and 19.605 cM. A region at 47.870 cM was defined by a single QTL explaining 7.9% phenotypic variation for salinity tolerance.

Three QTL with significant LOD scores above the genome-wide LOD thresholds were identified across two regions of linkage group seven (Table 4.5; Fig. 4.13). The LOD scores for the QTL ranged from 3.49 to 7.65. Two of the QTL were identified from the pixel analysis and one QTL was identified from the visual rating assessment. All three QTL were identified from the environment 2018SL. Two QTL explaining 7.0 and 12.2% phenotypic variation for salinity tolerance were identified at a region between 50.435 and 50.535 cM. A region at 71.544 cM was defined by a single QTL explaining 7.1% phenotypic variation for salinity tolerance.

A89 parent map

Four QTL with significant LOD scores above the genome-wide LOD thresholds were identified across two regions of linkage group one (Table 4.6; Fig. 4.14). The LOD scores for the QTL ranged from 3.81 to 6.24. Two of the QTL were identified from the visual rating assessment and the other two QTL were identified from the pixel analysis. Two of the QTL were identified from the environment 2017LS and two QTL were identified from the environment 2017SL. Two QTL explaining 7.5 and 7.6% phenotypic variation for salinity tolerance were identified at a region between 18.683 and 18.783 cM. Two QTL explaining 7.5 and 9.8% phenotypic variation for salinity tolerance were identified at a region between 26.933 and 27.033 cM.

Five QTL with significant LOD scores above the genome-wide LOD thresholds were identified across three regions of linkage group two (Table 4.6; Fig. 4.14). The LOD scores for the QTL ranged from 4.53 to 7.83. Three of the QTL were identified from the visual rating assessment and the remaining two QTL were identified from the pixel analysis. Two of the QTL were identified from the environment 2017LS, one QTL was identified from the environment 2017SL, one QTL was identified from the environment 2018SL, and the remaining QTL was identified from the combined data from all three environmental locations. Three QTL explaining between 8.5 and 8.7% phenotypic variation for salinity tolerance were identified at a region between 13.266 and 16.912 cM. One QTL explaining 7.3% phenotypic variation for salinity tolerance was identified at 69.068 cM. Another single QTL explaining 16.9% phenotypic variation for salinity tolerance was identified at 81.313 cM.

Nine QTL with significant LOD scores above the genome-wide LOD thresholds were identified across seven regions of linkage group three (Table 4.6; Fig. 4.14). The LOD scores for the QTL ranged from 3.28 to 9.53. Five of the QTL were identified from the pixel analysis and the remaining four QTL were identified from the visual rating assessment. Of the nine total QTL on linkage group three, one was identified from the environment 2017SL, four were identified from the environment 2018SL, and the remaining four QTL were identified from the combined data from all three environmental locations. Single QTL explaining 10.6, 5.8, 14.1, 8.2, 9.6, and 5.1% phenotypic variation for salinity tolerance were identified at 22.058, 26.487, 30.847, 35.520, 39.997, and 50.515 cM, respectively. Three QTL explaining between 4.9 and 6.0% phenotypic variation for salinity tolerance were identified at a region between 60.198 and 60.867.

Four QTL with significant LOD scores above the genome-wide LOD thresholds were identified across three regions of linkage group four (Table 4.6; Fig. 4.14). The LOD scores for the QTL ranged from 4.06 to 5.61. Three of the QTL were identified from the pixel analysis and one QTL was identified from the visual rating assessment. Two QTL were identified from the environment 2017LS, one QTL was identified from the environment 2017SL, and the remaining QTL was identified from the combined data from all three environmental locations. One QTL explaining 7.8% phenotypic variation for salinity tolerance was identified at 37.339 cM. One QTL explaining 8.8% phenotypic variation for salinity tolerance was identified at 62.788 cM. Two QTL explaining 6.5 and 7.1% phenotypic variation for salinity tolerance was identified at a region between 113.967 and 117.934 cM.

Five QTL with significant LOD scores above the genome-wide LOD thresholds were identified across three regions of linkage group five (Table 4.6; Fig. 4.14). The LOD scores for the QTL ranged from 4.14 to 9.41. Three of the QTL were identified from the pixel analysis and the remaining two QTL were identified from the visual rating assessment. All five QTL were identified from the environment 2017SL. One QTL explaining 9.6% phenotypic variation for salinity tolerance was identified at 32.790 cM. Two QTL explaining 15.3 and 16.8% phenotypic variation were identified at a region between 47.458 and 47.558 cM. Two QTL explaining 6.0 and 6.6% phenotypic variation for salinity tolerance were identified at 55.799 cM.

Two QTL with significant LOD scores above the genome-wide LOD thresholds were identified at a single region of linkage group six (Table 4.6; Fig. 4.14). The LOD scores for the QTL were 4.95 and 7.26. One QTL was identified from the visual rating

assessment and one QTL was identified from the pixel analysis. Both QTL were identified from the environment 2017SL. The two QTL explaining 10.0 and 11.6% phenotypic variation for salinity tolerance were identified at a region between 9.856 and 9.909 cM.

Two QTL with significant LOD scores above the genome-wide LOD thresholds were identified at a single region of linkage group seven (Table 4.6; Fig. 4.14). The LOD scores for the QTL were 3.43 and 9.04. One QTL was identified from the visual rating assessment and one QTL was identified from the pixel analysis. Both QTL were identified from the environment 2018SL. The two QTL explaining 5.1 and 14.6% phenotypic variation for salinity tolerance were identified at a region between 64.200 and 65.240 cM.

Discussion

Salinity stress is a growing concern among the turfgrass community. As a result, breeders are working to develop salinity tolerant cultivars of widely used turfgrass species such as perennial ryegrass (Duncan and Carrow, 1999; Koch et al., 2015; Lee et al., 2004; Marcum and Pessarakli, 2000; Pessarakli, 2007; Rose-Fricker and Wipff, 2001). Salinity tolerance is a multigenic, quantitatively inherited trait in perennial ryegrass (Koch et al., 2015). Researchers have documented greater than 100 salt stress induced genes and 300 salt stress repressed genes in the salt stress model plant, *Mesembryanthemum crystallinum* (Meyer et al., 1990). The general rationale for the

current study was to generate a better understanding of the underlying genetic basis for salinity tolerance in perennial ryegrass.

In total, fifteen major-effect QTL and forty-three minor-effect QTL for salinity tolerance were detected. Groups of coincident QTL were identified and partitioned to thirty-six target genomic regions, which will be useful for future studies and potential breeding applications. Major-effect QTL were defined as those QTL that explained 10.0%, or greater, phenotypic variation for salinity tolerance (Collard et al., 2005). Seven major-effect QTL were identified across five linkage groups on the I06 parent map, and eight major-effect QTL were identified across five linkage groups on the A89 parent map. Although greater than 10% phenotypic variation for salinity tolerance was explained by each of these QTL, many of the markers associated with these QTL were not consistently identified across the three environments in this study. Nonetheless, the genomic regions defined by these major-effect QTL should be investigated further to elucidate their potential role for salinity tolerance in perennial ryegrass.

Eleven QTL were identified using both visual rating and pixel analysis assessments. On the I06 parent map, QTL were identified at linkage groups three, four, five, and seven using both assessment methods. The markers closest to those QTL were 246729 for the QTL at linkage group three, G01_037 for the QTL at linkage group four, G04_043 for the QTL at linkage group five, and rv_1284 for the QTL at linkage group seven. On the A89 parent map, QTL were identified at linkage groups one, two, three, five, and six using both assessment methods. The markers closest to those QTL were G01_031 and PRE for the QTL at linkage group one, G03_054 for the QTL at linkage

group two, B3B8 for the QTL at linkage group three, 443395 and 406748 for the QTL at linkage group five, and LpSSR058 for the QTL at linkage group six.

These findings provide evidence of consistency in detecting these markers for the respective QTL regions; however, considering the high correlation between the data generated from visual ratings and pixel analysis, we anticipated identifying a larger number of shared markers from those two datasets. Nonetheless, the demonstrated ability to identify these eleven markers using different evaluation methods provides a reasoning for exploring those genomic regions in more detail.

In addition to observing consistency in marker identification among assessment methods, five QTL were also identified across multiple environments in the study. Three QTL were identified at linkage groups three, four, and five of the I06 parent map. The markers closest to those QTL were 190943 for the QTL at linkage group three, G01_037 for the QTL at linkage group four, and G04_043 for the QTL at linkage group five. Marker 190943 was identified from the 2018SL environment and the overall, pooled dataset from the three environments. Marker G01_037 was identified from the 2017SL environment and the overall, pooled dataset from the three environments. Marker G04_043 was identified from the 2017LS environment, the 2017SL environment, and the overall, pooled dataset from the three environments. Using the A89 parent map, QTL were identified at linkage groups two and three. The markers closest to those QTL were G03_054 for the QTL at linkage group two and B3B8 for the QTL at linkage group three. Marker G03_054 were identified from the 2017LS environment and the overall, pooled dataset from the three environments. Marker B3B8 was identified from the 2018SL environment and the overall, pooled dataset from the three environments. These results

indicate consistency in detecting these QTL, which suggest potential linkage between these QTL and the salinity tolerance trait in perennial ryegrass.

An additional, interesting finding was the identification of a QTL closely related to marker 618767, which was identified on linkage group three of both parent maps. The QTL was identified using the 2018SL phenotypic data with the I06 parent map and the overall, pooled data across the three environments with the A89 parent map. In the I06 parent map analysis, this QTL explained 11.3% total phenotypic variation for salinity tolerance. In the A89 parent map analysis, this QTL explained 9.6% total phenotypic variation for salinity tolerance. This QTL should be studied further to discern its role for salinity tolerance in perennial ryegrass.

In summary, this was the first reported effort to map QTL for salinity tolerance in perennial ryegrass. Thirty-six genomic regions were identified across the genetic linkage maps for the I06 and A89 parents. In addition, fifteen major-effect QTL were identified at these regions. Eleven QTL were identified using both visual ratings and pixel analysis to assess salinity tolerance, five QTL were identified at multiple environmental locations, and one QTL was identified on both parent maps.

Future work should include QTL confirmation studies using different environments and populations and dissecting the QTL regions identified in this study to determine their usefulness for marker-assisted selection breeding strategies. In addition, we will also study these QTL regions using techniques such as comparative genomics to identify possible genes and underlying mechanisms for salinity tolerance in perennial ryegrass and other closely related species. We also anticipate the completion of the perennial ryegrass reference genome in the near future (Byrne et al., 2015). This will be

a valuable resource for forthcoming studies with the I06 × A89 perennial ryegrass mapping population. Through these proposed efforts, we hope to better understand salinity tolerance in perennial ryegrass and other closely related species. This will be important for developing improved salt tolerant cultivars that can be irrigated with alternative water sources, which will ultimately contribute to fresh water conservation.

Literature cited

Beard, J.B. 1973. Turfgrass: Science and Culture. Prentice Hall, Englewood Cliffs, NJ.

Bernardo, R. 2002. Breeding for quantitative traits in plants. Stemma Press, Woodbury, MN, USA.

Brady, N.C., and R.R. Weil. 2004. Elements of the nature and properties of soils. Prentice Hall, Upper Saddle River, NJ.

Bushman, B.S., and S.E. Warnke. 2013. Genetic and genomic approaches for improving turfgrass. In: J.C. Stier, B.P. Horgan, and S.A. Bonos, editors, Turfgrass: biology, use, and management. ASA, CSSA, and SSSA, Madison, WI. p.683–712.

Byrne, S.L., M. Pfeifer, I. Nagy, I. Armstead, S. Swain, B. Studer, K.F.X. Mayer, J.D. Campbell, A. Czaban, S. Hentrup, F. Panitz, C. Bendixen, J. Hedegaard, M. Caccamo, T. Asp. 2015. A senty-based draft genome sequence for the forage grass *Lolium perenne*. Plant J. 84:816–826.

Carrow, R.N., and R.R. Duncan. 1998. Salt-affected turfgrass sites: Assessment and management. Ann Arbor Press. Chelsea, MI.

Carrow, R.N., and R.R. Duncan. 2012. Best management practices for saline and sodic turfgrass soils. CRC Press, Boca Raton, FL.

Churchill, G.A., and R.W. Doerge. 1994. Empirical threshold values for quantitative trait mapping. Genetics 138:963–971.

Cogan, N.O.I., K.F. Smith, T. Yamada, M.G. Francki, A.C. Vecchies, E.S. Jones, G.C. Spangenberg, and J.W. Forster. 2005. QTL analysis and comparative genomics of herbage quality traits in perennial ryegrass (*Lolium perenne* L.). Theor. Appl. Genet. 110:364–380.

Collard, B.C.Y., M.Z.Z. Jahufer, J.B. Brouwer, and E.C.K. Pang. 2005. An introduction to markers, quantitative trait loci (QTL) mapping and marker-assisted selection for crop improvement: The basic concepts. Euphytica 142:169–196. Doi:10.1007/s10681-005-1681-5

Curley, J., S.C. Sim, S. Warnke, S. Leong, and R. Barker. 2005. QTL mapping of resistance to gray leaf spot in ryegrass. Theor. Appl. Genet. 111:1107–1117.

Curley, J., N. Chakraborty, S. Chang, and G. Jung. 2008. QTL mapping of resistance to gray leaf spot in ryegrass: Consistency of QTL between two mapping populations. J. Korean Turf. Sci. 22:85–100.

Dean, D.E., D.A. Devitt, L.S. Verchick, and R.L. Morris. 1996. Turfgrass quality, growth, and water use influenced by salinity and water stress. Agron. J. 88:844–849. doi:10.2134/agronj1996.00021962008800050026x

Dellavalle, N.B. 1992. Determination of specific conductance in supertatant 1:2 soil:water solution In: Handbook on reference methods for soil analysis. Soil and Plant Analysis Council, Athens, GA. P.44–50.

Dumsday, J.L., K.F. Smith, J.W. Forster, and E. Jones, 2003. SSR-based genetic linkage analysis of resistance to crown rust (*Puccinia coronate* f. sp. *lolii*) in perennial ryegrass (*Lolium perenne* L.). Plant Pathol. 52:628–637.

Duncan, R.R., and R.N. Carrow. 1999. Turfgrass molecular genetic improvement for biotic/edaphic stress resistance. Advances in Agronomy 67:233–305.

Friell, J., E. Watkins, and B. Horgan. 2013. Salt tolerance of 74 turfgrass cultivars in nutrient solution culture. Crop Sci. 53:1743–1749.

Funk, C.R., and B.B. Clarke. 1989. Turfgrass breeding – with special reference to turf-type perennial ryegrass, tall fescue, and endophytes. In: H. Takotoh, editor, Proceedings of the 6th International Turfgrass Research Conference, Tokyo, Japan. 31 July – 5 Aug. 1989. p.3–10.

Grinberg, N.F., A. Lovatt, M. Hegarty, A. Lovatt, K.P. Skot, R. Kelly, T. Blackmore, D. Thorogood, R.D. King, I. Armstead, W. Powell, L. Skot. 2016. Implementation of genomic prediction in *Lolium perenne* (L.) breeding populations. Front. Plant Sci. 7:133

Havlin, J.L., J.D. Beaton, S.L. Tisdale, and W.L. Nelson. 2005. Soil fertility and fertilizers: an introduction to nutrient management. Prentice Hall, Upper Saddle River, NJ.

Hayes, A.R., C.F. Mancino, and I.L. Pepper. 1990. Irrigations of turfgrass with secondary sewage effluent: I. Soil and leachate water quality. Agron. J. 82:939–943. doi:10.2134/agronj1990.00021962008200050020x

Jensen, L.B., H. Muylle, P. Arens, C.H. Andersen, P.B. Holm, M. Ghesquiere, B. Julier, T. Lubberstedt, K.K. Nielsen, J.D. Riek, I. Roldan-Ruiz, N. Roulund, C. Taylor, B. Vosman, P. Barre. 2005. Development and mapping of a public reference set of SSR markers in *Lolium perenne* L. Mol. Ecol. Notes doi:10.1111/j.1471–8286.2005.01043.x

Jung, G., D.P. Coyne, P.W. Skroch, J. Nienhuis, E. Arnaud-Santana, J. Bokosi, H.M. Ariyarathne, J.R. Steadman, J.S. Beaver, and S.M. Kaeppler. 1996. Molecular markers associated with plant architecture and resistance to common blight, web blight, and rust in common beans. J. Am. Soc. Hortic. Sci. 121:794–803.

Karcher, D.E., C.J. Purcell, M.D. Richardson, L.C. Purcell, and K.W. Hignight. 2017. A new java program to rapidly quantify several turfgrass parameters from digital images. Agron. Abr. P. 109313.

Kjelgren, R., L. Rupp, D. Kilgren. 2000. Water conservation in urban landscapes. HortScience 35:1037–1040.

Koch, M.J., and S.A. Bonos. 2010. An overhead irrigation screening technique for salinity tolerance in cool-season turfgrasses. Crop Sci. 50:2613–2619.

Koch, M.J., and S.A. Bonos. 2011. Salinity tolerance of cool-season turfgrass cultivars under field conditions. Appl. Turfgrass Sci. doi:10.1094/ATS-2011-0725-01-RS

Koch, M.J., W.A. Meyer, and S.A. Bonos. 2015. Inheritance of salinity tolerance in perennial ryegrass. Crop Sci. 55:1834–1842.

Kopecky, D., M. Havrankova, J. Loureiro, S. Castro, A.J. Lukaszewski, J. Bartos, J. Kopecka, J. Dolezel. 2010. Physical distribution of homeologous recombination in individual chromosomes of *Festuca pratensis* in *Lolium multiflorum*. Cytogenetic and Genome Research 129:162–172.

Lander, E., and D. Botstein. 1989. Mapping Mendelian factors underlying quantitative traits using RFLP linkage maps. Genetics 121:185–199.

Langridge, P., and K. Chalmers. 2004. The principle: identification and application of molecular markers. In: H. Lorz and G. Wenzel, editors, Biotechnology in agriculture and forestry: molecular marker systems in plant breeding and crop improvement. Springer-Verlag Berlin Heidelberg, Germany. p. 3–22.

Lee, G.J., R.N. Carrow, and R.R. Duncan. 2004. Salinity tolerance of selected seashore paspalums and bermudagrasses: Root and verdure responses and criteria. HortScience 39:1136–1142.

Leinauer, B., and D.A. Devitt. 2013. Irrigation science and technology. In: J.C. Stier, B.P. Horgan, and S.A. Bonos, editors, Turfgrass: biology, use, and management. ASA, CSSA, and SSSA, Madison, WI. p.1075–1132.

Lespinasse, D., L. Grivet, V. Troispoux, M. Rodier-Goud, F. Pinard, M. Sequin. 2000. Identification of QTL involved in the resistance to South American leaf blight (*Microcyclus ulei*) in the rubber tree. Theor. Appl. Genet. 100:975–984.

Li, H. 2011. A quick method to calculate QTL confidence interval. J. Genet. 90:355–360.

Marcum, K.B. 2006. Use of saline and non-potable water in the turfgrass industry: Constraints and developments. Agric. Water Manage. 80:132–146.

Marcum, K.B., and M. Pessarakli. 2000. Salinity tolerance of 35 bermudagrass cultivars. Agron. Abstr. 169.

Meyer, G., J.M. Schmitt, and H.J. Bohnert. 1990. Direct screening of a small genome: Estimation of the magnitude of plant gene expression during adaptation to high salt. Mol. Gen. Genet. 224:347–356.

Montiagne, F. 2002. Water pressure. Nat. Geogr. 202:2–33.

Muylle, H., J. Baert, E. Van Bockstaele, J. Pertijs, and I. Roldan-Ruiz. 2005. Four QTL determine crown rust (*Puccinia coronate* f. sp. *lolii*) resistance in a perennial ryegrass (*Lolium perenne*) population. Heredity 95:348–357.

Pessarakli, M. 2007. Saltgrass (*Distichlis spicata*), a potential future turfgrass species with minimum maintenance/management cultural practices. In: Handbook of Turfgrass Management and Physiology, Edited by: Pesarakli, M. 57–63. Boca Raton, FL: CRC Press.

Pfender, W., M. Saha, E. Johnson, M. Slabaugh. Mapping with RAD (restriction-site associated DNA) markers to rapidly identify QTL for stem rust resistance in *Lolium perenne*. Theor. Appl. Genet. 122:1467–1480.

Portyanko, V.A., G. Chen, H.W. Rines, R.L. Phillips, K.J. Leonard, G.E. Ochocki, D.D. Stuthman. 2005. Quantitative trait loci for partial resistance to crown rust, *Puccinia coronoata*, in cultivated oat, *Aevena sativa* L. Theor. Appl. Genet. 111:313–324.

Qian, Y.L., and B. Mecham. 2005. Long-term effect of recycled wastewater irrigation on soil chemical properties on golf course fairways. Agron. J. 97:717–721.0 doi:10.2134/agronj2004.0140

Rose-Fricker, C., and J. Wipff. 2001. Breeding for salt tolerance in cool-season turfgrasses. Int. Turf. Soc. Res. J. 9:206–212.

Sartie, A.M., C. Matthew, H.S. Easton, and M.J. Faville. 2011. Phenotypic and QTL analyses of herbage-production related traits in perennial ryegrass (*Lolium perenne* L.).Euphytica182:295–315. doi:10.1007/s10681-0110400-7

Schejbel, B., L.B. Jensen, Y. Xing, T. Lubberstedt. 2007. QTL analysis of crown rust resistance in perennial ryegrass under conditions of natural and artificial infection. Plant Breed 126:347–352.

Shannon, M.C., and C.M. Grieve. 1999. Tolerance of vegetable crops to salinity. Sci. Hortic. (Amsterdam) 78:19–27.

Sim, S., K. Diesburg, M. Casler, and G. Jung. 2007. Mapping and comparative analysis of QTL for crown rust resistance in an Italian × perennial ryegrass population.

Phytopathology 97:767–776. doi:10.1094/PHYTO-97-6-0767

Singh, B.D. and Singh, A.K. 2015. Marker-assisted plant breeding: principles and practices. Springer, New Delhi

Steinke, K., and E.H. Ervin. 2013. Turfgrass ecology. In: J.C. Stier, B.P. Horgan, and S.A. Bonos, editors, Turfgrass: biology, use, and management. ASA, CSSA, and SSSA, Madison, WI. p.347–382.

Studer, B., T. Asp, U. Frei, S. Hentrup, H. Meally, A. Guillard, S. Barth, H. Muylle, Roldan-Ruiz, P. Barre, C. Koning, Boucoiran, G. Uenk-Stunnenberg, O. Dolstra, L. Skot, K.P. Skot, L.B. Turner, M. O. Humphreys, R. Kolliker, N. Roulund, K.K. Nielson, T. Lubberstedt. 2008. Expressed sequence tag-derived microsatellite markers of perennial ryegrass (*Lolium perenne* L.). Mol. Breed. 21:533–548.

Tanksley, S.D., N.D. Young, A.H. Paterson, M.W. Bonierbale. 1993. RFLP mapping in plant breeding: new tools for an old science. Bio/Technol. 7:257–264.

Terrell, E.E. 1968. A taxonomic revision of the genus *Lolium*. Technical Bulletin No. 1392. United States Department of Agriculture, Washington, D.C.

Thorogood, D. 2003. Perennial ryegrass (*Lolium perenne* L.), p. 75-105. In: M.D. Casler and R.R. Duncan, editors, Turfgrass biology, genetics, and breeding. John Wiley and Sons, Hoboken, NJ. p.75–106.

Van Ooijen, J.W. 2006. JoinMap 4.0, software for the calculation of genetic linkage maps in experimental populations. Kyazma B.V., Wageningen, Netherlands

Van Ooijen, J.W. 2009. MapQTL 6, software for the mapping of quantitative trait loci in experimental populations of diploid species. Kyzma B.V. Wageningen, Netherlands

Wang, D., R. Karle, A.F. Iezzoni. 2000. QTL analysis of flower and fruit traits in sour cherry. Theor. Appl. Genet. 100:535–544.

Xu, Y. 2010. Molecular plant breeding. CAB International, Wallingford. p. 734.

Yamada, T., E.S. Jones, N.O.I. Cogan, A.C. Vecchies, T. Nomura, H. Hisano, Y. Shimamoto, K.F. Smith, M.D. Hayward, and J.W. Forster. 2004. QTL analysis of morphological, developmental, and winter hardiness-associated traits in perennial ryegrass. Crop Sci. 44:925–935.

Table 4.1 Mean green cover as determined via visual ratings for the I06 × A89 perennial ryegrass population and each parent genotype on 28 Sep 2017 and 4 Sep 2018 at the Rutgers Plant Science Research and Extension Farm in Adelphia, NJ.

Environment[a]	Population Mean	Parent I06 Mean	Parent A89 Mean
2017LS	4.4[b]	5.7	2.0
2017SL	5.5	7.0	3.8
2018SL	5.5	5.7	2.6
Overall	5.1	6.1	2.8

[a] Freehold loamy sand soil during 2017 (2017LS), Holmdel sandy loam soil during 2017 (2017SL), Holmdel sandy loam soil during 2018 (2018SL).
[b] Green cover as estimated using a visual rating scale where 0 represented approximately 0% green cover and 10 represented approximately 100% green cover.

Table 4.2 Mean percent green cover as determined via pixel analysis for the I06 × A89 perennial ryegrass population and each parent genotype on 28 Sep 2017 and 4 Sep 2018 at the Rutgers Plant Science Research and Extension Farm in Adelphia, NJ.

Environment[a]	Population Mean	Parent I06 Mean	Parent A89 Mean
2017LS	32.4	41.6	15.2
2017SL	61.0	72.7	42.5
2018SL	56.9	58.8	29.4
Overall	50.1	57.7	29.0

[a] Freehold loamy sand soil during 2017 (2017LS), Holmdel sandy loam soil during 2017 (2017SL), Holmdel sandy loam soil during 2018 (2018SL).

Table 4.3 Analysis of variance for mean green cover as determined via visual ratings for the I06 × A89 perennial ryegrass mapping population on 28 Sep 2017 and 4 Sep 2018 at the Rutgers Plant Science Research and Extension Farm in Adelphia, NJ.

Sources of variation	*df*	*F* VALUE	*P* > *F*
Environment	2	1.07	0.4004
Rep(Environment), Error 1	6		
Genotype	119	2.78	<0.0001
Genotype x Environment	237	1.42	0.0003
Genotype x Rep(Environment), Error 2	711		
Error 3	127		

Table 4.4 Analysis of variance for mean percent green cover as determined via pixel analysis for the I06 × A89 perennial ryegrass mapping population on 28 Sep 2017 and 4 Sep 2018 at the Rutgers Plant Science Research and Extension Farm in Adelphia, NJ.

Sources of variation	*df*	*F* VALUE	*P* > *F*
Environment	2	6.19	0.0347
Rep(Environment), Error 1	6		
Genotype	119	2.67	<0.0001
Genotype x Environment	237	1.43	0.0002
Genotype x Rep(Environment), Error 2	711		
Error 3	127		

Table 4.5 Summary of the twenty-seven quantitative trait loci (QTL) identified for salinity tolerance at sixteen distinct genomic regions across six linkage groups of the I06 parent map. A multiple QTL model mapping analysis was conducted with phenotypic data for salinity tolerance generated from visual ratings and pixel analysis of field trials during 2017 on a loamy sand soil (2017LS) and a sandy loam soil (2017SL) and during 2018 on a sandy loam soil (2018SL) at the Rutgers Plant Science Research and Extension Farm in Adelphia, NJ.

Environment	QTL name[a]	LG	Position (cM)	Marker[b]	Allele means[c]		KW[d]	LOD[e]	R^2(%)[f]	99% CI (cM)[g]
					Allele a	Allele b				
2017LS	qI06STVIS-1	1	21.194	362271	4.8	4.2	*	6.16	6.4	19.394-21.673
Overall	qI06STVIS-32	1	33.793	1008765	5.5	5.1	**	12.40	24.2	32.180-34.293
2017LS	qI06STVIS-2	1	42.460	241687	3.9	4.7	***	6.56	6.9	39.187-42.460
2017LS	qI06STVIS-3	1	55.045	199191	4.3	4.8	*	6.53	6.8	53.573-55.545
2018SL	qI06STPA-6	3	42.125	533016	64.0	54.3	**	4.27	8.9	42.125-42.125
2017LS	qI06STVIS-8	3	44.935	246729	4.1	4.7	*	5.92	6.1	44.935-44.935
2017LS	qI06STPA-2	3	44.935	246729	30.0	35.3	**	7.70	14.9	44.935-44.935
2018SL	qI06STPA-7	3	45.637	382073	55.6	62.4	*	3.99	8.2	45.637-45.659
2018SL	qI06STVIS-27	3	49.847	604294	5.4	6.1	*	3.97	5.9	49.547-50.147
2017LS	qI06STVIS-9	3	53.793	419919	4.8	4.2	**	5.10	5.0	53.593-54.593

Table 4.5 (continued)

Environment	QTL name	LG	Position (cM)	Marker	Allele means		KW	LOD	R^2(%)	99% CI (cM)
					Allele a	Allele b				
Overall	qI06STPA-13	3	54.993	190943	52.4	49.7	**	10.01	15.3	53.693-57.422
2018SL	qI06STPA-8	3	55.693	190943	64.3	53.4	****	4.57	9.4	55.293-56.622
2018SL	qI06STVIS-28	3	58.509	618767	5.2	6.2	****	7.17	11.3	58.278-58.509
2017SL	qI06STVIS-18	4	58.695	G01_024	5.2	5.8	**	4.46	6.1	58.629-59.495
2017SL	qI06STVIS-19	4	61.411	G01_037	5.1	5.9	**	6.17	8.7	60.111-62.576
Overall	qI06STPA-15	4	62.676	G01_037	47.8	52.9	****	10.79	16.2	59.511-65.076
2017LS	qI06STVIS-10	4	73.454	G01_075	4.7	4.1	**	5.61	5.8	70.254-76.457
2017LS	qI06STVIS-11	5	86.138	G04_043	4.9	4.2	****	8.16	8.8	78.338-88.892
Overall	qI06STPA-16	5	88.638	G04_043	53.9	48.9	***	7.31	10.6	85.638-88.992
2017SL	qI06STVIS-22	5	88.892	G04_043	5.9	5.3	**	5.56	7.6	88.692-88.992
2017LS	qI06STPA-3	5	88.892	G04_043	37.0	29.9	*****	5.01	8.9	87.838-88.992
2017LS	qI06STPA-4	6	18.424	173167	30.8	35.2	*	3.21	5.7	18.360-18.424

Table 4.5 (continued)

Environment	QTL name	LG	Position (cM)	Marker	Allele means		KW	LOD	R^2(%)	99% CI (cM)
					Allele a	Allele b				
Overall	qI06STVIS-39	6	19.605	83270	5.0	5.4	**	4.29	7.6	19.535-19.605
2017SL	qI06STVIS-23	6	47.870	889747	5.3	5.8	*	5.65	7.9	47.563-47.970
2018SL	qI06STPA-9	7	50.435	rv_1284	54.5	62.0	**	3.49	7.0	50.035-50.583
2018SL	qI06STVIS-30	7	50.535	rv_1284	5.2	6.2	****	7.65	12.2	50.135-50.683
2018SL	qI06STPA-10	7	71.544	327535	54.4	60.8	*	3.51	7.1	71.503-72.044

[a] Name of QTL, indicates parent background (parent I06) and assessment method used to determine salinity tolerance (VIS = visual rating, PA = pixel analysis).
[b] Name of marker closest to a given QTL.
[c] The mean phenotypic value of progeny carrying the 'a' or 'b' allele of each marker.
[d] Kruskal-Wallis analysis. *, **, ***, ****, ***** Significant at $P \leq 0.1$, 0.05, 0.01, 0.005, and 0.0005 levels, respectively.
[e] The LOD values of the QTL determined by multiple QTL model (MQM) mapping.
[f] Proportion of phenotypic variation explained by a given QTL.
[g] A 99% confidence interval for the QTL length (cM) as determined using the 2-LOD approach.

Table 4.6 Summary of the thirty-one quantitative trait loci (QTL) identified for salinity tolerance at sixteen distinct genomic regions across six linkage groups of the A89 parent map. A multiple QTL model mapping analysis was conducted with phenotypic data for salinity tolerance generated from visual ratings and pixel analysis of field trials during 2017 on a loamy sand soil (2017LS) and a sandy loam soil (2017SL) and during 2018 on a sandy loam soil (2018SL) at the Rutgers Plant Science Research and Extension Farm in Adelphia, NJ.

Environment	QTL name[a]	LG	Position (cM)	Marker[b]	Allele means[c]		KW[d]	LOD[e]	R^2(%)[f]	99% CI (cM)[g]
					Allele a	Allele b				
2017LS	qA89STPA-1	1	18.683	G01_031	37.1	30.9	***	5.92	7.5	16.228-18.983
2017LS	qA89STVIS-1	1	18.783	G01_031	4.9	4.2	**	4.08	7.6	16.228-19.083
2017SL	qA89STVIS-10	1	26.933	PRE	6.0	5.3	**	3.81	7.5	26.533-28.702
2017SL	qA89STPA-13	1	27.033	PRE	66.8	58.3	***	6.24	9.8	26.733-28.202
Overall	qA89STPA-30	2	13.266	G03_054	48.6	53.8	**	6.92	8.6	7.666-17.312
2017LS	qA89STVIS-4	2	15.066	G03_054	4.2	4.8	**	4.53	8.5	6.466-17.512
2017LS	qA89STPA-5	2	16.912	G03_054	30.6	35.8	**	6.77	8.7	10.666-17.312
2018SL	qA89STVIS-17	2	69.068	140065	6.1	5.3	**	4.74	7.3	68.245-69.768
2017SL	qA89STVIS-12	2	81.313	942096	5.3	5.9	**	7.83	16.9	79.913-81.504
Overall	qA89STPA-34	3	22.058	409081	48.2	52.8	**	8.85	10.6	21.958-22.299

Table 4.6 (continued)

Environment	QTL name	LG	Position (cM)	Marker	Allele means		KW	LOD	R^2(%)	99% CI (cM)
					Allele a	Allele b				
2017SL	qA89STPA-16	3	26.487	187703	56.7	63.5	*	3.89	5.8	26.487-26.587
Overall	qA89STVIS-26	3	30.847	215744	5.1	5.7	***	6.22	14.1	30.394-31.147
2018SL	qA89STPA-23	3	35.520	675811	52.6	61.4	**	5.50	8.2	35.320-35.625
Overall	qA89STVIS-27	3	39.997	618767	5.7	5.1	****	4.45	9.6	39.381-40.097
2018SL	qA89STVIS-18	3	50.515	639475	5.4	6.1	**	3.42	5.1	46.036-53.815
2018SL	qA89STPA-25	3	60.198	B3B8	63.8	54.9	***	3.87	5.6	57.998-64.367
Overall	qA89STPA-35	3	60.498	B3B8	54.5	48.6	****	5.38	6.0	58.498-65.867
2018SL	qA89STVIS-19	3	60.867	B3B8	6.3	5.4	***	3.28	4.9	57.598-67.467
2018SL	qA89STPA-17	4	37.339	521831	59.7	67.5	*	5.12	7.8	35.439-40.539
Overall	qA89STVIS-28	4	62.788	194509	4.9	5.4	*	4.06	8.8	61.988-63.445
2017LS	qA89STPA-9	4	113.967	442336	36.4	29.5	****	5.22	6.5	113.897-114.267
2017LS	qA89STPA-10	4	117.934	489733	35.7	30.5	**	5.61	7.1	117.877-117.934

Table 4.6 (continued)

Environment	QTL name	LG	Position (cM)	Marker	Allele means		KW	LOD	R^2(%)	99% CI (cM)
					Allele a	Allele b				
2017SL	qA89STPA-18	5	32.790	401622	67.4	57.0	****	6.11	9.6	29.289-32.790
2017SL	qA89STVIS-14	5	47.458	443395	6.0	5.3	**	8.07	16.8	46.958-48.315
2017SL	qA89STPA-19	5	47.558	443395	66.1	58.3	**	9.41	15.3	47.058-48.315
2018SL	qA89STVIS-20	5	55.799	406748	6.0	5.3	**	4.31	6.6	55.799-56.147
2018SL	qA89STPA-26	5	55.799	406748	61.8	54.2	**	4.14	6.0	55.799-56.147
2017SL	qA89STVIS-16	6	9.856	LpSSR058	5.2	5.8	*	4.95	10.0	9.556-11.309
2017SL	qA89STPA-20	6	9.909	LpSSR058	56.8	65.2	**	7.26	11.6	9.656-10.909
2018SL	qA89STVIS-23	7	64.200	G07_088	6.1	4.9	****	3.43	5.1	62.316-64.300
2018SL	qA89STPA-28	7	65.240	DLF008	62.3	49.0	*****	9.04	14.6	65.235-65.340

[a] Name of QTL, indicates parent background (parent A89) and assessment method used to determine salinity tolerance (VIS = visual rating, PA = pixel analysis).
[b] Name of marker closest to a given QTL.
[c] The mean phenotypic value of progeny carrying the 'a' or 'b' allele of each marker.
[d] Kruskal-Wallis analysis. *, **, ***, ****, ***** Significant at $P \leq 0.1$, 0.05, 0.01, 0.005, and 0.0005 levels, respectively.
[e] The LOD values of the QTL determined by multiple QTL model (MQM) mapping.
[f] Proportion of phenotypic variation explained by a given QTL.
[g] A 99% confidence interval for the QTL length (cM) as determined using the 2-LOD approach.

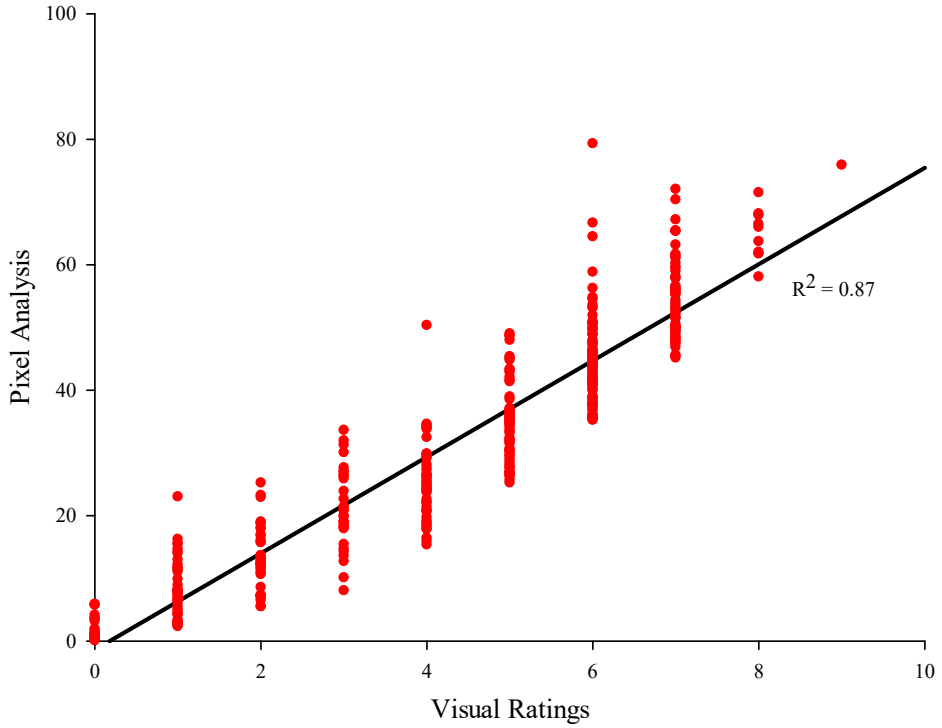

Figure 4.1 Linear regression analysis between visual ratings and pixel analysis for salinity stress response of turfgrass plants on a loamy sand soil after salinity stress periods of 2017 at the Rutgers Plant Science Research and Extension Farm in Adelphia, NJ.

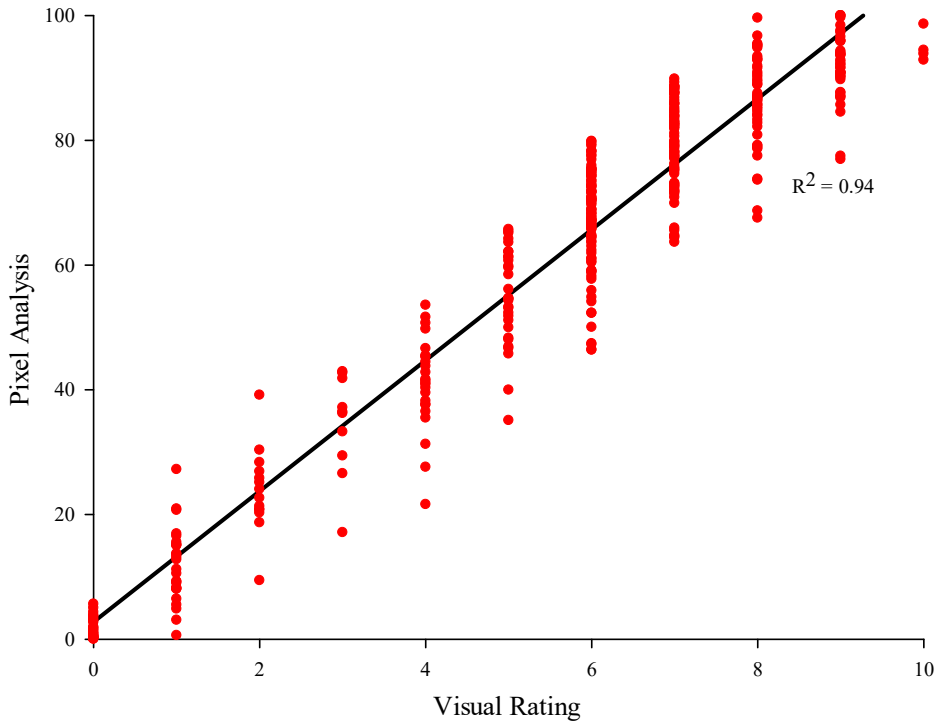

Figure 4.2 Linear regression analysis between visual ratings and pixel analysis for salinity stress response of turfgrass plants on a sandy loam soil after salinity stress periods of 2017 at the Rutgers Plant Science Research and Extension Farm in Adelphia, NJ.

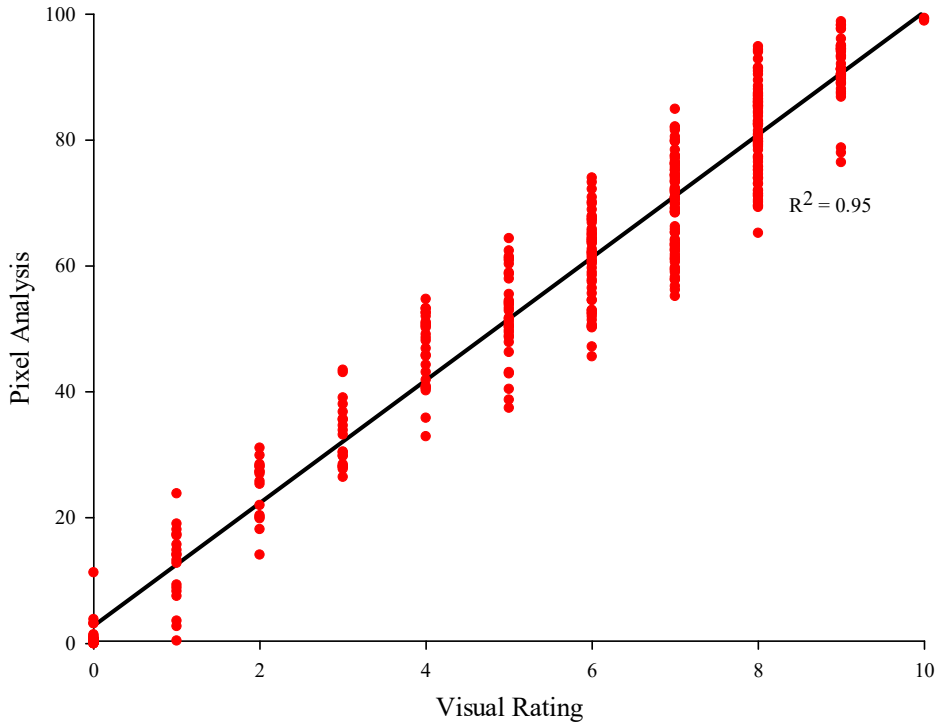

Figure 4.3 Linear regression analysis between visual ratings and pixel analysis for salinity stress response of turfgrass plants on a sandy loam soil after salinity stress periods of 2018 at the Rutgers Plant Science Research and Extension Farm in Adelphia, NJ.

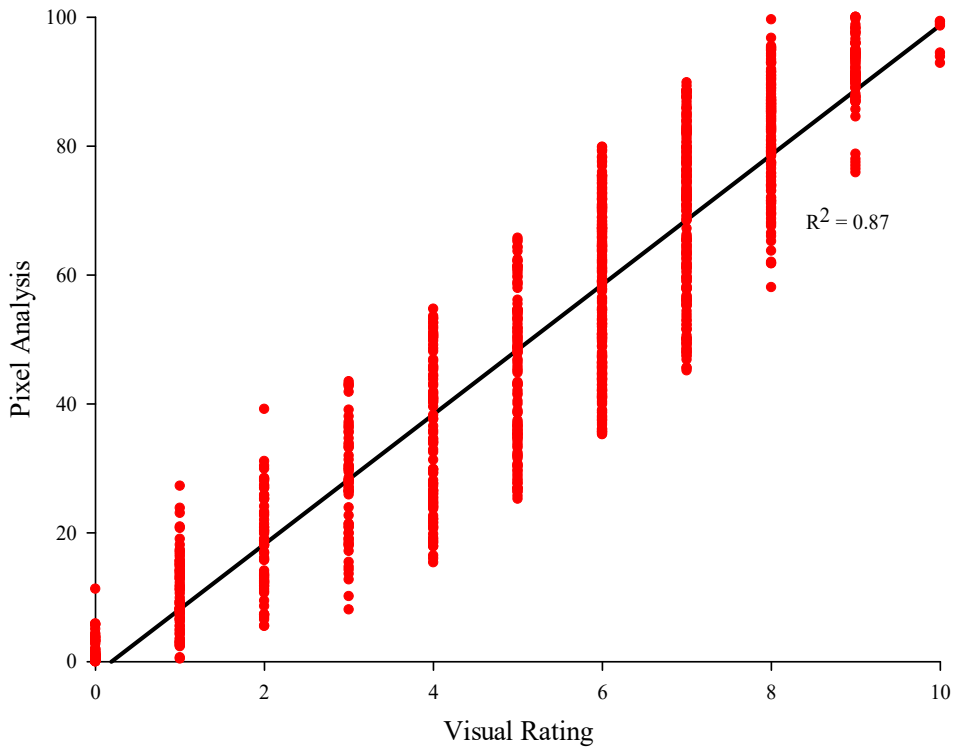

Figure 4.4 Linear regression analysis between visual ratings and pixel analysis for salinity stress response of turfgrass plants on a loamy sand soil and a sandy loam soil after salinity stress periods of 2017 and on a sandy loam soil after salinity stress periods of 2018 at the Rutgers Plant Science Research and Extension Farm in Adelphia, NJ.

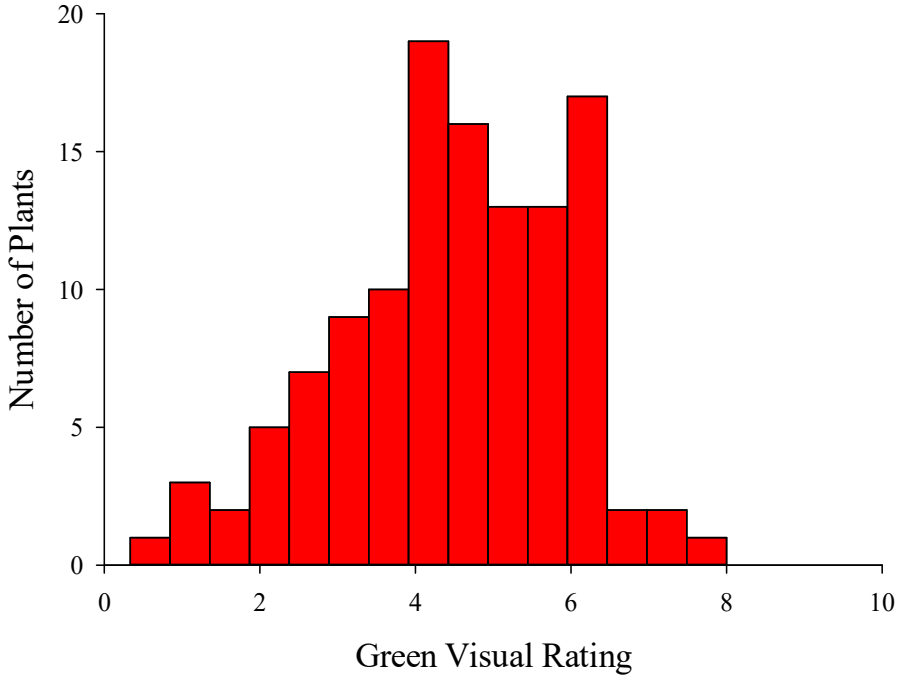

Figure 4.5 Frequency distribution for mean green visual rating for the I06 × A89 perennial ryegrass mapping population on a loamy sand soil after salinity stress periods of 2017 at the Rutgers Plant Science Research and Extension Farm in Adelphia, NJ. The Visual rating scale ranged from 0 to 10, where 0 represented approximately 0% green cover and 10 represented approximately 100% green cover.

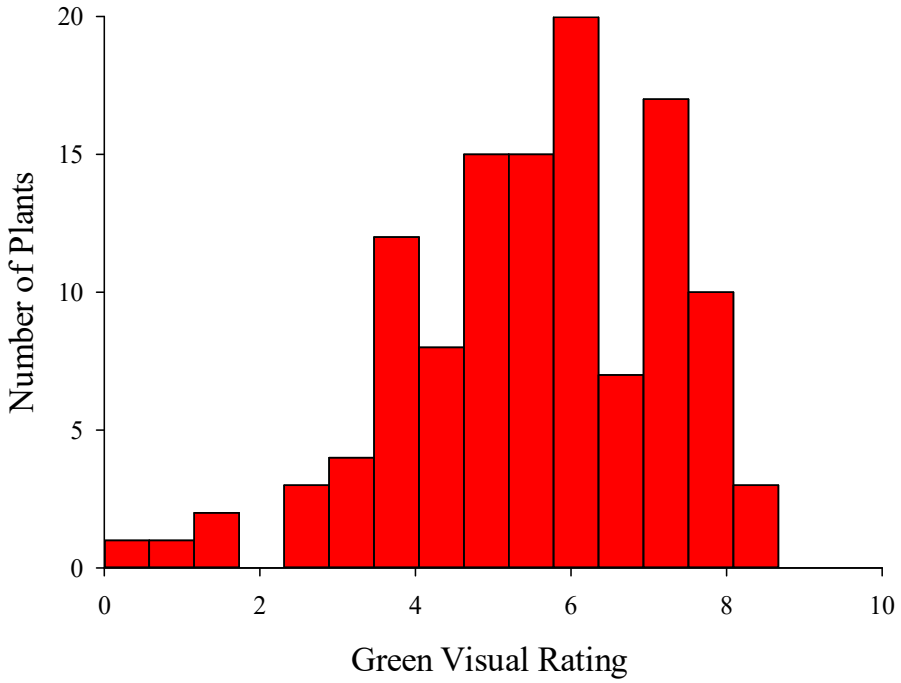

Figure 4.6 Frequency distribution for mean green visual rating for the I06 × A89 perennial ryegrass mapping population on a sandy loam soil after salinity stress periods of 2017 at the Rutgers Plant Science Research and Extension Farm in Adelphia, NJ. The Visual rating scale ranged from 0 to 10, where 0 represented approximately 0% green cover and 10 represented approximately 100% green cover.

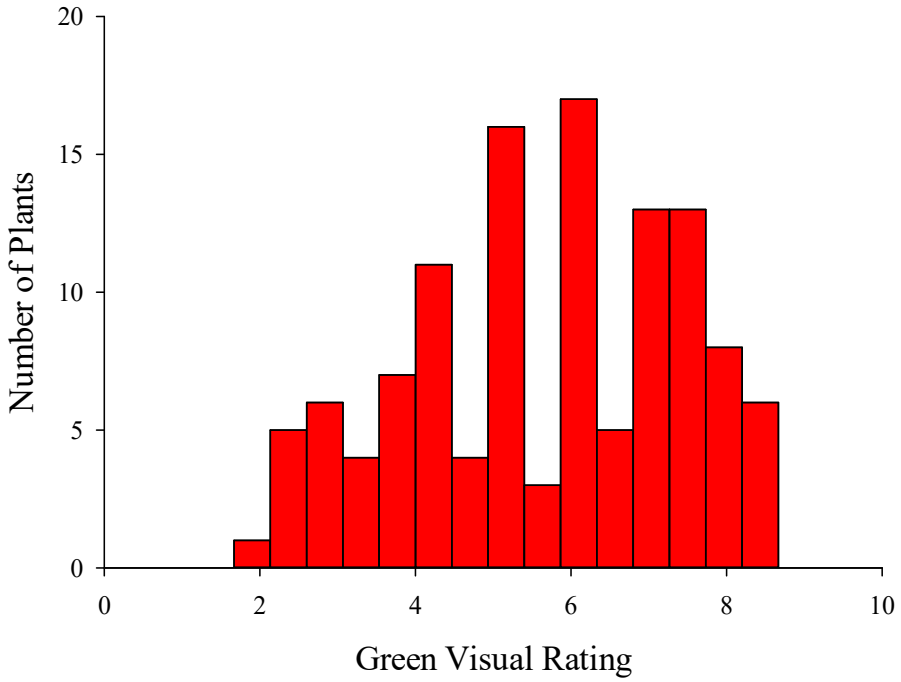

Figure 4.7 Frequency distribution for mean green visual rating for the I06 × A89 perennial ryegrass mapping population on a sandy loam soil after salinity stress periods of 2018 at the Rutgers Plant Science Research and Extension Farm in Adelphia, NJ. The Visual rating scale ranged from 0 to 10, where 0 represented approximately 0% green cover and 10 represented approximately 100% green cover.

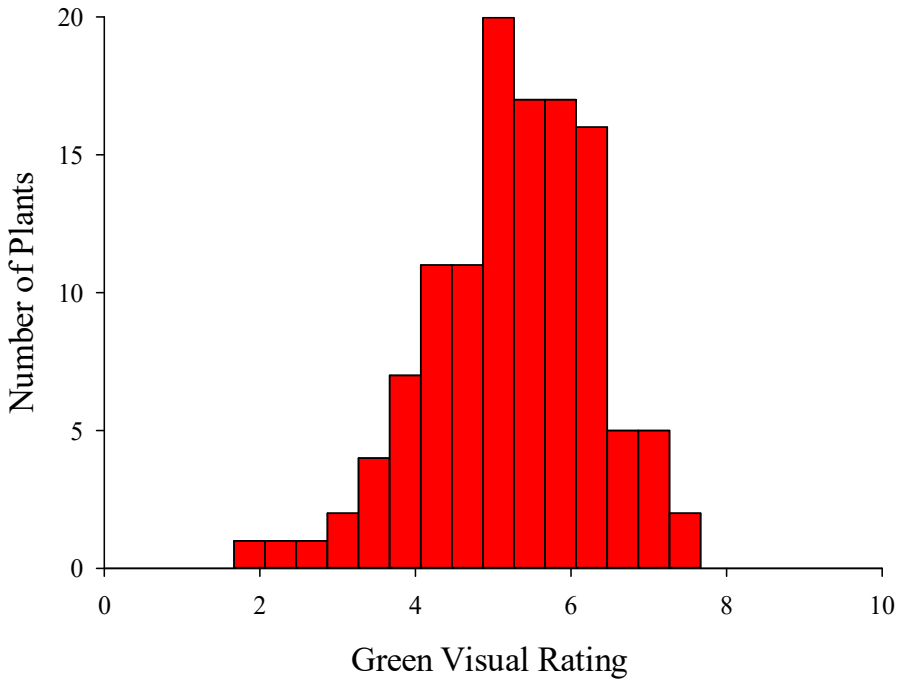

Figure 4.8 Frequency distribution for mean green visual rating for the I06 × A89 perennial ryegrass mapping population on a loamy sand soil and a sandy loam soil after salinity stress periods of 2017 and on a sandy loam soil after salinity stress periods of 2018 at the Rutgers Plant Science Research and Extension Farm in Adelphia, NJ. The Visual rating scale ranged from 0 to 10, where 0 represented approximately 0% green cover and 10 represented approximately 100% green cover.

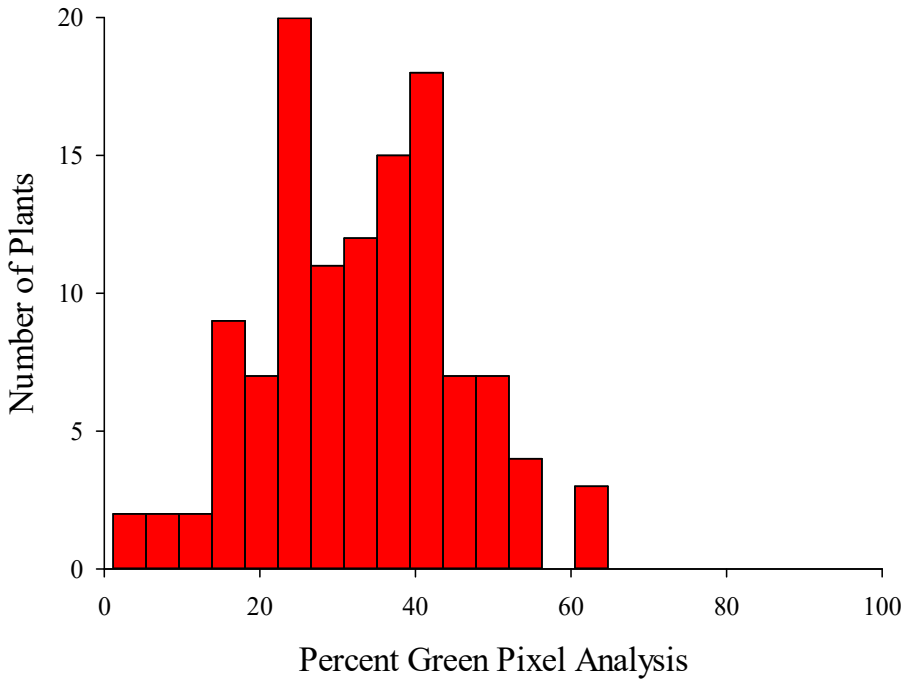

Figure 4.9 Frequency distribution for mean percent green as determined via pixel analysis for the I06 × A89 perennial ryegrass mapping population on a loamy sand soil after salinity stress periods of 2017 at the Rutgers Plant Science Research and Extension Farm in Adelphia, NJ.

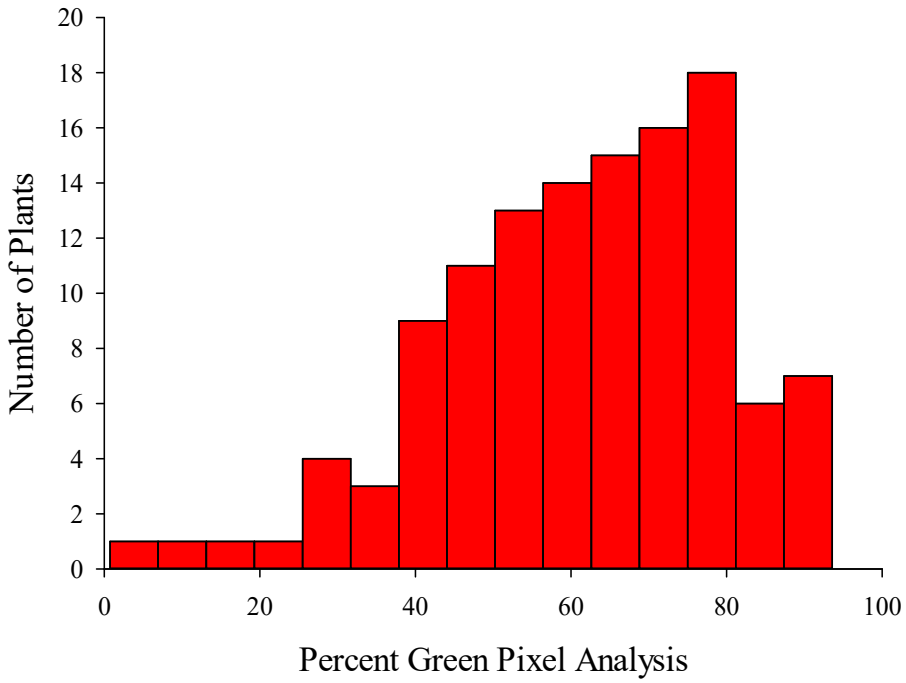

Figure 4.10 Frequency distribution for mean percent green as determined via pixel analysis for the I06 × A89 perennial ryegrass mapping population on a sandy loam soil after salinity stress periods of 2017 at the Rutgers Plant Science Research and Extension Farm in Adelphia, NJ.

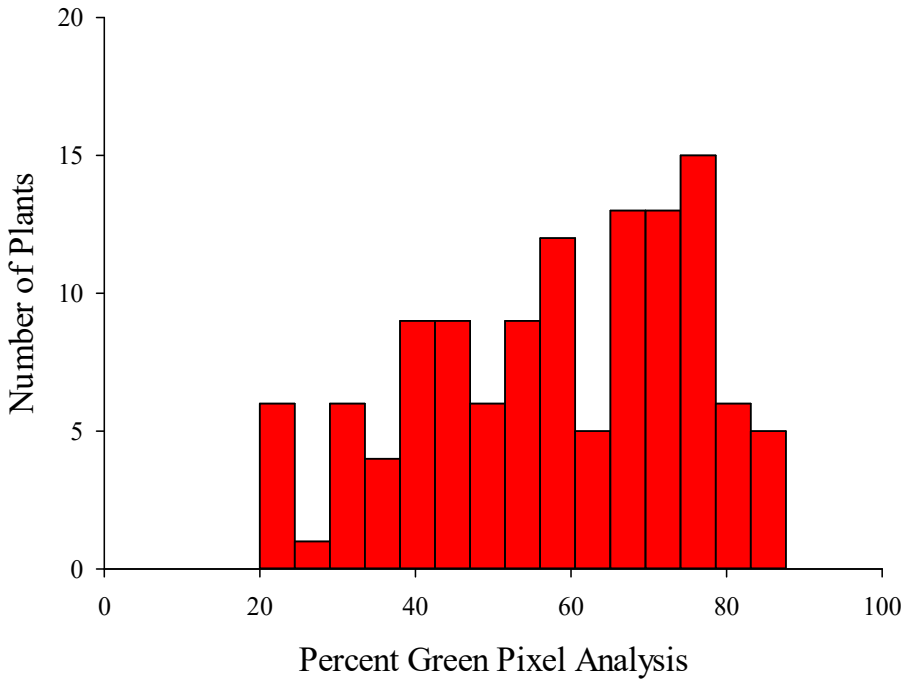

Figure 4.11 Frequency distribution for mean percent green as determined via pixel analysis for the I06 × A89 perennial ryegrass mapping population on a sandy loam soil after salinity stress periods of 2018 at the Rutgers Plant Science Research and Extension Farm in Adelphia, NJ.

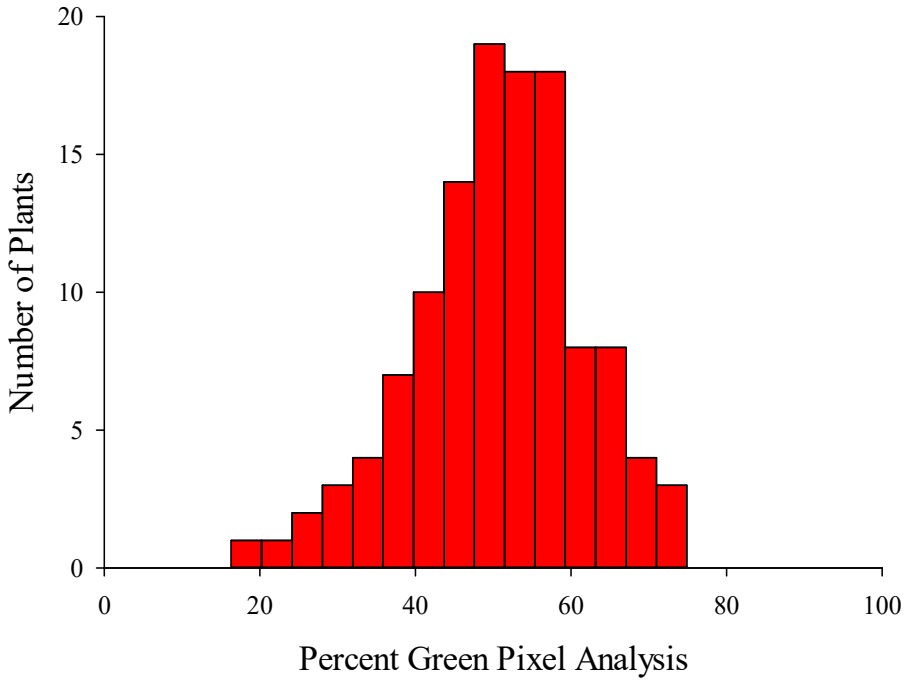

Figure 4.12 Frequency distribution for mean percent green as determined via pixel analysis for the I06 × A89 perennial ryegrass mapping population on a loamy sand soil and a sandy loam soil after salinity stress periods of 2017 and on a sandy loam soil after salinity stress periods of 2018 at the Rutgers Plant Science Research and Extension Farm in Adelphia, NJ.

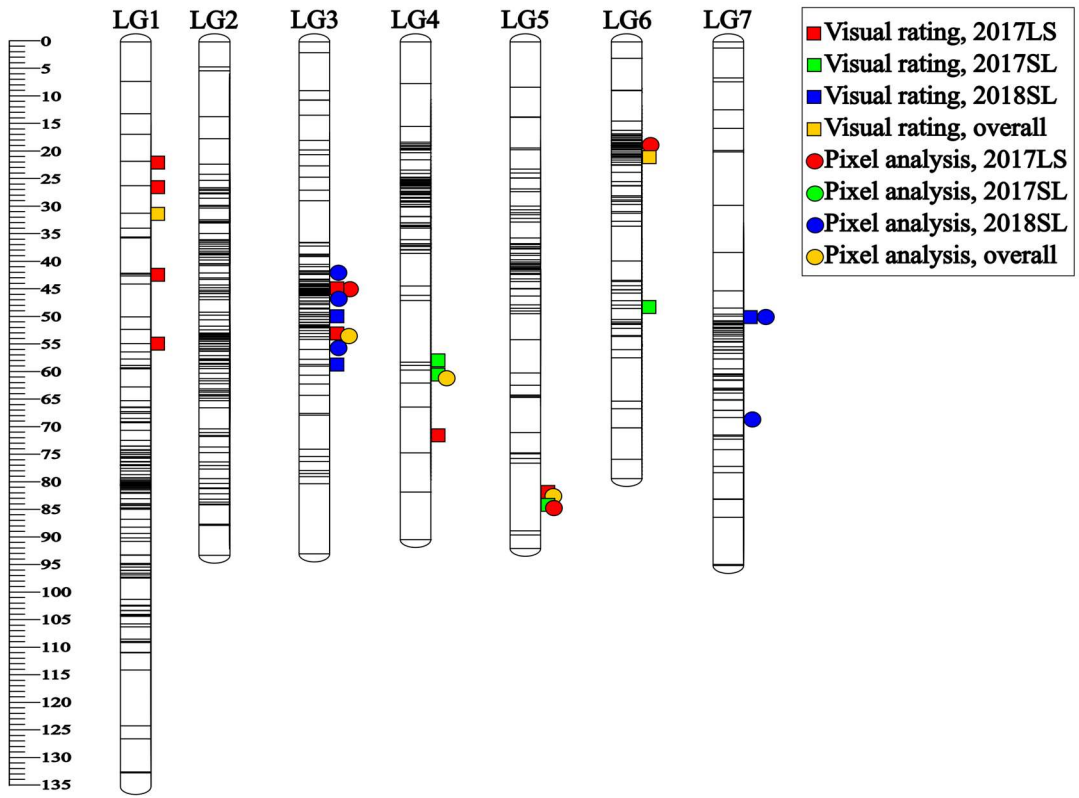

Figure 4.13 Summary of the quantitative trait loci (QTL) identified for salinity tolerance on the I06 parent map. A multiple QTL model mapping analysis was conducted with phenotypic data for salinity tolerance generated from visual ratings and pixel analysis of field trials during 2017 on a loamy sand soil (2017LS) and a sandy loam soil (2017SL) and during 2018 on a sandy loam soil (2018SL) at the Rutgers Plant Science Research and Extension Farm in Adelphia, NJ. The genetic map distance (cM) is provided to the left, and linkage group (LG) numbers are indicated at the top of each linkage group.

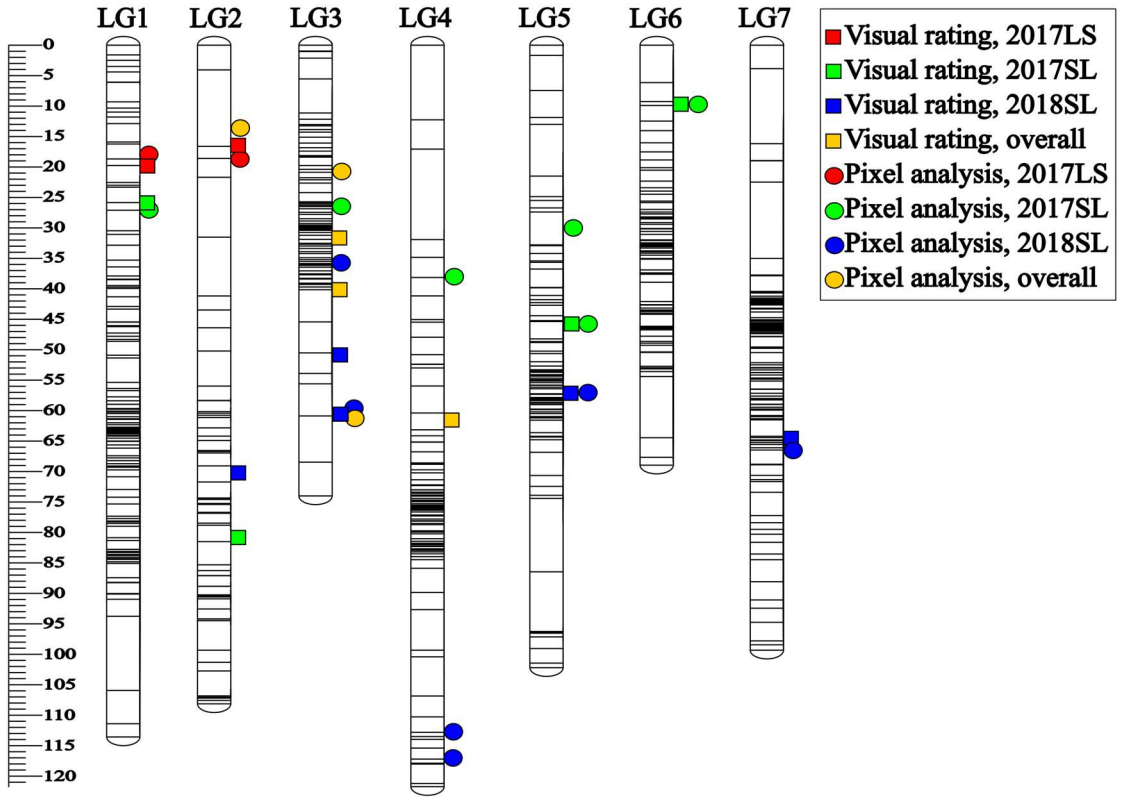

Figure 4.14 Summary of the quantitative trait loci (QTL) identified for salinity tolerance on the A89 parent map. A multiple QTL model mapping analysis was conducted with phenotypic data for salinity tolerance generated from visual ratings and pixel analysis of field trials during 2017 on a loamy sand soil (2017LS) and a sandy loam soil (2017SL) and during 2018 on a sandy loam soil (2018SL) at the Rutgers Plant Science Research and Extension Farm in Adelphia, NJ. The genetic map distance (cM) is provided to the left, and linkage group (LG) numbers are indicated at the top of each linkage group.

CHAPTER V

QUANTITATIVE TRAIT LOCUS MAPPING FOR DOLLAR SPOT RESISTANCE IN PERENNIAL RYEGRASS

Abstract

Dollar spot, caused by *Clarireedia jacksonii* C. Salgado, L.A. Beirn, B.B. Clarke, and J.A. Crouch, is an economically important disease of perennial ryegrass (*Lolium perenne* L.). Genetic resistance to dollar spot is an important disease management strategy; however, research in this area on perennial ryegrass is limited. Thus, the purpose of this study was to improve our understanding of the underlying genetic factors for dollar spot resistance in perennial ryegrass. A quantitative trait locus (QTL) analysis was conducted using the I06 × A89 pseudo-F_2 perennial ryegrass mapping population. The QTL analyses were conducted with the individual I06 and A89 parent maps and phenotypic data for dollar spot severity collected from field trials at the New Jersey Agricultural Experiment Station in New Brunswick, NJ during 2017 and 2018. Twelve major-effect QTL and nine minor-effect QTL were identified from the I06 and A89 parent genetic linkage maps. Coincident QTL were mapped to four distinct genomic regions and were consistently identified using multiple evaluation methods for dollar spot severity and/or multiple environments. This is the first reported effort for QTL mapping

of dollar spot resistance in perennial ryegrass. The QTL regions identified herein will be important for future studies regarding the genetic basis for dollar spot resistance in perennial ryegrass. These findings will aid in the development of marker-assisted selection techniques for breeding applications, dollar spot resistance gene and mechanism discovery, and comparative genomics investigations for dollar spot resistance using closely related plant species. Ultimately, these efforts will lead to the development of perennial ryegrass cultivars with improved resistance to dollar spot, potentially decreasing cultural and chemical inputs for effective dollar spot disease management.

Introduction

Perennial ryegrass (*Lolium perenne* L.) is a diploid (2n = 2x = 14), cool-season forage and turfgrass species with seven chromosomes and a genome size of approximately 2.5 Gb (Beard, 1973; Funk and Clarke, 1989; Kopecky et al., 2010; Terrell, 1968; Thorogood, 2003). This medium to high density, bunch-type perennial is native to temperate regions of Asia, North Africa, and Europe and is managed as a turfgrass in general landscaping areas, parks, racetracks, golf fairways and roughs, and athletic fields (Beard, 1973; Beard and Beard, 2005, Thorogood, 2003). Current breeding efforts for turf-type perennial ryegrass including improving resistance to important diseases such as dollar spot (Bonos and Huff, 2013; Bonos et al., 2006; Brilman, 2005; Thorogood, 2003).

Dollar spot is an economically important foliar disease that occurs throughout the world on many warm- and cool-season turfgrass species (Smiley et al., 2005; Watschke

et al., 2013). More money is spent by U.S. golf courses to manage dollar spot than any other turfgrass disease (Smiley et al., 2005; Vargas, 1994). In the U.S., dollar spot of cool-season turfgrass species, such as perennial ryegrass, is caused by the fungal pathogen *Clarireedia jacksonii* C. Salgado, L.A. Beirn, B.B. Clarke, and J.A. Crouch (formerly *Sclerotinia homoeocarpa* F.T. Bennet) (Salgado-Salazar et al., 2018). Unfortunately, research on the genetic basis for dollar spot resistance in perennial ryegrass is limited (Bonos and Huff, 2013). However, studies on creeping bentgrass (*Agrostis stolonifera* L.), suggest that dollar spot resistance is quantitatively inherited and largely influenced by additive gene effects (Bonos, 2006, 2011; Bonos et al., 2003; Chakraborty et al., 2006). Research has linked higher activity of oxalate oxidase, an enzyme that degrades the pathogenicity factor oxalic acid to CO_2 and H_2O_2, to enhanced dollar spot resistance in resistant creeping bentgrass plants, compared with dollar spot susceptible creeping bentgrass plants (DaRoche and Hammerschmidt, 2004). Thus, it is suggested that an increase in oxalate oxidase production is a possible mechanism for dollar spot resistance in creeping bentgrass (Orshinsky et al., 2012; Rioux, 2014).

A recurrent phenotypic selection breeding scheme has been widely and successfully applied to perennial ryegrass breeding programs to produce composite cultivars with improved traits (Bonos and Huff, 2013; Bonos et al., 2006; Brilman, 2005; Thorogood, 2003). However, phenotypic selection for quantitative traits, particularly for perennial crop breeding, can be laborious and time-consuming (Grinberg et al., 2016). Marker assisted selection based on quantitative trait locus (QTL) mapping has been successfully implemented to overcome limitations of phenotypic selection for

quantitative traits (Curley et al., 2005; Lespinasse et al., 2000; Portyanko et al., 2005; Tanksley et al., 1993; Wang et al., 2000).

The QTL mapping approach has been used to identify QTL in perennial ryegrass for traits such as disease resistance for stem rust (*Puccinia graminis* subsp. *graminicola* Z. Urb.), crown rust (*Puccinia coronata* Corda), and gray leaf spot (*Pyricularia oryzae* Cavara) diseases, vernalization response, winter hardiness, herbage quality characteristics, and morphological and developmental traits (Bushman and Warnke, 2013; Cogan et al., 2005; Curley et al., 2005; Curley et al., 2008; Dumsday et al., 2003; Jensen et al., 2005; Muylle et al., 2005; Pfender et al., 2011; Sartie et al., 2011; Schejbel et al., 2007; Sim et al., 2007; Studer et al., 2008; Yamada et al., 2004). The initial step for the QTL mapping procedure is developing an appropriate mapping population and constructing a genetic linkage map that is densely populated with markers (Bernardo, 2002; Langridge and Chalmers, 2004; Singh and Singh, 2015; Xu, 2010). Recently, high-density genetic linkage maps were constructed using the I06 × A89 perennial ryegrass population (Chapters II and III). This is a pseudo-F_2 population composed of 2 parent genotypes and 118 progeny genotypes that segregate for dollar spot resistance.

The objectives for this research were (i) to conduct QTL analyses using the I06 × A89 population to detect genomic regions involved in dollar spot resistance for perennial ryegrass and (ii) to identify molecular markers associated with dollar spot resistance for potential future use in a marker-assisted selection breeding approach.

Materials and methods

Mapping population

A pseudo-F_2 perennial ryegrass population was constructed to analyze QTL for dollar spot resistance (Chapter II). A controlled cross-fertilization was conducted using two diploid heterozygous genotypes (I06 and A89) at the New Jersey Agricultural Experiment Station in New Brunswick, NJ during the summer of 2016. Seeds were collected from parent I06 on 22 Aug 2016 and germinated in round pots (15.2 cm diameter). Each of the resulting 118 pseudo-F_2 progeny were transplanted to a single cell (5.1 × 5.1 cm) of a plastic flat and assigned a unique mapping population identifier on 14 Sep 2016.

Genetic linkage mapping

Genetic linkage maps were constructed for each parent, I06 and A89, using the doubled haploid two-way pseudo testcross approach in JoinMap 4.1 (Van Ooijen, 2006) as described previously (Chapter III). The I06 map included 848 SNPs and 52 SSRs mapped across a total distance of 677.5 cM with an average marker density of 0.75 cM. The A89 map included 769 SNPs and 35 SSRs mapped across a total distance of 687.9 cM with an average marker density of 0.86 cM. Both the I06 and A89 marker datasets and both genetic linkage maps were used for QTL mapping analyses.

Field assessment for dollar spot resistance

Three clonal replicates of progeny genotypes (n=118) and twenty-four clonal replicates of parental genotypes (n=2) were initially established in single cells (6.4 × 6.4 cm) of plastic flats containing Pro-mix (Premier Tech Ltd., Riviere-du-Loup, QC) growing media and grown in greenhouse conditions for four weeks. During this period, plants were fertilized biweekly with a balanced fertility source (10N-4.4P-8.3K) and irrigated daily. On 19 Apr 2017, the mapping population was established in a mowed spaced-plant trial at the Rutgers Horticultural Research Farm II in North Brunswick, NJ for evaluation of dollar spot resistance. A randomized complete block design was used for the experimental layout of the field trial. The trial was conducted in two environments (2017 and 2018), and the same plants were used during both years of this study.

The field trial was inoculated with two virulent isolates (PRG and JP236941) of *C. jacksonii* on 15 Jun 2017 and 28 Jun 2018. Inoculum was prepared based on a modified protocol from that outlined by Bonos et al. (2003). In detail, 900 g of Kentucky bluegrass (*Poa pratensis* L.) seed and 300 ml of water were added to foil pans and autoclaved two times, with each autoclaving event consisting of 20 min sterilization at 121°C. Fungal isolates were grown on potato dextrose agar (39 g agar L^{-1}) for 21 days under 24 hour fluorescent light. A 90 mm diameter Petri plate of a given isolate was cut into 1 cm^2 pieces and added to the 900 g of sterilized Kentucky bluegrass seed. Inoculated foil pans of seeds were grown for 4 weeks at 23°C. The pans were shaken daily to prevent clump formation. After 28 days, the infested seeds were spread on a bench top and dried for 4 days. The inoculum was passed through a sieve (2 × 10 mm)

and stored in plastic bags. Inoculum was applied to the mapping population at a rate of 0.8 g m^{-2} using a drop spreader (The Scotts Company, Marysville, OH, USA).

Individual clones of the mapping population were evaluated for dollar spot resistance during the growing seasons of 2017 and 2018 when phenotypic variation was at maximum. Assessments for dollar spot resistance included visual ratings and pixel analysis for dollar spot severity. Visual ratings were performed to estimate the percentage of leaf tissue from each plant that was affected by dollar spot disease. These data were recorded as dollar spot severity using a 0-10 rating scale where zero represented approximately 0% diseased leaf tissue, one represented approximately 10% diseased leaf tissue, two represented approximately 20% diseased leaf tissue, three represented approximately 30% diseased leaf tissue, four represented approximately 40% diseased leaf tissue, five represented approximately 50% diseased leaf tissue, six represented approximately 60% diseased leaf tissue, seven represented approximately 70% diseased leaf tissue, eight represented approximately 80% diseased leaf tissue, nine represented approximately 90% diseased leaf tissue, and ten represented approximately 100% diseased leaf tissue. Digital images of each plant were taken with a light box when phenotypic variation for dollar spot disease was at maximum. The images were subjected to a pixel analysis for dollar spot severity, assessed as percent non-green leaf tissue using TurfAnalyzer software (Karcher et al., 2017). Data for dollar spot severity were subjected to analysis of variance using the ANOVA procedure in SAS (SAS Institute, NC, USA) and used to assign a phenotypic mean for each genotype, which was used for QTL analysis. In addition, the relationship between visual rating and pixel analysis for

dollar spot severity was determined by a simple linear regression analysis using the REG procedure in SAS (SAS Institute, NC, USA).

Quantitative trait locus analysis

The I06 × A89 parent genetic linkage maps, marker datasets for all markers included in the linkage maps, and phenotypic data for dollar spot resistance were used for QTL mapping analyses in MapQTL 6 (Van Ooijen, 2009). Permutation testing was conducted to establish genome-wide logarithm of odds (LOD) thresholds using 10,000 permutations and at $\alpha = 0.05$ significance level (Churchill and Doerge, 1994). The QTL regions were initially identified by the nonparametric Kruskal-Wallis analysis and interval mapping (IM) procedures with default parameters including a regression algorithm with a mapping step size of 1.0 cM and a maximum number of neighboring markers equal to 5 (Jung et al., 1996; Lander and Botstein, 1989). The automatic cofactor selection (ACS) tool was used to detect significantly ($P < 0.02$) associated markers, which were subsequently used for multiple QTL model (MQM) mapping. The MQM mapping procedures were implemented with default parameters as described for the IM mapping procedures. The QTL positions were defined by the locations where LOD scores reached maximum values. The 2-LOD support intervals were used to calculate 99% confidence intervals (Lander and Botstein, 1989; Li, 2011). The percentage of phenotypic variation explained by each marker (R^2) was calculated as part of the analyses. Major-effect QTL were defined by R^2 values ≥ 10.0, and minor-effect QTL were defined by R^2 values < 10.0 (Collard et. al., 2005).

Results

Field assessment for dollar spot resistance

Percent disease data generated by visual ratings and pixel analysis were not well correlated, as evidenced by coefficient of determination values of 0.33 and 0.62 for the 2017 and 2018 datasets, respectively (Figs. 5.2, 5.3). The coefficient of determination for the overall, combined dataset was 0.42 (Fig. 5.4). Continuous phenotypic variation for percent disease was observed among the individuals of the mapping population generated from the cross between dollar spot susceptible I06 and dollar spot resistant A89 among all environments (Tables 5.1, 5.2. Figs. 5.5-5.10).

A summary of mean dollar spot severity generated by visual ratings is presented in Table 5.1. Mean dollar spot severity for the progeny genotypes was 2.8 and 3.0 during 2017 and 2018, respectively. The overall progeny mean dollar spot severity averaged across both years of the study was 2.9. Mean dollar spot severity for the dollar spot susceptible I06 parent genotype was 5.5 and 5.2 during 2017 and 2018, respectively. The overall parent I06 mean dollar spot severity averaged across both year of the study was 5.4. Mean dollar spot severity for the dollar spot resistant A89 parent genotype was 1.2 and 1.3 during 2017 and 2018, respectively. The overall parent A89 mean dollar spot severity averaged across both years of the study was 1.2.

A summary of mean dollar spot severity generated by pixel analysis is presented in Table 5.2. Mean dollar spot severity for the progeny genotypes was 42.2 and 39.4 during 2017 and 2018, respectively. The overall progeny mean dollar spot severity

averaged across both years of the study was 40.8. Mean dollar spot severity for the dollar spot susceptible I06 parent genotype was 47.4 and 51.3 during 2017 and 2018, respectively. The overall parent I06 mean dollar spot severity averaged across both years of the study was 49.4. Mean dollar spot severity for the dollar spot resistant A89 parent genotype was 30.8 and 26.7 during 2017 and 2018, respectively. The overall parent A89 mean dollar spot severity averaged across both years of the study was 28.7.

The analyses of variance for dollar spot severity as determined via visual ratings and pixel analysis were similar (Tables 5.3, 5.4). The interaction effect, genotype × environment, significantly affected mean dollar spot severity as determined by visual ratings ($P < 0.0001$) and pixel analysis ($P < 0.0001$). The main effect, genotype, significantly affected mean dollar spot severity as determined by visual ratings ($P < 0.0001$) and pixel analysis ($P < 0.0001$). The main effect, environment, did not significantly affect mean dollar spot severity as determined by visual ratings ($P = 0.6136$) and pixel analysis ($P = 0.2045$). Accordingly, QTL analyses were conducted using the phenotypic means for each genotype at each environment (2017 and 2018). Additionally, the QTL analyses were conducted on the overall datasets, which were generated by combining the data across both years of the study to increase the consistency in the observed genotype mean response.

Quantitative trait locus analysis

The QTL mapping analyses for dollar spot resistance were conducted using dollar spot severity as determined by both visual ratings and pixel analysis. Progeny genotype means were generated from each of the two environments (2017 and 2018) separately

and pooled, as the overall progeny genotype means. In total, twelve major-effect QTL and nine minor-effect QTL were identified at 15 distinct genomic regions across the two parent genetic linkage maps (Tables 5.5, 5.6; Figs. 5.11, 5.12). Two QTL were identified using both assessment methods (visual ratings and pixel analysis) for dollar spot severity, and three QTL were identified at more than one environment. The following sections describe the QTL mapping results from each of the parent maps, separately.

I06 parent map

Six major-effect QTL and six minor-effect QTL for dollar spot resistance were identified at eight distinct genomic regions across six linkage groups of the I06 parent map (Table 5.5; Fig. 5.11). The LOD scores ranged from 3.34 to 10.17, and the percent phenotypic variation for dollar spot resistance explained by the QTL ranged from 4.3 to 26.1. Three QTL were identified from environment 2017, five QTL were identified from environment 2018, and four QTL were identified from the combined data for 2017 and 2018. Seven QTL were identified using pixel analysis, and five QTL were identified using visual ratings. Two QTL were identified across multiple environments, and one QTL was identified using both assessment methods (visual ratings and pixel analysis) for dollar spot severity.

Five QTL were identified at linkage group one (Table 5.5; Fig. 5.11). Four of the QTL were defined by a single marker (DLF_027) that was detected across multiple environments using both the visual ratings and pixel analysis methods for dollar spot severity. These QTL explained between 8.5 and 26.1% phenotypic variation for dollar

spot severity depending on the environment and evaluation method from which they were identified. Another QTL, defined by marker B3B7, was identified at environment 2017 and explained 8.7% phenotypic variation for dollar spot severity.

A single QTL, defined by marker LpSSR112, was identified at linkage group two and explained 6.3% phenotypic variation for dollar spot severity (Table 5.5; Fig. 5.11). This QTL was detected at environment 2017 using the pixel analysis method for assessing dollar spot severity. Similarly, one QTL, defined by marker 357005, was also identified at linkage group three (Table 5.5; Fig. 5.11). This QTL was detected at environment 2018 using the pixel analysis method and explained 4.3% phenotypic variation for dollar spot severity.

Three QTL with significant LOD scores above the genome-wide LOD thresholds were defined by markers G01_037 and G01_075 and identified across two regions of linkage group four (Table 5.5; Fig. 5.11). The LOD scores for these QTL ranged from 3.81 to 5.15. Two of the QTL were identified from the pixel analysis and the remaining QTL was identified from the visual rating assessment. Two of the QTL were defined by a single marker (G01_075) that was detected across multiple environments. These QTL explained 12.7 and 12.9% phenotypic variation for dollar spot severity depending on the environment from which they were detected. Another QTL was identified using the combined dataset from 2017 and 2018 and explained 8.6% phenotypic variation for dollar spot severity.

A single QTL explaining 6.4% phenotypic variation for dollar spot severity was defined by marker G03_069 and identified at linkage group six (Table 5.5; Fig. 5.11). This QTL was detected at environment 2018 using the visual rating assessment for dollar

spot severity. Similarly, one QTL, defined by marker rv_1284, was identified at linkage group seven (Table 5.5; Fig. 5.11). This QTL was detected at environment 2017 using the pixel analysis method and explained 10.7% phenotypic variation for dollar spot severity.

A89 parent map

Six major-effect QTL and three minor-effect QTL for dollar spot resistance were identified at seven distinct genomic regions across five linkage groups of the A89 parent map (Table 5.6; Fig. 5.12). The LOD scores ranged from 3.36 to 8.70, and the percent phenotypic variation for dollar spot resistance explained by the QTL ranged from 4.9 to 15.5. Two QTL were identified from environment 2017, six QTL were identified from environment 2018, and one QTL was identified from the combined data for 2017 and 2018. Three QTL were identified using pixel analysis, and six QTL were identified using visual ratings. One QTL was identified across multiple environments, and one QTL was identified using both assessment methods (visual ratings and pixel analysis) for dollar spot severity.

Three QTL were identified at linkage group one (Table 5.6; Fig. 5.12). One of the QTL explaining 12.8% phenotypic variation for dollar spot severity was identified by pixel analysis at environment 2018. The other two QTL explaining 14.2 and 15.5% phenotypic variation for dollar spot severity were located at a region between 50.520 and 51.305 cM. These two QTL were both identified from the visual rating assessment for

dollar spot severity; however, they were identified at different environments and were defined by two different markers (rv_0244 and 527181).

Three QTL with significant LOD scores above the genome-wide LOD thresholds were identified across two regions of linkage group five (Table 5.6; Fig. 5.12). The LOD scores for these QTL ranged from 3.94 to 4.82. Two of the QTL were identified from the visual rating assessment and the remaining QTL was identified from the pixel analysis. Two of the QTL were located at a region between 32.915 and 35.653 cM. These two QTL were identified from different evaluation methods (visual rating and pixel analysis) for dollar spot severity, but were both identified at environment 2018. These QTL explained 5.8 and 10.9% phenotypic variation for dollar spot severity when identified from visual ratings and pixel analysis, respectively. The third QTL on this linkage group explained 13.5% phenotypic variation for dollar spot severity and was identified using visual ratings.

A single QTL explaining 10.4% phenotypic variation for dollar spot severity was identified at linkage group two (Table 5.6; Fig. 5.12). This QTL was detected at environment 2017 using the visual rating assessment for dollar spot severity. Similarly, one QTL was also identified at linkage group six (Table 5.6; Fig. 5.12). This QTL was detected at environment 2018 using the visual rating assessment and explained 4.9% phenotypic variation for dollar spot severity. Another single QTL explaining 9.9% phenotypic variation for dollar spot severity was identified at linkage group seven (Table 5.6; Fig. 5.12). This QTL was detected at environment 2018 using the pixel analysis for dollar spot severity.

Discussion

A continuous phenotypic variation for dollar spot resistance was observed during 2017 and 2018 for the I06 × A89 perennial ryegrass population. These findings are consistent with prior observations in creeping bentgrass (Bonos et al., 2003; Chakraborty et al., 2006; Honig et al., 2014) and indicate that dollar spot resistance may be a quantitatively inherited trait in perennial ryegrass as well. We conducted QTL analyses using phenotypic data collected during 2017 and 2018 along with two separate genetic linkage maps, one for each parent of the I06 × A89 mapping population. Dollar spot resistance was quantified as dollar spot severity using two assessment methods, visual ratings and pixel analysis. Thus, there were twelve datasets for QTL mapping analyses.

The visual rating data and pixel analysis data were not well correlated for dollar spot severity in this study. This could have been caused by an overestimation of disease severity ratings using the pixel analysis method, which treats non-green pixels as disease. However, other stress factors, such as heat and drought, for example, could have caused discoloration among the turfgrass plants. Thus, QTL identified with data generated from pixel analysis should be cautiously considered as QTL associated with dollar spot resistance, and those QTL should be studied further to elucidate these concerns.

In total, twelve major-effect QTL and nine minor-effect QTL for dollar spot resistance were detected. Groups of coincident QTL were identified and partitioned to fifteen genomic regions, which will be useful for future studies and potential breeding applications. As defined by Collard et al. (2005), major-effect QTL were those that explained 10.0%, or greater, phenotypic variation for dollar spot severity. Accordingly, six major-effect QTL were identified at linkage groups one, four, and seven on the I06

parent map, and six major-effect QTL were identified at linkage groups one, four, and five on the A89 parent map. The genomic regions defined by these major-effect QTL should be investigated further to elucidate their potential role for dollar spot resistance in perennial ryegrass.

Our findings support claims from previous reports, which indicate that major-effect QTL are more consistently detected across environments than QTL with smaller effects (Paterson et al., 1991; Portyanko et al., 2005; Zou et al., 2000). Specifically, we observed consistency in QTL detection using multiple assessment methods (visual rating and pixel analysis) and multiple environments in our analyses. Two major-effect QTL were consistently identified using both visual ratings and pixel analysis and mapped to linkage group one of the I06 parent map and linkage group five of the A89 parent map. Three major-effect QTL were also consistently identified across multiple environments and mapped to linkage groups one and four of the I06 parent map and linkage group one of the A89 map.

A single marker (DLF_027) defined the QTL on linkage group one of the I06 parent map. This QTL was identified across multiple environments using both assessment methods. The LOD scores for this QTL ranged from 4.53 to 10.17 using the 2018 and overall datasets, respectively. The percent phenotypic variation for dollar spot severity explained by this QTL ranged from 8.5 to 26.1 using the 2018 and overall datasets, respectively, thus suggesting that this maker (or region) might be a target for future analysis. A single marker (G01_075) defined the QTL located on linkage group four of the I06 parent map that was identified across multiple environments. The LOD scores for this QTL were 4.10 and 5.15 using the overall and 2018 datasets, respectively.

The percent phenotypic variation for dollar spot severity explained by this QTL were 12.7 and 12.9 using the overall and 2018 datasets, respectively. Two markers (rv_0244 and 527181) were closely associated with the QTL on linkage group one of the A89 parent map that was identified across multiple environments. The LOD scores for this QTL were 5.67 and 8.70 using the 2017 and 2018 datasets, respectively. The percent phenotypic variation for dollar spot severity explained by this QTL were 14.2 and 15.5 using the 2018 and 2017 datasets, respectively. Two markers (G04_043 and rv_11112) were closely associated with the QTL on linkage group five of the A89 parent map that was identified using both assessment methods. The LOD scores for this QTL were 3.94 and 4.05, and the percent phenotypic variation for dollar spot severity explained were 5.8 and 10.9.

Consistent detection of the four QTL described above suggests potential linkage between these QTL and the dollar spot resistance trait in perennial ryegrass. These findings support gene number calculations for dollar spot resistance in creeping bentgrass, which range from two to five genes (Bonos et al., 2003). This evidence provides a reason for exploring these genomic regions in more detail to discern their potential role for dollar spot resistance in perennial ryegrass. Previous studies in creeping bentgrass have suggested that an increase in oxalate oxidase production is a mechanism for dollar spot resistance (Daroche and Hammerschmidt, 2004; Orshinsky et al., 2012; Rioux, 2014). Future work should investigate if these genomic regions are related to production of oxalate oxidase or related compounds.

In summary, this was the first reported effort to map QTL for dollar spot resistance in perennial ryegrass. Fifteen regions were identified across the genetic

linkage maps for the I06 and A89 parents. In addition, twelve major-effect QTL were identified at these regions. Two QTL were identified using both visual ratings and pixel analysis to assess dollar spot severity, and three QTL were identified at multiple environmental locations.

Future work should include QTL confirmation studies using additional environments and populations. We will also investigate the QTL regions identified in this study to determine their usefulness for marker-assisted selection breeding strategies for dollar spot resistance in perennial ryegrass. In addition, these QTL regions will also be studied using techniques such as comparative genomics to identify possible genes (oxalate oxidase, for example) and underlying mechanisms for dollar spot resistance in perennial ryegrass and other closely related species. A completed perennial ryegrass reference genome is expected be available in the near future (Byrne et al., 2015). This will be a valuable resource for forthcoming studies such as marker discovery and comparative genomics that should be conducted with the I06 × A89 perennial ryegrass mapping population. Through these proposed efforts, we hope to better understand dollar spot resistance in perennial ryegrass and other closely related species. This work will be important for developing dollar spot resistant cultivars, which will potentially decrease fungicide input requirements to maintain desirable turf quality characteristics.

Literature cited

Beard, J.B. 1973. Turfgrass: Science and Culture. Prentice Hall, Englewood Cliffs, NJ.

Beard, J.B., and H.J. Beard. 2005. Beard's Turfgrass Encyclopedia for Golf Courses, Grounds, Lawns, Sports Fields. Michigan State University Press

Bernardo, R. 2002. Breeding for quantitative traits in plants. Stemma Press, Woodbury, MN, USA.

Bonos, S.A., and D.R. Huff. 2013. Cool-season grasses: biology and breeding. In: J.C. Stier, B.P. Horgan, and S.A. Bonos, editors, Turfgrass: biology, use, and management. ASA, CSSA, and SSSA, Madison, WI. p.591–660

Bonos, S.A., B.B. Clarke, and W.A. Meyer. 2006. Breeding for disease resistance in the major cool-season turfgrasses. Annu. Rev. Phytopathol. 44:213–234

Bonos, S.A., M.D. Casler, and W.A. Meyer. 2003. Inheritance of dollar spot resistance in creeping bentgrass. Crop Sci. 43: 2189–2196

Brilman, L.A. 2005. Turfgrass breeding in the United States: public private cool- and warm-season. Int. Turf. Soc. Res. 10:508–515

Bushman, B.S., and S.E. Warnke. 2013. Genetic and genomic approaches for improving turfgrass. In: J.C. Stier, B.P. Horgan, and S.A. Bonos, editors, Turfgrass: biology, use, and management. ASA, CSSA, and SSSA, Madison, WI. p.683–712.

Byrne, S.L., M. Pfeifer, I. Nagy, I. Armstead, S. Swain, B. Studer, K.F.X. Mayer, J.D. Campbell, A. Czaban, S. Hentrup, F. Panitz, C. Bendixen, J. Hedegaard, M. Caccamo, T. Asp. 2015. A senty-based draft genome sequence for the forage grass *Lolium perenne*. Plant J. 84:816–826.

Chakraborty, N., J. Curley, S. Warnke, M.D. Casler, and G. Jung. 2006. Mapping QTL for dollar spot resistance in creeping bentgrass (*Agrostis stolonifera* L.). Theor. Appl. Genet. 113:1421–1435.

Churchill, G.A., and R.W. Doerge. 1994. Empirical threshold values for quantitative trait mapping. Genetics 138:963–971.

Cogan, N.O.I., K.F. Smith, T. Yamada, M.G. Francki, A.C. Vecchies, E.S. Jones, G.C. Spangenberg, and J.W. Forster. 2005. QTL analysis and comparative genomics of herbage quality traits in perennial ryegrass (*Lolium perenne* L.). Theor. Appl. Genet. 110:364–380

Collard, B.C.Y, M.Z.Z. Jahufer, J.B. Brouwer, and E.C.K. Pang. 2005. An introduction to markers, quantitative trait loci (QTL) mapping and marker-assisted selection for crop improvement: the basic concepts. Euphytica. 142:169–196

Curley, J., N. Chakrabory, S. Chang, and G. Jung. 2008. QTL mapping of resistance to gray leaf spot in ryegrass: consistency of QTL between two mapping populations. Kor. Turfgrass Sci. 22:85–100

Curley, J., S.C. Sim, S. Warnke, S. Leong, and R. Barker. 2005. QTL mapping of resistance to gray leaf spot in ryegrass. Theor. Appl. Genet. 111:1107–1117

DaRocha, A.B., R. Hammerschmidt. 2004. Increase in oxalate oxidase activity in bentgrass response to *Sclerotinia homoeocarpa* and chemical treatment. Phytopahthology 94:S157.

Dumsday, J.L., K.F. Smith, J.W. Forster, and E. Jones, 2003. SSR-based genetic linkage analysis of resistance to crown rust (*Puccinia coronate* f. sp. *lolii*) in perennial ryegrass (*Lolium perenne* L.). Plant Pathol. 52:628–637

Funk, C.R., and B.B. Clarke. 1989. Turfgrass breeding – with special reference to turf-type perennial ryegrass, tall fescue, and endophytes. In: H. Takotoh, editor, Proceedings of the 6th International Turfgrass Research Conference, Tokyo, Japan. 31 July – 5 Aug. 1989. p.3–10.

Grinberg, N.F., A. Lovatt, M. Hegarty, A. Lovatt, K.P. Skot, R. Kelly, T. Blackmore, D. Thorogood, R.D. King, I. Armstead, W. Powell, L. Skot. 2016. Implementation of genomic prediction in *Lolium perenne* (L.) breeding populations. Front. Plant Sci. 7:133

Honig, J.A., C. Kubik, M. Majewski, C. Poulsen, E. Weibel, K. Amundsen, S.E. Warnke, W.A. Meyer, S.A. Bonos. 2014. A PCR-based linkage map of *Agrostis stolonifera* and identification of QTL markers for dollar spot resistance. Mol. Breeding 34:185–203.

Jensen, L.B., J.R. Andersen, U. Frei, Y. Xing, C. Taylor, P.B. Holm, and T. Lubberstedt. 2005. QTL mapping of vernalization response in perennial ryegrass (*Lolium perenne* L.) reveals co-location with an orthologue of wheat *VRN1*. Theor. Appl. Genet. 110:527–536

Jung, G., D.P. Coyne, P.W. Skroch, J. Nienhuis, E. Arnaud-Santana, J. Bokosi, H.M. Ariyarathne, J.R. Steadman, J.S. Beaver, and S.M. Kaeppler. 1996. Molecular markers associated with plant architecture and resistance to common blight, web blight, and rust in common beans. J. Am. Soc. Hortic. Sci. 121:794–803.

Karcher, D.E., C.J. Purcell, M.D. Richardson, L.C. Purcell, and K.W. Hignight. 2017. A new java program to rapidly quantify several turfgrass parameters from digital images. Agron. Abr. P. 109313.

Kopecky, D., M. Havrankova, J. Loureiro, S. Castro, A.J. Lukaszewski, J. Bartos, J. Kopecka, J. Dolezel. 2010. Physical distribution of homeologous recombination in individual chromosomes of *Festuca pratensis* in *Lolium multiflorum*. Cytogenetic and Genome Research 129:162–172.

Lander, E., and D. Botstein. 1989. Mapping Mendelian factors underlying quantitative traits using RFLP linkage maps. Genetics 121:185–199

Langridge, P., and K. Chalmers. 2004. The principle: identification and application of molecular markers. In: H. Lorz and G. Wenzel, editors, Biotechnology in agriculture and forestry: molecular marker systems in plant breeding and crop improvement. Springer-Verlag Berlin Heidelberg, Germany. p. 3–22

Lespinasse, D., L. Grivet, V. Troispoux, M. Rodier-Goud, F. Pinard, M. Sequin. 2000. Identification of QTL involved in the resistance to South American leaf blight (*Microcyclus ulei*) in the rubber tree. Theor. Appl. Genet. 100:975–984.

Li, H. 2011. A quick method to calculate QTL confidence interval. J. Genet. 90:355–360.

Muylle, H., J. Baert, E. Van Bockstaele, J. Pertijs, and I. Roldan-Ruiz. 2005. Four QTL determine crown rust (*Puccinia coronate* f. sp. *lolii*) resistance in a perennial ryegrass (*Lolium perenne*) population. Heredity 95:348–357

Orshinsky, A.M., J. Hu, S.O. Opiyo, V. Reddyvari-Channarayappa, T.K. Mitchell, M.J. Boehm. 2012. RNA-Seq analysis of the *Sclerotinia homoeocarpa* – creeping bentgrass pathosystem. Plos One 7:e41140.

Paterson, A.H., S. Damon, J.D. Hewitt, D. Zamir, H.D. Rabinowitch, S.E. Lincoln, E.S. Lander, and S.D. Tanksley. 1991. Mendelian factors underlying quantitative traits in tomato: Comparison across species, generations, and environments. Genetics 127:181–197.

Pfender, W., M. Saha, E. Johnson, M. Slabaugh. Mapping with RAD (restriction-site associated DNA) markers to rapidly identify QTL for stem rust resistance in *Lolium perenne*. Theor. Appl. Genet. 122:1467–1480.

Portyanko, V.A., G. Chen, H.W. Rines, R.L. Phillips, K.J. Leonard, G.E. Ochocki, D.D. Stuthman. 2005. Quantitative trait loci for partial resistance to crown rust, *Puccinia coronoata*, in cultivated oat, *Aevena sativa* L. Theor. Appl. Genet. 111:313–324.

Rioux, R.A. 2014. New insights on the biology and host-pathogen interactions of the dollar spot pathogen *Sclerotinia homoeocarpa*. Doctoral dissertation, University of Wisconsin-Madison, Madison, WI.

Salgado-Salazar, C., L.A. Beirn, A. Ismaiel, M. J. Boehm, I. Carbone, A.I. Putman, L.P. Tredway, B.B. Clarke, and J.A. Crouch. 2018. *Clarireedia*: A new fungal genus

comprising four pathogenic species responsible for dollar spot disease of turfgrass. Fungal Biol. 122:761–773

Sartie, A.M., C. Matthew, H.S. Easton, and M.J. Faville. 2011. Phenotypic and QTL analyses of herbage-production related traits in perennial ryegrass (*Lolium perenne* L.).Euphytica182:295–315. doi:10.1007/s10681-0110400-7

Schejbel, B., L.B. Jensen, Y. Xing, T. Lubberstedt. 2007. QTL analysis of crown rust resistance in perennial ryegrass under conditions of natural and artificial infection. Plant Breed 126:347–352.

Sim, S., K. Diesburg, M. Casler, and G. Jung. 2007. Mapping and comparative analysis of QTL for crown rust resistance in an Italian × perennial ryegrass population. Phytopathology 97:767–776

Singh, B.D. and Singh, A.K. 2015. Marker-assisted plant breeding: principles and practices. Springer, New Delhi.

Smiley, R.W., Dernoeden, P.H., Clarke, B.B. 2005. Compendium of Turfgrass Diseases. St. Paul, MN: Am. Phytopathol. Soc. 3rd ed. 167pp.

Studer, B., T. Asp, U. Frei, S. Hentrup, H. Meally, A. Guillard, S. Barth, H. Muylle, Roldan-Ruiz, P. Barre, C. Koning, Boucoiran, G. Uenk-Stunnenberg, O. Dolstra, L. Skot, K.P. Skot, L.B. Turner, M. O. Humphreys, R. Kolliker, N. Roulund, K.K. Nielson, T. Lubberstedt. 2008. Expressed sequence tag-derived microsatellite markers of perennial ryegrass (*Lolium perenne* L.). Mol. Breed. 21:533–548.

Tanksley, S.D., N.D. Young, A.H. Paterson, M.W. Bonierbale. 1993. RFLP mapping in plant breeding: new tools for an old science. Bio/Technol. 7:257–264.

Terrell, E.E. 1968. A taxonomic revision of the genus *Lolium*. Technical Bulletin No. 1392. United States Department of Agriculture, Washington, D.C.

Thorogood, D. 2003. Perennial ryegrass (*Lolium perenne* L.), p. 75-105. In: M.D. Casler and R.R. Duncan, editors, Turfgrass biology, genetics, and breeding. John Wiley and Sons, Hoboken, NJ. p.75–106.

Van Ooijen, J.W. 2006. JoinMap 4.0, software for the calculation of genetic linkage maps in experimental populations. Kyazma B.V., Wageningen, Netherlands

Van Ooijen, J.W. 2009. MapQTL 6, software for the mapping of quantitative trait loci in experimental populations of diploid species. Kyzma B.V. Wageningen, Netherlands

Vargas, J.M., Jr. 1994. Management of Turfgrass Diseases. 2nd ed. Lewis Publ., Boca Raton, FL

Wang, D., R. Karle, A.F. Iezzoni. 2000. QTL analysis of flower and fruit traits in sour cherry. Theor. Appl. Genet. 100:535–544.

Watschke, T.L., P.H. Dernoeden, and D.J. Shetlar. 2013. Managing Turfgrass Pests. 2nd ed. CRC Press, Boca Raton, FL.

Xu, Y. 2010. Molecular plant breeding. CAB International, Wallingford. p. 734.

Yamada, T., E.S. Jones, N.O.I. Cogan, A.C. Vecchies, T. Nomura, H. Hisano, Y. Shimamoto, K.F. Smith, M.D. Hayward, and J.W. Forster. 2004. QTL analysis of morphological, developmental, and winter hardiness-associated traits in perennial ryegrass. Crop Sci. 44:925–935

Zou, J.H., X.B. Pan, Z.X. Chen, J.Y., Xu, J.F. Lu, W.X. Zhai, L.H. Zhu. 2000. Mapping quantitative trait loci controlling sheath blight resistance in two rice cultivars. Theor. Appl. Genet. 101:569–573.

Table 5.1 Mean dollar spot severity as determined via visual ratings for the I06 × A89 perennial ryegrass population on 23 Aug 2017 and 28 Aug 2018 at the Rutgers Horticultural Research Farm II in North Brunswick, NJ.

Environment	Population Mean	Parent I06 Mean	Parent A89 Mean
2017	2.8[a]	5.5	1.2
2018	3.0	5.2	1.3
Overall	2.9	5.4	1.2

[a] Dollar spot severity as estimated using a visual rating scale where 0 represented approximately 0% diseased leaf tissue and 10 represented approximately 100% diseased leaf tissue.

Table 5.2 Mean dollar spot severity (percent non-green area) as determined via pixel analysis for the I06 × A89 perennial ryegrass population on 23 Aug 2017 and 28 Aug 2018 at the Rutgers Horticultural Research Farm II in North Brunswick, NJ.

Environment	Population Mean	Parent I06 Mean	Parent A89 Mean
2017	42.2	47.4	30.8
2018	39.4	51.3	26.7
Overall	40.8	49.4	28.7

Table 5.3 Analysis of variance for mean dollar spot severity as determined via visual ratings for the I06 × A89 perennial ryegrass population on 23 Aug 2017 and 28 Aug 2018 at the Rutgers Horticultural Research Farm II in North Brunswick, NJ.

Sources of variation	*df*	*F* VALUE	*P* > *F*
Environment	1	0.30	0.6136
Rep(Environment), Error 1	4		
Genotype	119	4.41	<0.0001
Genotype x Environment	119	2.05	<0.0001
Genotype x Rep(Environment), Error 2	476		
Error 3	84		

Table 5.4 Analysis of variance for mean dollar spot severity (percent non-green area) as determined via pixel analysis for the I06 × A89 perennial ryegrass population on 23 Aug 2017 and 28 Aug 2018 at the Rutgers Horticultural Research Farm II in North Brunswick, NJ.

Sources of variation	*df*	*F* VALUE	*P* > *F*
Environment	1	2.29	0.2045
Rep(Environment), Error 1	4		
Genotype	119	6.76	<0.0001
Genotype x Environment	119	1.71	<0.0001
Genotype x Rep(Environment), Error 2	476		
Error 3	84		

Table 5.5 Summary of the twelve quantitative trait loci (QTL) identified for dollar spot resistance across six linkage groups of the I06 parent map. A multiple QTL model mapping analysis was conducted with phenotypic data for dollar spot severity generated from visual ratings and pixel analysis of field trials during 2017 and 2018 at the Rutgers Horticultural Research Farm II in North Brunswick, NJ.

Environment	QTL name[a]	LG	Position (cM)	Marker[b]	Allele means[c]		KW[d]	LOD[e]	R^2(%)[f]	99% CI (cM)[g]
					Allele a	Allele b				
Overall	qI06DSPA-6	1	0.000	DLF_027	44.8	36.7	*******	4.75	15.0	0.000-2.000
Overall	qI06DSVIS-4	1	0.000	DLF_027	3.4	2.2	*******	10.17	26.1	0.000-2.200
2018	qI06DSVIS-1	1	0.700	DLF_027	2.4	3.4	****	6.23	8.5	0.000-2.900
2018	qI06DSPA-4	1	1.000	DLF_027	44.2	34.1	*******	4.53	11.2	0.000-2.000
2017	qI06DSPA-1	1	13.035	B3B7	38.8	46.7	**	4.36	8.7	13.035-13.635
2017	qI06DSPA-2	2	71.363	LpSSR112	40.5	45.4	**	3.57	6.3	71.263-71.413
2018	qI06DSVIS-2	3	46.440	357005	2.7	3.3	**	3.34	4.3	46.358-46.640
Overall	qI06DSVIS-5	4	61.876	G01_037	3.3	2.6	****	3.81	8.6	59.511-63.976
2018	qI06DSPA-5	4	73.254	G01_075	35.5	44.5	******	5.15	12.9	69.254-77.557
Overall	qI06DSPA-7	4	73.254	G01_075	37.9	45.1	******	4.10	12.7	69.254-77.557
2018	qI06DSVIS-3	6	51.251	G03_069	2.4	3.4	****	4.79	6.4	51.193-51.951
2017	qI06DSPA-3	7	50.335	rv_1284	39.6	45.3	****	5.90	10.7	50.135-50.583

[a] Name of QTL, indicates parent background (parent I06) and assessment method used to determine dollar spot severity (VIS = visual rating, PA = pixel analysis).
[b] Name of marker closest to a given QTL.
[c] The mean phenotypic value of progeny carrying the 'a' or 'b' allele of each marker.
[d] Kruskal-Wallis analysis. **, ****, ******, *******, Significant at $P \leq 0.05$, 0.005, 0.0005, and 0.0001 levels, respectively.
[e] The LOD values of the QTL determined by multiple QTL model (MQM) mapping.
[f] Proportion of phenotypic variation explained by a given QTL.
[g] A 99% confidence interval for the QTL length (cM) as determined using the 2-LOD approach.

Table 5.6 Summary of the nine quantitative trait loci (QTL) identified for dollar spot resistance across five linkage groups of the A89 parent map. A multiple QTL model mapping analysis was conducted with phenotypic data for dollar spot severity generated from visual ratings and pixel analysis of field trials during 2017 and 2018 at the Rutgers Horticultural Research Farm II in North Brunswick, NJ.

Environment	QTL name[a]	LG	Position (cM)	Marker[b]	Allele means[c]		KW[d]	LOD[e]	R^2(%)[f]	99% CI (cM)[g]
					Allele a	Allele b				
2018	qA89DSPA-1	1	22.996	LG1_B3B7	33.3	45.4	*****	4.70	12.8	22.847-23.096
2018	qA89DSVIS-3	1	50.520	LG1_rv_0244	2.5	3.4	**	8.70	14.2	49.920-51.105
2017	qA89DSVIS-1	1	51.305	527181	2.4	2.9	*	5.67	15.5	51.305-52.751
2017	qA89DSVIS-2	4	64.128	942062	2.4	3.1	***	3.73	10.4	63.745-65.128
2018	qA89DSPA-2	5	32.915	LG5_G04_043	35.5	43.5	*****	4.05	10.9	32.890-33.515
2018	qA89DSVIS-4	5	35.653	LG5_rv_1112	3.5	2.6	*****	3.94	5.8	35.653-35.653
Overall	qA89DSVIS-6	5	42.667	982455	3.1	2.6	**	4.82	13.5	42.567-43.505
2018	qA89DSVIS-5	6	52.726	565070	3.2	2.7	*	3.36	4.9	52.441-52.726
2018	qA89DSPA-3	7	43.274	965847	42.3	37.3	**	3.69	9.9	43.250-43.274

[a] Name of QTL, indicates parent background (parent A89) and assessment method used to determine dollar spot severity (VIS = visual rating, PA = pixel analysis).
[b] Name of marker closest to a given QTL.
[c] The mean phenotypic value of progeny carrying the 'a' or 'b' allele of each marker.
[d] Kruskal-Wallis analysis. *, **, ***, ***** Significant at $P \leq 0.1$, 0.05, 0.01, and 0.001 levels, respectively.
[e] The LOD values of the QTL determined by multiple QTL model (MQM) mapping.
[f] Proportion of phenotypic variation explained by a given QTL.
[g] A 99% confidence interval for the QTL length (cM) as determined using the 2-LOD approach.

Figure 5.1 Dollar spot susceptible parent I06 (left) and dollar spot resistant parent A89 (right) under high dollar spot disease pressure during 2017 at the Rutgers Horticultural Research Farm II in North Brunswick, NJ.

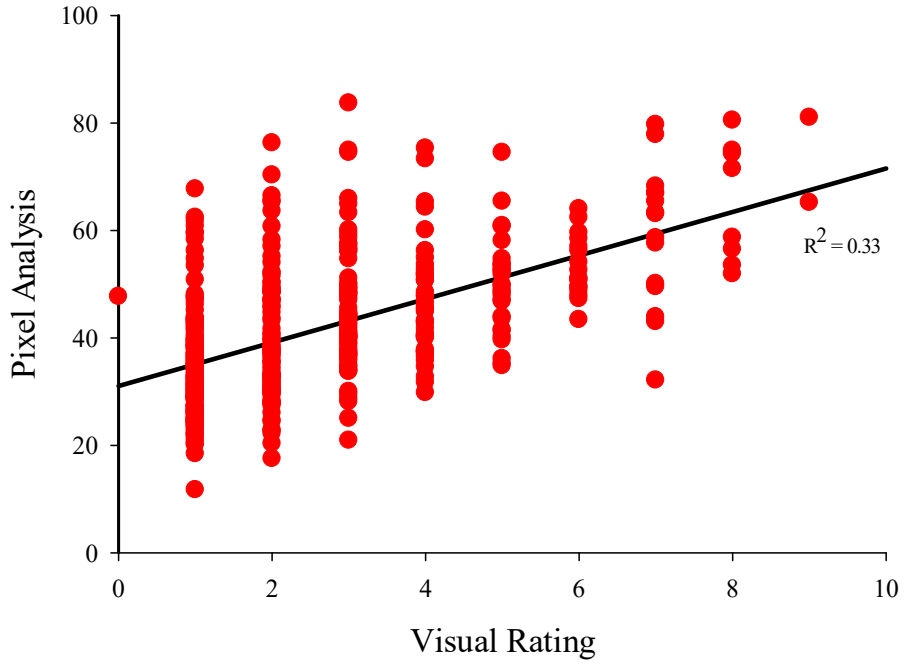

Figure 5.2 Linear regression analysis between visual ratings and pixel analysis for dollar spot severity on 23 Aug 2017 at the Rutgers Plan Biology Research and Extension Farm in North Brunswick, NJ.

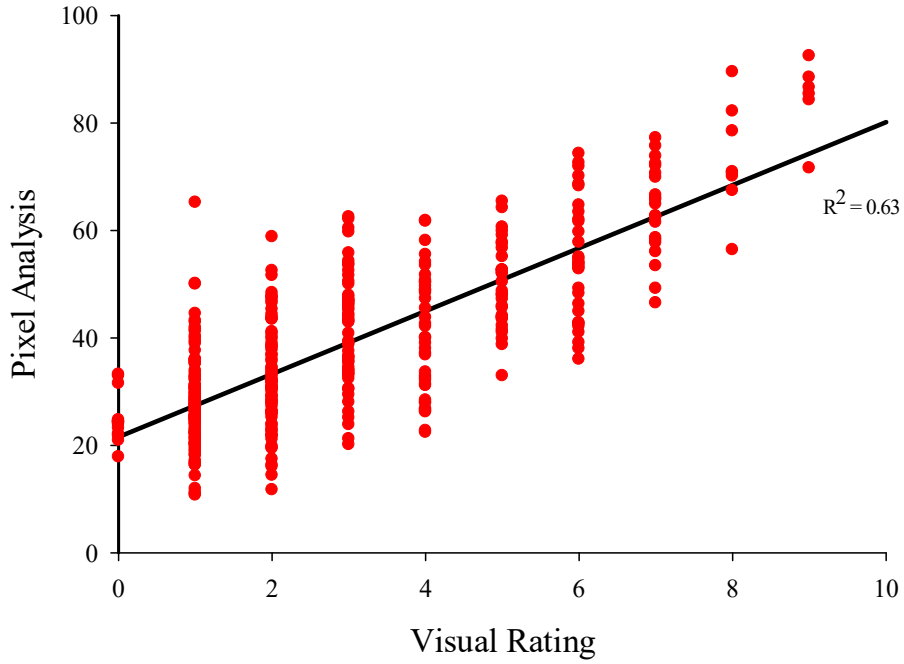

Figure 5.3 Linear regression analysis between visual ratings and pixel analysis for dollar spot severity on 28 Aug 2018 at the Rutgers Plan Biology Research and Extension Farm in North Brunswick, NJ.

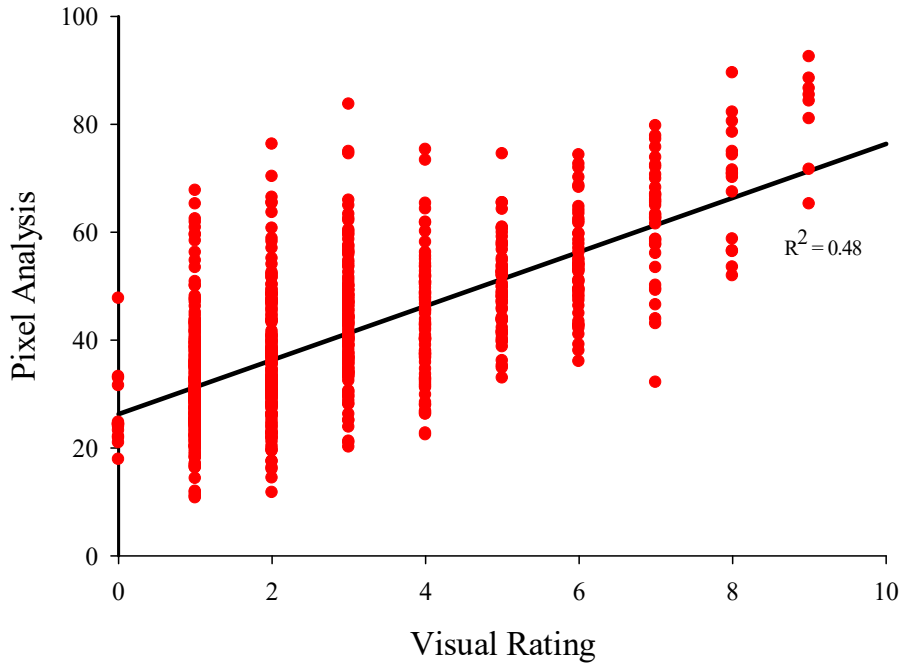

Figure 5.4 Linear regression analysis between visual ratings and pixel analysis for dollar spot severity on 23 Aug 2017 and 28 Aug 2018 at the Rutgers Plan Biology Research and Extension Farm in North Brunswick, NJ.

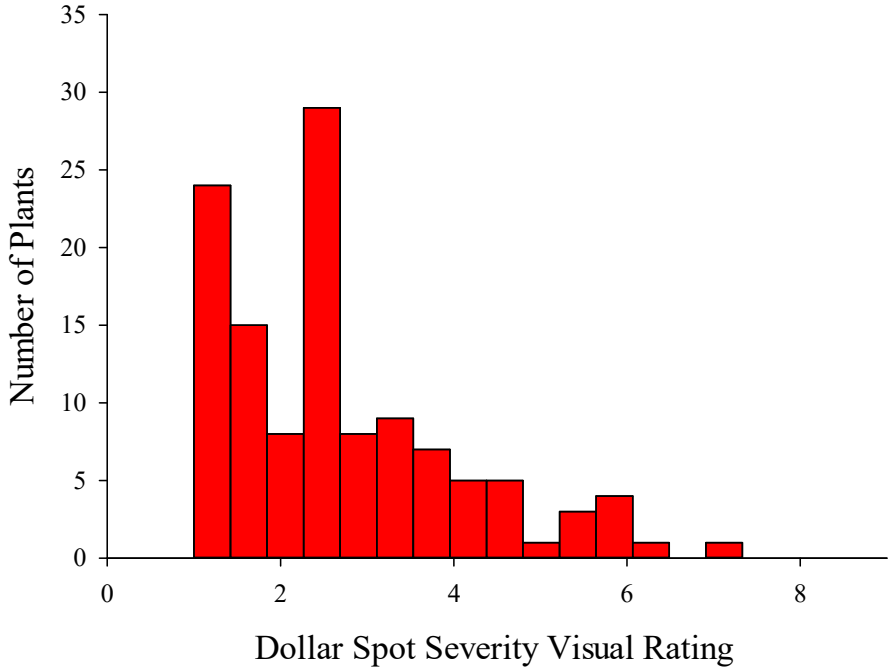

Figure 5.5 Frequency distribution for mean dollar spot severity (percent diseased area) as determined via visual ratings for the I06 × A89 perennial ryegrass mapping population on 23 Aug 2017 at the Rutgers Plan Biology Research and Extension Farm in North Brunswick, NJ. Dollar spot severity was estimated using a visual rating scale where 0 represented approximately 0% diseased leaf tissue and 10 represented approximately 100% diseased leaf tissue.

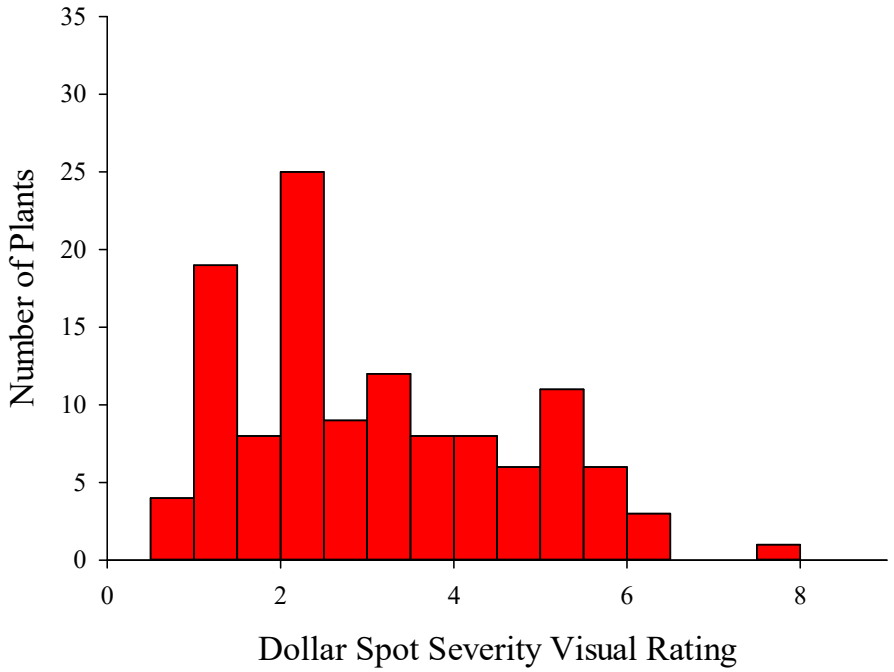

Figure 5.6 Frequency distribution for mean dollar spot severity (percent diseased area) as determined via visual ratings for the I06 × A89 perennial ryegrass mapping population on 28 Aug 2018 at the Rutgers Plan Biology Research and Extension Farm in North Brunswick, NJ. Dollar spot severity was estimated using a visual rating scale where 0 represented approximately 0% diseased leaf tissue and 10 represented approximately 100% diseased leaf tissue.

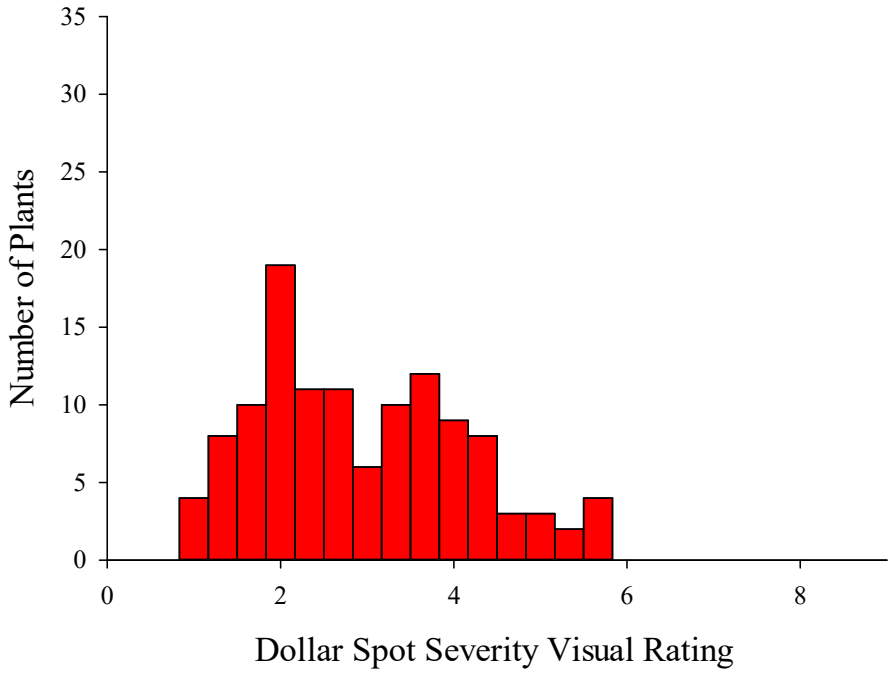

Figure 5.7 Frequency distribution for mean dollar spot severity (percent diseased area) as determined via visual ratings for the I06 × A89 perennial ryegrass mapping population on 23 Aug 2017 and 28 Aug 2018 at the Rutgers Plan Biology Research and Extension Farm in North Brunswick, NJ. Dollar spot severity was estimated using a visual rating scale where 0 represented approximately 0% diseased leaf tissue and 10 represented approximately 100% diseased leaf tissue.

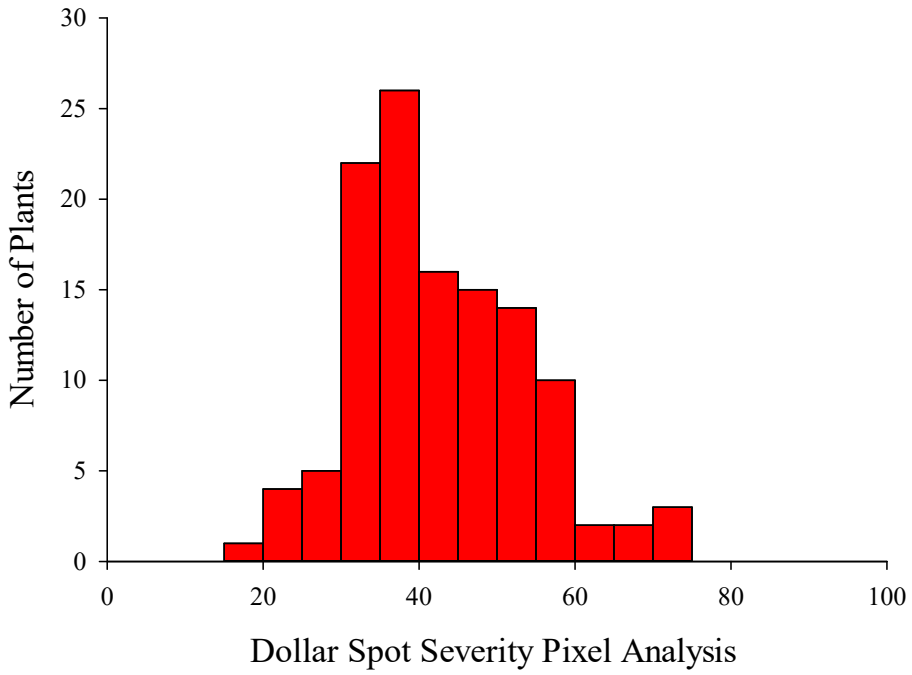

Figure 5.8 Frequency distribution for mean dollar spot severity (percent non-green area) as determined via pixel analysis for the I06 × A89 perennial ryegrass mapping population on 23 Aug 2017 at the Rutgers Plan Biology Research and Extension Farm in North Brunswick, NJ.

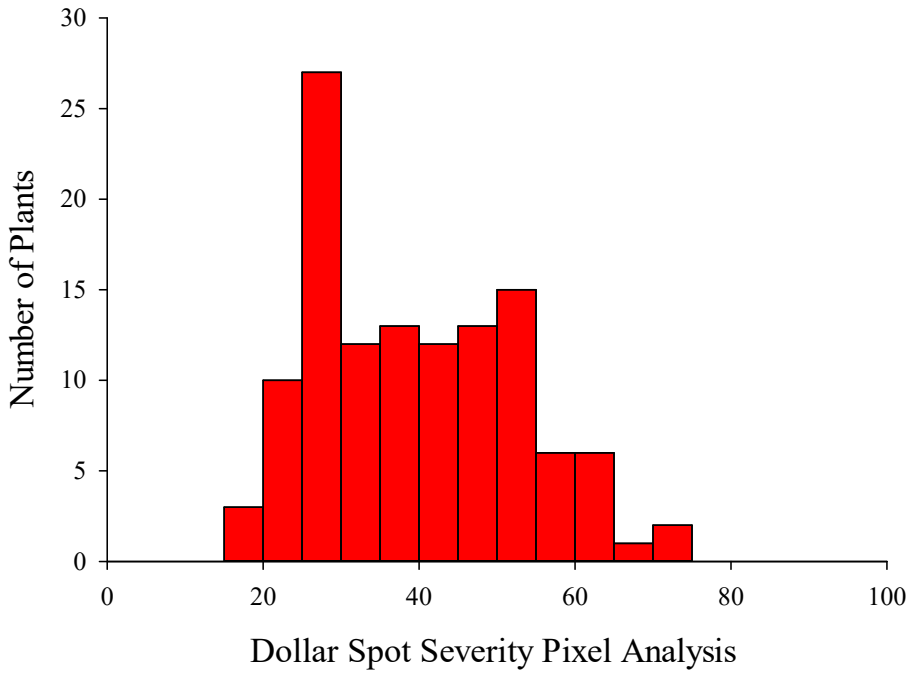

Figure 5.9 Frequency distribution for mean dollar spot severity (percent non-green area) as determined via pixel analysis for the I06 × A89 perennial ryegrass mapping population on 28 Aug 2018 at the Rutgers Plan Biology Research and Extension Farm in North Brunswick, NJ.

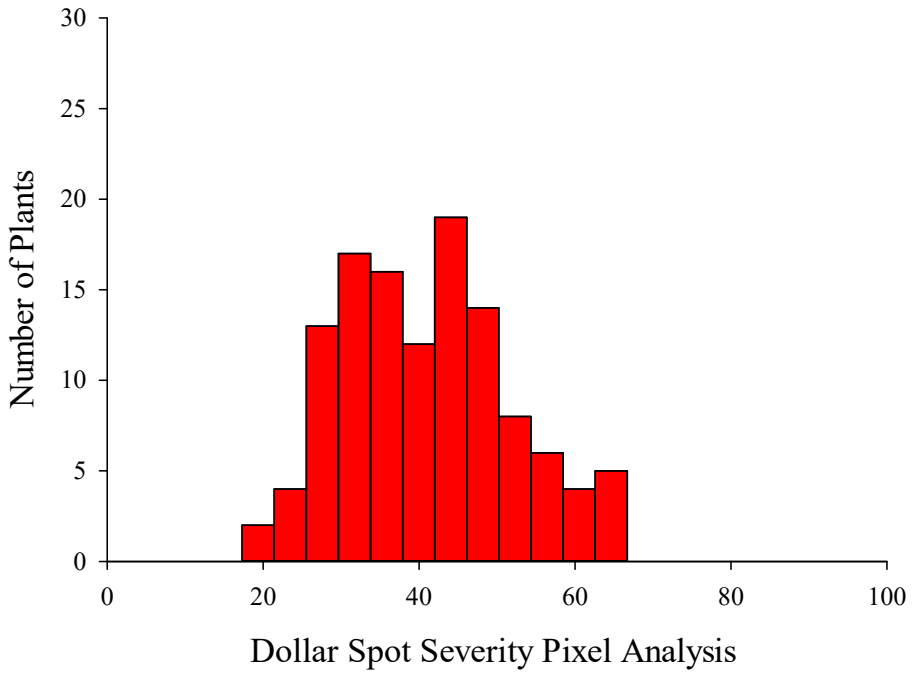

Figure 5.10 Frequency distribution for mean dollar spot severity (percent non-green area) as determined via pixel analysis for the I06 × A89 perennial ryegrass mapping population on 23 Aug 2017 and 28 Aug 2018 at the Rutgers Plan Biology Research and Extension Farm in North Brunswick, NJ.

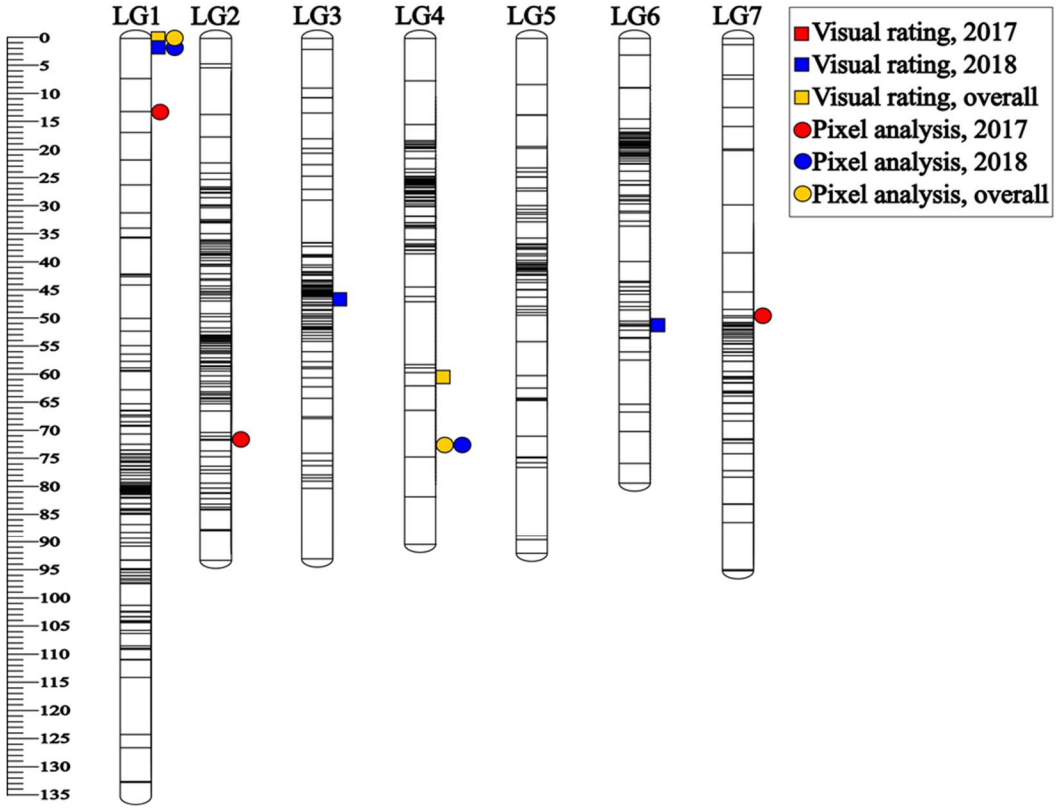

Figure 5.11 Summary of the quantitative trait loci (QTL) identified for dollar spot resistance on the I06 parent map. A multiple QTL model mapping analysis was conducted with phenotypic data for dollar spot severity generated from visual ratings and pixel analysis of a field trial on 23 Aug 2017 and 28 Aug 2018 at the Rutgers Plant Science Research and Extension Farm in Adelphia, NJ. The genetic map distance (cM) is provided to the left, and linkage group (LG) numbers are indicated at the top of each individual linkage group.

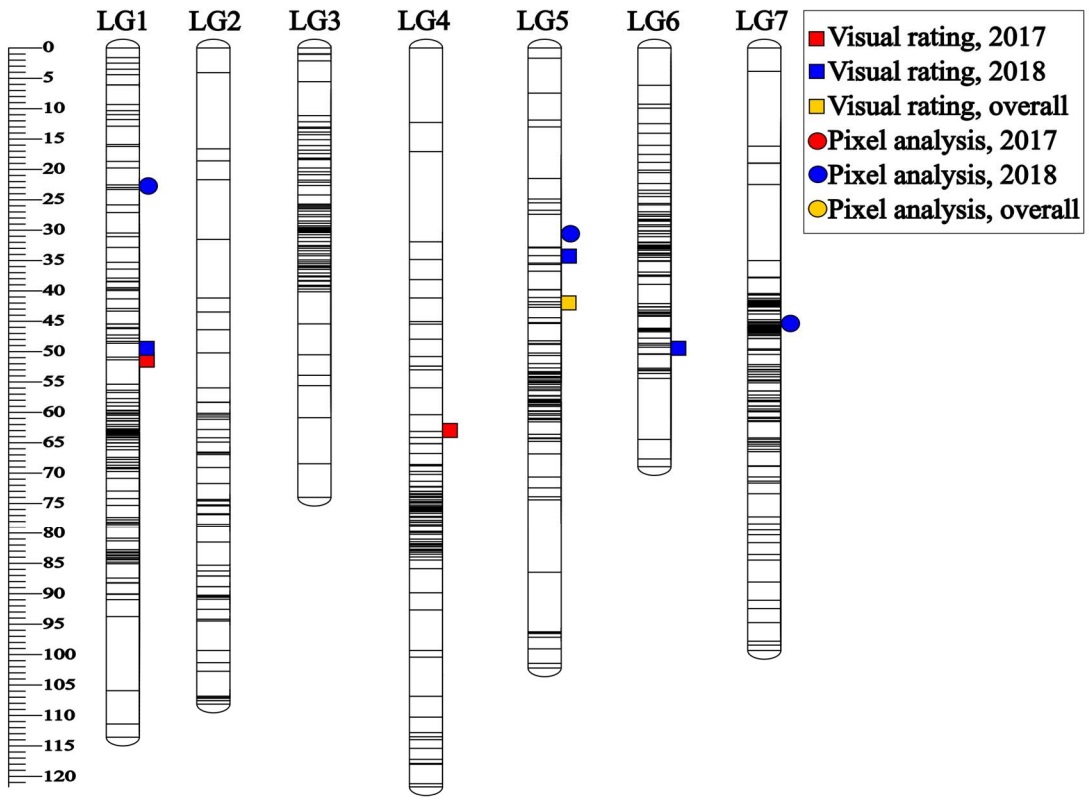

Figure 5.12 Summary of the quantitative trait loci (QTL) identified for dollar spot resistance on the A89 parent map. A multiple QTL model mapping analysis was conducted with phenotypic data for dollar spot severity generated from visual ratings and pixel analysis of a field trial on 23 Aug 2017 and 28 Aug 2018 at the Rutgers Plant Science Research and Extension Farm in Adelphia, NJ. The genetic map distance (cM) is provided to the left, and linkage group (LG) numbers are indicated at the top of each individual linkage group.

CHAPTER VI

QUANTITATIVE TRAIT LOCUS MAPPING FOR GROWTH HABIT MORPHOLOGY TRAITS IN PERENNIAL RYEGRASS

Abstract

Perennial ryegrass (*Lolium perenne* L.) is a widely used cool-season turfgrass species. Breeding for turf-type perennial ryegrass is challenging because morphological traits that are desirable for turf quality characteristics often do not align with morphological traits that are desirable for seed production. For turfgrass purposes, a prostrate growth habit contributes to low mowing tolerance, enhanced heat tolerance and winter hardiness, and improved traffic tolerance. However, an upright growth habit contributes to improved seed ripening and harvesting conditions for seed production purposes. Thus, the rationale of this study was to improve our understanding of the genetic basis for growth habit morphology in perennial ryegrass. We conducted a quantitative trait locus (QTL) analysis using the I06 × A89 pseudo-F_2 perennial ryegrass mapping population. The QTL analyses were conducted with the individual I06 and A89 parent maps and phenotypic data for growth habit, seedhead angle, plant height, vegetative plant width, and total plant width collected from field nurseries during 2017 and 2018. QTL were identified for growth habit (n=11), seedhead angle (n=2), plant height (n=7), vegetative plant width (n=5), and total plant width (n=3) from the I06 and A89 parent genetic linkage maps. Four QTL were identified across multiple

environments, and two QTL were significantly associated with multiple morphological traits. This is the first reported effort for QTL mapping of growth habit traits in turf-type perennial ryegrass. These findings will be useful for future studies regarding the genetic basis for assessing growth habit morphology in perennial ryegrass.

Introduction

Perennial ryegrass (*Lolium perenne* L.) is a major cool-season turf and forage grass native to temperate regions of Asia, North Africa, and Europe (Beard, 1973; Funk and Clarke, 1989; Terrell, 1968; Thorogood, 2003). The genome size of this diploid (2n = 2x = 14) species is approximately 2.5 Gb (Beard, 1973; Kopecky et al., 2010). With the exception of Antarctica, this medium to high density, bunch-type perennial is grown on every continent and is managed as a turfgrass in general landscaping areas, parks, racetracks, golf fairways and roughs, and athletic fields (Beard, 1973; Beard and Beard, 2005; Thorogood, 2003). Moreover, perennial ryegrass is used in lower latitudes to overseed warm-season turf to increase density and green color during winter dormancy periods (Beard and Beard, 2005; Thorogood, 2003; Turgeon, 2008).

The breeding of turf-type perennial ryegrass is challenging because morphological traits that contribute to improved turf quality characteristics are not necessarily desirable for seed production. Research of various turfgrass species has demonstrated that a prostrate growth habit, compared to an upright growth habit, is beneficial for turf quality and health traits including improved low mowing tolerance (Inguagiato et al., 2009; Younger, 1969), enhanced heat tolerance and winter hardiness

(Beard, 1973; Cohen, 1980), and improved traffic tolerance (Chen et al., 2016). Accordingly, turf-type perennial ryegrass has been selected for prostrate growth habit and, thus, has been widely utilized for turf applications (Funk and Clarke, 1989). However, an upright growth habit provides benefits for seed production including conditions that favor better seed ripening and easier harvesting because the seedheads are not lying on or near the ground. Therefore, a better understanding of the genetic control mechanisms for growth habit morphology will enable manipulation of this trait in breeding programs (Yamada et al., 2004).

With regard to the underlying genetic basis for growth habit morphology in perennial ryegrass, research is limited. Quantitative trait locus (QTL) analyses have been conducted for morphological and developmental traits (Yamada et al., 2004) and forage quality traits (Cogan et al., 2005). Forty-two QTL were identified for herbage quality traits including crude protein content, estimated in vivo dry-matter digestibility, neutral detergent fiber content, estimated metabolisable energy, and water-soluble carbohydrate content (Cogan et al., 2005). Nine QTL were identified for morphological and developmental traits including plant height, plant type (growth habit), tiller size, leaf length, and leaf width (Yamada et al., 2004). Two QTL for plant height were identified on linkage groups one and three, and three QTL for plant type were identified on linkage groups four and seven.

More recently, a turf-type perennial ryegrass mapping population was developed that segregates for morphological traits related to growth habit (Chapter II). This population is a valuable resource for better understanding the genetic basis of perennial ryegrass growth habit. Thus, the objective of this research was to conduct QTL analyses

using the I06 × A89 population to identify genomic regions associate with growth habit morphology for perennial ryegrass.

Materials and methods

Mapping population

During the summer of 2016, a pseudo-F_2 population was developed to analyze QTL for morphological traits related to growth habit in perennial ryegrass (Chapter II). Two diploid heterozygotes, I06 and A89, were used as parental genotypes. A cross-fertilization between the prostrate clone (maternal parent, I06) and the upright clone (paternal parent, A89) was conducted at the New Jersey Agricultural Experiment Station in New Brunswick, NJ. Maternally derived seeds were sown into 15.2 cm diameter round pots on 22 Aug 2016 and allowed to germinate. On 14 Sep 2016, the resulting 118 pseudo-F_2 progeny were transferred to single cells (5.1 × 5.1 cm) of plastic flats and given a unique mapping population label.

Genetic linkage mapping

Genetic linkage maps were constructed in JoinMap 4.1 (Van Ooijen, 2006) for the I06 parent and the A89 parent using the doubled haploid two-way pseudo testcross approach (Chapter III). A total of 848 SNPs and 52 SSRs were mapped across a total distance of 677.5 cM on the I06 parent map, yielding an average marker density of 0.75

cM. A total of 769 SNPs and 35 SSRs were mapped across a total distance of 687.9 cM on the A89 parent map, with an average marker density of 0.86 cM. Both genetic linkage maps and both marker datasets were used for QTL mapping analyses.

Field assessment for morphological traits

The I06 × A89 mapping population was established in two spaced-plant field nurseries at the Rutgers Plant Science Research and Extension Farm in Adelphia, NJ and studied for growth habit morphology during the summers of 2017 and 2018. Each nursery was arranged in a randomized complete block design and there were three replicates of each progeny genotype (n=118) and 24 replicates of each parent genotype (n=2); plants were spaced 61 cm apart at planting. The 2017 field nursery was initially established in single cells (6.4 × 6.4 cm) of plastic flats filled with Pro-mix (Premier Tech Ltd., Riviere-du-Loup, QC) growing media during December 2016. The plants were vernalized in a non-heated greenhouse throughout the winter months and transplanted to the field nursery on 12 Apr 2017. The 2018 nursery was initially established in single cells (6.4 × 6.4 cm) of plastic flats filled with Pro-mix growing media during September 2017 and grown in greenhouse conditions for four weeks. During this period, plants were fertilized biweekly with a balanced fertility source (10N-4.4P-8.3K) and irrigated daily. The plants were established in the field nursery on 17 Oct 2017.

Morphological traits studied included growth habit, seedhead angle, plant height, vegetative plant width, and total plant width. Growth habit was assessed for each plant on 27 Jun 2017 and 11 Jun 2018 using a visual rating scale that ranged from 1 to 9, where

1 represented an extremely prostrate growth habit and 9 represented an extremely upright growth habit. Seedhead angle was assessed for each plant on 29 Jun 2017 and 12 Jun 2018 using a protractor to measure the average seedhead angle (degree) from the ground level (Fig. 6.1). Plant height was assessed for each plant on 27 Jun 2017 and 13 Jun 2018 by measuring the maximum distance (mm) from the base of the plant to the top of the foliar leaf tissue. Vegetative plant width was assessed for each plant on 29 Jun 2017 and 11 Jun 2018 by measuring the maximum distance (mm) from one side of the plant foliar leaf tissue to the other. Total plant width was assessed for each plant on 28 Jun 2017 and 13 Jun 2018 by measuring the maximum distance (mm) from one side of the plant seedheads to the other. Thus, the difference between the vegetative plant width and total plant width measurements was that the total plant width measurement included the width with seedheads while the vegetative plant width measurement only included the width of the foliar leaf tissue.

All morphological trait data were subjected to an analysis of variance (ANOVA) using SAS (SAS Institute, NC, USA). The data were summarized for each of the two environments (2017 and 2018) and used to assign phenotypic means for each genotype, which were used for QTL analyses.

Quantitative trait locus analysis

The I06 × A89 parent genetic linkage maps, marker datasets for all markers included in the linkage maps, and phenotypic data for growth habit, seedhead angle, plant height, vegetative plant width, and total plant width were used for QTL mapping analyses in MapQTL 6 (Van Ooijen, 2009). Permutation testing was conducted to establish

genome-wide logarithm of odds (LOD) thresholds using 10,000 permutations and at $\alpha = 0.05$ significance level (Churchill and Doerge, 1994). Initially, QTL were identified by interval mapping (IM) procedures with default parameters including a regression algorithm with a mapping step size of 1.0 cM and a maximum number of neighboring markers equal to 5 (Jung et al., 1996; Lander and Botstein, 1989). The automatic cofactor selection (ACS) tool was used to detect significantly ($P < 0.02$) associated markers, which were subsequently used for multiple QTL model (MQM) mapping. The MQM mapping procedures were implemented with default parameters as described for the IM mapping procedures. The QTL positions were defined by the locations where LOD scores reached maximum values. The 2-LOD support intervals were used to calculate 99% confidence intervals (Lander and Botstein, 1989; Li, 2011). The percentage of phenotypic variation explained by each marker (R^2) was calculated as part of the analyses. Major-effect QTL were defined by R^2 values ≥ 10.0, and minor-effect QTL were defined by R^2 values < 10.0 (Collard et. al., 2005).

Results

Field assessment for morphological traits

Continuous phenotypic variation was observed for all traits among the individuals of the mapping population generated from the cross between parent I06 and parent A89

during both years (Tables 6.1-6.5; Figs. 6.2-6.16). The following sections describe the results for the analyses of variance and each of the morphological traits, separately.

Analyses of Variance

The analyses of variance for the morphological traits are presented in Tables 6.6-6.10. The interaction effect, genotype × environment, significantly affected mean growth habit ($P < 0.0001$), mean seedhead angle ($P = 0.0069$), mean plant height ($P < 0.0001$), mean vegetative plant width ($P = 0.0025$), and mean total plant width ($P < 0.0001$). The main effect, genotype, significantly affected mean growth habit ($P < 0.0001$), mean seedhead angle ($P < 0.0001$), mean plant height ($P < 0.0001$), mean vegetative plant width ($P < 0.0001$), and mean total plant width ($P < 0.0001$). The main effect, environment, did not significantly affect mean growth habit ($P = 0.1640$) or mean seedhead angle ($P = 0.7494$), but did significantly affect mean plant height ($P = 0.0050$), mean vegetative plant width ($P = 0.0002$), and mean total plant width ($P = 0.0016$). Accordingly, QTL analyses were conducted using the phenotypic means for each genotype at each environment (2017 and 2018). Additionally, the QTL analyses were conducted on the overall datasets, which were generated by combining the data across both years of the study to increase the consistency in the observed genotype mean response.

Growth habit

A summary of the growth habit data is presented in Table 6.1 and Figs. 6.2-6.4. Mean growth habit for the progeny genotypes was 5.2 and 4.7 during 2017 and 2018, respectively. The overall progeny mean growth habit averaged across both years of the study was 5.0. Mean growth habit for the I06 parent genotype was 3.0 and 3.4 during 2017 and 2018, respectively. The overall parent I06 mean growth habit averaged across both years of the study was 3.2. Mean growth habit for the A89 parent genotype was 7.8 and 7.9 during 2017 and 2018, respectively. The overall parent A89 mean growth habit averaged across both years of the study was 7.8.

Seedhead angle

A summary of the seedhead angle data is presented in Table 6.2 and Figs. 6.5-6.7. Seedhead angle was assessed for each plant using a protractor to measure the average seedhead angle (degree) from the ground level (Fig. 6.1). Mean seedhead angle for the progeny genotypes was 69.3 and 70.1 degrees during 2017 and 2018, respectively. The overall progeny mean seedhead angle averaged across both years of the study was 69.7 degrees. Mean seedhead angle for the I06 parent genotype was 63.5 and 64.9 degrees during 2017 and 2018, respectively. The overall parent I06 mean seedhead angle averaged across both years of the study was 64.2 degrees. Mean seedhead angle for the A89 parent genotype was 83.0 and 78.9 degrees during 2017 and 2018, respectively. The overall parent A89 mean seedhead angle averaged across both years of the study was 81.1 degrees.

Plant height

A summary of the plant height data is presented in Table 6.3 and Figs. 6.8-6.10. Mean plant height for the progeny genotypes was 427.8 and 493.4 mm during 2017 and 2018, respectively. The overall progeny mean plant height averaged across both years of the study was 460.4 mm. Mean plant height for the I06 parent genotype was 422.0 and 577.3 mm during 2017 and 2018, respectively. The overall parent I06 mean plant height averaged across both years of the study was 496.3 mm. Mean plant height for the A89 parent genotype was 447.6 and 470.5 mm during 2017 and 2018, respectively. The overall parent A89 plant height averaged across both years of the study was 458.3 mm.

Vegetative plant width

A summary of the vegetative plant width data is presented in Table 6.4 and Figs. 6.11-6.13. Mean vegetative plant width for the progeny genotypes was 310.3 and 477.9 mm during 2017 and 2018, respectively. The overall progeny mean vegetative plant width averaged across both years of the study was 393.6 mm. Mean vegetative plant width for the I06 parent genotype was 349.6 and 525.9 mm during 2017 and 2018, respectively. The overall parent I06 mean vegetative plant width averaged across both years of the study was 433.9 mm. Mean vegetative plant width for the A89 parent genotype was 250.0 and 344.8 mm during 2017 and 2018, respectively. The overall

parent A89 mean vegetative plant width averaged across both years of the study was 294.2 mm.

Total plant width

A summary of the total plant width data is presented in Table 6.5 and Figs 6.14-6.16. Mean total plant width for the progeny genotypes was 926.7 and 973.4 mm during 2017 and 2018, respectively. The overall progeny mean total plant width averaged across both years of the study was 949.9 mm. Mean total plant width for the I06 parent genotype was 1057.5 and 1123.6 mm during 2017 and 2018, respectively. The overall parent I06 mean total plant width averaged across both years of the study was 1089.1 mm. Mean total plant width for the A89 parent genotype was 717.1 and 551.0 mm during 2017 and 2018, respectively. The overall parent A89 mean total plant width averaged across both years of the study was 639.6 mm.

Quantitative trait locus analysis

The QTL mapping analyses were conducted using progeny means for growth habit, seedhead angle, plant height, vegetative plant width, and total plant width. Progeny genotype means were generated from each of the two years (2017 and 2018) separately and pooled, as the overall progeny genotype means. Six major-effect QTL and five minor-effect QTL were identified for visual growth habit from the two parent genetic linkage maps (Tables 6.11, 6.12; Figs. 6.17, 6.18). Two major-effect QTL were identified for seedhead angle from the two parent genetic linkage maps (Tables 6.11,

6.12; Figs. 6.17, 6.18). Six major-effect QTL and one minor-effect QTL were identified for plant height from the two parent genetic linkage maps (Tables 6.11, 6.12; Figs. 6.17, 6.18). Four major-effect QTL and one minor-effect QTL were identified for vegetative plant width from the two parent genetic linkage maps (Tables 6.11, 6.12; Figs. 6.17, 6.18). Three major-effect QTL were identified for total plant width from the two parent genetic linkage maps (Tables 6.11, 6.12; Figs. 6.17, 6.18). Quantitative trait loci for growth habit (n=1), plant height (n=2), vegetative plant width (n=1), and total plant width (n=1) were identified across multiple environments, and two of the identified QTL were significantly associated with multiple morphological traits. The following sections describe the QTL mapping results from each of the parent maps, separately.

I06 parent map

Seventeen major-effect QTL and four minor-effect QTL for morphological traits were identified at sixteen distinct genomic regions across six linkage groups of the I06 parent map (Table 6.11; Fig. 6.17). The LOD scores ranged from 3.26 to 8.70, and the percent phenotypic variation explained by the QTL ranged from 7.2 to 22.1. The seventeen major effect QTL were identified across linkage groups two, three, four, five, six, and seven of the I06 parent map. In addition, groups of coincident QTL were identified at linkage groups two, four and seven.

From the 2017 study, QTL were identified for growth habit (n=4), seedhead angle (n=1), plant height (n=2), and vegetative plant width (n=1). From the 2018 study, QTL were identified for growth habit (n=3), plant height (n=1), vegetative plant width (n=2),

and total width (n=2). From the overall, combined data, QTL were identified for growth habit (n=1), plant height (n=1), vegetative plant width (n=2), and total plant width (n=1). One of the identified QTL (defined by marker G01_024 on the I06 parent map) was significantly associated with both growth habit and plant height.

A QTL, defined by marker LpSSR112 on linkage group two of the I06 parent map, was identified for total plant width across multiple environments. The LOD scores for this QTL ranged from 3.68 to 4.58, and the percent phenotypic variation for total plant width explained ranged from 10.6 to 13.1. Another QTL, defined by marker G01_024 on linkage group four of the I06 parent map, was identified for growth habit and plant height across multiple environments. The LOD scores for this QTL ranged from 4.21 to 6.23. The percent phenotypic variation for growth habit explained ranged from 13.6 to 15.4, and the percent phenotypic variation for plant height explained ranged from 13.6 to 15.7. A final QTL, defined by marker B5G4 on linkage group seven of the I06 parent map, was identified for vegetative plant width across multiple environments. The LOD scores for this QTL ranged from 5.14 to 6.07 using the 2018 and overall datasets, respectively. The percent phenotypic variation for vegetative plant width explained ranged from 12.6 to 15.5 using the 2018 and overall datasets, respectively.

A89 parent map

Four major-effect QTL and three minor-effect QTL for morphological traits were identified at five distinct genomic regions across four linkage groups of the A89 parent map (Table 6.12; Fig. 6.18). The LOD scores ranged from 3.23 to 6.45, and the percent

phenotypic variation explained by the QTL ranged from 8.5 to 16.5. The four major effect QTL were identified across linkage groups two, four, six, and seven of the A89 parent map. In addition, a single group of coincident QTL was identified at linkage group two.

From the 2017 study, a single QTL was identified for seedhead angle. From the 2018 study, QTL were identified for growth habit (n=1), plant height (n=1), and vegetative plant width (n=2). From the overall, combined data, a QTL was identified for vegetative plant width. No significant QTL were identified for total plant width in A89 parent..

A QTL, defined by marker G03_054 on linkage group two of the A89 parent map, was identified for growth habit and plant height across multiple environments. The LOD scores for this QTL ranged from 3.23 to 4.86. The percent phenotypic variation for growth habit explained was 9.9, and the percent phenotypic variation for plant height explained ranged from 9.5 to 14.6.

Discussion

We conducted QTL analyses using phenotypic data for growth habit morphology collected during 2017 and 2018 along with two separate genetic linkage maps, one for each parent of the I06 × A89 mapping population. Phenotypic data included growth habit, seedhead angle, plant height, vegetative plant width, and total plant width. Thus, there were thirty datasets for QTL mapping analyses. The 2017 study was planted during the spring of 2017 and evaluated for growth habit morphology-related traits during the

summer of 2017. The 2018 study was planted in the field during the fall of 2017 and evaluated for growth habit morphology-related traits during the summer of 2018. The difference in establishment timing between the two years resulted in larger plants for the 2018 study, as observed for the plant height, vegetative plant width, and total plant width data.

In total, twenty-one major-effect QTL and seven minor-effect QTL for the growth habit morphology-related traits were detected. As defined by Collard et al. (2005), major-effect QTL were those that explained 10.0%, or greater, phenotypic trait variation. The genomic regions defined by the major-effect QTL identified in this study should be investigated further to elucidate their potential role for growth habit morphology in perennial ryegrass. The coincident QTL identified in this study can be partitioned to four target genomic regions at linkage groups two, four, and seven of the I06 parent map and linkage group two of the A89 parent map. These genomic regions will potentially be useful for future studies and potential breeding applications.

Four of the QTL identified in this study were detected using data from both years of this study, and two of those QTL were associated with multiple morphological traits. Consistent detection of these four QTL suggests potential linkage between these QTL and growth habit morphology in perennial ryegrass. Of great interest, is the coincident detection of QTL for plant height and growth habit on linkage group 4 of the I06 parent map and linkage group two of the A89 parent map. This evidence provides a reason for exploring these genomic regions in more detail to discern their potential role for these morphological traits in perennial ryegrass. Yamada et al. (2004) identified two QTL for plant height located at perennial ryegrass linkage groups one and three. We identified

seven QTL for plant height in this study, but those QTL were located on linkage groups two, four, and five of the I06 parent map and linkage groups two and seven of the A89 parent map. Yamada et al. (2004) also identified three QTL for growth habit at linkage groups four and seven. In this study, we identified eleven QTL for growth habit, which were located on linkage groups two, three, four, and seven of the I06 parent map and linkage groups two, four, and six of the A89 parent map. Thus, these reports warrant further investigations into the genomic regions associated with the growth habit QTL on linkage groups four and seven of the perennial ryegrass linkage maps.

In summary, this was the first reported effort to map QTL for growth habit morphology in turf-type perennial ryegrass. Twenty-one major-effect QTL and seven minor-effect QTL were identified at twenty-one distinct genomic regions across the two parent genetic linkage maps. Twenty-one regions were identified across the genetic linkage maps for the I06 and A89 parents. Four QTL were identified across multiple environments, and two QTL were significantly associated with multiple traits.

Moving forward, QTL confirmation studies should be conducted using additional populations and environments. The QTL regions identified herein should also be investigated to determine their usefulness for marker-assisted selection breeding strategies for growth habit traits in perennial ryegrass. Additional techniques such as comparative genomics should also be used to identify possible genes and underlying mechanisms for growth habit morphology in perennial ryegrass and other closely related species. The completion of a proposed perennial ryegrass reference genome will be a valuable resource for forthcoming studies with the I06 × A89 perennial ryegrass mapping population (Byrne et al., 2015). Through these proposed efforts, we hope to better

understand growth habit morphology in perennial ryegrass and other closely related species.

Literature cited

Beard, J.B. 1973. Turfgrass: Science and Culture. Prentice Hall, Englewood Cliffs, NJ.

Beard, J.B., and H.J. Beard. 2005. Beard's Turfgrass Encyclopedia for Golf Courses, Grounds, Lawns, Sports Fields. Michigan State University Press

Byrne, S.L., M. Pfeifer, I. Nagy, I. Armstead, S. Swain, B. Studer, K.F.X. Mayer, J.D. Campbell, A. Czaban, S. Hentrup, F. Panitz, C. Bendixen, J. Hedegaard, M. Caccamo, T. Asp. 2015. A senty-based draft genome sequence for the forage grass *Lolium perenne*. Plant J. 84:816–826.

Chen, J., C. Thammina, W. Li, H. Yu, H. Yer, R. El-Tanbouly, M. Marron, L. Katin-Grazzini, Y. Chen, J. Inguagiato, R.J. McAvoy, K. Guillard, X. Zhang, Y. Li. 2016. Isolation of prostrate turfgrass mutants via screening dwarf phenotype and characterization of a perennial ryegrass prostrate mutant. Horticulture Research 3:16003. doi:10.1038/hortres.2016.3

Churchill, G.A., and R.W. Doerge. 1994. Empirical threshold values for quantitative trait mapping. Genetics 138:963–971.

Cogan, N.O.I., K.F. Smith, T. Yamada, M.G. Francki, A.C. Vecchies, E.S. Jones, G.C. Spangenberg, and J.W. Forster. 2005. QTL analysis and comparative genomics of herbage quality traits in perennial ryegrass (*Lolium perenne* L.). Theor. Appl. Genet. 110:364–380.

Cohen, R.P. 1980. Evaluating perennial ryegrass (*Lolium perenne* L.) for cold hardiness through alcohol bath freezing and measurement of subcrown internodes. Master thesis, Univ. of Vermont, Burlington, VT.

Collard, B.C.Y, M.Z.Z. Jahufer, J.B. Brouwer, and E.C.K. Pang. 2005. An introduction to markers, quantitative trait loci (QTL) mapping and marker-assisted selection for crop improvement: the basic concepts. Euphytica. 142:169–196

Funk, C.R., and B.B. Clarke. 1989. Turfgrass breeding – with special reference to turf-type perennial ryegrass, tall fescue, and endophytes. In: H. Takotoh, editor, Proceedings of the 6th International Turfgrass Research Conference, Tokyo, Japan. 31 July – 5 Aug. 1989. p.3–10.

Inguagiato, J., J. Murphy, B.B. Clarke. 2009. Anthracnose disease and annual bluegrass putting green performance affected by mowing practices and lightweight rolling. Crop Sci. 49: 1454–1462.

Jung, G., D.P. Coyne, P.W. Skroch, J. Nienhuis, E. Arnaud-Santana, J. Bokosi, H.M. Ariyarathne, J.R. Steadman, J.S. Beaver, and S.M. Kaeppler. 1996. Molecular

markers associated with plant architecture and resistance to common blight, web blight, and rust in common beans. J. Am. Soc. Hortic. Sci. 121:794–803.

Kopecky, D., M. Havrankova, J. Loureiro, S. Castro, A.J. Lukaszewski, J. Bartos, J. Kopecka, J. Dolezel. 2010. Physical distribution of homeologous recombination in individual chromosomes of *Festuca pratensis* in *Lolium multiflorum*. Cytogenetic and Genome Research 129:162–172.

Lander, E., and D. Botstein. 1989. Mapping Mendelian factors underlying quantitative traits using RFLP linkage maps. Genetics 121:185–199

Li, H. 2011. A quick method to calculate QTL confidence interval. J. Genet. 90:355–360.

Terrell, E.E. 1968. A taxonomic revision of the genus *Lolium*. Technical Bulletin No. 1392. United States Department of Agriculture, Washington, D.C.

Thorogood, D. 2003. Perennial ryegrass (*Lolium perenne* L.), p. 75-105. In: M.D. Casler and R.R. Duncan, editors, Turfgrass biology, genetics, and breeding. John Wiley and Sons, Hoboken, NJ. p.75–106.

Turgeon, A.J. 2008. Turfgrass management, Eighth Edition. Pearson Prentice Hall, Upper Saddle River, NJ.

Van Ooijen, J.W. 2006. JoinMap 4.0, software for the calculation of genetic linkage maps in experimental populations. Kyazma B.V., Wageningen, Netherlands

Van Ooijen, J.W. 2009. MapQTL 6, software for the mapping of quantitative trait loci in experimental populations of diploid species. Kyzma B.V. Wageningen, Netherlands

Yamada, T., E.S. Jones, N.O.I. Cogan, A.C. Vecchies, T. Nomura, H. Hisano, Y. Shimamoto, K.F. Smith, M.D. Hayward, and J.W. Forster. 2004. QTL analysis of morphological, developmental, and winter hardiness-associated traits in perennial ryegrass. Crop Sci. 44:925–935

Younger, V.B. 1969. Physiology of growth and development. In A.A. Hanson and F.V. Juska (ed.) Turfgrass Science. ASA, Madison, WI. p.187–216.

Table 6.1 Mean growth habit for the I06 × A89 perennial ryegrass population and each parent genotype on 27 Jun 2017 and 11 Jun 2018 at the Rutgers Plant Science Research and Extension Farm in Adelphia, NJ.

Environment	Population Mean	Parent I06 Mean	Parent A89 Mean
2017	5.2[a]	3.0	7.8
2018	4.7	3.4	7.9
Overall	5.0	3.2	7.8

[a] Mean growth habit as assessed for each plant using a visual rating scale that ranged from 1 to 9, where 1 represented an extremely prostrate growth habit and 9 represented an extremely upright growth habit.

Table 6.2 Mean seedhead angle (degree) for the I06 × A89 perennial ryegrass population and each parent genotype on 29 Jun 2017 and 12 Jun 2018 at the Rutgers Plant Science Research and Extension Farm in Adelphia, NJ.

Environment	Population Mean	Parent I06 Mean	Parent A89 Mean
2017	69.3[a]	63.5	83.0
2018	70.1	64.9	78.9
Overall	69.7	64.2	81.1

[a] Mean seedhead angle as assessed for each plant using a protractor to measure the average seedhead angle (degree) from the ground level.

Table 6.3 Mean plant height (mm) for the I06 × A89 perennial ryegrass population and each parent genotype on 27 Jun 2017 and 13 Jun 2018 at the Rutgers Plant Science Research and Extension Farm in Adelphia, NJ.

Environment	Population Mean	Parent I06 Mean	Parent A89 Mean
2017	427.8[a]	422.0	447.6
2018	493.4	577.3	470.5
Overall	460.4	496.3	458.3

[a] Mean plant height as assessed for each plant by measuring the maximum distance (mm) from the base of the plant to the top of the foliar leaf tissue.

Table 6.4 Mean vegetative plant width (mm) for the I06 × A89 perennial ryegrass population and each parent genotype on 29 Jun 2017 and 11 Jun 2018 at the Rutgers Plant Science Research and Extension Farm in Adelphia, NJ.

Environment	Population Mean	Parent I06 Mean	Parent A89 Mean
2017	310.3[a]	349.6	250.0
2018	477.9	525.9	344.8
Overall	393.6	433.9	294.2

[a] Mean vegetative plant width as assessed for each plant by measuring the maximum distance (mm) from one side of the plant foliar leaf tissue to the other.

Table 6.5 Mean total plant width (mm) for the I06 × A89 perennial ryegrass population and each parent genotype on 28 Jun 2017 and 13 Jun 2018 at the Rutgers Plant Science Research and Extension Farm in Adelphia, NJ.

Environment	Population Mean	Parent I06 Mean	Parent A89 Mean
2017	926.7[a]	1057.5	717.1
2018	973.4	1123.6	551.0
Overall	949.9	1089.1	639.6

[a] Mean total plant width as assessed for each plant by measuring the maximum distance (mm) from one side of the plant seedheads to the other.

Table 6.6 Analysis of variance for mean growth habit of the I06 × A89 perennial ryegrass mapping population on 27 Jun 2017 and 11 Jun 2018 at the Rutgers Plant Science Research and Extension Farm in Adelphia, NJ.

Sources of variation	*df*	*F* VALUE	*P* > *F*
Environment	1	2.90	0.1640
Rep(Environment), Error 1	4		
Genotype	119	6.58	< 0.0001
Genotype × Environment	119	2.98	< 0.0001
Genotype × Rep(Environment), Error 2	476		
Error 3	79		

Table 6.7 Analysis of variance for mean seedhead angle (degree) of the I06 × A89 perennial ryegrass mapping population on 29 Jun 2017 and 12 Jun 2018 at the Rutgers Plant Science Research and Extension Farm in Adelphia, NJ.

Sources of variation	*df*	*F* VALUE	*P* > *F*
Environment	1	0.12	0.7494
Rep(Environment), Error 1	4		
Genotype	119	1.92	< 0.0001
Genotype × Environment	119	1.41	0.0069
Genotype × Rep(Environment), Error 2	476		
Error 3	79		

Table 6.8 Analysis of variance for mean plant height (mm) of the I06 × A89 perennial ryegrass mapping population on 27 Jun 2017 and 13 Jun 2018 at the Rutgers Plant Science Research and Extension Farm in Adelphia, NJ.

Sources of variation	*df*	*F* VALUE	*P* > *F*
Environment	1	31.40	0.0050
Rep(Environment), Error 1	4		
Genotype	119	6.18	< 0.0001
Genotype × Environment	119	1.70	< 0.0001
Genotype × Rep(Environment), Error 2	476		
Error 3	79		

Table 6.9 Analysis of variance for mean vegetative plant width (mm) of the I06 × A89 perennial ryegrass mapping population on 29 Jun 2017 and 11 Jun 2018 at the Rutgers Plant Science Research and Extension Farm in Adelphia, NJ.

Sources of variation	*df*	*F* VALUE	*P* > *F*
Environment	1	185.47	0.0002
Rep(Environment), Error 1	4		
Genotype	119	4.08	< 0.0001
Genotype × Environment	119	1.48	0.0025
Genotype × Rep(Environment), Error 2	476		
Error 3	79		

Table 6.10 Analysis of variance for mean total plant width (mm) of the I06 × A89 perennial ryegrass mapping population on 28 Jun 2017 and 13 Jun 2018 at the Rutgers Plant Science Research and Extension Farm in Adelphia, NJ.

Sources of variation	*df*	*F* VALUE	*P* > *F*
Environment	1	57.22	0.0016
Rep(Environment), Error 1	4		
Genotype	119	7.17	< 0.0001
Genotype × Environment	119	2.22	< 0.0001
Genotype × Rep(Environment), Error 2	476		
Error 3	79		

Table 6.11 Summary of the twenty-one quantitative trait loci (QTL) identified for morphological traits across six linkage groups of the I06 parent map. A multiple QTL model mapping analysis was conducted with phenotypic data for growth habit, seedhead angle, plant height, vegetative plant width, and total plant width during 2017 and 2018 at the Rutgers Plant Science Research and Extension Farm in Adelphia, NJ.

Environment	QTL name[a]	LG	Position (cM)	Marker[b]	Allele means[c]		KW[d]	LOD[e]	R^2(%)[f]	99% CI (cM)[g]
					Allele a	Allele b				
Overall	qI06VPW-4	2	63.248	573029	390.1	401	*	4.62	11.3	63.148-63.365
2018	qI06TPW-1	2	71.413	LpSSR112	1015.4	955.8	*****	3.68	10.6	71.263-71.513
Overall	qI06TPW-1	2	71.413	LpSSR112	987	9273.1	*******	4.58	13.1	71.263-71.513
2017	qI06VPW-1	2	76.276	B5G4	323.3	296.4	*******	8.12	22.1	75.476-77.506
2017	qI06PH-1	2	82.565	700519	410.1	445.7	*****	4.02	12.6	82.565-83.443
2017	qI06GH-1	2	86.762	102066	5.0	5.4	*	3.46	7.2	85.962-87.593
2018	qI06GH-5	3	22.518	237101	4.4	4.8	**	5.29	13.6	21.357-24.418
2017	qI06GH-2	3	50.864	124981	5.4	5.0	*	4.57	9.7	50.864-50.864
2018	qI06TPW-2	3	59.098	G02_079	1026.4	952.2	******	4.28	12.0	58.709-59.698
2018	qI06GH-7	3	78.401	322447	4.8	4.4	**	3.88	9.5	78.135-78.701
2017	qI06GH-3	4	19.255	287810	5.0	5.4	*	8.70	20.1	19.140-19.255
Overall	qI06GH-8	4	58.529	G01_024	5.3	4.6	*******	5.68	15.4	58.429-59.495
2017	qI06GH-4	4	58.629	G01_024	5.7	4.8	*******	6.23	13.6	58.429-59.495
2017	qI06PH-2	4	58.695	G01_024	451.1	410.7	******	4.21	13.6	58.429-59.495
Overall	qI06PH-2	4	58.695	G01_024	479.1	444.3	*******	5.01	15.7	58.529-59.495

Table 6.11 (continued)

Environment	QTL name[a]	LG	Position (cM)	Marker[b]	Allele means[c]		KW[d]	LOD[e]	R^2(%)[f]	99% CI (cM)[g]
					Allele a	Allele b				
2018	qI06PH-4	5	76.438	G05_094	476.1	502.2	******	4.75	13.3	75.566-85.438
2017	qI06SHA-1	6	25.449	667180	67.4	70.3	*	6.85	19.6	24.168-25.549
2018	qI06VPW-2	6	45.595	835392	493.8	477.3	**	3.26	7.7	45.595-45.895
2018	qI06GH-6	7	61.414	G07_088	4.8	4.4	***	4.35	11.0	61.414-61.814
Overall	qI06VPW-5	7	76.876	B5G4	408.7	382.2	*******	6.07	15.5	75.776-77.406
2018	qI06VPW-3	7	77.006	B5G4	494.1	468	*******	5.14	12.6	75.776-77.406

[a] Name of QTL, indicates parent background (parent I06) and morphological trait (GH = growth habit, SHA = seedhead angle, PH = plant height, VPW = vegetative plant width, TPW = total plant width).
[b] Name of marker closest to a given QTL.
[c] The mean phenotypic value of progeny carrying the 'a' or 'b' allele of each marker.
[d] Kruskal-Wallis analysis. *, **, ***, *****, ******, *******, Significant at $P \leq 0.1$, 0.05, 0.01, 0.001, 0.0005, and 0.0001 levels, respectively.
[e] The LOD values of the QTL determined by multiple QTL model (MQM) mapping.
[f] Proportion of phenotypic variation explained by a given QTL.
[g] A 99% confidence interval for the QTL length (cM) as determined using the 2-LOD approach.

Table 6.12 Summary of the seven quantitative trait loci (QTL) identified for morphological traits across four linkage groups of the A89 parent map. A multiple QTL model mapping analysis was conducted with phenotypic data for growth habit, seedhead angle, plant height, vegetative plant width, and total plant width during 2017 and 2018 at the Rutgers Plant Science Research and Extension Farm in Adelphia, NJ.

Environment	QTL name[a]	LG	Position (cM)	Marker[b]	Allele means[c]		KW[d]	LOD[e]	R^2(%)[f]	99% CI (cM)[g]
					Allele a	Allele b				
Overall	qA89GH-3	2	0.000	G03_054	5.1	4.6	****	3.82	9.9	8.966-17.412
2017	qA89PH-1	2	16.612	G03_054	445.1	405.1	******	4.86	14.6	9.066-16.612
Overall	qA89PH-3	2	16.612	G03_054	471.6	442.3	******	3.23	9.5	7.966-17.422
2017	qA89GH-1	4	1.300	LpSSRH01E10	4.8	5.6	******	6.45	16.5	0.000-4.700
Overall	qA89SHA-1	6	32.546	892594	68.0	70.7	***	3.45	10.1	32.444-32.646
2017	qA89GH-2	6	53.145	899889	4.9	5.5	****	3.35	8.5	53.145-53.245
2018	qA89PH-2	7	57.611	LpSSR017	506.6	482.4	****	3.85	11.6	57.448-57.711

[a] Name of QTL, indicates parent background (parent A89) and morphological trait (GH = growth habit, SHA = seedhead angle, PH = plant height).
[b] Name of marker closest to a given QTL.
[c] The mean phenotypic value of progeny carrying the 'a' or 'b' allele of each marker.
[d] Kruskal-Wallis analysis. ***, ****, ****** Significant at $P \leq 0.1$, 0.005, 0.01, and 0.0005 levels, respectively.
[e] The LOD values of the QTL determined by multiple QTL model (MQM) mapping.
[f] Proportion of phenotypic variation explained by a given QTL.
[g] A 99% confidence interval for the QTL length (cM) as determined using the 2-LOD approach.

Figure 6.1 Measurement of seedhead angle for individuals of the I06 × A89 perennial ryegrass mapping population.

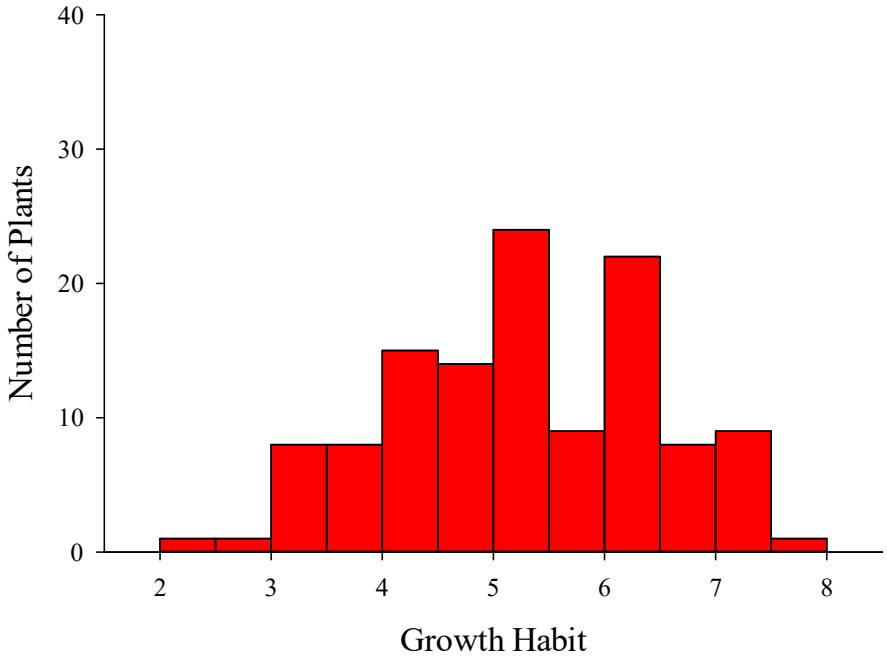

Figure 6.2 Frequency distribution for mean growth habit of the I06 × A89 perennial ryegrass mapping population on 27 Jun 2017 at the Rutgers Plant Science Research and Extension Farm in Adelphia, NJ. Growth habit was assessed for each plant using a visual rating scale that ranged from 1 to 9, where 1 represented an extremely prostrate growth habit and 9 represented an extremely upright growth habit.

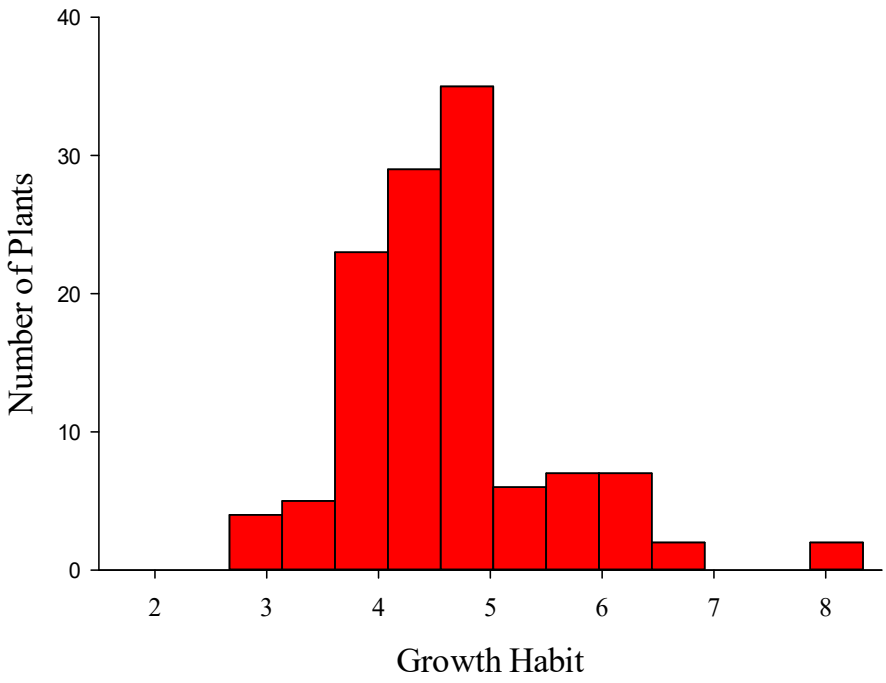

Figure 6.3 Frequency distribution for mean growth habit of the I06 × A89 perennial ryegrass mapping population on 11 Jun 2018 at the Rutgers Plant Science Research and Extension Farm in Adelphia, NJ. Growth habit was assessed for each plant using a visual rating scale that ranged from 1 to 9, where 1 represented an extremely prostrate growth habit and 9 represented an extremely upright growth habit.

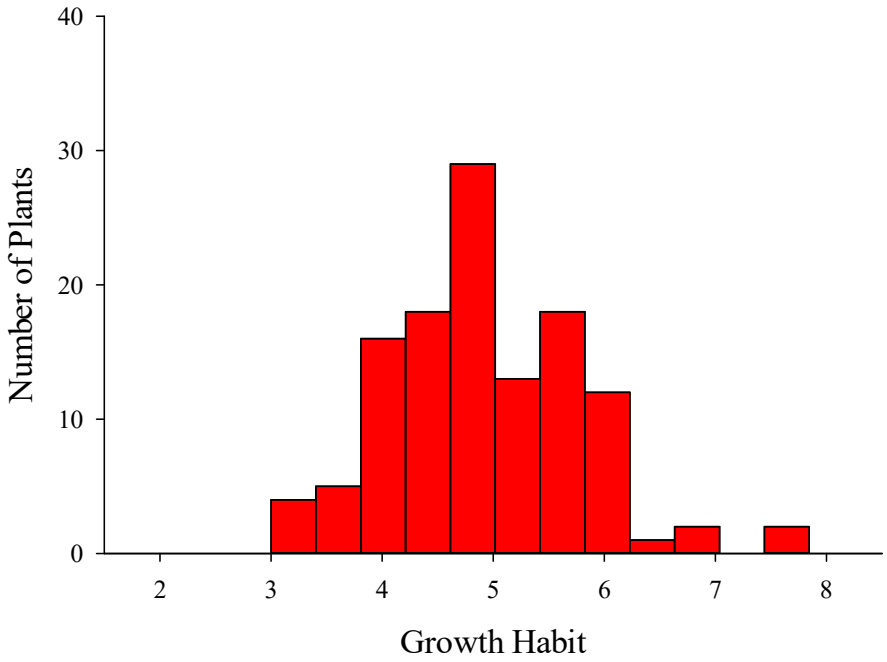

Figure 6.4 Frequency distribution for mean growth habit of the I06 × A89 perennial ryegrass mapping population on 27 Jun 2017 and 11 Jun 2018 at the Rutgers Plant Science Research and Extension Farm in Adelphia, NJ. Growth habit was assessed for each plant using a visual rating scale that ranged from 1 to 9, where 1 represented an extremely prostrate growth habit and 9 represented an extremely upright growth habit.

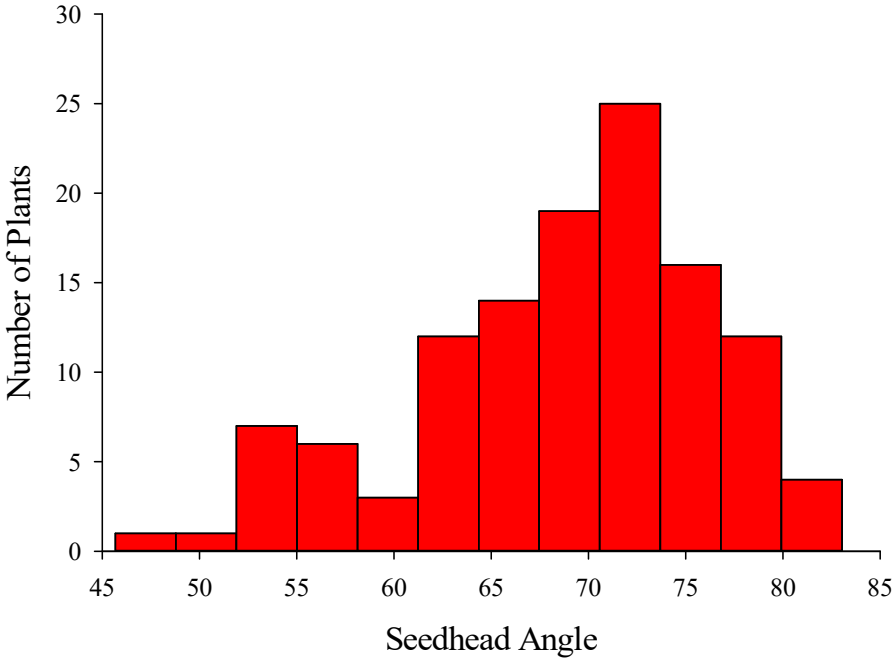

Figure 6.5 Frequency distribution for mean seedhead angle (degree) of the I06 × A89 perennial ryegrass mapping population on 29 Jun 2017 at the Rutgers Plant Science Research and Extension Farm in Adelphia, NJ. Seedhead angle was assessed for each plant using a protractor to measure the average seedhead angle from the ground level.

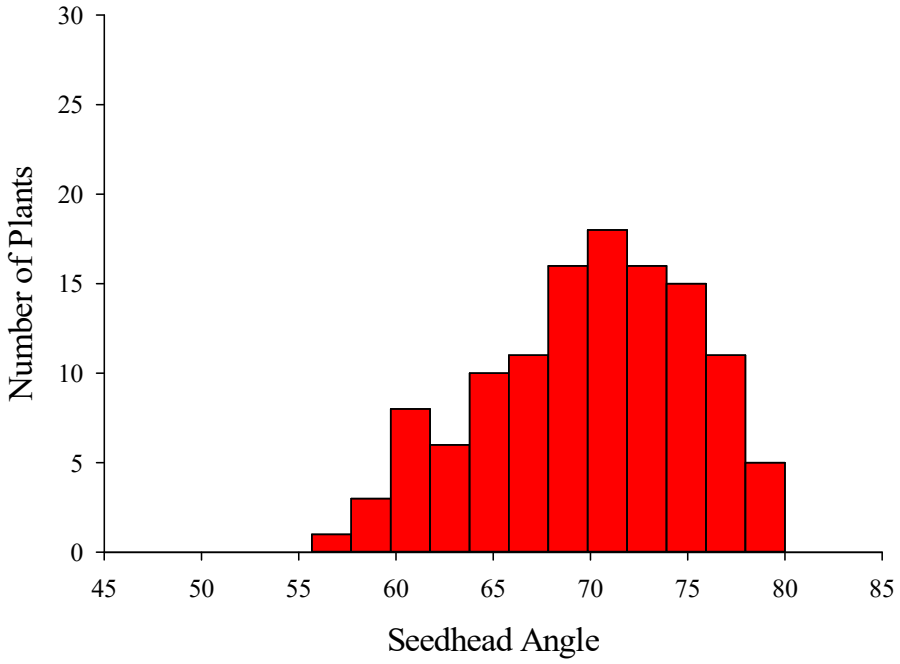

Figure 6.6 Frequency distribution for mean seedhead angle (degree) of the I06 × A89 perennial ryegrass mapping population on 12 Jun 2018 at the Rutgers Plant Science Research and Extension Farm in Adelphia, NJ. Seedhead angle was assessed for each plant using a protractor to measure the average seedhead angle from the ground level.

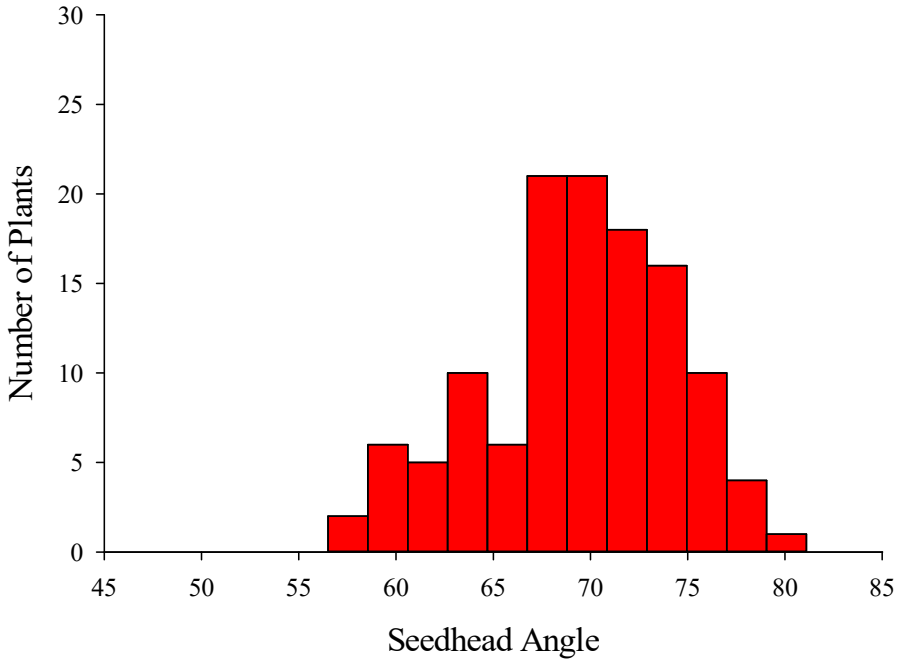

Figure 6.7 Frequency distribution for mean seedhead angle (degree) of the I06 × A89 perennial ryegrass mapping population on 29 Jun 2017 and 12 Jun 2018 at the Rutgers Plant Science Research and Extension Farm in Adelphia, NJ. Seedhead angle was assessed for each plant using a protractor to measure the average seedhead angle from the ground level.

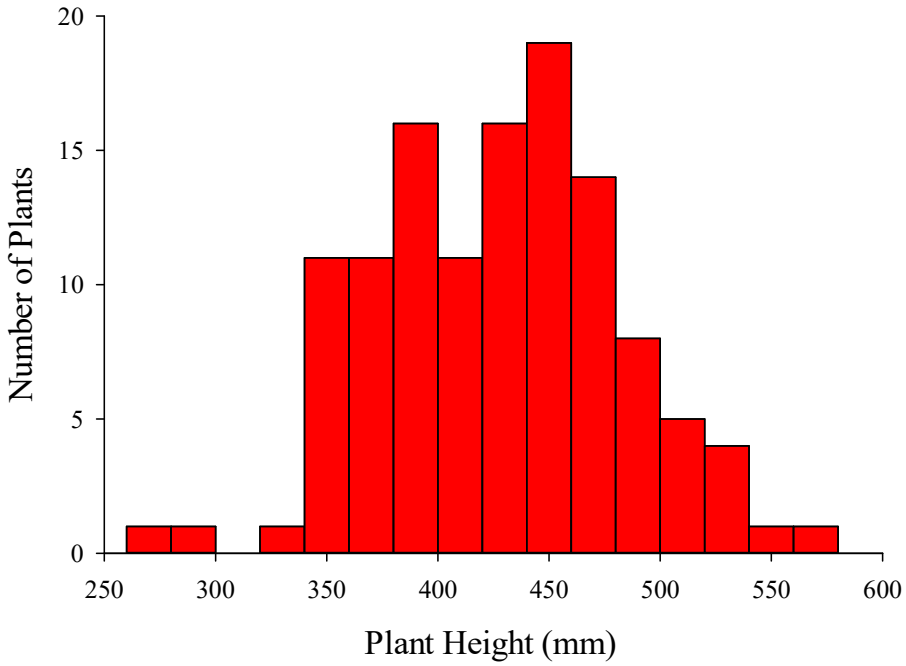

Figure 6.8 Frequency distribution for mean plant height (mm) of the I06 × A89 perennial ryegrass mapping population on 27 Jun 2017 at the Rutgers Plant Science Research and Extension Farm in Adelphia, NJ. Plant height was assessed for each plant by measuring the maximum distance (mm) from the base of the plant to the top of the foliar leaf tissue.

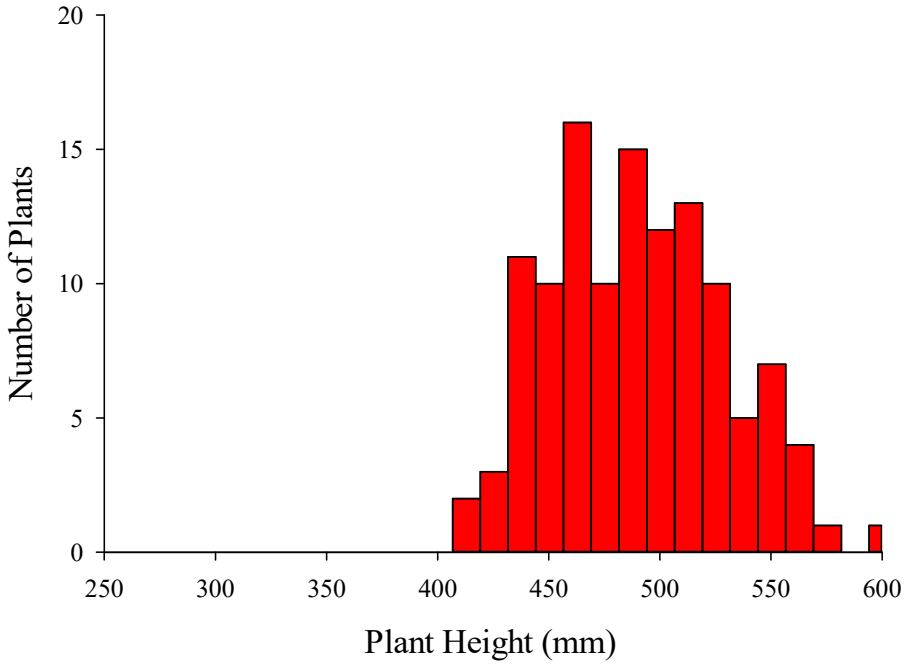

Figure 6.9 Frequency distribution for mean plant height (mm) of the I06 × A89 perennial ryegrass mapping population on 13 Jun 2018 at the Rutgers Plant Science Research and Extension Farm in Adelphia, NJ. Plant height was assessed for each plant by measuring the maximum distance (mm) from the base of the plant to the top of the foliar leaf tissue.

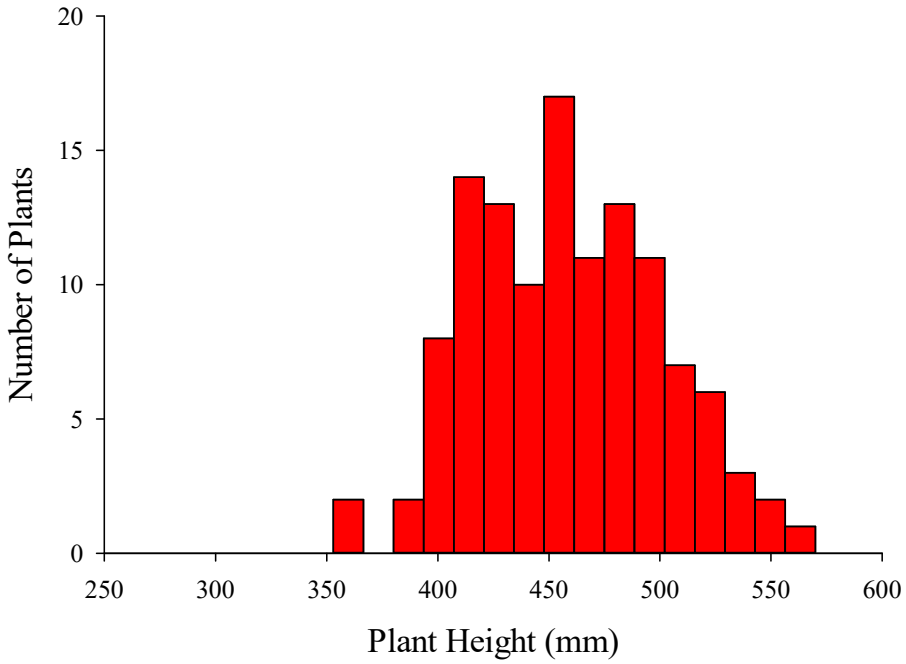

Figure 6.10 Frequency distribution for mean plant height (mm) of the I06 × A89 perennial ryegrass mapping population on 27 Jun 2017 and 13 Jun 2018 at the Rutgers Plant Science Research and Extension Farm in Adelphia, NJ. Plant height was assessed for each plant by measuring the maximum distance (mm) from the base of the plant to the top of the foliar leaf tissue.

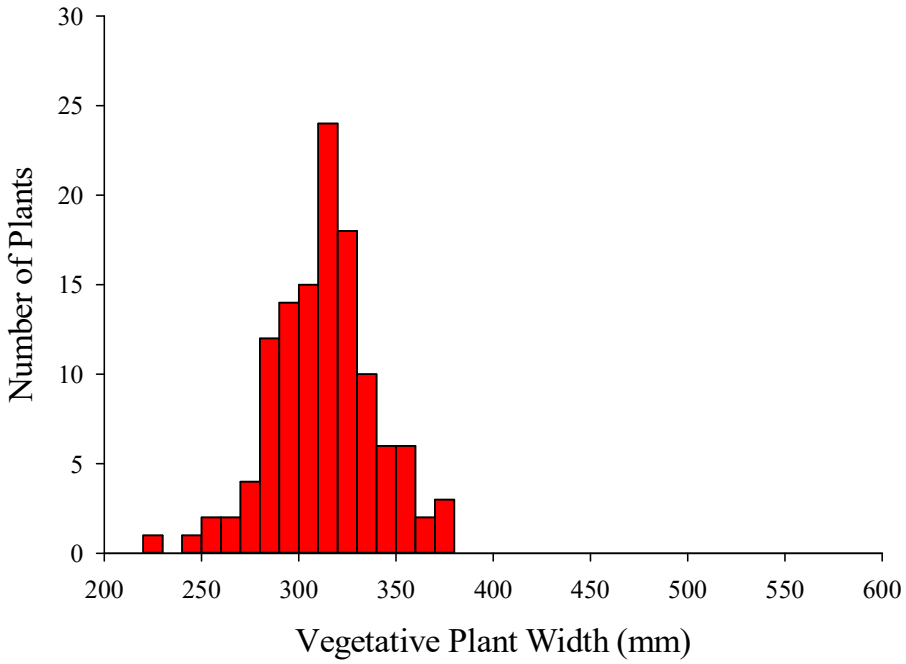

Figure 6.11 Frequency distribution for mean vegetative plant width (mm) of the I06 × A89 perennial ryegrass mapping population on 29 Jun 2017 at the Rutgers Plant Science Research and Extension Farm in Adelphia, NJ. Vegetative plant width was assessed for each plant by measuring the maximum distance (mm) from one side of the plant foliar leaf tissue to the other.

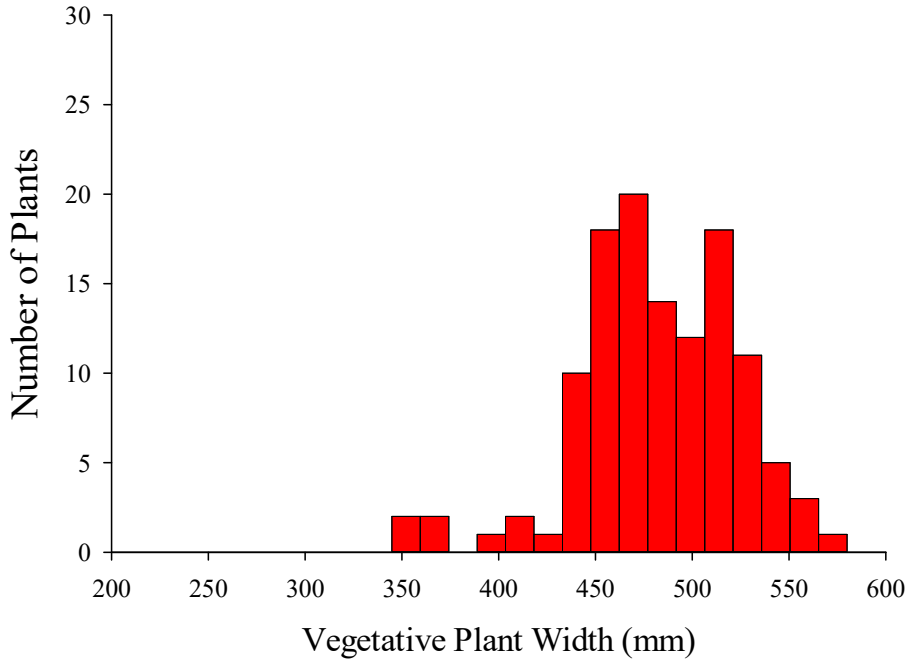

Figure 6.12 Frequency distribution for mean vegetative plant width (mm) of the I06 × A89 perennial ryegrass mapping population on 11 Jun 2018 at the Rutgers Plant Science Research and Extension Farm in Adelphia, NJ. Vegetative plant width was assessed for each plant by measuring the maximum distance (mm) from one side of the plant foliar leaf tissue to the other.

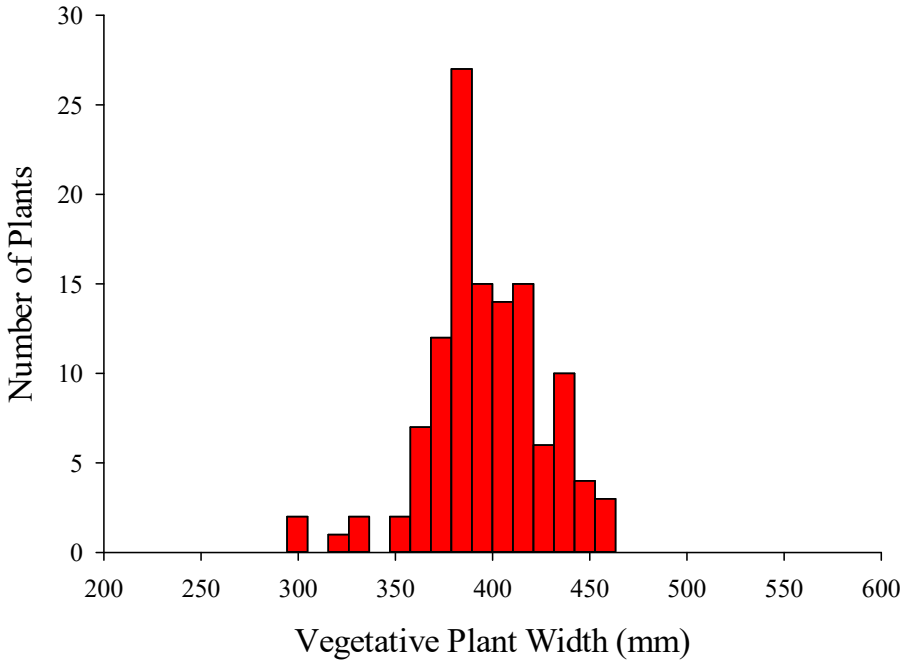

Figure 6.13 Frequency distribution for mean vegetative plant width (mm) of the I06 × A89 perennial ryegrass mapping population on 29 Jun 2017 and 11 Jun 2018 at the Rutgers Plant Science Research and Extension Farm in Adelphia, NJ. Vegetative plant width was assessed for each plant by measuring the maximum distance (mm) from one side of the plant foliar leaf tissue to the other.

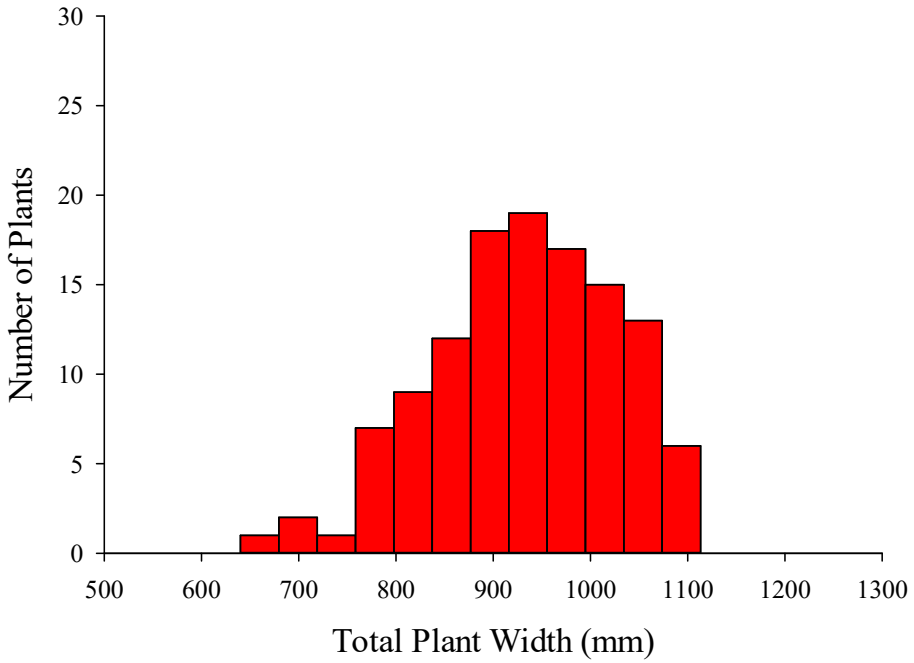

Figure 6.14 Frequency distribution for mean total plant width (mm) of the I06 × A89 perennial ryegrass mapping population on 28 Jun 2017 at the Rutgers Plant Science Research and Extension Farm in Adelphia, NJ. Total plant width was assessed for each plant by measuring the maximum distance (mm) from one side of the plant seedheads to the other.

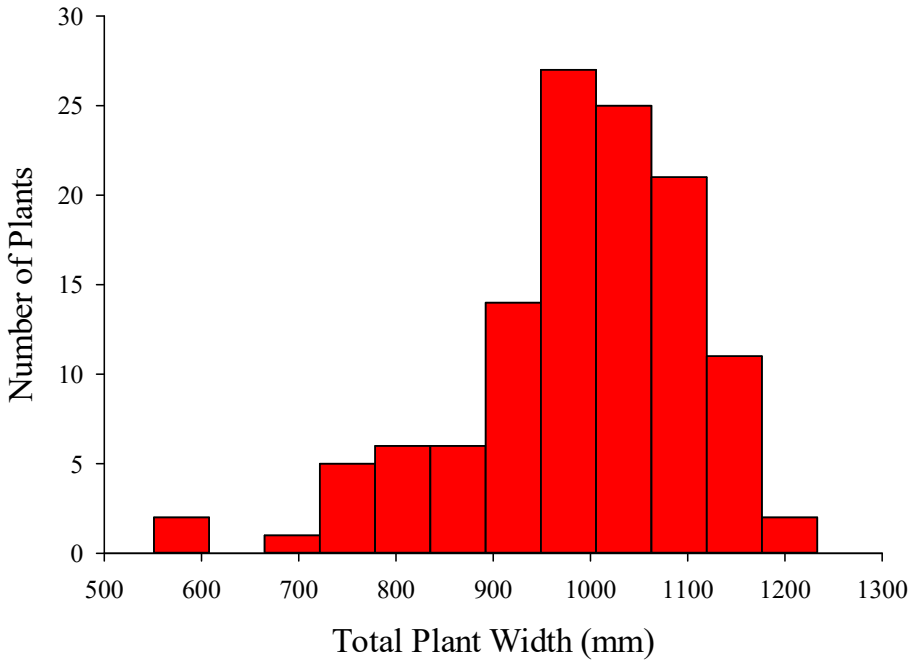

Figure 6.15 Frequency distribution for mean total plant width (mm) of the I06 × A89 perennial ryegrass mapping population on 13 Jun 2018 at the Rutgers Plant Science Research and Extension Farm in Adelphia, NJ. Total plant width was assessed for each plant by measuring the maximum distance (mm) from one side of the plant seedheads to the other.

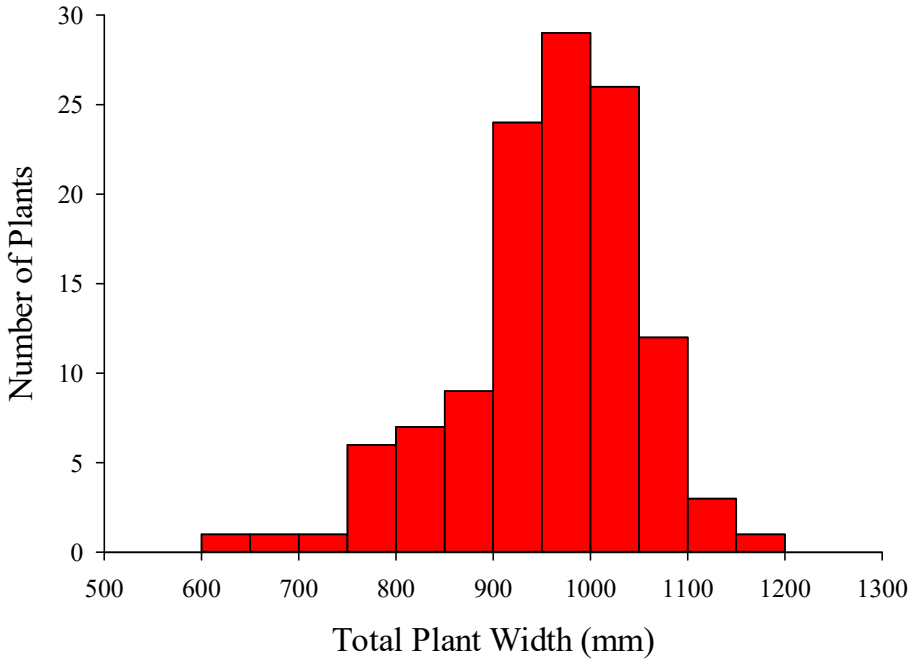

Figure 6.16 Frequency distribution for mean total plant width (mm) of the I06 × A89 perennial ryegrass mapping population on 28 Jun 2017 and 13 Jun 2018 at the Rutgers Plant Science Research and Extension Farm in Adelphia, NJ. Total plant width was assessed for each plant by measuring the maximum distance (mm) from one side of the plant seedheads to the other.

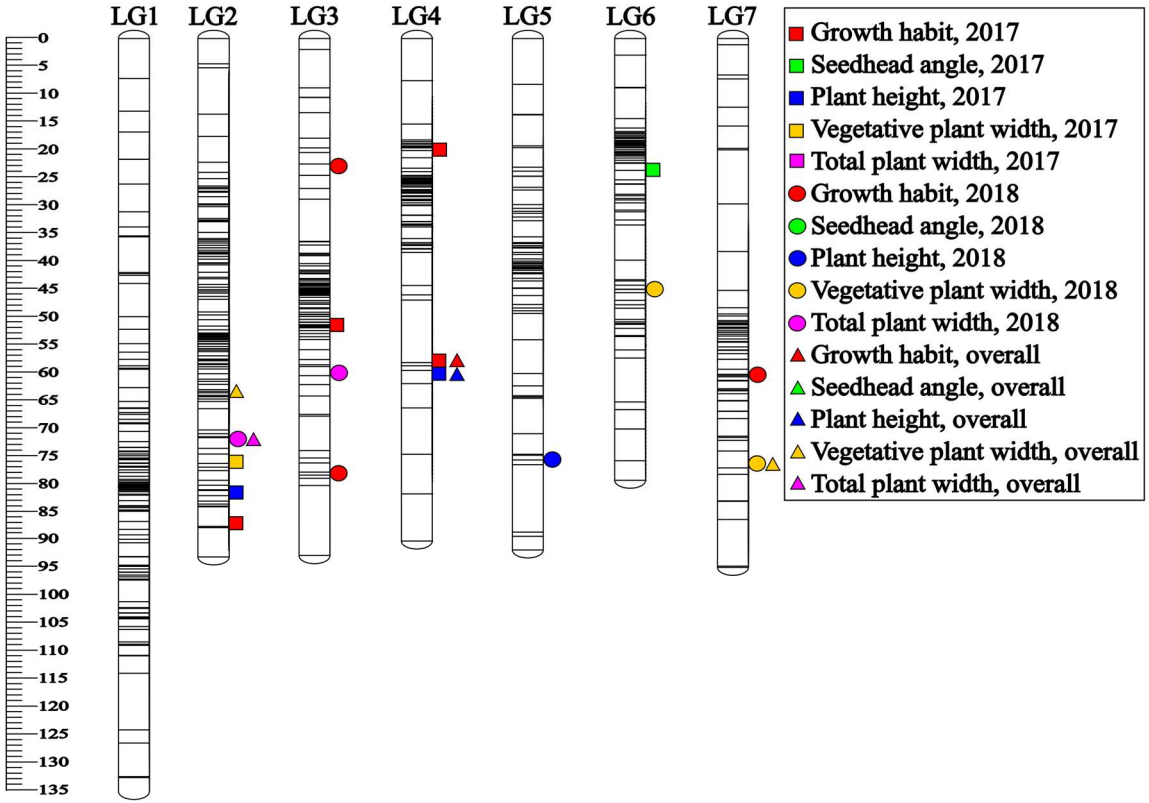

Figure 6.17 Summary of the quantitative trait loci (QTL) identified for morphological traits on the I06 parent map. A multiple QTL model mapping analysis was conducted with phenotypic data for growth habit, seedhead angle, plant height, vegetative plant width, and total plant width during 2017 and 2018 at the Rutgers Plant Science Research and Extension Farm in Adelphia, NJ. The genetic map distance (cM) is provided to the left, and linkage group (LG) numbers are indicated at the top of each individual linkage group.

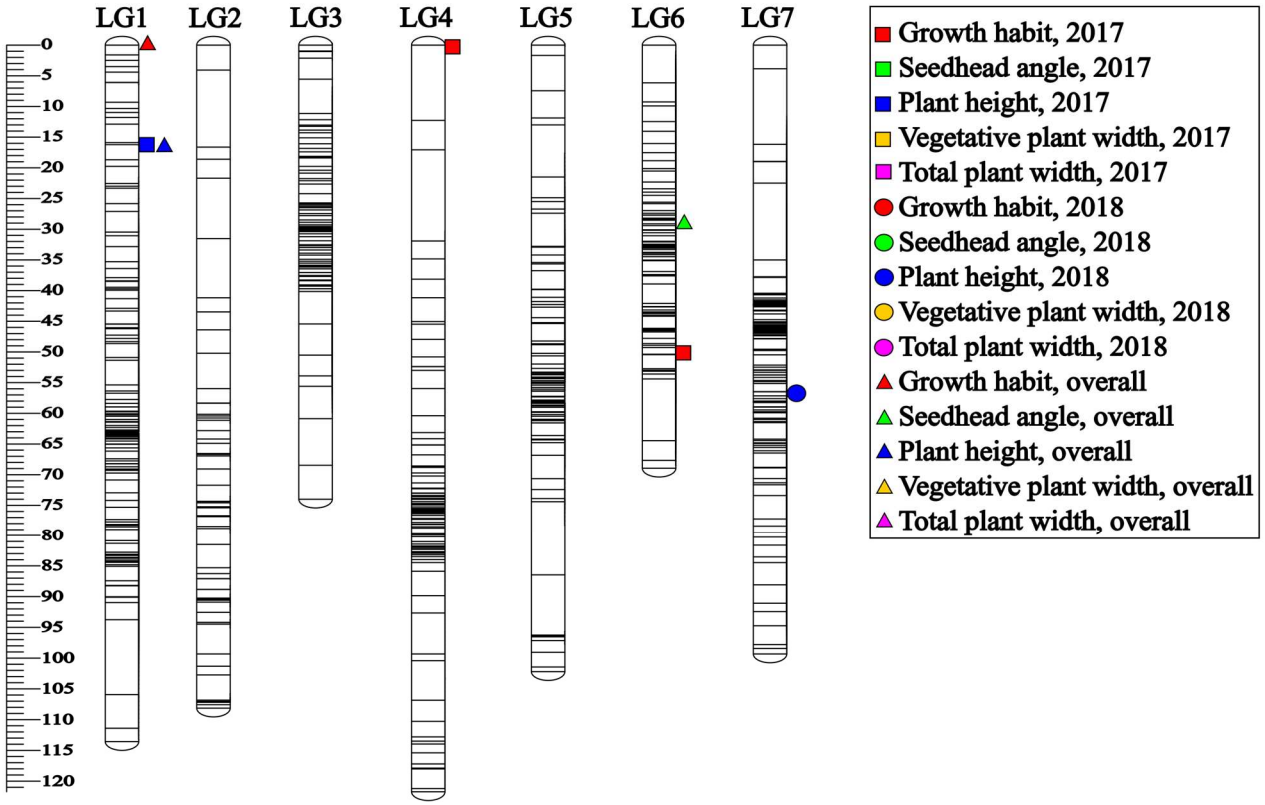

Figure 6.18 Summary of the quantitative trait loci (QTL) identified for morphological traits on the A89 parent map. A multiple QTL model mapping analysis was conducted with phenotypic data for growth habit, seedhead angle, plant height, vegetative plant width, and total plant width during 2017 and 2018 at the Rutgers Plant Science Research and Extension Farm in Adelphia, NJ. The genetic map distance (cM) is provided to the left, and linkage group (LG) numbers are indicated at the top of each individual linkage group.

CHAPTER VII

THESIS CONCLUSION

Turfgrass breeding programs will continue to breed turf-type perennial ryegrass for improved tolerance to abiotic and biotic factors such as salinity stress and dollar spot disease. Molecular breeding tools will be required to efficiently improve these types of quantitatively inherited traits. Strategies such as marker-assisted selection, which is based on quantitative trait locus (QTL) mapping, will be implemented in modern plant breeding programs to compliment traditional, field-based breeding approaches. These tools will enable breeders to dissect the complex, quantitative traits and, ultimately, identify markers and/or genes associated with these traits.

This research provided a basis for establishing a marker-assisted selection breeding program for salinity tolerance, dollar spot resistance, and morphological traits in perennial ryegrass. The I06 × A89 perennial ryegrass mapping population, which includes 118 pseudo-F_2 progeny, was developed from a cross between two diverse parent genotypes. The I06 parent (maternal) is salinity tolerant and dollar spot susceptible and has a prostrate growth habit and light green leaf color. The A89 parent (paternal) is susceptible to salinity stress and dollar spot resistant and has an upright growth habit and dark green leaf color. The usefulness of this mapping population was demonstrated in this dissertation through studies for salinity tolerance, dollar spot resistance, and growth habit morphology. It is anticipated that leaf color morphology will also be studied using

this mapping population. In addition, the diverse I06 and A89 parents should be studied in detail to identify other meaningful traits that segregate between the two parent genotypes and could be studied using this mapping population.

High-density genetic linkage maps were constructed for both the I06 and A89 parents. In total, 900 markers were included in the I06 parent dataset and mapped to a total distance of 677.5 cM, yielding an average marker density of 0.75 cM. Similarly, 804 markers were included in the A89 parent dataset and mapped to a total distance of 687.9 cM, yielding an average marker density of 0.86 cM. These high-density genetic linkage maps were useful for QTL studies in this dissertation and should be useful for future QTL studies with this population. We are hopeful that a reference genome will be completed for perennial ryegrass in the near future. By aligning our DNA sequencing reads to the reference genome, we could potentially recover and map additional markers to our parent genetic linkage maps; this would facilitate finer QTL mapping results. Moreover, we anticipate the development of improved computational software for linkage map construction and hope to construct integrated parent linkage maps, which will also be useful for future QTL mapping purposes.

The QTL analyses for salinity tolerance resulted in the identification of fifteen major-effect QTL and forty-three minor-effect QTL. Eleven salinity tolerance QTL were identified using both visual ratings and pixel analysis evaluation methods for salinity tolerance, seven salinity tolerance QTL were identified across multiple environmental locations, and one salinity tolerance QTL was identified across both parent maps. The QTL identified in this study should be validated through studies in additional environments and using additional perennial ryegrass mapping populations. The QTL

that are repeatedly detected through these studies will be most useful in identifying markers or genes for salinity tolerance in perennial ryegrass.

The QTL analyses for dollar spot resistance resulted in the identification of twelve major-effect QTL and nine minor-effect QTL. Coincident dollar spot resistance QTL were mapped to four distinct genomic regions and were consistently identified using multiple evaluation methods for dollar spot severity and/or multiple environments. Studies in additional environments and using additional perennial ryegrass mapping populations should be conducted to confirm the QTL for dollar spot resistance identified in this study.

The QTL analyses for growth habit morphology-related traits resulted in the identification of twenty-one major effect QTL and seven minor-effect QTL. Four QTL were identified across both years of the study, and two growth habit morphology QTL were significantly associated with multiple growth habit morphology-related traits. QTL validation studies should be conducted for the QTL identified in this study. These validation studies should be conducted using additional perennial ryegrass mapping populations and in different environments. The QTL that are repeatedly detected through these studies will be most useful in identifying markers or genes for growth habit morphology-related traits in perennial ryegrass.

In summary, the work presented herein includes the first reported efforts for QTL mapping of salinity tolerance and dollar spot resistance in perennial ryegrass. Further, this is the first report of QTL mapping for growth habit morphology-related traits in turf-type perennial ryegrass. These findings will be useful for future studies involving development of marker-assisted selection techniques for breeding applications, gene and

mechanism discovery, and comparative genomics investigations using closely related plant species. These efforts will be used to develop improved perennial ryegrass cultivars, which will ultimately contribute to the sustainability of the turfgrass industry. Moreover, as indicated above, the I06 × A89 perennial ryegrass population will be useful to further study these and additional traits in perennial ryegrass, and the high-density genetic linkage map constructed in this dissertation will be a valuable resource for future QTL studies in turf-type perennial ryegrass breeding.

APPENDIX A

SUPPLEMENTARY MATERIAL FOR GENETIC LINKAGE MAPPING STUDIES

Table A.1 Library set, sample name, barcode identifier, total read number, and retained read number for parent and progeny genotypes of the I06 × A89 perennial ryegrass mapping population.

Library set	Sample name	Barcode	Total reads	Retained reads
1	I06	ATTAT	15118570	12840063
1	I06	ACTGCGAT	12965922	12365328
1	A89	CACCA	16737490	14706271
1	A89	TTCGTT	11193548	10576673
1	P1G001	TGCTT	15917542	14165746
1	P1G002	GAAGTG	14216212	13462635
1	P1G003	TCTTGG	14854764	14114595
1	P1G004	ACAACT	14575562	13818618
1	P1G005	CTAAGCA	15620608	15131676
1	P1G006	TAGCCAA	16369882	15802586
1	P1G007	GTTCACA	15471852	14878753
1	P1G008	GCCTACCT	14004286	13593293
1	P1G009	AAGACGCT	13492798	13075491
1	P1G010	CCATCCAA	13441420	12959204
1	P1G011	TGACGCCA	13568478	13122358
1	P1G012	CAGATA	14138938	13271485
1	P1G013	TAGCGGAT	14790076	14347089
1	P1G014	TATTCGCAT	15309332	14872104
1	P1G015	CCGAACA	17446066	16973767
1	P1G016	GGAAGACAT	16573330	16124008

Table A.1 (continued)

Library set	Sample name	Barcode	Total reads	Retained reads
1	P1G017	GGCTTA	15531492	14810743
1	P1G018	AACGCACATT	14513510	14051793
1	P1G019	GAGCGACAT	14719550	14287573
1	P1G020	CCTTGCCATT	14972688	14561763
1	P1G021	GGTATA	14602774	13986469
1	P1G022	GCGCTCA	14167246	13777012
1	P1G023	ATATAA	12818972	12033510
1	P1G024	TGGCAACAGA	13738866	13343174
1	P1G025	CTCGTCG	13721716	13242358
1	P1G026	AATTAG	14337158	13580610
1	P1G027	GGAACGA	12758772	12308004
1	P1G028	ACTGCT	14338790	13426971
1	P1G029	CGTGGACAGT	12893974	12562747
1	P1G030	TGGCACAGA	13769748	13349650
1	P1G031	GCAAGCCAT	14751264	14370059
1	P1G032	CGCACCAATT	11476920	11216103
1	P1G033	CTCGCGG	13152070	12753991
1	P1G034	AACTGG	14377170	13658658
1	P1G035	ATGAGCAA	14064050	13634476
1	P1G036	CTTGA	16208582	14522476
1	P1G037	GCGTCCT	13269030	12885103
1	P1G038	ACCAGGA	14074650	13551625

Table A.1 (continued)

Library set	Sample name	Barcode	Total reads	Retained reads
1	P1G039	CCACTCA	14368346	13945941
1	P1G040	TCACGGAAG	11590902	11211476
1	P1G041	TATCA	14775552	13442059
1	P1G042	ATATCGCCA	14098310	13713317
1	P1G403	CTCTA	14585518	13441878
1	P1G044	GGTGCACATT	13088092	12695823
2	I06	ATTAT	11442386	9867645
2	I06	ACTGCGAT	11555744	11097975
2	A89	CACCA	10402626	9087835
2	A89	TTCGTT	33084488	31702845
2	P1G045	TGCTT	13567708	12169268
2	P1G046	GAAGTG	12109110	11396782
2	P1G047	TCTTGG	13485510	12865753
2	P1G048	ACAACT	12330554	11824251
2	P1G049	CTAAGCA	13101820	12636855
2	P1G050	TAGCCAA	12582570	12009069
2	P1G051	GTTCACA	13855928	13304625
2	P1G052	GCCTACCT	12816682	12436675
2	P1G053	AAGACGCT	13558628	13079413
2	P1G054	CCATCCAA	12742298	12309977
2	P1G055	TGACGCCA	13595340	13121187
2	P1G056	CAGATA	13395932	12671233

Table A.1 (continued)

Library set	Sample name	Barcode	Total reads	Retained reads
2	P1G057	TAGCGGAT	12256560	11823752
2	P1G058	TATTCGCAT	13165434	12763734
2	P1G059	CCGAACA	13391456	12955024
2	P1G061	GGAAGACAT	10599914	10240241
2	P1G062	GGCTTA	12630300	12091239
2	P1G063	AACGCACATT	12602018	12223750
2	P1G064	GAGCGACAT	11848358	11470037
2	P1G065	CCTTGCCATT	11272444	10977565
2	P1G066	GGTATA	12327706	11803020
2	P1G067	GCGCTCA	12102184	11714500
2	P1G068	ATATAA	11956228	11266328
2	P1G069	TGGCAACAGA	11797284	11424941
2	P1G070	CTCGTCG	11525938	11112346
2	P1G071	AATTAG	13446328	12804524
2	P1G073	ACTGCT	12836190	12099294
2	P1G074	CGTGGACAGT	10545290	10306169
2	P1G075	TGGCACAGA	12435070	12035384
2	P1G076	GCAAGCCAT	11548938	11151779
2	P1G078	CGCACCAATT	12310058	12035662
2	P1G079	CTCGCGG	11904438	11485664
2	P1G080	AACTGG	12239010	11661311
2	P1G081	ATGAGCAA	12248404	11810601

Table A.1 (continued)

Library set	Sample name	Barcode	Total reads	Retained reads
2	P1G082	CTTGA	13165870	11855213
2	P1G083	GCGTCCT	11738788	11341552
2	P1G084	ACCAGGA	11783432	11297335
2	P1G086	TCACGGAAG	10552132	10242376
2	P1G087	TATCA	12248270	11241687
2	P1G088	ATATCGCCA	11455970	11157479
2	P1G089	CTCTA	11828380	10987477
2	P1G090	GGTGCACATT	11863052	11551246
3	I06	ATTAT	12616320	10941711
3	I06	ACTGCGAT	46782476	44548819
3	A89	CACCA	33859196	31766673
3	P1G091	TGCTT	9397062	8330341
3	P1G092	GAAGTG	13726832	12951331
3	P1G093	TCTTGG	14798734	14059862
3	P1G094	ACAACT	14437130	13724581
3	P1G095	CTAAGCA	14121320	13624798
3	P1G096	TAGCCAA	13952752	13368173
3	P1G097	GTTCACA	14142078	13531216
3	P1G098	GCCTACCT	12569626	12058353
3	P1G099	AAGACGCT	14371828	13746064
3	P1G100	CCATCCAA	13965144	13358049
3	P1G101	TGACGCCA	13501148	12993159

Table A.1 (continued)

Library set	Sample name	Barcode	Total reads	Retained reads
3	P1G102	CAGATA	14188960	13425736
3	P1G103	TAGCGGAT	13834572	13248293
3	P1G104	TATTCGCAT	14090128	13566722
3	P1G105	CCGAACA	13857642	13361035
3	P1G106	GGAAGACAT	12814750	12215525
3	P1G107	GGCTTA	13217358	12466614
3	P1G108	AACGCACATT	13864272	13274930
3	P1G109	GAGCGACAT	13923300	13372585
3	P1G110	CCTTGCCATT	14040310	13489716
3	P1G111	GGTATA	13468550	12816657
3	P1G112	GCGCTCA	12097868	11667075
3	P1G113	ATATAA	11934598	11240699
3	P1G114	TGGCAACAGA	12395948	11965024
3	P1G115	CTCGTCG	11585194	11146570
3	P1G116	AATTAG	11182580	10519772
3	P1G117	GGAACGA	12433124	11960829
3	P1G118	ACTGCT	14857168	13894984
3	P1G119	CGTGGACAGT	10689080	10388968
3	P1G122	CGCACCAATT	11632470	11288519
3	P1G123	CTCGCGG	13135002	12664438
3	P1G124	AACTGG	12256542	11623575
3	P1G125	ATGAGCAA	11506026	11077161

Table A.1 (continued)

Library set	Sample name	Barcode	Total reads	Retained reads
3	P1G126	CTTGA	12066686	10854764
3	P1G127	GCGTCCT	11466780	11049970
3	P1G128	ACCAGGA	11912576	11393606
3	P1G130	TCACGGAAG	11024132	10629075
3	P1G131	TATCA	12152858	11123309
3	P1G060	CTCTA	10253160	9465687
3	P1G077	GGTGCACATT	9659846	9367557
4	I06	ATTAT	23848330	23265836
4	A89	CACCA	24320978	24104307

Table A.2 Characteristics for the set of framework SSR markers used for genetic linkage mapping of the I06 × A89 perennial ryegrass mapping population.

Marker name	SSR motif	Primer sequence (5' – 3')	Polymorphic	LG
14GA1	(CT)25	F–GTTTGCATTCCTTGTGCT R–TCCTTGGGTGTGTCTACG	No	3
25CA1	(GT)16	F–ATCGAGTGCACATTTCGT R–TGTGATCGATGGTGCATA	No	3
B1A10	(CA)12	F–GCGACAGGAGTGAACACTGA R–TAAGGCGTAAGGCAGCAGTG	No	3
B1A2	(GA)14	F–GTGCAGCAGTTTGAATTGGA R–AGCATCGGGAGCTATGAATG	No	3
B1A8[a]	(TG)7	F–GACTTTCAGGCATCGGTCAT R–CCCAGCTCCATTCTTAATGC	Yes	6
B1B3	(TG)7	F–AGGTGTCCTGTTGCTTTGGA R–TTTACCCCCAGGGATCAAAT	No	3
B1B6	(CTT)4(GT)2	F–GGAGCTGCATCTTTCTTGCT R–GCAAACCCAGACACCCATTA	Yes	1

Table A.2 (continued)

Marker name	SSR motif	Primer sequence (5' – 3')	Polymorphic	LG
B1C8	(CA)8(CT)6	F–TTCTGGCCATGTTGATTTGC R–GTCTACGGGTTGGAGCAGTG	No	7
B1C9	(CT)8	F–GAGCCGATGCACAGGTTACT R–AAAGGAAGCCGGCTAATCAC	Yes	3
B2F1	(CA)5	F–CCAACCATATGCAACGATGA R–TCCATTTGTTCTTGGGGAGA	No	5
B2G6A	(TGA)8	F–CCAACTAGACAAAGGGGATTG R–GGAGAGCACCATTCATCCAT	No	1
B3A1	(AC)5(AG)5	F–CTTGTCGTCCTTGTTGGGAG R–ATATTCTGGATCGTGGCGTT	Yes	2
B3A3	(GT)8	F–GGGTGAAGTGCTCTTTGTGA R–ATGGTGAAGGCCTGAAACTG	No	7
B3B7	(TG)9	F–AGGCGACCAATACGTCTGTC R–ATCTCTGATGGCTTTGTGGC	Yes	1

Table A.2 (continued)

Marker name	SSR motif	Primer sequence (5' – 3')	Polymorphic	LG
B3B8	(TG)10	F–TGTCATGTCCGCTGTCTACG R–GAGAGTGGGCGATCATCTTC	Yes	3
B3C10	(CTC)4	F–CTACAACTCCGTGCTGCTGA R–TGCATGGTTTCTCAAATGCT	Yes	7
B3C11	(CATG)3(TG)9	F–ATTCACCTCGCTCGAAAATG R–AACACCAAGCTAGCCACCAC	Yes	7
B3C5	(GT)8	F–TGTCATGTTCAGAAAGTGCG R–TGTCCACATAAATGCACCTCA	Yes	7
B3D12	(TC)7	F–GGGCATCACTGAGAAGAGGA R–TACAAAGGAAGTCGGGCATC	Yes	2
B3D2	(AT)4	F–ATACGAGCGAATTGCCTCTC R–TCTCCCATCGCTTATGTTCC	No	1
B3D4	(CG)4	F–AAACCCATACCGACATACCG R–GGCGTCTGTGAGAGTGAGTG	No	6

Table A.2 (continued)

Marker name	SSR motif	Primer sequence (5' – 3')	Polymorphic	LG
B3E6	(AG)4(GT)7	F–CTGTAACAACAGCCGCTGAG R–GTCTCGAGCACAGGAGTTCA	Yes	3
B4C4	(GT)4(GT)3(TC)3(CT)6	F–TGCATGCACCCTTGTAGC R–GGAGACTTTGTGTGTGCAGC	No	7
B4D7	(CT)10	F–CGGGAGCTCTCTCTCCTTCT R–TCCAGAACCTTCTCGAGGTC	Yes	1
B4D9	(TC)10(TC)4	F–GACGTCATACCTGCGTGCTA R–GCGAATCAAAGAAGCATGTG	Yes	4
B5E1	(CA)3(CA)5	F–AAACATCAACGGAAGGATGC R–TGATATGCATTGTGATGGAGG	No	5
B5G4	(CA)8	F–TGGAGTTGTGGACCTTTTCC R–AGATGCTGGTTGGTTTCCAG	Yes	7
DLF008	(ACT)7	F–CCGTTGCTTGATACTTGGAC R–GAACGAGCATTCTTCCTTTCT	Yes	7

Table A.2 (continued)

Marker name	SSR motif	Primer sequence (5' – 3')	Polymorphic	LG
DLF013	(GTT)6(GCT)3	F–GTAGTCCAGCGGAGGTCAAT R–ATAGCAAACGTTGGCACACAT	No	3
DLF020	(CGA)5	F–ATGACGACGAGGAGGAAT R–ATAGCGACGAGAGAAAGGTAA	Yes	7
DLF025	(CT)10	F–CGGCGAGAAGCTAACAGA R–TCACGGAGAGGGCAAGT	No	4
DLF027	(TA)11	F–CGCTTTGTCAACTCATACC R–CAAACCCGTTCTTCTACATT	Yes	1
G01-001	(CCA)5	F–AGGGAAAGCGAAAAACCCTA R–GTCGAGGACTGGAAAACCAA	No	7
G01-002	(AG)7	F–CAAGACCAAACCGAGAGAGG R–TCTCCTCCTCGACTTCCAGA	Yes	6
G01-007	(GCA)5	F–CCTCAGCAGCAGTTACAGCA R–GGCTGGGTTGTGAATGAAGT	No	3

Table A.2 (continued)

Marker name	SSR motif	Primer sequence (5' – 3')	Polymorphic	LG
G01-013	(AG)6	F–AGGAGGATGTTGGCATGAAG R–GGGAAGTTCACGACATCCAC	No	4
G01-024	(CCA)5	F–AAGTTCCCGTTGGAGGATCT R–ATGCCGACATTAGGAACCAC	Yes	4
G01-025	(AAT)4	F–GCTTTGCAGACGAAGGTCTC R–GGCACAGAACCGTTGCTAAT	No	1
G01-027	(AT)6	F–CACGTAATTTCGTCGTCCAT R–CATGCGGTCCGTCTTTATTT	Yes	6
G01-031	(ATG)6	F–ATGAACACCCAGGATTGGAA R–TGTATGCAGCTCAGGGTTTG	Yes	1
G01-033	(TGA)5	F–ATTAATCGCCCTCGTTCAAA R–AAAATCCACGGGTCACACAT	Yes	5
G01-035	(AGA)4	F–CACTTGCCAGTGGTAGCAGA R–CTTAGTGCGAGCAACACCAA	No	6

Table A.2 (continued)

Marker name	SSR motif	Primer sequence (5' – 3')	Polymorphic	LG
G01-037	(GA)6	F–CAAGGCTTTGCATCTGTGAA R–TCGGGAGAACTGGAAACAAC	Yes	4
G01-038	(GTA)6	F–AAGAGCCTGATTTGCCAAGA R–GGGACGAATTCTCTGGAGTG	No	6
G01-040	(GT)7	F–CAAGATGCATGGATGGAATG R–GCATGTGACAGACACGACCT	Yes	2
G01-043	(AG)9ataa(AG)10	F–AGCCGCTCAACTTTGAAGAA R–TTGGTGGTGGTGAAGTTGAA	No	2
G01-044	(GAT)5	F–ACCATTGCAGGGATCAAAGA R–ATTATGCCCCCTCTGAGCTT	No	3
G01-045	(GAT)5	F–TGCTAAAACAGCAGCCAATG R–TTGAACATGGGAATGCACTG	Yes	5
G01-047	(GT)7	F–CCCCAGAGCATCCCATAATA R–CCACGGAAAGCTAGGACTTG	Yes	6

Table A.2 (continued)

Marker name	SSR motif	Primer sequence (5' – 3')	Polymorphic	LG
G01-048	(GAA)4	F–TGGTCATTGCCAGCATCTAC R–TCATTAGGGCTTGGGAACTG	Yes	6
G01-053	(CGG)5	F–GAAAAGGTTGGGGGTTTGTT R–CGAAGAGGCGGTAGATCTTG	Yes	3
G01-054	(TGG)5	F–AGACCAGCACGAGGTGAAGT R–TGCATGCTAATTCCAGGTTG	No	2
G01-059	(CTG)4	F–GACATTGGGGGTACATGGAG R–CTTTCATCATTGGGCAACCT	No	3
G01-063	(TA)6	F–GTGGTGCAGTTTGGTCAATG R–GACGCAACAAAACTTGTGGA	No	1
G01-068	(CAG)5	F–GCATCCATGTCTCCAAGGAA R–TAGGCCCCATCATCAGTTTC	No	1
G01-075	(TGC)4	F–ATAGACGAGGTCGGGTTCCT R–CGCTGATAGCACCTTCTTCC	Yes	4

Table A.2 (continued)

Marker name	SSR motif	Primer sequence (5' – 3')	Polymorphic	LG
G01-079	(ATG)4	F–GTCACTCCCATTCCCTACGA R–GATAGCTGATAGCACCGAACG	Yes	1
G01-080	(CTC)6	F–TCTGCAACTTGCGTTGTTTC R–GCCGTAAAAGACCGTTGTGT	Yes	5
G01-081	(CGA)5	F–CTGCCCTTCGATCTGAACAT R–ATCAGTCCAGGAGCAGGAAG	No	6
G01-086	(GCCG)4	F–GGAGATGGCACTCTCTCGTC R–CGATCCAACGGAGGAACTAA	No	6
G01-094	(CGC)7	F–ACTCTCCCGTCGTCTCCAC R–TGCTTACCCTTGCTCCACTT	No	5
G01-095	(GCC)5	F–CACTCTTCCTCCCGGATCA R–GGATCCTCATGTCGATGTCC	No	5
G01-097	(AGCT)4	F–TCCTGATCCCTATTGGCTTG R–TGGTAAGCACAACGAATCCA	No	6

Table A.2 (continued)

Marker name	SSR motif	Primer sequence (5' – 3')	Polymorphic	LG
G01-098	(CTC)4	F–GAGAAGTTCCGCAAGAGGTG R–GCAAGACGAAGACGAAGAGG	No	3
G02-004	(CAT)5	F–CCGCGAGTAGAAAAAGAGGA R–AGTGGGGGAGTTGAAAACCT	Yes	7
G02-013	(GTT)4	F–AGAGGAGGAGGCCTGAAAAG R–CCGAAGACACGAAACAGGAT	No	3
G02-014	(TG)6	F–TTGAGCTGCGTGATCTCATC R–TCAGGCAATCACGATTATGG	No	1
G02-016	(CCG)4	F–ACTCAGCGAGGGAGGAGAC R–CTCAGCTTGAGAAGGGGATG	No	1
G02-017	(CCG)	F–CCTCATCCCAAACCCTAACC R–AGCTCCTTCTCCTCCCTGAC	Yes	1
G02-021	(CG)6	F–CTTCCTCGCCTCCTCTCCT R–CGAGCTTGTAGTTGCTGTCG	No	5

Table A.2 (continued)

Marker name	SSR motif	Primer sequence (5' – 3')	Polymorphic	LG
G02-022	(GTG)4	F–GGTGCTCCAATGGACAAGAT R–CGCCAACAAGGAGCTCTATC	No	7
G02-025	(TGG)5	F–GAGTTTGAAGATCCCCGTGA R–GCCATGATGCAGAAGAAGGT	No	2
G02-029	(GTC)5	F–CTTCCAATTCCAAGCGATCT R–GCTGCCTTCTCCTTCTTGG	Yes	4
G02-032	(CAT)5	F–ATCGTGTGCCTGGAAACTG R–CAAGCAGCAAAGTTGCACAT	Yes	3
G02-035	(TC)7	F–GCGACTCTCGTTTCCTTGTC R–CGGATTCAACTGCAATCAGA	Yes	4
G02-037	(TA)6	F–AGGCGTCACAGTTGGAAGAG R–TCCTTTTATCGCATTCACGA	No	1
G02-043	(TGTA)5	F–CTGACCATAAATCCCGCTGT R–GCTGCACTATAAGGCCAAGG	No	6

Table A.2 (continued)

Marker name	SSR motif	Primer sequence (5' – 3')	Polymorphic	LG
G02-047	(TG)11	F–GCCTTTGTCCTTGGAAATCA R–TCCAAAACGATTCAGAAGCA	No	1
G02-048	(GT)6	F–GTGTGTTCCTGTCGTGGATG R–TGCTATGTGTTGCTCCTTGC	No	7
G02-049	(TGTA)5	F–CCGGTTGACGGAGTTGTAGT R–GCTTACAAGGTGCCGAAGAG	Yes	2
G02-053	(ATT)4	F–GGCGTGTGACATAGGCAAT R–AAAACCACCATCCCTATCCTG	No	6
G02-057	(GCG)4	F–CTGCTATCTCGGCCAGTCAT R–GAAAGGGATTGCATCTCGAA	Yes	5
G02-058	(CCG)5	F–GCAAACGCTCACAGAAACAG R–GACCTTGTTGACGCCGTAAT	Yes	1
G02-069	(AGA)4	F–GCTGCAGATGATGATGAGGA R–TAGGGTTGAGGAGGAGAGCA	No	6

Table A.2 (continued)

Marker name	SSR motif	Primer sequence (5' – 3')	Polymorphic	LG
G02-075	(TAG)5	F–GCCGGGTGTAGGACTGTAAA R–CTTCCCAAGATCACCACGAT	No	3
G02-079	(AG)6	F–GGAAACCAACAAGCAAGAAGA R–GACCGAATCGAAATTCAGGA	Yes	3
G02-080	(CAG)5	F–CGACCACAAGGAGAAGAAGG R–GACATGTCACGCATCACACA	Yes	4
G02-081	(CG)7	F–GATCACCCGTCCGTCTCC R–CGATGTCGGAGCTGGTTTAT	No	7
G02-092	(AGC)5	F–ACCAATTCCCCACCTCATCT R–AGGTCTCGACGCTCTTCTTG	No	3
G02-098	(GCC)5	F–GGCACGGACCTAGGGTTT R–ATGGTGTTGTCGGTCCTCAT	No	6
G03-002	(GAA)4	F–GCATCCTCTACGCGCTCTAC R–GAAAAGCTGAGGCAACCAAG	Yes	1

Table A.2 (continued)

Marker name	SSR motif	Primer sequence (5' – 3')	Polymorphic	LG
G03-003	(CCT)4	F–GGAGATGGCACTCTCTCGTC R–CGATCCAACGGAGGAACTAA	No	6
G03-015	(ATA)4	F–AGTGTGACGGCACTGAGATG R–CCACCTAGAGGTTGGAGCAG	Yes	6
G03-020	(TGTCG)4	F–ACCCAACTTACGCACTCCAG R–TTCCATGCAACAGGTACAGC	Yes	3
G03-028	(GCC)4	F–CCCCTGTAGTCCCTCCTCTC R–TGAGTCCGTTGTCGTTGTTC	No	2
G03-030	(AGG)4	F–AACTGAAACAAGCCGATGCT R–CTTACGCAACTCCTCCTTCG	No	2
G03-039	(CTG)4	F–GCTCCAGGACTTCTTCAACG R–TTGGTGGGATGGTGTGTTC	Yes	4
G03-049	(TGA)4	F–AAGCCCTTCCTTTACCTTGC R–ACCGACTCTTGTACGAAGCAC	No	1

Table A.2 (continued)

Marker name	SSR motif	Primer sequence (5' – 3')	Polymorphic	LG
G03-052	(GCG)4	F–AGTCGACTGACCCGATGAAC R–AAGCCGTGCTTCAGGTAGAA	No	5
G03-054	(GTA)4	F–TGGACTTACCTGGGGTTCTG R–TTCCTCATCCAACATGCAAA	Yes	2
G03-055	(AAGA)4	F–CCACTGACAAACCCTCACCT R–AATGCTGCCCTCCTCCTAAT	Yes	7
G03-058	(GCA)4	F–CCTGTACCAAAAGCGTCCAG R–CATTTTACTTGCCAGCAGCA	No	2
G03-063	(TGA)4	F–ACATCCCCAGTCTGCGATAG R–ACATCAAGGGAGCCAATGTC	No	5
G03-065	(CAG)4	F–GTCGTCCTCATCATCGTCCT R–TTACAATCGCGACGGACATA	Yes	4
G03-069	(AAG)4	F–GGGACTGGACGATAAGGTGA R–GGAACAAGAGAGCTGGTGGA	Yes	6

Table A.2 (continued)

Marker name	SSR motif	Primer sequence (5' – 3')	Polymorphic	LG
G03-073	(CGA)4	F–AACCGGCTCTACACCATCAC R–CAAAGCTCACAACGCCTACA	No	7
G03-074	(GAT)4	F–CTGATGCGGAGAGCATTGTA R–CAGTGGGAGAAATCGGTGAT	No	4
G03-079	(CAG)4	F–CAGAGCTGCTCCATGTTCAA R–AAAGTGGCCTTCAACCTCCT	Yes	6
G03-089	(CTCC)4	F–TCACCAACACCACACTCCTC R–GCTGCTCGTACTGCTGTAG	Yes	3
G03-094	(AGA)4	F–GCATCTACGCACAGGGAAAT R–ATAGCCAACACCTTGCCATC	No	3
G03-096	(GGT)4	F–CTATGGTGCAGCAAGGACAA R–CGACACAGCCGTATCTCTCA	No	5
G03-099	(TCC)4	F–CGAATCGGAAGCAAATCG R–GGCACTCGTCCGAGATAGAC	No	4

Table A.2 (continued)

Marker name	SSR motif	Primer sequence (5' – 3')	Polymorphic	LG
G04-002	(GGT)4	F–GACGTCCCTTTCCTCCTCTT R–ATATATACAGGCGCGGATGC	Yes	7
G04-030	(GCC)4	F–ATGCAGCCCACAGTGACCTA R–GAATCTGGCAGTGCTTGAGG	No	2
G04-043	(AGG)4	F–TCAAACCCACCACTTTGACA R–GCCTCTCTCCCGTTTCCTAT	Yes	5
G04-048	(CGG)4	F–GAGCAAAGACACCAGCATCA R–AGAATCCCTTCCCCTTCTCA	No	7
G04-054	(AAG)4	F–GGTGGAACAGAGGAAGCAAA R–GAGGACGAGGTCTCGAACAG	Yes	3
G04-056	(GATCT)4	F–CAAGGGTGTGGCGATTAACT R–ATCGGCATCATCATCAGACA	Yes	6
G04-057	(CCGA)4	F–GTGCTCCTCCTTGTCTTTCG R–ACATTGAGCCATCCAGCATT	No	3

Table A.2 (continued)

Marker name	SSR motif	Primer sequence (5' – 3')	Polymorphic	LG
G04-059	(AGA)4	F–GAAAGACAAAGCGACGAAGG R–AGTGGTCTTTCCTGCTTCCA	Yes	2
G04-061	(TAG)4	F–GGCTGGTGTGTGTGAATTGT R–TGTTCATCCATACCAGTTCAGC	No	4
G04-064	(CAG)4	F–AGTGAAGGCCTACGCAAAAG R–CAGGTCTGTCAACCCAACCT	No	3
G04-065	(GTG)4	F–AACAAGGAATGCGGAGAAGA R–GCTTCCACAAGGAAGAAAGG	No	2
G04-067	(CAC)4	F–TGGCAGTACAAATAGCTGAACG R–TTGCAGGTTTCTGTGCACTC	Yes	3
G04-074	(ACG)4	F–AAGGTGCTGGAGAAGGTGAA R–AAAAGGCTGGTGTGGAGATG	No	3
G04-081	(GCG)4	F–AGTCGCTCGTGGAGAAGAAG R–AAGCAGGAAGCAGCTAGCAC	Yes	3

Table A.2 (continued)

Marker name	SSR motif	Primer sequence (5' – 3')	Polymorphic	LG
G04-098	(AAG)4	F–GAGGAAGCAAAACAGCACAA R–GAGGACGAGGTCTCGAACAG	Yes	3
G04-099	(TACG)4	F–AAGTTCACCGGCAAGAACAC R–GCCGAATCCATCACTGAAAC	Yes	4
G05-022	(TGG)4	F–GAGGAGGACGACGAGTTCTG R–ATCCTCTCCTTGTCCCTCGT	No	6
G05-023	(GAT)5	F–GCGAAACCACCAAGTGATCT R–GCATGTCAGGTCATCACACC	No	3
G05-024	(GCG)4	F–GCAACCTCGTAGACCACCTC R–CAATCTTGATGGTCGCGATA	No	3
G05-028	(GGA)4	F–GACCTCACCTCACCAAGCTC R–CTTCAAGAGCCTTGCTCACC	No	3
G05-030	(GCT)5	F–GGGGAAGGAAGTCAGGTCTC R–GCCAACAAACAGAGACAGCA	No	5

Table A.2 (continued)

Marker name	SSR motif	Primer sequence (5' – 3')	Polymorphic	LG
G05-033	(AGC)4	F–GCAGCTTCCTTCCAACACTT R–GCACGCTAAGTTTCGGTGTT	Yes	5
G05-041	(AGG)4	F–TAACGGCGGATAGATTGCTC R–GTCGGAGTCAGAGTCGAAGG	No	6
G05-044	(CTC)4	F–GACCGATTGGAACCAACAAC R–CGATGCTTTCAGCGGTTAAT	No	5
G05-046	(GCA)5	F–TACCTCCAGCAACAGCTTCA R–TTCTGAAACTGGCTGCAATG	No	6
G05-052	(CCA)5	F–TTGGTTGCAGCACTGATTTC R–TTGCTGCTTTCTGTTTGTGG	No	4
G05-065	(TCT)6	F–ATGAAGATCGCCACTCACCT R–TGCTGCTGCTACCGTTCTTA	Yes	5
G05-070	(CT)7	F–CCCATTCTTCTGATCCTCCA R–CATCTGCCATGTGATGCTCT	Yes	3

Table A.2 (continued)

Marker name	SSR motif	Primer sequence (5' – 3')	Polymorphic	LG
G05-071	(TTC)5	F–CTGGTCCGGTCAGTCAGTCT R–TTTGCTGGACAAACTGCAAC	No	5
G05-078	(CGA)5	F–CGAGTACAGGCACATCGAGA R–CAACAGTGTGCCTGGCTAGA	No	7
G05-081	(AG)10	F–CCAACCAGAAGAGTCGGAAG R–AGGGTCTCGGAGATGCTG	No	1
G05-082	(TA)6	F–GACGGCAGGTACTGGACAAT R–TTCCTAGGTCGGTAGGCAAA	No	2
G05-088	(TG)4	F–TGGAGACATGGAGGAGAACC R–CGTGCACAACAGAAAAACCA	No	3
G05-089	(CTG)5	F–AAGTGCGCTGCTTGACACTA R–AGGGCACAACATGCACTTTA	Yes	3
G05-090	(GA)7	F–CAGAAGAGGCTCAAGCAACC R–CACACAACCAGTGCTCATTTG	No	3

Table A.2 (continued)

Marker name	SSR motif	Primer sequence (5' – 3')	Polymorphic	LG
G05-092	(GGC)8	F–GCCTCCTCAAACCCTAACCT R–TGCGAGAACTTGATCTGGTG	No	5
G05-094	(CTG)5	F–GAGATGTACCCGGAGACCAA R–TTAGATGTGTCGAGCGATGG	Yes	5
G05-099	(GGA)5	F–AGCCTTCTTTGGGAGAGGAG R–TCCTCTCTGGCAGTTCTGGT	No	5
G05-100	(CCT)5	F–AGAATATCGCGCGAGGAAG R–CCTTCTCGTTCATGGCTGAT	Yes	2
G05-109	(ACC)4	F–TGCAGACGGGACTGTAACTG R–TTGAAAACAGAGCCGAAACC	No	3
G05-112	(GCC)4	F–AGCGGCTAGGACCGAGTT R–AAACCATGGCTTGTCTCGTT	Yes	7
G05-121	(TGC)4	F–CGTCTTCACCAAGATCGACA R–TTGCGATCCATGCACTATACA	No	4

Table A.2 (continued)

Marker name	SSR motif	Primer sequence (5' – 3')	Polymorphic	LG
G05-124	(TTC)4	F–TCGGACGCTACCTAACCATC R–GGTTGTCCTGGACGTAGACC	No	1
G05-127	(CCA)4(GCA)4	F–AAATGTTGTCCGGTGAGAGG R–GATGAGCGGTCTCTTCTTGC	No	1
G05-129	(TGC)4	F–CTTTTGCTTCTGCACCTTCC R–AAACCACCAGCAGATGAAGC	Yes	2
G05-134	(CGC)4	F–CCTGGGTTCCACCTTCTCTT R–GCGGGCTGTAGACGAAGTAG	No	3
G06-006	(GAT)4	F–GTGGATCCAGAGTTGGCACT R–CTCCCTCGTCCATTGACATT	No	4
G06-021	(GGC)4	F–ACGCCATTACTCCTGTCCAC R–ATCTCCTCGGAGACGCACT	No	7
G06-028	(ATG)4	F–TGGAGGATTGAGTGCTACCC R–CCATGATGCCACACACAAAT	No	7

Table A.2 (continued)

Marker name	SSR motif	Primer sequence (5' – 3')	Polymorphic	LG
G06-029	(ATA)4	F–TTGTCGAAGCTGGTGATCTG R–GGCATTCCGTTTGGATAATG	No	3
G06-031	(GCC)4	F–GCCGAGTTCAACCTTTCAGA R–GCTTCCCCTGCTCTTCTTCT	No	3
G06-039	(TCG)4	F–AGAAGGCTCGTCGGGTCTA R–CCCAACCAGGTCAAGAAGAA	No	6
G06-049	(TTA)4	F–TGTAATCGTACCCCCAGCTC R–TTGACTGCCTGAAACTGCAC	No	1
G06-065	(TGT)4	F–TCCCAGTGACCCTCTGGTAG R–AATCCAGTACATCGGCAAGG	Yes	6
G06-079	(GCCG)4	F–GCAACGACGAGGAGATCAAT R–ACCACCGGTGAGTACATTGC	No	7
G06-088	(AG)6	F–GGAGCGGTGATCAAAGAGAA R–AGCCGTTTGAGGCAAAACTA	No	3

Table A.2 (continued)

Marker name	SSR motif	Primer sequence (5' – 3')	Polymorphic	LG
G06-089	(AGA)4	F–AGATGGGAGGTGATCAGGTG R–GAATCTTGGCAGAAGCCCTA	Yes	4
G06-096	(TTG)4	F–GATCTTGCAGGCCGTCTAAC R–GCCAGCGTCTTTATTTAGGC	No	5
G07-024	(CTT)4	F–ACACCTCCACTCCACACTCC R–ATTCTGAGAGCACCCACCAC	No	5
G07-034	(CTCCAC)4	F–ACCAGCAACCGACGAAAC R–GCCGCTGTAGTGGAAGAAGA	No	3
G07-037	(CCG)4	F–CCGAGTCCAGCTCAATCTTC R–ATCCGCCAGAACTCGTAGTC	No	2
G07-038	(GCT)4	F–GACGCACAACTGCAACAACT R–TCTTGACTTCTTCTTGCTTGGA	No	6
G07-056	(CCGCT)4	F–CAAAGAAGTCACGCACCAAA R–GCTGGTGTAGCAGATGAGCA	No	6

Table A.2 (continued)

Marker name	SSR motif	Primer sequence (5' – 3')	Polymorphic	LG
G07-058	(GCC)4	F–AAGGAGCTCCAGCAAGATGA R–AGCCGTTTGAGGCAAAACTA	No	3
G07-065	(CTC)4	F–CTCCACTCCAGTCCACAACC R–GAACATGGAGAGGGTCAGGA	No	5
G07-066	(GCA)4	F–TTTCGGGAGGTGGTAGAAGA R–GTAGGTGGACCTGGTGCTGT	Yes	7
G07-071	(TCC)4	F–CATCTATGCTCCTTGTCCACTCT R–AACGAATCCGATCGAAACAG	No	3
G07-074	(AGC)4	F–GAAGCACATCGACGAGATCA R–ATGGCATTGATACCCTCCAC	No	1
G07-083	(AAG)4	F–ACTGTGGGAGATGACGAACC R–CCTCCAAGCCAATAAAGCAG	No	3
G07-088	(CTA)4	F–CCGGGACAGAAACTGATGAT R–CGAGCATTCTTCCTTTCTCC	Yes	7

Table A.2 (continued)

Marker name	SSR motif	Primer sequence (5' – 3')	Polymorphic	LG
G07-097	(ACG)4	F–TCAAGGCCCTACAGAACCAC R–AGGCCAAGGGATAAATCGAG	No	1
G07-098	(AAG)4(AGA)4	F–ACTGAGGCAGTGGAAGAGGA R–TGCAACCAAAATAACCACCA	Yes	2
LP165	(CT)14	F–CCATCACCTCCACTAT R–AGCTCGCAGTCTGTTG	Yes	7
LP204A	(CT)20	F–GAGCTTCTCTCGATCCT R–AGTGGATGTGACTACA	No	4
LP20A	(GA)16(A)5(GA)4	F–ACCGCTGTGCTAAATCTG R–ATGCGCTGCTGTCTGCCCT	No	4
LP8A	(CT)17	F–TGACTTCTCTCGATCCT R–ATGTGACTACAAAACCA	No	4
LpSSR006	(CT)23	F–CAATGGAGTCCCAACAG R–TACCTGGGCAAATCTTG	Yes	4

Table A.2 (continued)

Marker name	SSR motif	Primer sequence (5' – 3')	Polymorphic	LG
LpSSR011	(CA)15(CA)9	F–AAATGTTCATCGTATCG R–CAGGTCCCTGCTTAC	Yes	4
LpSSR017	(GA)26(GA)2(GA)2	F–TGAGCACCATGAAGGAG R–GGTTGTCCGCAGGTATT	Yes	7
LpSSR020	(GA)5(GA)2(GA)16	F–GGGGAAATACAGTTCTGC R–GATGCTCCTGCCTACTTTA	Yes	7
LpSSR021	(GA)21	F–AACAAGTCAATGGACAGATT R–TTTGTTTTCCCTTTTGG	Yes	2
LpSSR023	(GT)4(GT)19(GA)23	F–ATGCACGGGTTTTATTCATT R–CGCGAGGCTTAAGGTGT	No	4
LpSSR026	(CT)25	F–GCAAAGTGTACAACCTCT R–ACTCACGTATCTCATAGGA	No	5
LpSSR027	(CT)17	F–CACCACCTTCTCCAAC R–AACAAGCACTTAGGAACA	No	1

Table A.2 (continued)

Marker name	SSR motif	Primer sequence (5' – 3')	Polymorphic	LG
LpSSR057	(GA)21	F–TAGCCTCCAGAAACAAAGTC R–CATAGCAGTACAGCCAGTCA	No	1
LpSSR058	(GA)14	F–CGATGAACTCAAGGGGGATT R–GCACCGGTCTAGGGACAGAA	Yes	6
LpSSR059	(CT)20	F–GATCGGATCGGTACAGGAGA R–GAAGCGCACCTTCTGTTTCT	No	5
LpSSR066	(TG)24	F–GCCAGTGCCCATTCCGATAA R–CCCCACTCCAACCAAAGCAA	Yes	7
LpSSR071	(CTT)2(GTT)2(CTT)2	F–GGAAGTGGGGGCAGCAG R–GCAACAACGCAACACCCTAA	No	2
LpSSR076	(CA)28	F–CCCATACTTCGAGGCATAAA R–AAATTCCCCCATCAGAGAAC	No	2
LpSSR082	(CA)25	F–CTAAACTAAATGTTCATCGT R–CCTGCTTACTCCTGTT	Yes	4

Table A.2 (continued)

Marker name	SSR motif	Primer sequence (5' – 3')	Polymorphic	LG
LpSSR085	(CA)47	F–GCCAGATCCCTTGTAGAAG R–GCACCATTTAAAACCAAAGA	Yes	1
LpSSR089A	(TG)(TG)2(TG)9	F–TGTGTTTCCGTGTTTCCTTG R–CCAAAATCGAGAAAATGGTTC	No	4
LpSSR091	(TG)25	F–CACTCTCGGTCTCGCCTTAT R–TTCGCATGCATACAACACAT	No	7
LpSSR100	(TG)8(TG)2	F–AATACTTGAGTTGGCATTTC R–CGGCTCACTGAACATTC	No	3
LpSSR112	(CA)20	F–GACCCCGAGACAGCCTA R–ACGCATATGGTCTTCAGAA	Yes	2
LPSSRH01A02	(CA)27	F–AAAGACCGCATACGAAGT R–AACCAAAGCCTCAAGACA	No	5
LpSSRH01E10	(CA)10	F–CGCAGCTTAATTTAGTC R–GCTTTGAGTATGTAAAGTT	Yes	4

Table A.2 (continued)

Marker name	SSR motif	Primer sequence (5' – 3')	Polymorphic	LG
LPSSRH01H06	(CA)9	F–ATTGACTGGCTTCCGTGTT R–CGCGATTGCAGATTCTTG	No	4
LPSSRH02C11	(CA)4(CA)4	F–TGGAATAACGATGAAAAF R–CATCACGAATTAACAAGAG	No	3
M10-138	(CA)13	F–TAGAGGATCAGTTGCATC R–TAGTTCCGAGTTAGCTGA	Yes	3
M144	(CT)16	F–CAGAAGGAGGTCGTCGA R–CTGAAACCTAGGCTATCTGAG	Yes	4
M15-185	(GA)5(GA)17	F–GGTCTGGTAGACATGCCTAC R–TACCAGCACAGGCAGGTTC	Yes	2
M16B	(GA)28	F–TGCTGTGGCTCTTGTGAC R–AGCCGAGGCTCAGCTCGA	No	1
M4136	(GA)27	F–AGAGACCATCACCAAGCC R–TCTGGAAGATTTCCTTG	Yes	2

Table A.2 (continued)

Marker name	SSR motif	Primer sequence (5' – 3')	Polymorphic	LG
M4213	(GT)9	F–CACCTCCCGCTGCATGGCATGT R–TACAACGACATGTCAAGGT	No	1
PR14	(GT)12	F–CCTTTTCGCCTTCGTA R–CACCAACATTGCCGAGTG	No	4
PR24	(GT)16	F–TGCTGTGATGCTGAATG R–GTATAGTACCCATTCCGTTGTC	Yes	2
PR25	(GT)15	F–AGGGTTCGTCTGCATTC R–CCTGCATACATTCATCCA	No	1
PR3	(CA)22	F–GTATAGTACCCATTCCGT R–GCCGCCCTGCCATGCTG	No	2
PR37	(GT)18	F–TCTGCATTCGTTGTCTCACTG R–GAGCCGTCGCACCCCTG	No	1
PR39	(CA)17	F–CATTCATCCACGTTAGAC R–CTTCCACGACTGCTTC	No	1

Table A.2 (continued)

Marker name	SSR motif	Primer sequence (5' – 3')	Polymorphic	LG
PR8	(GT)42	F–AGGGTTCGTCTGCATTC R–GCCGTCGCACCCCTG	No	1
PRE	(CA)12	F–CATTCATCCACGTTAGAC R–GTTAGGTTCGTCTGCAT	Yes	1
PRG	(CA)13	F–GCCGAGTGTCATCAAGGT R–CTTTTTCGCCTTCGTA	Yes	4
rv-0005	(TAGA)22	F–GGCAACTAGGAGAAAAATGAGAA R–GATTGTAGTAGTGGGTAATCCT	Yes	7
rv-0244	(CT)21	F–CAGATTGCAACTCACGAGGA R–ATTTTCCCGTCTGTATTGCG	Yes	1
rv-0454	(CT)19	F–AGATGTGAGCTGTGTGCCTT R–CGATATATCAGCCTCACGCA	Yes	4
rv-0641	(CT)10	F–TGCATAACTTCACTGCAGCATA R–AGAAACTCGGTAGAAGGACCTC	Yes	6

Table A.2 (continued)

Marker name	SSR motif	Primer sequence (5' – 3')	Polymorphic	LG
rv-0659	(CT)19(CA)11	F–TCTCTCCAAGTTCCTCTTCTGC R–TCTGCTTCCATCAAGAAAGGTT	Yes	1
rv-0663	(CT)15	F–ATTAGTTCAAACACCCGCAAGT R–CGTCTGCACCTCTACAGCATAG	Yes	7
rv-0706	(CT)18	F–TTCATGTTAGCCCTCCTGTTTT R–AATCAAGCCATCTCGTCCTCTA	Yes	2
rv-0757	(CT)27	F–AGATGATGATGCAGTGGACAAG R–CACCACTTCAATCACGCAGTAT	Yes	5
rv-0913	(CT)9	F–GGCTTACAGCGAAGAAGACATT R–CAGTTGAGCTCATTGGAGACAC	Yes	1
rv-0941	(CT)9	F–ACTTGCATAGCGTACAAGCAAA R–AAAAACTGTACACTGCGCTCAC	Yes	4
rv-0959	(TAA)9	F–GTAAACTGGGTTGATGGGATGT R–CATTGTACGATTTATGCTTCTCCA	Yes	2

Table A.2 (continued)

Marker name	SSR motif	Primer sequence (5' – 3')	Polymorphic	LG
rv-0985-1	(CT)18	F–CTTATTATTGCAAGCGATGGTG R–GTATCGTCCCTCAGTCCTTTTG	Yes	6
rv-0992	(TAA)11	F–CAATGCCATCACCAACACTACT R–TTTTGTAGCATGGAGAGATTACCA	Yes	4
rv-1112	(CT)11	F–TTTGTTAGCCCGTCCTTACCTA R–AACATGTGGAATGGAATGGAAT	Yes	5
rv-1133	(CG)8	F–CGGTTCTGAATTTTCTGCTTCT R–AAAGCTGAGAACCGAATCCATA	Yes	3
rv-1266	(CAG)10	F–AAGAGGAAACAAATGGCAACAT R–AGCTTCCTTACATGCTCTGTAT	Yes	6
rv-1284	(TA)9	F–TTTGACTATTTCTCGCACTTCG R–GAATTCCGCACATATCCAAACT	Yes	7
rye012	(CA)23	F–GGTCTAATTGTCGTCCTTTC R–GAGTGATTTGGAGGTGAGAA	Yes	4

Table A.2 (continued)

Marker name	SSR motif	Primer sequence (5' – 3')	Polymorphic	LG
rye014	(CA)26	F–CTGCTCTGTGTTTGTGTGAC R–GCCTTTCATCGTTACTGTCT	Yes	6
uni001	(AC)17	F–AGCCACACTTTACCTAATGCTG R–CCCGCAAAACTTACAATTAAA	Yes	3

[a] The markers that successfully mapped to the maternal and paternal parent maps are presented in boldface font.